RAMAN BAND INTENSITIES OF THIOETHERS AND THIOLS

A Thesis Submitted for the Degree of

Doctor of Philosphy

by

JOSEPHINE ANNE ELLWOOD

ROYAL HOLLOWAY AND BEDFORD
NEW
COLLEGE
LIBRARY

Chemistry Department

Royal Holloway and Bedford New College

University of London

October 1989

ProQuest Number: 10096237

All rights reserved

INFORMATION TO ALL USERS
The quality of this reproduction is dependent upon the quality of the copy submitted.

In the unlikely event that the author did not send a complete manuscript
and there are missing pages, these will be noted. Also, if material had to be removed,
a note will indicate the deletion.

ProQuest 10096237

Published by ProQuest LLC(2016). Copyright of the Dissertation is held by the Author.

All rights reserved.
This work is protected against unauthorized copying under Title 17, United States Code.
Microform Edition © ProQuest LLC.

ProQuest LLC
789 East Eisenhower Parkway
P.O. Box 1346
Ann Arbor, MI 48106-1346

To Peter

ABSTRACT

Raman spectroscopy is potentially a useful technique for the analysis of thioethers and thiols because of the characteristic set of bands which appears in the C-S stretching region.

A review of previous studies on Raman band intensity measurements is presented in which the experimental difficulties and influencing factors are given.

An experimental system has been developed around a Coderg PHO Raman spectrometer for the measurement of absolute Raman band intensities. This includes the novel use of a Pockels cell for the accurate determination of depolarisation ratios. Carbon tetrachloride has been assessed as a suitable internal standard for use with this system.

Raman band intensities are given for five thioethers and two thiols. Several bands are identified as being characteristic of sulphur-containing hydrocarbons. Analysis of bands in the C-S stretching region is accomplished by considering the intensity contributions provided by individual groups in the molecule, resulting in a successful prediction of the C-S stretching band intensities for t-butane thiol.

In addition, temperature studies have been conducted for ethyl methyl sulphide in order to attempt calculation of the energy barrier between the two conformations.

A computer programme has been developed for the theoretical calculation of Raman band frequencies and intensities. Molecular parameters have been derived for dimethyl sulphide, including an *ab initio* force field. Tests for transferability

of these data to ethyl methyl sulphide and deuterated dimethyl sulphide have produced encouraging results.

A study of infra-red intensities of thioethers has been carried out. This is an extension of some previous work in which the necessity to resolve individual bands is eliminated. For several discrete spectral regions quantification is made of the effects of a sulphur atom on C-H band intensities, thus allowing successful intensity predictions for other molecules studied.

Suggestions for further work in this field are given.

ACKNOWLEDGEMENTS

I wish to thank Dr Derek Steele for his help and advice during the course of this work and during the preparation of this Thesis.

The financial support of British Petroleum plc is gratefully acknowledged.

CONTENTS

	Page
1. MEASUREMENT OF ABSOLUTE RAMAN BAND INTENSITIES	1
1.1 Introduction	1
1.2 Theory of Raman Spectroscopy	2
1.3 The Development of Raman Intensity Measurements	6
1.4 Theory of Raman Band Intensities	9
1.4.1 Molecular Polarisability Tensor	9
1.4.2 Depolarisation Ratios	11
1.4.3 Placzek's Molecular Polarisability Theory	13
1.4.4 Wolkenstein Bond Polarisability Theory	16
1.5 Raman Intensity Measurements in Liquids	18
1.6 A Brief Description of the Work Covered in this Thesis	21
2. AN EXPERIMENTAL SYSTEM FOR THE MEASUREMENT OF ABSOLUTE RAMAN INTENSITIES	23
2.1 Instrumentation	23
2.2 Use of a Pockels Cell for the Measurement of Depolarisation Ratios	24
2.3 Computer Programme for the Accumulation and Interpretation of Data	30
2.3.1 Routine for Fitting to the Sum of One or More Damped Lorentzian Band Contours	32
2.4 Calibration of the Spectrometer for Variation of Efficiency with Frequency	34
2.4.1 Experimental Procedure	34
2.4.2 Results	36
2.5 Assessment of Carbon Tetrachloride as an Internal Standard	41
2.5.1 Experimental Procedure	44
2.5.2 Results	45
3. RAMAN BAND INTENSITY MEASUREMENTS OF THIOETHERS AND THIOLS	48
3.1 Introduction	48
3.2 Experimental Procedure	48
3.3 Results	52
3.3.1 Estimation of Experimental Error	52
3.3.2 Interpretation of Results	57
3.3.2.1 C-S Stretching Bands	58
3.3.2.2 C-H Bending and Stretching Bands	65
3.4 Deuterated Dimethyl Sulphide Compared with Dimethyl Sulphide	69
3.5 Ethyl Methyl Sulphide Temperature Studies	72
3.5.1 Introduction	72
3.5.2 Experimental Results	78

Page

4. THEORETICAL CALCULATION OF RAMAN BAND INTENSITIES 83

4.1 The Wolkenstein Assumptions 83
4.2 Description of the Method Used for Intensity Calculation 83
4.2.1 Input Data for Theoretical Calculation Programme 84
4.2.2 Vibrational Frequency Calculation 87
4.2.3 Raman Band Intensity Calculation 91
4.3 *Ab Initio* Calculation of a Force Field for Dimethyl Sulphide 96
4.3.1 The Gaussian 82 Package 97
4.3.2 Experimental Procedure for Dimethyl Sulphide 100
4.3.3 Force Field Results 103
4.4 Polarisability Data for Dimethyl Sulphide 109
4.5 Optimisation of Data for Dimethyl Sulphide 110
4.5.1 Force Field 110
4.5.2 Polarisability Data 111
4.6 Results 113
4.6.1 Water 113
4.6.2 Dimethyl Sulphide 113
4.6.3 Dimethyl Sulphide-d6 115
4.6.4 Ethyl Methyl Sulphide 117

5. USE OF INFRA-RED BAND INTENSITIES IN STRUCTURAL ANALYSIS 121

5.1 Introduction 121
5.2 Measurement of Infra-red Band Intensities 122
5.3 Experimental Procedure 125
5.4 Results 127
5.4.1 Review of Studies of n-Alkanes and Methyl n-Alkyl Ketones 127
5.4.2 Thioethers - Infra-red Intensity Results 128
5.5 Prediction of Infra-Red Intensities 134
5.5.1 Stretching Intensities 134
5.5.1.1 Calculation of S Effect on α and β CH_2 Group Intensities 134
5.5.1.2 Prediction of Infra-Red Intensity for Methyl n-Propyl Sulphide 137
5.5.2 Bending Intensities 139
5.5.2.1 Prediction of Infra-Red Intensities for Dihexyl Sulphide and Dioctyl Sulphide 142

6. CONCLUSIONS AND SUGGESTIONS FOR FURTHER WORK 143

6.1 Experimental System for the Measurement of Raman Band Intensities 143
6.2 Raman Band Intensity Measurements of Thioethers and Thiols 144
6.3 Theoretical Calculation of Raman Band Intensities 146
6.4 Infra-Red Band Intensities of Thioethers 147
6.5 Conclusions 148

Page

7. REFERENCES 149

APPENDIX A
Theory of the Pockels Cell 153

APPENDIX B
Raman Spectrum of Chloroform 154

APPENDIX C
Programme for Polynomial Fit Calculations 156

APPENDIX D
Raman Spectra of Thioethers and Thiols 158
Dimethyl Sulphide 158
Dimethyl Sulphide-d6 160
Ethyl Methyl Sulphide 162
Diethyl Sulphide 164
Methyl n-Propyl Sulphide 166
Ethane Thiol 168
t-Butane Thiol 170

APPENDIX E
Data Files for Theoretical Calculation Programme 172
Dimethyl Sulphide 172
Dimethyl Sulphide-d6 176
Ethyl Methyl Sulphide - *Gauche* 180
Ethyl Methyl Sulphide - *Trans* 183

APPENDIX F
Self Consistent Field Method 186

APPENDIX G
Gaussian 82 Data File for Dimethyl Sulphide 187

APPENDIX H
Theoretical Calculation Results 188
Dimethyl Sulphide 188
Dimethyl Sulphide-d6 189
Ethyl Methyl Sulphide - *Gauche* 190
Ethyl Methyl Sulphide - *Trans* 191

APPENDIX I
Infra-Red Spectra of Thioethers
Dimethyl Sulphide 192
Ethyl Methyl Sulphide 193
Diethyl Sulphide 194
Methyl n-Propyl Sulphide 195
Di-n-Hexyl Sulphide 196

APPENDIX J
Plots of Intensity *versus* Number of CH_2 Units for Thioethers 197

LIST OF TABLES

Page

CHAPTER 2

2.1: Comparison of Depolarisation Ratios of Chloroform as Measured with a Pockels Cell with Literature Values 29

2.2: Variation of Intensity Results with Frequency Observed During Calibration with NPL Calibrated Tungsten Lamp 36

2.3: Adjustment of Black Body Radiation Intensities to take into Account Spectrometer Intensity Variation 37

2.4: Comparison of Observed and Calculated Antistokes/Stokes Band Intensity Ratios (I_{AS}/I_S) for Carbon Tetrachloride 39

2.5: Carbon Tetrachloride: Variation of Relative Band Intensities with Laser Wavelength 44

2.6: Carbon Tetrachloride: Variation of Relative Band Intensities with Temperature 45

2.7: Relative Raman Band Intensities for Diphenyl Acetylene, Neat and in Carbon Tetrachloride Solution 46

CHAPTER 3

3.1: Raman Band Intensities (I) and Depolarisation Ratios (ρ) for Thioethers and Thiols 53

3.2: Calculation of Experimental Error for Methyl n-Propyl Sulphide 55

3.3: Relative Band Intensities for Solutions of Thioethers and Thiols in Carbon Tetrachloride 56

3.4: Calculation of CV Between Individual Intensity Measurements for Methyl n-Propyl Sulphide in Carbon Tetrachloride Solution 56

3.5: Comparison of Observed and Literature Raman Band Frequencies for Dimethyl Sulphide 58

3.6: Comparison of Observed and Literature Raman Band Frequencies for Ethyl Methyl Sulphide 59

3.7: Integrated C-S Stretching Intensities for Thioethers and Thiols Studied 60

Page

3.8: Some Characteristic Raman Bands and Intensities Due to C-H Vibrations 66

3.9: C-H Stretching Region: Comparison of Calculated Intensity per C-H Bond for Thioethers and Thiols Studied (2700 - 3000 cm^{-1}) 67

3.10: Investigation of C-H Intensity Contribution for Bonds Adjacent and Non-Adjacent to Sulphur 69

3.11: Comparison of Raman Band Frequencies and Intensities for $S(CH_3)_2$ and $S(CD_3)_2$ 71

3.12: F-Sum Rule for Dimethyl Sulphide 72

3.13: Ethyl Methyl Sulphide: Relative Intensities of the C-S Stretching Bands as a Function of Temperature 79

3.14: Ethyl Methyl Sulphide - Solution in Carbon Tetrachloride: Variation of Relative Intensities of 658 cm^{-1} and 458 cm^{-1} Bands with Temperature 79

CHAPTER 4

4.1: Rate of Change of (-DE/DR) with Change in Molecular Parameter, R, for Dimethyl Sulphide 105

4.2: Non-Scaled *Ab Initio* Force Field for Dimethyl Sulphide 106

4.3: Scaled Force Constants for Dimethyl Sulphide (Scaling Factors Based on Pulay's Values) 108

4.4: Examples of Bond Polarisabilities and Polarisability Derivatives for Some Simple Hydrocarbons 109

4.5: Initial Polarisability Values Used in DMS Calculations 110

4.6: Optimised Force Field for Dimethyl Sulphide 112

4.7: Optimised Polarisability Values for Dimethyl Sulphide 112

4.8: Dimethyl Sulphide: Comparison of Theoretical and Experimental Vibrational Frequencies 114

4.9: Dimethyl Sulphide: Comparison of Theoretical and Experimental Raman Band Intensities and Depolarisation Ratios 115

Page

4.10: Dimethyl Sulphide-d6: Comparison of Theoretical and Experimental Vibrational Frequencies and Relative Band Intensities 116

4.11: Ethyl Methyl Sulphide: Comparison of Theoretical and Experimental Vibrational Frequencies 118

4.12: Ethyl Methyl Sulphide: Comparison of Theoretical and Experimental Raman Band Intensities and Depolarisation Ratios 120

CHAPTER 5

5.1: Infra-red Intensities in the Region 3000 - 2800 cm^{-1} for Varying Concentrations of Thioethers in Carbon Tetrachloride 130

5.2: Infra-Red Absorption Intensities of 25 cm^{-1} Regions for 5% Solutions of Thioethers in Carbon Tetrachloride 131

5.3: Infra-Red Intensities per CH_2 or CH_3 Unit over 25 cm^{-1} Regions between 1500 and 1350 cm^{-1} 140

5.4: Bending Intensities for α and β CH_2 Units over 25 cm^{-1} Regions Determined for Thioethers 140

5.5: Comparison of Predicted and Observed Infra-Red Intensities over 25 cm^{-1} Regions for Dihexyl Sulphide and Dioctyl Sulphide 140

LIST OF FIGURES

Page

CHAPTER 1

1.1: Rayleigh Scattering 3

1.2: Raman Scattering (Stokes Lines) 3

1.3: Raman Scattering (Antistokes Lines) 3

1.4: Stokes and Antistokes Lines of Carbon Tetrachloride (Schematic) 5

1.5: Directions of Planes of Polarisation of the Incident and Scattered Radiation 11

CHAPTER 2

2.1: Schematic Diagram of Apparatus 25

2.2: a) Pockels Cell Off b) Pockels Cell On 27

2.3: Integration between Band Minima 31

2.4: Graph to Show Variation of Spectrometer Efficiency with Wavelength 40

2.5: Normal Modes of Vibration for Carbon Tetrachloride 41

2.6: Raman Spectrum of Carbon Tetrachloride 43

CHAPTER 3

3.1: Coderg Temperature Controller Unit 51

3.2: Plot of C-H Stretching Intensity *per* C-H Bond *versus* Number of CH_2 Bonds 67

3.3: Rotational Isomers of Ethyl Methyl Sulphide 73

3.4: Change in Potential Energy with Conformation for Ethyl Methyl Sulphide 73

3.5: C-S Stretching Bands of Ethyl Methyl Sulphide 75

3.6: C-S Stretching Modes of Ethyl Methyl Sulphide 76

3.7: Energy Barrier Calculation for Ethyl Methyl Sulphide 82

CHAPTER 4

4.1: Molecular Energy Curve 100

4.2: Dimethyl Sulphide Molecule 103

CHAPTER 5

5.1: Half Band Width 123

5.2: Plot of intensity *versus* Concentration for Thioethers 129

CHAPTER 1

MEASUREMENT OF ABSOLUTE RAMAN BAND INTENSITIES

1. MEASUREMENT OF ABSOLUTE RAMAN BAND INTENSITIES

1.1 Introduction

The aim of this project was to investigate the possibility of using Raman band intensity measurements to detect and identify various thioethers and thiols. One application of this work could be to follow the elimination of these compounds from crude oil. Thioethers and thiols are found in large quantities in crude oil and are a great nuisance, the main reason being their tendency to oxidise to acidic substances on burning. One current problem arising from this is the formation of acid rain.

Raman spectroscopy would seem to be an ideal method for looking at these compounds as the main feature which distinguishes them from other hydrocarbons, the carbon-sulphur bond, produces a very prominent set of stretching bands in the Raman spectrum. This is not the case with infra-red spectroscopy. Raman spectroscopy has the added advantage that minimal sample preparation is necessary. It was hoped that by measuring the Raman band intensities of a series of the compounds of interest a method might be established for use in quantitative analyses. Included in this work was an attempt to establish the molecular parameters that would permit the prediction and analysis of the spectra of thioethers.

1.2 Theory of Raman Spectroscopy

Raman spectroscopy is a technique by which information about energy levels of molecules is accumulated by studying the light inelastically scattered by them.[1,2]

When a beam of radiation passes through any transparent substance light is scattered. Most of this scattered light has a frequency which is the same as that of the incident light, and this is known as Rayleigh scattering (see Figure 1.1). It is Rayleigh scattering that is responsible for the blue colour of the sky. As light from the sun passes through the earth's atmosphere, Rayleigh scattering occurs and since the extent of scattering is proportional to the fourth power of the frequency, the light at the blue end of the spectrum is scattered much more strongly than that at the red end. Thus the sky appears to be blue.

During the scattering process new frequencies are added. These result from the photons either gaining or losing energy during inelastic collisions with molecules. If a molecule absorbs energy from a photon during collision and is excited to a higher energy level, then the photon will emerge from the collision with lower energy and hence a lower frequency. The resulting Raman lines are then known as Stokes lines (see Figure 1.2). If, however, the molecules are already excited they may be able to transfer energy to the photons by dropping to a lower energy level. The emergent photons will then have increased energy and therefore a higher frequency. These Raman lines are known as Antistokes lines (see Figure 1.3). The difference between the frequency of the Raman

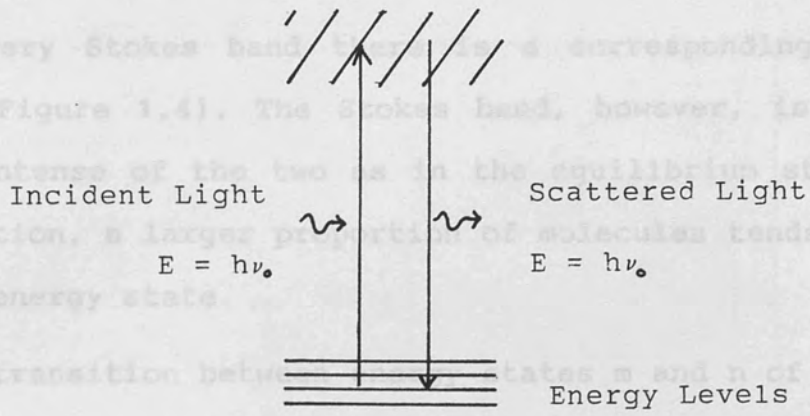

Figure 1.1: Rayleigh Scattering

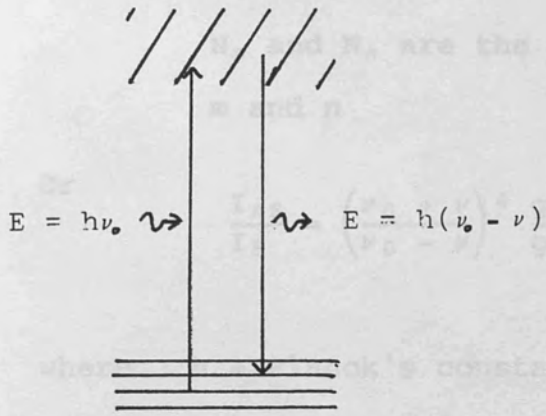

Vibrational Frequency = ν

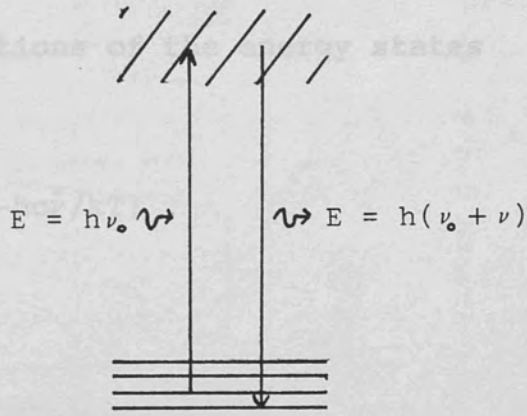

Vibrational Frequency = ν

Figure 1.2: Raman Scattering (Stokes Lines)

Figure 1.3: Raman Scattering (Antistokes Lines)

scattered radiation and the incident radiation is equivalent to a vibrational frequency.

For every Stokes band there is a corresponding Antistokes band (Figure 1.4). The Stokes band, however, is usually the more intense of the two as in the equilibrium state, before excitation, a larger proportion of molecules tends to be in a lower energy state.

For a transition between energy states m and n of a molecule, the ratio of intensities of Antistokes lines, I_{AS}, to Stokes lines, I_S, is given by:

$$\frac{I_{AS}}{I_S} = \left(\frac{\nu_0 + \nu}{\nu_0 - \nu}\right)^4 \frac{N_m}{N_n}$$

where ν_0 = frequency of incident radiation

ν = vibrational frequency, i.e. the difference between the incident and scattered radiation frequencies

N_m and N_n are the populations of the energy states m and n

Or

$$\frac{I_{AS}}{I_S} = \left(\frac{\nu_0 + \nu}{\nu_0 - \nu}\right)^4 \frac{g_m}{g_n} \exp(-hc\bar{\nu}/kT)$$

where h = Planck's constant

k = Boltzmann's constant

c = speed of light

T = temperature (K)

g_m and g_n = degeneracies of energy states m and n

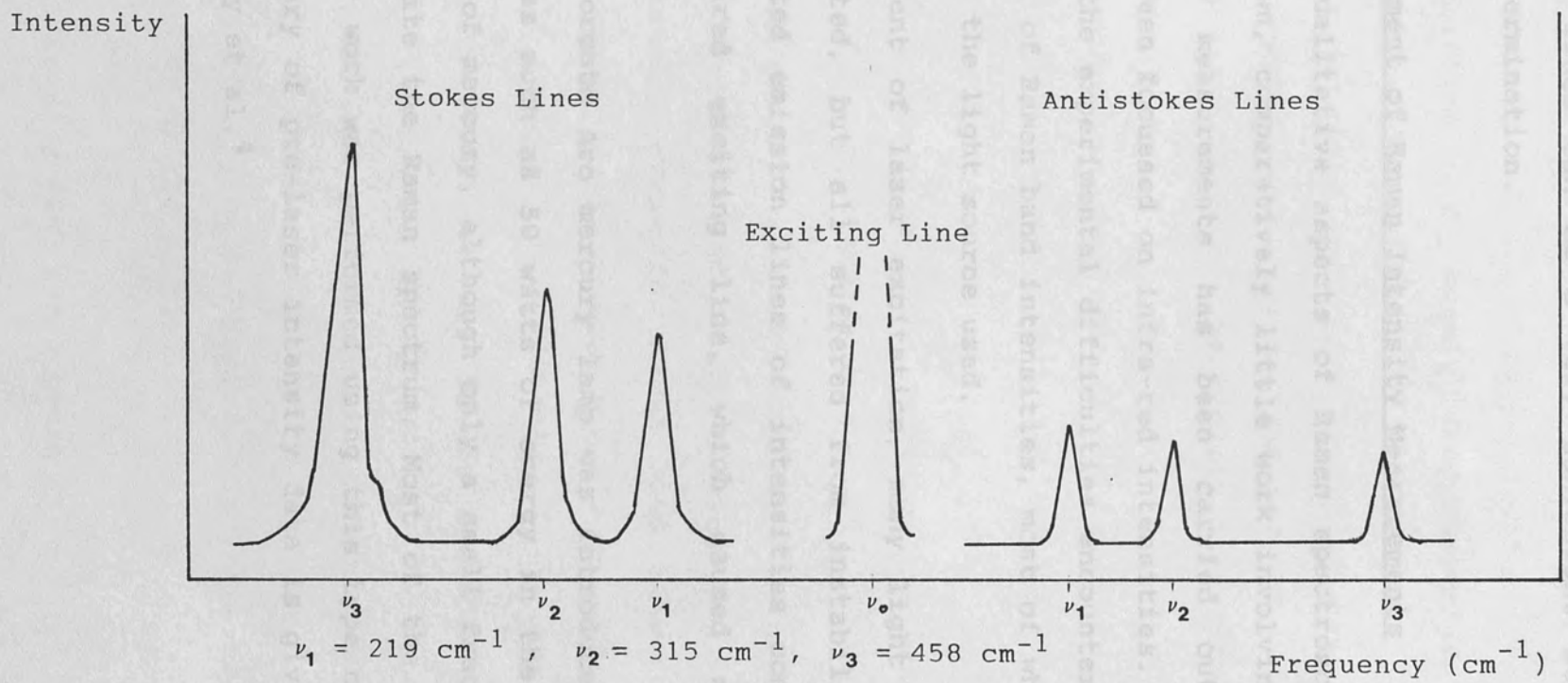

Figure 1.4: Stokes and Antistokes Lines of Carbon Tetrachloride (Schematic)

It can be seen from this expression that the ratio varies with temperature and so the comparative measurement of Stokes and Antistokes lines can be a very convenient method of temperature determination.

1.3 The Development of Raman Intensity Measurements

Although the qualitative aspects of Raman spectroscopy are quite well known, comparatively little work involving Raman band intensity measurements has been carried out; more attention has been focussed on infra-red intensities. This is mainly due to the experimental difficulties encountered with the measurement of Raman band intensities, most of which are associated with the light source used.

Before the advent of laser excitation, many light sources were investigated, but all suffered from instability and produced unwanted emission lines of intensities comparable with the desired exciting line, which caused multiple excitations.[3]

In 1952, the Toronto Arc mercury lamp was introduced. This could radiate as much as 50 watts of energy in the 4538 Å emission lines of mercury, although only a small fraction of this could excite the Raman spectrum. Most of the earlier Raman intensity work was performed using this type of light source. A summary of pre-laser intensity data is given in a review by Murphy et al.[4]

With the relatively recent introduction of laser excitation, however, many of the experimental problems have been eliminated. The laser has many advantages over other light sources. For example:

(1) Laser radiation is highly monochromatic, which eliminates the possiblity of multiple excitation.

(2) The laser is plane polarised, enabling the accurate measurement of depolarisation ratios (see Section 1.4.2).

(3) The high power density of the radiation produces better quality spectra.

(4) The small cross-sectional area of the laser beam and the fact that it is directional permit the use of very small sample quantities.

Hence a renewed interest is being taken in the measurement and application of Raman intensity data.

Among the first people to look seriously at Raman band intensities were Bernstein and Allen.[5] In 1955 they proposed a standard intensity scale for Raman band intensities of liquids and attempted to set up such a scale using the carbon tetrachloride 458 cm^{-1} band as a standard.

To do this, several factors had to be considered. These included:

(1) Correction for convergence error due to non-transverse irradiation.

(2) Spectral sensitivity of the photomultiplier tube.

(3) Optical density of the sample.

(4) Reflection loss.

(5) Change of intensity with temperature.

Up to this time, several workers had taken into account one or two of these corrections, but none had considered them all. Bernstein and Allen managed to evaluate standard intensities for the Raman bands of CH_2Cl_2, $CHCl_3$ and CCl_4.

In 1958, Yoshino and Bernstein[6] set up an experimental procedure for the measurement of Raman intensities of gases, and proposed a set of correction factors based on experimental and expected results.

This procedure was adapted in 1961 by Golden and Crawford[7] who set out to determine absolute gas-phase Raman intensities. For the measurement of absolute Raman intensities a standard is required whose intensity per molecule is known or can be calculated. One possibility for this is to measure the intensity ratio of the Raman and Rayleigh lines, and this is the method which was used by Yoshino and Bernstein.[6] For this it is necessary to subtract the background intensity of the evacuated tube and to use an absorption filter to weaken the Rayleigh line.

However, Golden and Crawford suggested an alternative method. As a standard they used the $J = 1 \rightarrow 3$ pure rotational transition of hydrogen ($\nu = 587\ cm^{-1}$), the line intensity of which can be determined. This is a much more straightforward method for routine experiments as it is independent of the level of background intensity and thus eliminates possible errors arising from the presence of the absorption filter.

In 1964, Schrotter and Bernstein[8] simplified the experimental procedure of Yoshino and Bernstein and adapted the apparatus for the investigation of vapours. They used the pure rotational $J = 1 \rightarrow 3$ line in hydrogen as an internal standard and measured the absolute Raman intensities of several organic compounds.

1.4 Theory of Raman Band Intensities

1.4.1 Molecular Polarisability Tensor

The extent of Raman scattering depends on the polarisability of the molecule.[1,2] When a molecule is placed in a static electric field it is distorted, the positively charged nuclei being attracted to the negative pole of the field, and the electrons to the positive pole. This separation of charges causes an induced dipole to be set up in the molecule and the molecule is said to be polarised.

The size of the induced dipole, μ, can be expressed as:

$$\mu = \alpha E$$

where E is the magnitude of the applied field and α is the polarisability tensor,

$$\alpha = \begin{bmatrix} \alpha_{xx} & \alpha_{xy} & \alpha_{xz} \\ \alpha_{yx} & \alpha_{yy} & \alpha_{yz} \\ \alpha_{zx} & \alpha_{zy} & \alpha_{zz} \end{bmatrix}$$

This polarisability tensor defines the creation of the electric dipole by the electric field. In general, the components of the two vectors are non-parallel. If the

molecular coordinate system is rotated, however, the tensor will change until at a certain position the induced dipole will be parallel to the inducing field, and α will take on a unique diagonal form:

$$\alpha = \begin{bmatrix} \alpha_1 & 0 & 0 \\ 0 & \alpha_2 & 0 \\ 0 & 0 & \alpha_3 \end{bmatrix}$$

The terms α_1, α_2 and α_3 are known as the principal polarisabilities.

In Raman spectroscopy there are two polarisability functions which are of particular interest:

(1) Mean polarisability, $\bar{\alpha}$

$$\bar{\alpha} = \tfrac{1}{3}(\alpha_{xx} + \alpha_{yy} + \alpha_{zz}) = \tfrac{1}{3}(\alpha_1 + \alpha_2 + \alpha_3)$$

(2) Anisotropy polarisability squared, γ^2

$$\gamma^2 = \tfrac{1}{2}[(\alpha_{xx} - \alpha_{yy})^2 + (\alpha_{yy} - \alpha_{zz})^2 + (\alpha_{zz} - \alpha_{xx})^2 + 6(\alpha_{xy}^2 + \alpha_{yz}^2 + \alpha_{zx}^2)]$$

$$= \tfrac{1}{2}[(\alpha_1 - \alpha_2)^2 + (\alpha_2 - \alpha_3)^2 + (\alpha_3 - \alpha_1)^2]$$

The anisotropy polarisability squared describes the way in which the molecular polarisability changes with orientation.

Both $\bar{\alpha}$ and γ^2 are rotational invariants and are therefore physically observable for a sample containing randomly orientated molecules. The mean values of the squares of the tensor elements for a molecule in an isotropic fluid can be expressed in terms of $\bar{\alpha}$ and γ^2 as follows:

$$\alpha_{xx}^2 = \alpha_{yy}^2 = \alpha_{zz}^2 = \frac{1}{45}(45\bar{\alpha}^2 + 4\gamma^2) \quad \text{(Equation 1.1)}$$

$$\alpha_{xy}^2 = \alpha_{yz}^2 = \alpha_{zx}^2 = \gamma^2/15 \quad \text{(Equation 1.2)}$$

1.4.2 Depolarisation Ratios

A laser is normally polarised in a plane perpendicular to the plane of propagation and when using laser excitation, one very useful easily measurable quantity which can be obtained from experiment is that of the depolarisation ratio, ρ.

The depolarisation ratio is defined as the ratio of the intensity of scattered light polarised in a plane perpendicular to the plane of polarisation of the incident light to the intensity of scattered light polarised in a plane parallel to this plane.

Consider the arrangement shown in Figure 1.5 where I is the intensity of radiation and the subscripts $_V$ and $_H$ represent the orientation of the plane of polarisation (where there are two subscripts the first refers to the incident radiation and the second to the scattered radiation):

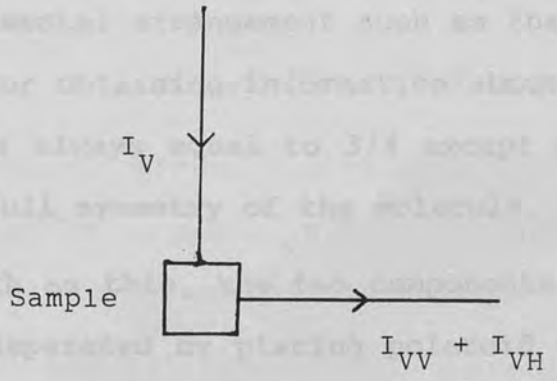

Figure 1.5: Directions of Planes of Polarisation of the Incident and Scattered Radiation

For a non-polarised source of radiation the scattered light would have the following components:

$$I_{VV},\ I_{HH},\ I_{VH} \text{ and } I_{HV}$$

Consider a fully symmetric transition of an isotropic molecule such as carbon tetrachloride. On reaching the sample, only light which is polarised in the vertical direction can be scattered at right angles to the direction of radiation. For this reason, I_{HH} will be dependent on the anisotropy of the molecule and will have an equivalent value to I_{VH} and I_{HV}.

The value of ρ for the optical arrangement in Figure 1.5 can be expressed as:

$$\rho = \frac{I_{VH}}{I_{VV}} = \frac{I_{yz}}{I_{yy}} \approx \frac{\mu_{yz}^2}{\mu_{yy}^2} = \frac{\alpha_{yz}^2 E_z^2}{\alpha_{yy}^2 E_y^2}$$

Therefore, using Equations 1.1 and 1.2:

$$\rho = \frac{(1/15)\gamma^2}{(1/45)(45\bar{\alpha}^2 + 4\gamma^2)} = \frac{3\gamma^2}{45\bar{\alpha}^2 + 4\gamma^2}$$

This is the normal expression for the depolarisation ratio for an experimental arrangement such as that shown, and it is very useful for obtaining information about the symmetry. The value of ρ is always equal to 3/4 except when the vibration retains the full symmetry of the molecule.

In a case such as this, the two components I_{VH} and I_{VV} would normally be separated by placing polaroid sheets between the sample and the analyser. In the work described in this thesis an alternative method was used for the determination of the

depolarisation ratios, using a Pockels cell. This method produces a slightly different expression for ρ and is described in more detail in Section 2.2.

1.4.3 Placzek's Molecular Polarisability Theory[9,10]

Placzek[11] showed that provided certain conditions are satisfied, Raman intensity can be expressed as a function of

$$(\nu_0, \nu_e)\left(\frac{\partial\alpha}{\partial Q}\right)^2$$

where ν_e = electronic frequency of the molecule

ν_0 = frequency of incident radiation

α = polarisability which is symmetric and real

Q = vibrational coordinate in the prescribed conditions

These conditions are:

(1) The vibrational frequency must be very much less than the exciting frequency which in turn must be very much less than any electronic excitation frequency of the molecule, or, in terms of the energies involved:

E_{elec}	>>	E_o	>>	E_{vib}
lowest electronic energy level		incident photon energy		vibrational energy level

(2) The electronic ground states must be non-degenerate.

(3) There must be no magnetic field present.

(4) The molecule must contain no unpaired electrons.

Conditions (3) and (4) ensure that the polarisability tensor is symmetric.

It is seen that these conditions are satisfied for the majority of molecules, and in such a situation the separate components of the polarisability tensor, α_{mn}, become molecular constants for any given transition from an initial state m to a final state n. The change in any component $\alpha_{\rho\sigma}$ on transferral of the molecule from one state to another can be given by:

$$(\alpha_{\rho\sigma})_{mn} = \int \psi_n^* \alpha_{\rho\sigma} \psi_m d\tau$$

where ψ_n^* = complex conjugate wavefunction of final state n

ψ_m = wavefunction of initial state state m

If $\alpha_{\rho\sigma}$ is expanded in a Taylor series, then the following is obtained:

$$(\alpha_{\rho\sigma})_{mn} = \int \psi_n^* \alpha_0 \psi_m d\tau + \sum_i (\partial\alpha/\partial Q_i) \int \psi_n^* Q_i \psi_m d\tau \quad \text{(Equation 1.3)}$$

where α_0 = static equilibrium molecular polarisability.

Q_i = normal vibrational coordinates for the ith vibration

The normal vibrational coordinates, Q, however, are very often used as a basis set, and in this situation Equation 1.3 can be simplified to:

$$(\alpha_{\rho\sigma})_{mn} = \alpha_0 \int \psi_n^* \psi_m d\tau + (\partial\alpha/\partial Q_i) \int \psi_n^* Q_i \psi_m d\tau \quad \text{(Equation 1.4)}$$

It has been shown that the first term on the right hand side of Equation 1.4 is related to Rayleigh scattering and the

second term to Raman scattering. The integral in the Rayleigh term is equal to zero by orthogonality unless n = m.

Two other established relationships are:

$$I = \frac{2^7\pi^5 I_0(\nu_0 + \nu)^4}{3^2c^4} \sum_{\rho\sigma} |(\alpha_{\rho\sigma})_{mn}|^2 \qquad \text{(Equation 1.5)}$$

and

$$\int \psi_n^* Q_i \psi_m d\tau = \sqrt{\frac{(n_i + 1)h}{8\pi^2\mu\nu}} \qquad \text{(Equation 1.6)}$$

where n_i is the lower vibrational quantum number.
μ is the reduced mass

Hence by substituting Equations 1.4 (considering only the second term) and 1.6 in Equation 1.5 we get

$$I = \frac{2^4\pi^3 I_0(\nu_0 + \nu)^4}{3^2c^4} \sum_i (\partial\alpha/\partial Q_i)^2 \frac{(n_i + 1)h}{\mu\nu} \qquad \text{(Equation 1.7)}$$

Thus we have an equation which gives the observed intensity of a Raman band.

In order to obtain an expression for the overall Raman effect it is necessary to sum over all the values of n; i.e. all vibrational energy levels must be taken into account. The population of each energy level is given by the Boltzmann factor

$$N = N_0 \exp(-nhc\bar{\nu}/kT)$$

where N = number of molecules per unit volume

N_0 = number of molecules per unit volume in the ground state.

It can be shown that the result of summing this over all values of n to obtain the total population is:

$$\Sigma N_0 \exp(-nhc\bar{\nu}/kT) = \frac{N_0}{1 - \exp(-hc\bar{\nu}/kT)}$$

Substituting into Equation 1.7, the total intensity of a Stokes band of frequency $(\nu_0 - \nu)$ is:

$$I = \frac{2^4\pi^3}{3^2c^4} \frac{hI_0N(\nu_0 - \nu)^4}{\mu\nu(1 - e^{-hc\bar{\nu}/kT})} \sum_{\rho\sigma}(\partial\alpha_{\rho\sigma}/\partial Q_i)^2 \qquad \text{(Equation 1.8)}$$

It can be seen from this expression that the intensity of a Raman band is

(a) directly proportional to $(\nu_0 - \nu)^4$

(b) inversely proportional to $\nu(1 - e^{-hc\bar{\nu}/kT})$

These two factors should therefore be taken into consideration when calculating absolute Raman intensities. However the 'ν' term in (b) arises from the mean square amplitude of vibration which is already accounted for in the programme for theoretical calculations (see Chapter 4). Therefore in order to facilitate comparison of experimentally observed intensities with those predicted theoretically this factor of ν was omitted from this second correction consideration.

1.4.4 Wolkenstein Bond Polarisability Theory

Wolkenstein's model is one in which the molecular polarisability gradient is broken down into bond contributions. The assumptions in this model are:

(1) The molecular polarisability is the sum of the atomic core polarisabilities (assumed spherical) and bond polarisabilities (assumed non-spherical). Since the wavelength of the exciting radiation is so large compared with the dimensions of the molecule it is assumed that the displacement of the centres of polarisabilties will have no effect on the overall polarisation. The molecular polarisability therefore reduces to a sum of several polarisability tensors, which are related to each other by rotation in space. Each polarisability tensor in its own natural coordinate system is diagonal with diagonal components being the principal polarisabilities, α_1, α_2 and α_3.

$$\begin{bmatrix} \alpha_1 & 0 & 0 \\ 0 & \alpha_2 & 0 \\ 0 & 0 & \alpha_3 \end{bmatrix}$$

To obtain the overall polarisability each tensor must be rotated to a common coordinate system. Corresponding elements can then be added to give the total polarisability.

(2) Each bond direction is defined as the principal axis of the polarisability tensor for that particular bond, whether it is in an equilibrium or deformed state.

(3) Deformation of one bond does not affect the bond polarisabilities and derivatives associated with any other bond.

(4) The bond polarisability derivatives are not changed by change in orientation, including angular deformation.

1.5 Raman Intensity Measurements in Liquids

In making a comparison between standard intensities in the gaseous and liquid phase it has been observed[8,12] that the intensity in the liquid is enhanced by a factor of between 1.5 and 3. This is because there are three effects which are present in liquids but which are not significant in gases. These are:

(a) The Optical Effect

(b) The Local Field Effect

(c) Intermolecular Interactions

(a) The Optical Effect

The optical effect arises from the fact that the light collection geometry is altered by refraction at the liquid-glass-air interface of the sample container.[13,14] The presence of this phenomenon and the need for a correction factor was first suggested by Woodward and George[15] in 1951, although they made no attempt to quantify the effect. In general the intensity of a band increases with the refractive index of the medium. This intensity change is especially significant when the light source is in the form of a cylindrical mercury arc arranged around the sample. It is much less of a problem when using laser excitation. If standard intensity measurements are to be made the best way to allow for this effect is to use an internal standard.[12] If an external standard is to be used then the refractive index of the standard and sample would not be the same and a correction factor would be required.

(b) <u>The Local Field Effect</u>

This arises from the dielectric nature of liquids. In the gaseous phase the molecules are free to rotate in space without restriction to orientation. This is not the case with liquids as in the liquid phase the influence of neighbouring molecules changes the electric field at the position of the molecule. The molecular polarisability can also be changed. Therefore it is the local field around a molecule and not the effective field in the medium which is responsible for the induced dipole moment which gives rise to Raman scattering.[14,16] Thus, if these two fields differ significantly then a local field correction must be applied. The correction factor which has been proven[13,17] to produce good agreement between gas and liquid data was put forward by Eckhardt and Wagner[18] and is given by:

$$L = \frac{n'}{n}\left(\frac{n^2 + 2}{3}\right)^2\left(\frac{n'^2 + 2}{3}\right)^2$$

where L = Local field correction

n = refractive index of liquid (or solution) at the wavelength of the incident radiation

n' = refractive index at wavelength of scattered radiation

When optical dispersion is small, as is usually the case, then $n' \approx n$ and the expression becomes

$$L = \left(\frac{n^2 + 2}{3}\right)^4$$

This implies that the scattering cross-section of a liquid is greater than the corresponding gas-phase cross-section by a factor equal to L. This theory assumes that the liquid is randomly orientated, non-associated and transparent to both the incident and scattered light. Since both Raman and Rayleigh scattering are affected to the same extent by the local field effect the correction is cancelled out in comparative measurements.

(c) Intermolecular Interactions

Intermolecular interactions[16] can affect the environment of a molecule and hence also the scattering cross-section. This effect has been observed by several workers. For example, Evans and Bernstein[19] saw two forbidden bands in the spectrum of carbon disulphide due to the interaction between the carbon atom of one molecule and the sulphur atom of another. These bands decreased in intensity on dilution.

Nestor and Lippincott[13] also noticed the effect. They used the local field corrections to compare liquid and gas phase intensities and found that agreement was good in all cases except in those of hydrogen bonded liquids. Thus, when such interactions are present, the change of intensity with concentration must be taken into consideration. In addition, variation of a solvent can affect the intensity of a Raman line. This is known as the solvent effect. It has been shown[20] that this is particularly significant when a solvent is present which has a strongly anisotropic molecular polarisability. In such a case a change in the molecular polarisability of the solute may be brought about.

1.6 A Brief Description of the Work Covered in this Thesis

The project had five main aims:

(1) To set up an experimental system for the accurate measurement of absolute Raman intensities.

(2) To measure the Raman band intensities of various thioethers and thiols and to evaluate the results in terms of possible quantitative applications.

(3) To establish the molecular parameters that would permit the prediction and analysis of the spectra of thioethers.

(4) To calculate theoretical Raman band intensities using a model based on the Wolkenstein assumptions.

(5) To carry out a brief study of the infra-red intensities of some thioethers.

The first stage was to adapt the existing instrumentation such that band intensities and depolarisation ratios could be measured accurately. This involved making certain additions to the system and necessitated calibration of the instrument for variation of efficiency with frequency. In addition to this was the development of the computer software used to accumulate and process the data. The chosen internal standard, carbon tetrachloride, was assessed for its suitability for use in this work.

Once established, the experimental system was used to determine the band intensities of five thioethers and two thiols. The results were compared and any trends observed were noted. Ethyl methyl sulphide was studied at various temperatures in an attempt to estimate the energy barrier between its two conformers.

To compare experimental results with predicted results, a Fortran programme was developed to calculate theoretical values for Raman band frequencies and intensities. An *ab initio* force field was calculated for the simplest molecule in the series, dimethyl sulphide, and a set of polarisability values was deduced from the experimental intensities. It is hoped that these parameters will transfer satisfactorily to larger molecules so that the programme can eventually be used to predict the spectrum of any molecule in the series which may be of interest. Some progress along these lines was made with ethyl methyl sulphide.

In addition to this work, preliminary investigations were made of the infra-red band intensities of several thioethers. Any emerging trend in the intensities across the series of compounds was noted and assessed for potential use in the prediction of the spectra of other molecules in the series.

CHAPTER 2

AN EXPERIMENTAL SYSTEM FOR THE MEASUREMENT OF ABSOLUTE RAMAN INTENSITIES

2. AN EXPERIMENTAL SYSTEM FOR THE MEASUREMENT OF ABSOLUTE RAMAN INTENSITIES

2.1 Instrumentation

Measurements were made using a Coderg PHO double monochromator, the signal passing through an RCA cooled (-30°C) gallium arsenide photomultiplier RCAC31034 into one channel of a Brookdeal SCI photon counting system. A Coherent model 52 2W argon ion laser was used as the radiating source.

To enable accurate measurements of absolute Raman band intensities to be made, it was necessary to adapt the existing spectroscopic system to satisfy the following criteria:

(1) Signal stabilities to better than 1%

(2) Accurate determination of depolarisation ratios

(3) Versatile software for data manipulation

(4) High efficiency through automation.

These requirements have led to several modifications to the instrument.

For the measurement of absolute Raman intensities it was also necessary to consider both the change in instrument efficiency and the variation of scattering intensity with frequency. These are described in Sections 2.3 and 2.4. Firstly, however, the instrument modifications will be described.

The first of these modifications was the introduction of a photocell. This photocell was placed in a position just prior to sample irradiation such that it could collect a small amount of laser radiation. The signal from the photocell was fed into the second channel of the photon counter. In this way a laser signal integration system could be used to control the counting period between grating steps as an alternative to fixed time signal counting, thus eliminating problems caused by small fluctuations in laser power.

A second addition to the instrument was that of a Pockels cell (Electro-Optics Developments Ltd., PC105), whose function was to allow accurate measurement of depolarisation ratios.

Figure 2.1 shows a schematic diagram of the apparatus.

2.2 Use of a Pockels Cell for the Measurement of Depolarisation Ratios

A Pockels cell is capable of rotating the plane of polarisation of a beam of radiation. This rotation is achieved by the application of a high voltage across the cell, the magnitude of which is directly proportional to the wavelength of the laser radiation. For 90° rotation the optimum voltage was found to be about 4200 volts at 514.5 nm. For stability the cell was maintained at $40^{o}C$ using a temperature control system (Electro-Optic Developments Ltd., TC15). (The theory of the Pockels cell is described briefly in Appendix A).

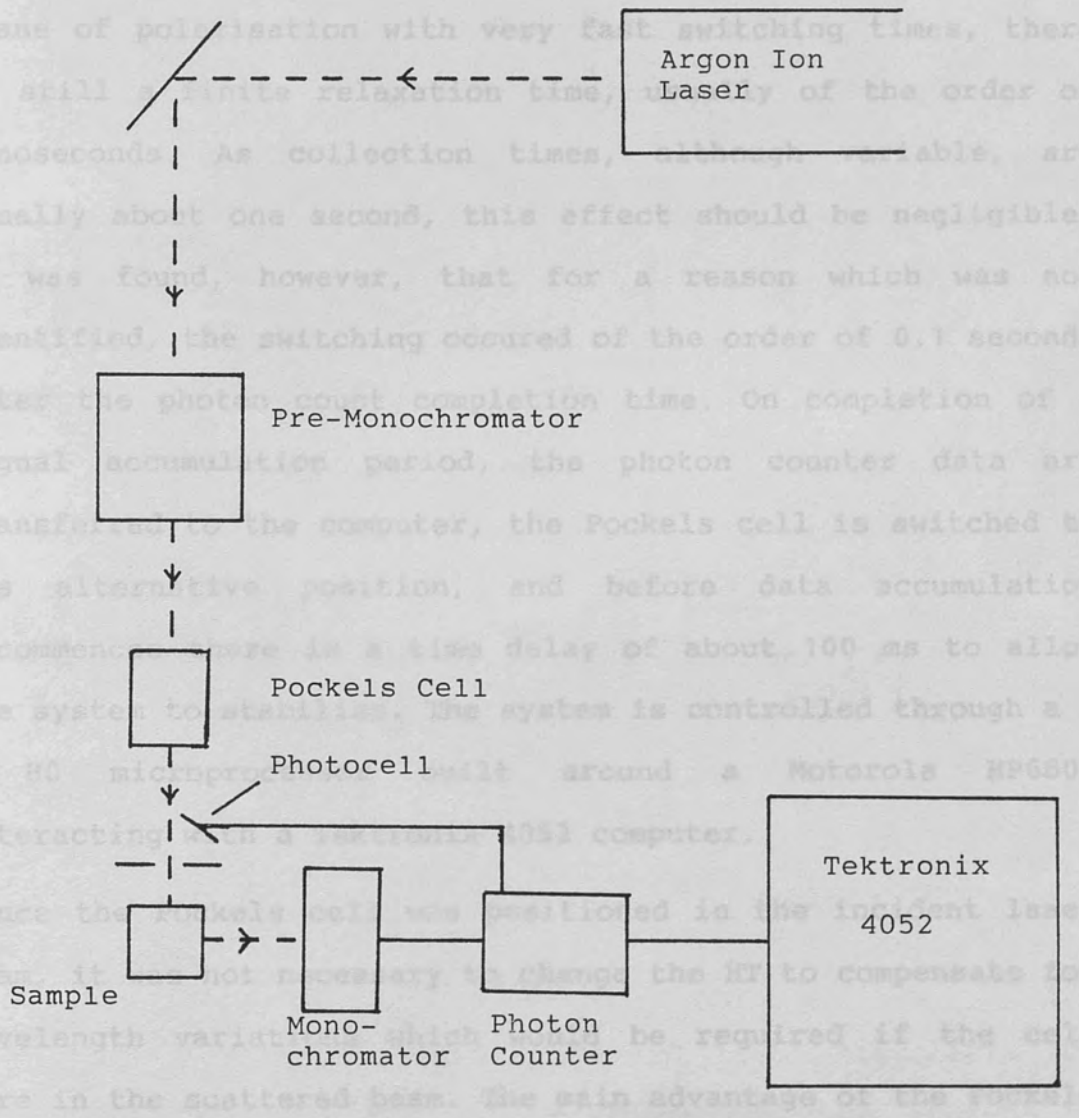

Figure 2.1: Schematic Diagram of Apparatus

The KDP Pockels cell was placed in the incident laser beam and, using an electronic valve switch to switch the operating voltage alternately to its maximum and minimum values for each grating step, it was possible to record the quantities I_{VV} and I_{VH} simultaneously.[20a]

Although the Pockels cell has the capability to rotate the plane of polarisation with very fast switching times, there is still a finite relaxation time, usually of the order of nanoseconds. As collection times, although variable, are usually about one second, this effect should be negligible. It was found, however, that for a reason which was not identified, the switching occured of the order of 0.1 seconds after the photon count completion time. On completion of a signal accumulation period, the photon counter data are transferred to the computer, the Pockels cell is switched to its alternative position, and before data accumulation recommences there is a time delay of about 100 ms to allow the system to stabilise. The system is controlled through a 2 x 80 microprocessor built around a Motorola HP6800 interacting with a Tektronix 4052 computer.

Since the Pockels cell was positioned in the incident laser beam, it was not necessary to change the HT to compensate for wavelength variations which would be required if the cell were in the scattered beam. The main advantage of the Pockels cell method over the polaroid sheet method (see Section 1.4.2) is that since no further analysers are required in the scattered beam the signal is increased by a factor of about 2. The polaroid sheet method also requires the laser power to remain constant throughout both scans. There is, however, a

slight change in the calculation of the depolarisation ratio with a Pockels cell. The maximum value now becomes 6/7 as opposed to the previous value of 3/4.

Consider in Figure 2.2 the usual 90° scattering geometry as described earlier.

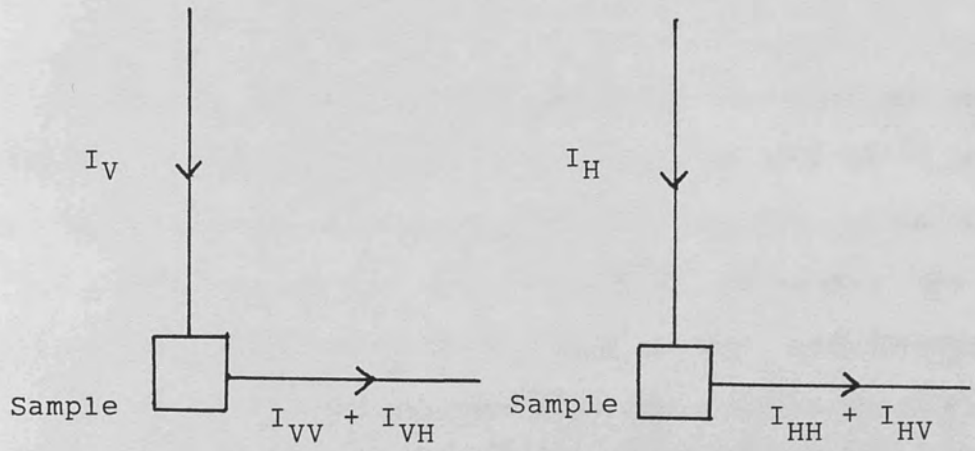

Figure 2.2: a) Pockels Cell Off b) Pockels Cell On

In Figure 2.2 a) the same scattered light components are present as in the polaroid sheet method, but instead of separating I_{VV} and I_{VH}, they are now measured collectively.

In Figure 2.2 b) the Pockels cell is on and the plane of polarisation of the incident radiation has been switched to the horizontal plane. The scattered light components are now I_{HH} and I_{HV} and these are again analysed collectively.

Using Equations 1.1 and 1.2 the depolarisation ratio, ρ, can be calculated.

$$\rho = \frac{I_{HH} + I_{HV}}{I_{VV} + I_{VH}} = \frac{(\gamma^2/15) + (\gamma^2/15)}{(45\bar{\alpha}^2 + 4\gamma^2)/45 + (\gamma^2/15)}$$

Therefore,

$$\rho = \frac{6\gamma^2}{45\bar{\alpha}^2 + 7\gamma^2}$$

Optimisation of the voltage settings was carried out using the carbon tetrachloride set of bands at 458 cm^{-1}. With this system ρ was measured as 0.035 (theoretical value should be zero). The origin of this residual intensity for the I_H arrangements was not apparent and optical realignment failed to reduce it. It was thought that this could be due to noise fluctuations in the power supply which was an old 1940s unit. The very fast Pockels cell response would transform these pulses into brief changes in the incident light polarisation. This value of 0.035 was therefore taken as a 'leakage'. For the bands at 219 cm^{-1} and 315 cm^{-1} the value 6/7 was achieved after allowing for the imperfection of the scrambler and optical transmission systems. Therefore spectra were thereafter corrected by a scaling factor as follows:

$$\text{corrected } \rho = \frac{[\rho_{(obs)} - 0.035]\rho_{315(true)}}{[\rho_{315(obs)} - 0.035]}$$

or

$$\text{corrected } \rho = \frac{\rho_{(obs)} - 0.035}{1.002} \qquad \text{(Equation 2.1)}$$

Equation 2.1 assumes that this discrepancy is linear over the whole range of depolarisation ratios. The mean value of ρ for depolarised bands was 0.894, the theoretical value being 0.857.

The linearity of the system was tested using measurements made on chloroform. The results are shown in Table 2.1 and it can be seen that the agreement with the literature values[21] for the liquid state is very good. For the 368 and 679 cm^{-1} A_1 bands agreement with the literature vapour phase results[22] is also good. The ratio for the 3020 cm^{-1} C-H stretch is increased in the liquid state as a result of hydrogen bonding.

Table 2.1: Comparison of Depolarisation Ratios of Chloroform as Measured with a Pockels Cell with Literature Values

$\bar{\nu}$	Depolarisation Ratio		
(cm^{-1})	Observed	Lit[21](liquid)[b]	Lit[22](vapour)[b]
263	0.868(15)[a]	0.857	
368	0.160(13)	0.130	0.130
670	0.022(8)	0.026	0.014
761	0.841(9)	0.857	
1219	0.862(22)	0.857	
3020	0.284(5)	0.280	0.182

a) Figures in brackets represent the coefficient of variation over three measurements

b) Values adjusted to correspond to maximum ρ value of 6/7 to allow direct comparison with Pockels cell results

The Raman spectrum of chloroform is shown in Appendix B.

2.3 Computer Programme for the Accumulation and Interpretation of Data

As mentioned previously, control of the spectrometer was accomplished from a Tektronix 4052 computer through a microprocessor. In order to improve the versatility and efficiency of the system, a programme was written to include options firstly on conditions for data collection, such as the choice to include polarisation measurements, and secondly on data manipulation. The menu driven options for data processing include:

(1) Background subtraction of a polynomial function in frequency.

(2) Plot over specified range.

(3) Alteration of maximum intensity.

(4) Correction for variation in instrument efficiency (see Section 2.4).

(5) Correction for variation of scattering intensity with frequency. Data points are scaled by the factor:

$$\frac{1 - \exp(-hc\bar{\nu}/kT)}{(\nu_0 - \nu)^4}$$

(6) Integration over specified range.

(7) Routine for the fitting to the sum of one or more damped Lorentzian contours. This includes integration of the bands, once fitted.

In processing a spectrum the data are first corrected for instrument efficiency and variation of intensity with frequency and the background is adjusted. Each band can then be integrated using one of two options.

(1) Integration over a specified range.

This method is a straightforward integration between two points, based on Simpson's Rule. It is most useful firstly where a band is very well separated from any other band and an accurate measurement can be made by integrating between the two points where the wings of the peak meet the baseline, and secondly where the bands are present in a group, too close to be separated. Intensities can then be calculated between band minima (see Figure 2.3).

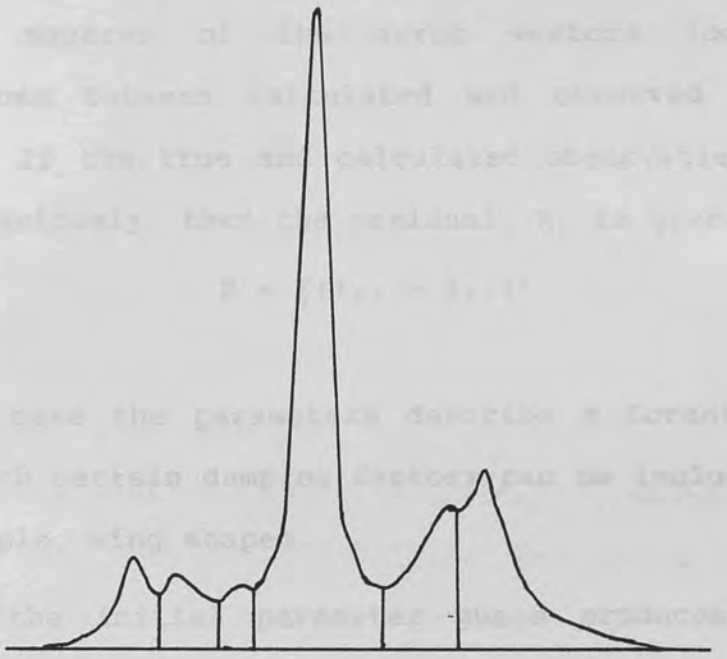

Figure 2.3: Integration between Band Minima

(2) Fitting to the sum of one or more damped Lorentzian band contours.

This routine was adapted for a spectral region containing 1, 2 or 3 bands which can be overlapping. An input of approximate dimensions for each band is required, plus certain damping factors, and from these is calculated the Lorentzian function which most closely fits the actual band

data. The individual band areas can then be calculated. The procedure is based on a least squares Jacobian method.

2.3.1 Routine for fitting to the sum of one or more damped Lorentzian band contours

Let the observables, in this case the spectral data points, be represented as a function of some parameters, p. The least squares problem is then to change the array p so that the sum of the squares of the error vectors (containing the differences between calculated and observed values) is a minimum. If the true and calculated observables are I_{ti} and I_{ci} respectively, then the residual, R, is given by:

$$R = \sum_i (I_{ci} - I_{ti})^2$$

In this case the parameters describe a Lorentzian function into which certain damping factors can be included to change, for example, wing shapes.

Suppose the initial parameter guess produces an array of calculated observables I^{o}_{ci}. Then it is necessary to know the parameter changes, Δp, which minimise R. The new calculated observable, I_{ci}, is given by:

$$I_{ci} = I^{0}_{ci} + \sum_j (\partial I_i / \partial p_j) \Delta p_j = I^{0}_{ci} + \sum_j J_{ij} \Delta p_j$$

where J_{ij} is the Jacobian matrix and defines the change of values of I_i with respect to p_j.

The residual, R, can therefore be expressed as:

$$R = \sum_i [(I_{ci}^0 - I_{ti}) + \sum_j J_{ij}\Delta p_j]^2$$

and

$$\partial R/\partial \Delta p_j = 2\sum_i\sum_j (I_{ci}^0 - I_{ti} + J_{ij}\Delta p_j)J_{ij} = 0 \quad \text{(Equation 2.3)}$$

Let $I_{ci}^0 - I_{ti}$ be written as the vector of errors, ϵ_i.

Equation 2.3 can then be expressed in matrix form.

$$\begin{bmatrix} J_{11} & J_{21} & .. & J_{i1} \\ J_{12} & J_{22} & .. & \\ . & & & \\ . & & & \\ J_{1j} & & & \end{bmatrix} \begin{bmatrix} \epsilon_1 \\ \epsilon_2 \\ . \\ . \\ \epsilon_i \end{bmatrix} = \begin{bmatrix} J_{11} & J_{21} & .. & J_{i1} \\ J_{12} & J_{22} & .. & \\ . & & & \\ . & & & \\ J_{1j} & & & \end{bmatrix} \begin{bmatrix} J_{11} & J_{12} & .. & J_{1j} \\ J_{21} & J_{22} & .. & \\ . & & & \\ . & & & \\ J_{i1} & & & \end{bmatrix} \begin{bmatrix} \Delta p_1 \\ \Delta p_2 \\ . \\ . \\ \Delta p_j \end{bmatrix}$$

or,

$$J^tE = (J^tJ)\Delta p \qquad \text{(Equation 2.4)}$$

It is often the case that not all observables are of equal reliability, and it may be necessary to weight the results. This is achieved by multiplying the error vector with a weighting matrix, W_i. W_i is a diagonal matrix with components equal to the weighting factor of each result. Equation 2.4 then becomes:

$$J^tWE = (J^tWJ)\Delta p$$

Provided that the set of linear equations is adequate to determine Δp, then the determinant of $J^tWJ \neq 0$ and the matrix may be inverted to give the optimum Δp as:

$$\Delta p = (J^tWJ)^{-1}J^tWE = c^{-1}J^tWE \qquad \text{(Equation 2.5)}$$

where $c = J^tWJ$

The programme goes through this routine three times, the second and third times using the new values of Δp calculated from the previous loop to form the initial guessed parameters.

2.4 Calibration of Spectrometer for Variation of Efficiency with Frequency

The efficiency of the spectrometer is known to change with frequency. Therefore, before making absolute band intensity measurements, it was necessary to monitor the instrument response over the frequency range of interest. This calibration was achieved using a standardised aged tungsten lamp, supplied by the National Physical Laboratory (NPL). Provided with the lamp was a set of tables giving the ratios of radiation intensity emitted by the lamp to radiation intensity emitted by a black body radiator for different wavelengths at various temperatures (obtained by running the lamp at specified currents and voltages).

Using this lamp it was possible to produce a polynomial equation in frequency which described the variation in instrument efficiency of light transmission relative to that of a black body radiator.

2.4.1 Experimental Procedure

The NPL calibrated tungsten lamp was used as a light source in place of the laser, and was situated in the sample compartment. In order to avoid interference from stray light the room was kept in darkness throughout the experiment.

Photon counter readings were taken manually from 21650 cm^{-1} to 12650 cm^{-1} at 50 cm^{-1} intervals. These readings were then fitted to a polynomial function in frequency using a computer programme written for the purpose (see Appendix C). From this function photon counter readings corresponding to the intermediate wavenumber values quoted in the NPL literature were calculated and hence the results could be adjusted to black body values using the correction factors provided. A second polynomial function in frequency was computed describing this efficiency variation and was added as an option to the data processing programme in the form of a correction factor.

Having completed the calibration it was necessary to test the system. To do this the Stokes and Antistokes intensities of the three main carbon tetrachloride bands were measured and their ratios compared with theory. The theoretical value of the Antistokes/Stokes ratio for any band can be found (after frequency correction) from:

$$\frac{I_{AS}}{I_S} = \exp(-hc\bar{\nu}/kT)$$

where I_{AS} = intensity of Antistokes band

I_S = intensity of Stokes band

The sample temperature was assumed to be 298K.

2.4.2 Results

Examples of intensity values obtained directly from the spectrometer at different frequency settings during the calibration can be seen in Table 2.2. In fitting results to a polynomial equation a reference frequency of 16000 cm^{-1} was chosen.

Table 2.2: Variation of Intensity Results with Frequency Observed During Calibration with NPL Calibrated Tungsten Lamp

Frequency (cm^{-1})	Observed Intensity	Frequency (cm^{-1})	Observed Intensity
12650	11026	17250	192488
12750	14612	17500	182888
13000	28052	17750	170684
13250	47734	18000	160648
13500	70110	18250	148452
13750	97290	18500	133504
14000	121492	18750	124326
14250	146212	19000	112916
14500	169374	19250	105128
14750	185056	19500	93936
15000	200950	19750	83624
15250	211700	20000	73964
15500	219244	20250	64458
15750	224928	20500	55332
16000	223884	20750	47526
16250	221342	21000	40258
16500	216438	21250	34606
16750	210074	21500	28632
17000	203052	21650	25834

Experimental conditions:

Slit = 8 cm^{-1}

Lamp set at current 0.661 A
voltage 1.458 V

Table 2.3: Adjustment of Black Body Radiation Intensities to take into Account Spectrometer Intensity Variation

λ (nm)	$\bar{\nu}$ (cm^{-1})	I_W (tungsten)	I_S	I_W/I_S x 10^6	$\frac{(I_W/I_S)_{\bar{\nu}}}{(I_W/I_S)_{16000cm^{-1}}}$
450	22222	15.65	10463	1495.75	1.236
460	21739	19.90	22160	898.01	0.742
470	21277	24.99	33684	741.90	0.613
480	20833	31.02	45845	676.63	0.559
490	20408	38.08	58946	646.01	0.534
500	20000	46.29	73085	633.37	0.523
510	19608	55.68	88146	631.68	0.522
520	19231	66.45	103890	639.62	0.528
530	18868	78.55	120007	654.55	0.541
540	18519	92.11	136099	676.79	0.559
550	18182	107.10	151852	705.29	0.583
560	17857	123.70	166859	741.34	0.613
570	17544	141.90	180735	785.13	0.649
580	17241	161.50	193206	835.90	0.691
590	16949	182.80	203900	896.52	0.741
600	16667	205.80	212567	968.17	0.800
610	16393	230.60	219000	1052.97	0.870
620	16129	257.00	222928	1152.84	0.953
630	15873	285.20	224204	1272.06	1.051
640	15625	315.20	222668	1415.56	1.170
610	16393	230.60	219174	1052.13	0.686
620	16129	257.00	222703	1154.00	0.952
630	15873	285.20	223972	1273.37	1.050
640	15625	315.20	222262	1418.15	1.190
650	15385	347.00	212270	1634.71	1.348
660	15152	380.10	208970	1818.92	1.500
670	14925	415.00	197520	2101.05	1.733
680	14706	451.10	183417	2459.42	2.028
690	14493	488.70	167055	2925.38	2.413
700	14286	527.30	149006	3538.78	2.919
710	14085	567.20	129898	4366.50	3.601
720	13889	608.50	110280	5517.77	4.551
730	13699	650.50	90907	7155.66	5.902
740	13514	692.90	72318	9581.29	7.902
750	13333	736.20	55039	13375.97	11.032
760	13158	780.10	39851	19575.42	16.145
770	12987	825.00	27126	30413.63	25.084

For the first polynomial fitting procedure the range was split into two and two functions were calculated. These were:

For the range 22222 cm^{-1} to 15625 cm^{-1}

$$I_S = 223909 - 5070v - 20160v^2 + 4105v^3 + 249v^4$$

(Equation 2.6)

and for the range 16393 cm^{-1} to 12987 cm^{-1}

$$I_S = 223676 - 5072v - 20414v^2 + 9496v^3 + 2830v^4$$

(Equation 2.7)

where I_S is the calculated photon counter reading and

$$v = \frac{\bar{\nu} - 16000}{1000}$$

At 16000 cm^{-1}, I_W, the ratio of the radiation intensity emitted by the lamp to the radiation intensity emitted by a black body radiator under the conditions used = 271.2.

From Equation 2.5, $I_W/I_S = 1210.31$

From Equation 2.6, $I_W/I_S = 1212.47$

I_W/I_S represents the ratio of the measured spectroscopic intensity to the black body radiation intensity.

The theoretical readings corresponding to the NPL tabulated frequencies, calculated from Equations 2.6 and 2.7, are shown in Table 2.3. It can be seen that for the region where the two functions overlap agreement between the calculated photon counter readings, I_S, is very good.

Let $I_W/I_S = I_C$

The polynomial function which the values of I_C fitted was found to be:

$$I_C = 1.04 - 0.44v + 0.12v^2 - 0.01v^3$$

$$v = \frac{\bar{\nu} - 16000}{1000}$$

where $\bar{\nu} = \bar{\nu}_0 - \bar{\nu}_{obs}$ for Stokes lines

$\bar{\nu} = \bar{\nu}_0 + \bar{\nu}_{obs}$ for Antistokes lines

$\bar{\nu}_0$ = frequency of incident radiation

This function was added as an efficiency correction option to the data processing programme. A plot of spectrometer efficiency versus wavelength is shown in Figure 2.4. The results for the carbon tetrachloride Antistokes/Stokes ratios are compared to calculated values in Table 2.4. It can be seen that agreement between theory and experiment is good. The theoretical values for T = 273K and 283K are shown for comparison.

Table 2.4: Comparison of Observed and Calculated Antistokes/Stokes Band Intensity Ratios (I_{AS}/I_S) for Carbon Tetrachloride

$\bar{\nu}$	Calculated I_{AS}/I_S			Observed I_{AS}/I_S (T = 298K)			
(cm^{-1})	T=273K	T=283K	T=298K	Run 1	Run 2	Run 3	Mean
219	0.3320	0.3350	0.3541	0.330	0.342	0.336	0.336
315	0.1900	0.2016	0.2175	0.210	0.213	0.210	0.211
458	0.0894	0.0974	0.1096	0.102	0.104	0.102	0.103

$I_{AS}/I_S = e^{-hc\bar{\nu}/kT}$

T = Absolute temperature

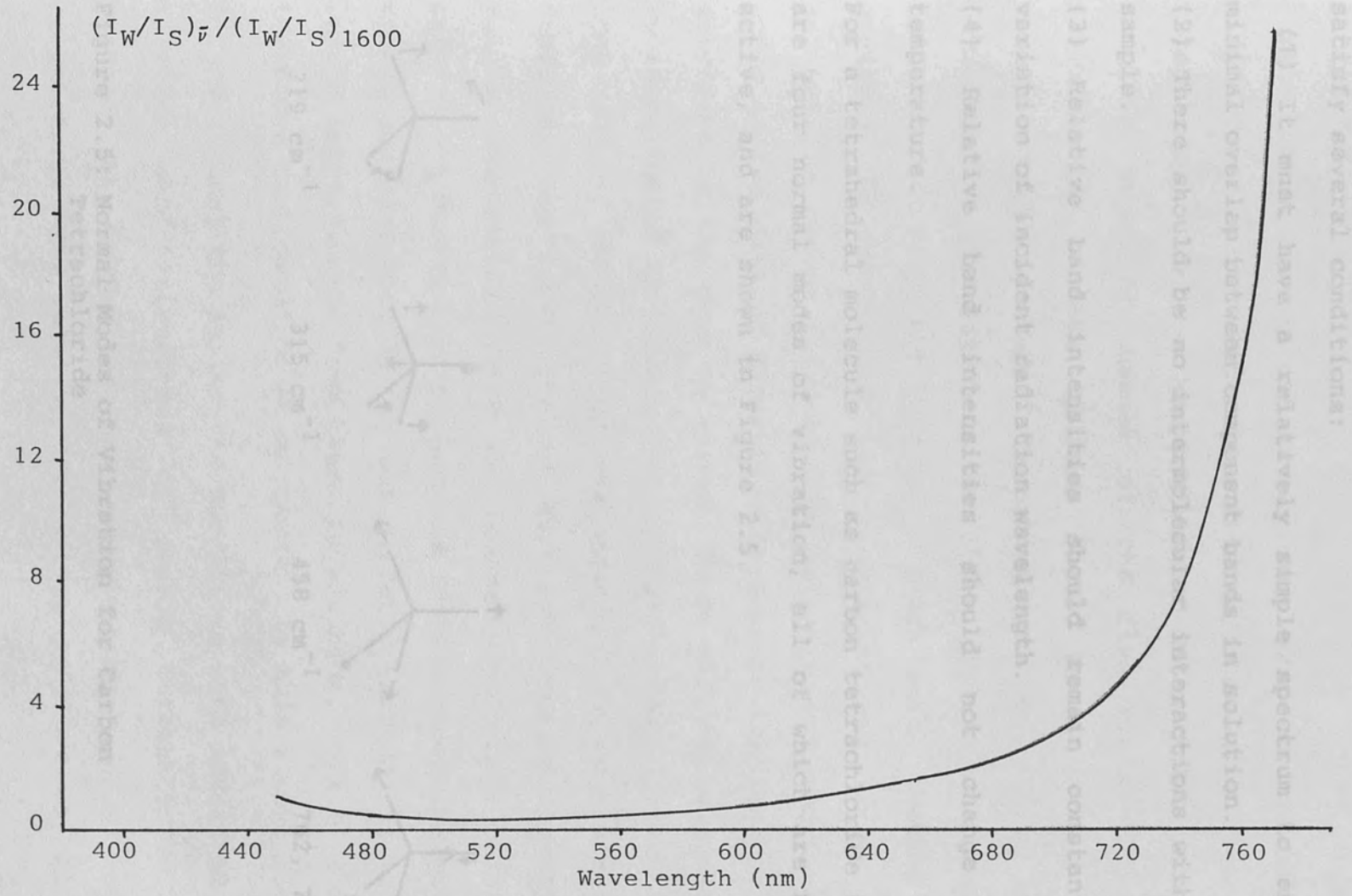

Figure 2.4: Graph to Show Variation of Spectrometer Efficiency with Wavelength

2.5 Assessment of Carbon Tetrachloride as an Internal Standard

To be a satisfactory internal standard a substance must satisfy several conditions:

(1) It must have a relatively simple spectrum to ensure minimal overlap between component bands in solution.

(2) There should be no intermolecular interactions with the sample.

(3) Relative band intensities should remain constant on variation of incident radiation wavelength.

(4) Relative band intensities should not change with temperature.

For a tetrahedral molecule such as carbon tetrachloride there are four normal modes of vibration, all of which are Raman active, and are shown in Figure 2.5.

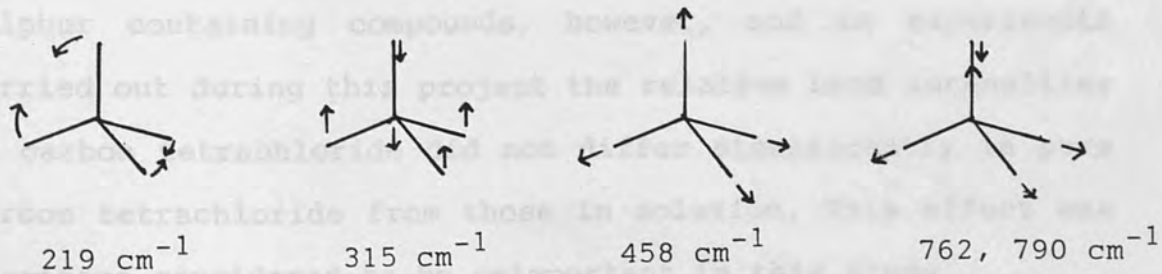

Figure 2.5: Normal Modes of Vibration for Carbon Tetrachloride

The Raman spectrum of carbon tetrachloride therefore contains just five bands, the positions of which are well documented.[5,21,23] An example of such a spectrum is shown in Figure 2.6.

Carbon tetrachloride has often been used as an internal standard in Raman intensity studies, mainly because the molecule has generally been considered to be inert. However, in 1968 intensity changes of the five bands of carbon tetrachloride on changing from 'inert' to electron-donating solvents were reported.[24] Donor solvents containing oxygen were found to have little or no effect, whereas with aromatic and amine donors, significant although small changes were observed. It was thought that complexing was taking place between the carbon tetrachloride molecule and either the π bonds in the case of aromatic molecules or the lone pair of electrons in the case of amines. Since all the molecules to be investigated in this project contain sulphur, which has a lone pair of electrons, it was important to consider these findings. The literature in question does not refer to sulphur containing compounds, however, and in experiments carried out during this project the relative band intensities of carbon tetrachloride did not differ significantly in pure carbon tetrachloride from those in solution. This effect was therefore considered to be unimportant in this study.

To ensure that the latter two conditions were satisfied, the relative band intensities of carbon tetrachloride were measured at several incident wavelengths and at various temperatures. The relative intensities of the bands at room

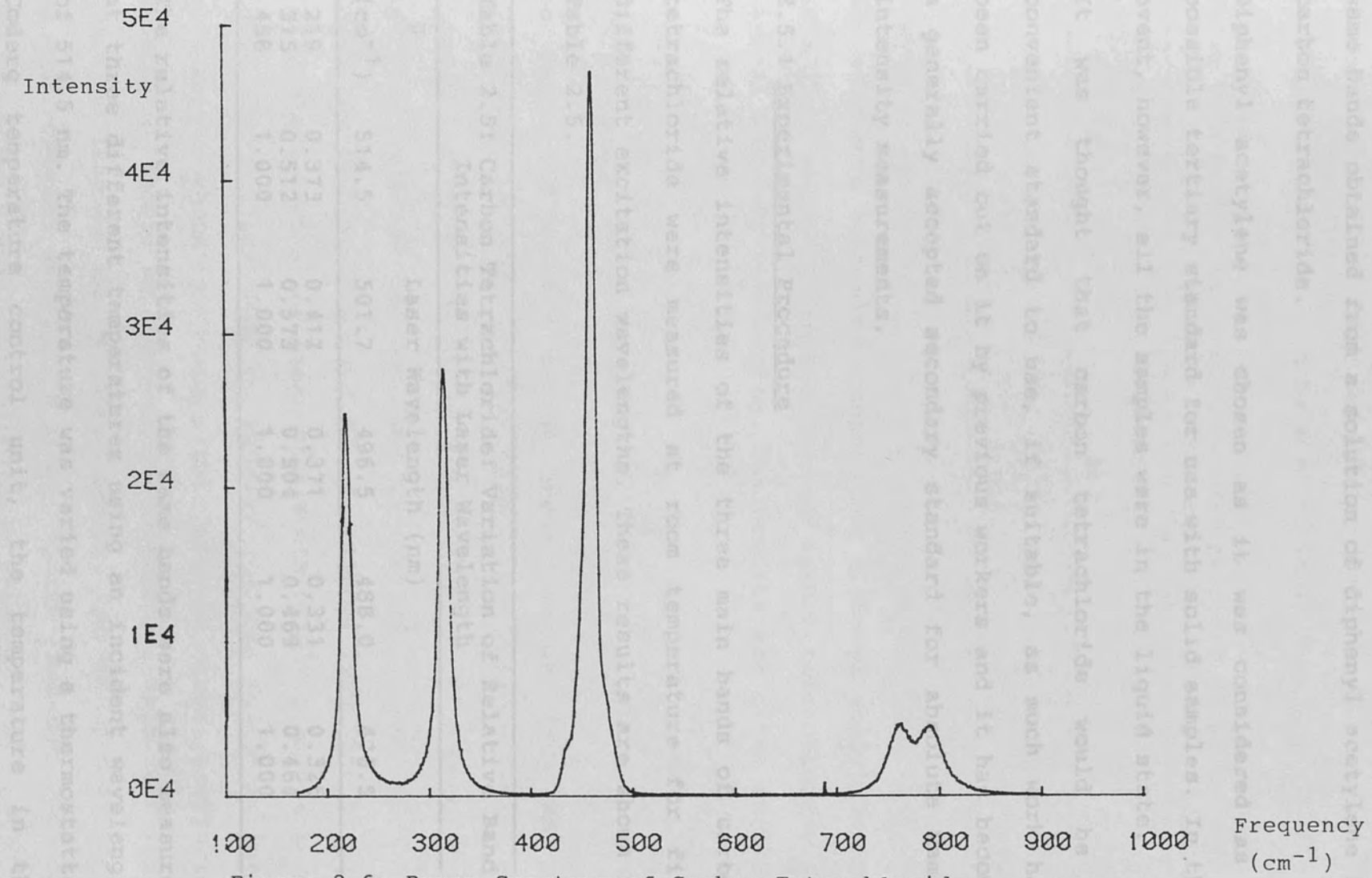

Figure 2.6: Raman Spectrum of Carbon Tetrachloride

temperature were also compared with the intensities of the same bands obtained from a solution of diphenyl acetylene in carbon tetrachloride.

Diphenyl acetylene was chosen as it was considered as a possible tertiary standard for use with solid samples. In the event, however, all the samples were in the liquid state.

It was thought that carbon tetrachloride would be a convenient standard to use, if suitable, as much work has been carried out on it by previous workers and it has become a generally accepted secondary standard for absolute Raman intensity measurements.

2.5.1 Experimental Procedure

The relative intensities of the three main bands of carbon tetrachloride were measured at room temperature for five different excitation wavelengths. These results are shown in Table 2.5.

Table 2.5: Carbon Tetrachloride: Variation of Relative Band Intensities with Laser Wavelength

$\bar{\nu}$	Laser Wavelength (nm)				
(cm^{-1})	514.5	501.7	496.5	488.0	476.5
219	0.373	0.412	0.371	0.331	0.326
315	0.512	0.573	0.504	0.469	0.464
458	1.000	1.000	1.000	1.000	1.000

The relative intensities of the same bands were also measured at three different temperatures using an incident wavelength of 514.5 nm. The temperature was varied using a thermostatted Coderg temperature control unit, the temperature in the

sample cell being monitored using a Keithley digital thermometer fitted with a remote temperature probe. The resulting intensities can be seen in Table 2.6.

Table 2.6: Carbon Tetrachloride: Variation of Relative Band Intensities with Temperature

$\bar{\nu}$ (cm^{-1})	Temperature (^{o}C) -10	20	61.5
219	0.405	0.436	0.420
315	0.560	0.617	0.577
458	1.000	1.000	1.000

Raman spectra were also obtained for diphenyl acetylene both as a pure solid and in solution in carbon tetrachloride for several incident wavelengths. The results are given in Table 2.7.

2.5.2 Results

In Table 2.5 a very slight trend can be seen. As the wavelength of the incident radiation gets shorter the intensities of the bands at 219 and 315 cm^{-1} both tend to decrease relative to the band at 458 cm^{-1}. However, this variation is very small and not considered important in this work, where a constant laser wavelength of 514.5 nm was to be used. The results show an anomaly for the 501.7 nm laser wavelength which suggests that perhaps this particular experiment should be repeated at some future date. The argon 501.7 nm line is fairly weak, however, and so is not likely to be chosen as a radiating source because of the correspondingly weak spectra which it produces.

Table 2.7: Relative Raman Band Intensities for Diphenyl Acetylene, Neat and in Carbon Tetrachloride Solution

	$\bar{\nu}$	Excitation Wavelength (nm)				
	(cm^{-1})	514.5	501.7	496.5	488.0	476.5
Diphenyl Acetylene neat	386	0.09	0.09	0.10	0.06	0.09
	539	0.16	0.15	0.17	0.13	0.16
	625	0.04	0.04	0.04	0.03	0.04
	997	1.00	1.00	1.00	1.00	1.00
	1141	2.32	2.19	2.16	2.30	2.50
	1482	0.28	0.21	0.25	0.31	0.35
	1593	3.34	2.86	3.11	3.91	4.39
	2222	8.48	6.64	6.68	10.48	10.99
Diphenyl Acetylene in CCl_4 solution	386	0.04	0.03	0.04	0.03	0.02
	539	0.12	0.14	0.08	0.11	0.11
	625	0.05	0.04	0.02	0.03	0.03
	997	1.00	1.00	1.00	1.00	1.00
	1141	1.97	1.92	1.94	1.98	2.08
	1482	0.24	0.22	0.21	0.27	0.29
	1593	2.59	2.37	2.38	2.93	3.25
	2222	7.32	6.00	6.03	7.87	7.72
Solvent bands (CCl_4)	219	0.41	0.41	0.32	0.29	0.29
	315	0.58	0.58	0.43	0.42	0.43
	458	1.00	1.00	1.00	1.00	1.00

In Table 2.6 the relative carbon tetrachloride band intensities do not appear to change significantly with temperature. Thus, studies involving temperature variation can be made without the development of standard intensity problems.

Considering all the information available about the nature and behaviour of its Raman bands, it was concluded that carbon tetrachloride would be a convenient and suitable standard for use in the studies to be carried out during the course of this project.

It was thought that diphenyl acetylene might be suitable as a tertiary standard if for some reason carbon tetrachloride could not be used, for example, in the solid state. The main disadvantage of diphenyl acetylene is that its spectrum contains more bands than ideally required, increasing the possibility of sample/standard band interference.

CHAPTER 3

RAMAN BAND INTENSITY MEASUREMENTS OF THIOETHERS AND THIOLS

3. RAMAN BAND INTENSITY MEASUREMENTS OF THIOETHERS AND THIOLS

3.1 Introduction

Raman spectroscopy is potentially useful for the analysis of thioethers and thiols because of the intense bands which result from the carbon-sulphur stretching motion. This could allow easy detection of such compounds in a mixture containing several different types of hydrocarbon.

A study of two thiols and five thioethers was carried out. The band frequencies and intensities of each were measured and examined in an attempt to identify some of the factors which determine them.

The molecules studied were dimethyl sulphide, ethyl methyl sulphide, diethyl sulphide, methyl n-propyl sulphide, dimethyl sulphide-d6, ethane thiol and t-butane thiol.

For ethyl methyl sulphide additional experiments were carried out to explore the change of the relative intensities of the bands in the carbon-sulphur stretching region with temperature. It was hoped that these would lead to information about the change in conformation about the carbon-sulphur bond with temperature.

3.2 Experimental Procedure

All experiments were carried out using the experimental system described in Chapter 2. Power at the sample was on average about 100 mW and 90° illumination was used. Since initially the photocell was in a developmental stage it was

not used. Great care was taken to ensure that the laser power remained constant throughout each experiment.

The raw data were stored on disk and then corrected for spectroscopic efficiency, as described in Section 2.4.2, and by the following correction factor:

$$\frac{1 - \exp(-hc\bar{\nu}/kT)}{(\nu_0 - \nu)^4}$$

where ν_0 = frequency of incident radiation

$\nu_0 - \nu$ = frequency shift of band centre from ν_0

T = temperature (K)

h = Planck's constant

k = Boltzmann constant

c = velocity of light

A background correction was also caried out.

For all samples the scattering intensities were measured at room temperature. These measurements were made using the band fitting procedure described in Section 2.3.1. Where complex groups of bands were present such that it was impossible to determine the exact positions, shapes and numbers of individual bands, for example, in the C-H stretch region, integrals were evaluated over ranges between frequencies at which intensity minima occured.

Since the interest in this work was in absolute Raman band intensities, it was necessary to express all the band intensities of the compounds studied relative to a standard band, the 458 cm^{-1} band of carbon tetrachloride. In order to do this, avoiding the problem of overlapping bands from two solution constituents, the following procedure was adopted.

The pure liquids were studied first, the band intensities being expressed relative to a strong, well defined band in the spectrum, usually the major C-S stretching band. Solutions of each sample in carbon tetrachloride were then prepared and the intensity of the reference band in the pure sample was measured relative to the 458 cm^{-1} band of carbon tetrachloride. The intensities of the remaining bands in the first spectrum could then also be expressed relative to this band.

For each compound several consecutive intensity measurements were made and the mean was calculated. For the carbon tetrachloride solution measurements an average of three scans each of at least three solutions was used. No evidence was found to suggest change in relative intensities for any compound on mixing with carbon tetrachloride.

To convert the relative Raman intensities to an absolute scale a value of 22.5 $cm^4\ g^{-1}$ for the 458 cm^{-1} band of carbon tetrachloride could be taken for the absolute intensity of the 458 cm^{-1} band of carbon tetrachloride.[4] However, in this thesis, to simplify analysis of the results, all band intensities have been reported relative to the carbon tetrachloride 458 cm^{-1} band. These band intensities, as measured with the Pockels cell 'off', refer to the quantity $45\bar{\alpha}^2 + 7\gamma^2$.

Depolarisation ratios were also obtained, using the Pockels cell method.

The ethyl methyl sulphide conformational studies were performed by varying the temperature of the sample.

Temperatures of -11, 18.4, 42.5, 54.5, 70, 80 and 90°C were used. For this a Coderg temperature controller unit was employed, with a Keithley digital thermometer with a remote probe to monitor the exact temperature in the cell (see Figure 3.1).

For measurement each sample was placed in a clear 1 cm diameter glass vial. Due to the high volatility of these compounds it was important to keep the vial tightly sealed at all times. For the temperature variation studies a sealed 0.5 cm diameter glass ampoule was used.

Solutions in carbon tetrachloride were made up by weight keeping both components in ice water throughout the process. The sulphur containing compound was the last component added in each case, the vial being sealed tightly immediately after the addition. Relative band intensities were expressed based on a 1:1 molar ratio of the two solution constituents.

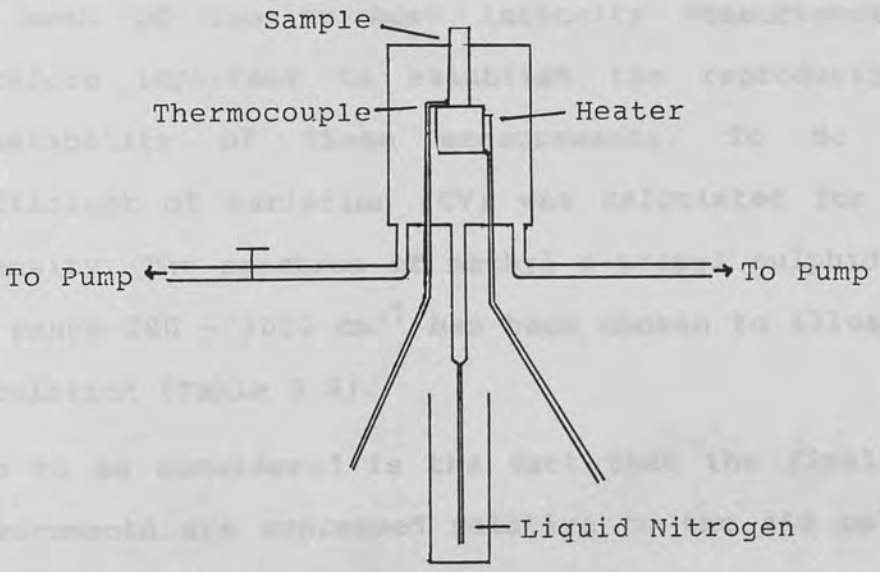

Figure 3.1: Coderg Temperature Controller Unit

All samples were used as supplied by the manufacturer without further purification, except for t-butane thiol which was distilled under vacuum at room temperature before use.

3.3 Results

The Raman spectra obtained from the series of thiols and thioethers listed in Section 3.1 are shown in Appendix D. All these spectra have been corrected as described above.

The frequencies and intensities of the observed bands are presented in Table 3.1. All intensities are expressed relative to the 458 cm^{-1} band of carbon tetrachloride (I_{458} = 100). Also shown are the depolarisation ratios, calculated and corrected as described in Chapter 2.

3.3.1 Estimation of Experimental Error

As mentioned previously, all band intensities reported are the mean of two or more intensity measurements. It is therefore important to establish the reproducibility and repeatability of these measurements. To do this the coefficient of variation (CV) was calculated for each band intensity. The spectrum of methyl n-propyl sulphide covering the range 200 - 1050 cm^{-1} has been chosen to illustrate this calculation (Table 3.2).

Also to be considered is the fact that the final intensity measurements are expressed relative to the 458 cm^{-1} band of carbon tetrachloride. To do this at least three scans of each of three separate solutions of each sample in carbon

Table 3.1 Raman Band Intensities (I) and Depolarisation Ratios (ρ) for Thioethers and Thiols

CH_3SCH_3			CD_3SCD_3			$CH_3SC_2H_5$			$C_2H_5SC_2H_5$			$CH_3S(n\text{-}C_3H_7)$			$(t\text{-}C_4H_9)SH$			C_2H_5SH			Assignment
$\tilde{\nu}$	I	ρ	$\tilde{\nu}$	I	ρ	$\tilde{\nu}$	I	ρ	$\tilde{\nu}$	I	ρ	$\tilde{\nu}$	I	ρ	$\tilde{\nu}$	I	ρ	$\tilde{\nu}$	I	ρ	
						223	4.4	0.74				241	4.3	0.00	241	4.6	0.70				
282	21.4	0.82	247	14.9	0.86	274	6.9	0.07	262	1.7	0.39	291	4.9	0.49							CSC/CCS
									309	7.9	0.19	316	4.2	0.48	329	4.1	0.72	334	12.2	0.37	
									337	8.5	0.38										
						355	12.8	0.61				356	2.0	0.24							
									385	8.3	0.61	380	5.2	0.31	380	10.5	0.68				
															411	1.6	0.38				
												430	4.8	0.47	432	0.6	-				
															454	6.1	0.39				
												511	0.5	0.21	520	1.3	0.21				
												563	0.2	0.10							
									641	21.4	0.12	647	13.6	0.21	621	33.0	0.44				
						658	38.6	0.35	658	27.8	0.13	669	6.3	0.43	665	5.3	0.48	660	68.9	0.25	
693	72.8	0.20	642	52.3	0.18	682	16.1	0.47	694	22.3	0.72	699	15.4	0.24	685	8.9	0.47				CS str
744	24.1	0.85	707	17.8	0.85	729	26.9	0.75	766	1.4	0.21	724	17.0	0.44	711	1.5	0.38	734	8.5	0.53	
												749	8.6	0.80							
												785	5.3	0.44	791	4.3	0.54				
			822	3.0	0.32							831	1.5	0.78	843	12.7	0.74				
												851	1.4	0.77	866	7.4	0.38	872	9.2	0.57	
												888	3.0	0.54							
												898	2.3	0.47							
						975	12.6	0.88	976	15.9	0.87	959	1.0	0.58	956	5.0	0.85	975	6.4	0.86	
															991	4.6	0.71				
									1004	1.5	0.61	1032	8.9	0.71							
									1021	6.5	0.52	1019	3.5	0.65							
									1039									1051	7.6	0.39	
						1050	5.5	0.49	1048	10.5	0.25	1093	3.6	0.57	1073	6.3	0.68	1093	8.8	0.40	
						1070	5.3	0.41	1075	6.2	0.39				1107	6.7	0.65				
												1214	0.8	0.58	1155	2.4	0.68				
												1245	1.7	0.60	1229	5.4	0.62				
						1244	3.0	0.74	1253	3.7	0.82				1267	1.6	0.67	1272	6.6	0.51	
						1269	2.8	0.41	1271	4.3	0.25	1292	3.2	0.75	1281	1.5	0.68				
															1299	3.6	0.71				
												1323	2.5	0.66	1319	1.3	0.70				
1333	1.9	0.48	1025	10.4	0.28	1324	1.5	0.83							1343	2.4	0.72				
									1379	2.6	0.70				1378	1.3	0.54				
1424	11.0	0.91	1044	13.2	0.00	1430	11.7	0.79	1431	12.7	0.83	1431	14.1	0.93							
1444	19.3	0.91				1450	23.9	0.93	1453	29.1	0.84	1443	21.3	0.98	1451	28.8	0.67	1450	83.9	0.17	
															2573	125.5	0.48	2571	173.7	0.24	SH str
															2685	7.6	0.62				
			1998	11.2	0.09	2728	4.5	0.32	2733	15.0	0.51	2735	7.2	0.43	2731	17.3	0.47	2733	11.4	0.00	$S\text{-}CH_2$ str
2834	28.6	0.00	2037	8.1	0.04	2836	19.7	0.35				2829	12.8	0.53							$S\text{-}CH_3$ str
2854	45.3	0.00	2085	21.3	0.07	2854	18.7	0.36				2847	289.4	0.01							
						2876	42.6	0.32	2875	196.5	0.44	2876	94.1	0.41	2877	383.9	0.40	2873	90.1	0.16	CH_3 sym str
															2905	133.1	0.48				
2914	240.4	0.19	2126	115.0	0.03	2915	163.8	0.32				2918	241.6	0.47							SCH_3 str
						2929	114.3	0.48	2932	522.4	0.53	2936	85.6	0.61	2923	160.5	0.45				SCH_2 str
																		2929	297.1	0.24	
2970	68.9	0.83							2964	165.1	0.85	2970	56.4	0.84	2964	129.0	0.75				
2987	86.7	0.87	2240	74.7	0.87	2967	138.3	0.86				2986	68.6	0.90							SCH_3 antisym str

tetrachloride were obtained. The result for each compound is therefore the mean of at least nine different measurements.

In Table 3.3 the mean band intensity value relative to the 458 cm^{-1} band of carbon tetrachloride is given for each solution for all the samples studied. The CV between solutions for each sample was calculated.

Table 3.4 gives the CVs between scans for each individual solution of methyl n-propyl sulphide.

The overall experimental error includes the repeatability of intensity measurements and the error arising from the preparation of the solutions.

From Table 3.2 it can be seen that the errors, expressed as CVs, range from 0.8% to 31.2%, the mean CV being 8.8%. In general the large errors arise from small intensity measurements.

The mean CV between separate solutions is 6.3% and between separate scans of an individual solution, 2.0%

In order to estimate the overall experimental error it is necessary to combine the errors from these three sources. The procedure is as follows:[25]

$$\text{Overall error} = (CV_1^2 + CV_2^2 + CV_3^2)^{1/2}$$
$$= (8.8^2 + 6.3^2 + 2^2)^{1/2}$$
$$= 11\%$$

where CV_1 = mean experimental intensity measurement error for pure sample

CV_2 = mean experimental intensity measurement error for chosen sample band relative to 458 cm^{-1} band in solution

CV_3 = mean error arising from preparation of sample solution in carbon tetrachloride

Table 3.2: Calculation of Experimental Error for Methyl n-Propyl Sulphide

ν	Relative Intensity (I_{647} = 100)				CV
(cm^{-1})	Run 1	Run 2	Run 3	Mean	(%)
241	33.9	27.1	33.2	31.4	11.9
291	39.2	32.0	36.5	35.9	10.1
316	33.9	28.6	29.4	30.6	9.3
356	16.4	13.9	14.2	14.8	9.2
380	40.4	39.1	35.4	38.3	6.8
430	12.9	11.6	11.1	11.9	7.8
511	3.6	4.2	3.8	3.9	7.9
563	1.8	1.0	1.2	1.3	31.2
647	100.0	100.0	100.0	100.0	-
669	46.6	48.7	44.9	46.7	4.1
699	114.6	111.3	113.2	113.0	1.5
724	125.3	126.3	124.2	125.3	0.8
749	61.7	64.0	63.6	63.1	1.9
785	37.6	39.0	-	38.3	2.6
831	11.3	9.4	11.5	10.7	10.8
851	11.6	10.3	10.0	10.6	8.0
888	23.4	20.4	23.4	22.4	7.7
898	15.1	19.3	17.3	17.2	12.2
959	9.2	6.4	6.7	7.4	20.7
1032	63.1	65.9	66.5	65.2	2.8

Mean CV = 8.8%

Table 3.3: Relative Band Intensities for Solutions of Thioethers and Thiols in Carbon Tetrachloride

Compound	$\bar{\nu}$ (cm^{-1})	$I_{\bar{\nu}}/I_{458}$ (mean)* Soln 1	Soln 2	Soln 3	Overall Mean	CV (%)
Dimethyl Sulphide	693	70.4	79.0	68.9	72.8	7.5
Dimethyl Sulphide-d6	642	51.7	56.8	48.4	52.3	8.1
Ethyl Methyl Sulphide	658	37.8	39.5	38.6	38.6	2.2
Diethyl Sulphide	641	23.7	22.5	18.1	21.4	13.8
Methyl Propyl Sulphide	647	14.0	13.3	13.5	13.6	2.4
t-Butane Thiol	621	35.5	33.1	30.5	33.0	7.6
Ethane Thiol	660	66.9	69.4	70.4	68.9	2.6

* Expressed relative to I_{458} = 100
Mean CV = 6.3%

Table 3.4: Calculation of CV Between Individual Intensity Measurements for Methyl n-Propyl Sulphide in Carbon Tetrachloride Solution

Solution No.	647 cm^{-1} Band Intensity (I_{458} = 100) Scan 1	Scan 2	Scan 3	CV (%)
1	32.2	32.1	32.2	0.2
2	29.7	31.2	31.2	2.8
3	31.0	30.0	31.9	3.1

Mean CV = 2.0%

3.3.2 Interpretation of Results

From the data shown in Table 3.1 it can be seen that the Raman spectra of thiols feature four main groups of bands in the following regions:

(1) 200 - 500 cm^{-1} (C-S-C bend/torsion)

(2) 590 - 750 cm^{-1} (C-S stretch)

(3) 1300 - 1450 cm^{-1} (C-H bend)

(4) 2500 - 3000 cm^{-1} (C-H stretch)

Spectra for the thiols show similar groupings of bands except that there are no C-S-C bending modes, but bands due to S-H stretching are observed at approximately 2570 cm^{-1} and due to C-S-H bending at approximately 330 cm^{-1}.

Several workers have studied the Raman spectra of thioethers and thiols.[26-32] The band frequencies observed here agree very well with those reported in the literature. Tables 3.5 and 3.6 show comparisons between experimental and literature band frequencies for dimethyl sulphide and ethyl methyl sulphide respectively.

Where band intensites have been reported in the literature they have been denoted simply as strong or weak etc.

Table 3.5: Comparison of Observed and Literature Raman Band Frequencies for Dimethyl Sulphide

Observed (This work)	Allkins[34]	Fonteyne[35]	Geisler[36]	Tentative Assignment
282	284	285	282	C-S-C bend
		480		
693	691	690	691	C-S sym str
744	742	742	744	C-S antisym str
		919		
	1032	1041		CH_3 rock
		1224		
1333	1331	1325	1326	CH_3 sym def
1424	1428	1426	1419	CH_3 antisym def
1444	1443		1436	CH_3 antisym def
		1609		
2834	2832	2832	2832	C-H str
2854	2854		2864	C-H str
2914	2916	2911	2908	C-H str
2970	2966		2962	C-H str
2987	2982	2980	2981	C-H str

3.3.2.1 C-S Stretching Bands

The bands due to the C-S stretching motions appear in the region 590-750 cm^{-1}. In the spectrum of dimethyl sulphide there are just two bands in this region, at 744 cm^{-1} due to the antisymmetric C-S-C stretch and at 693 cm^{-1} due to the symmetric C-S-C stretch. As the alkyl groups attached to sulphur become larger, more bands appear in this region because of the increased number of conformational isomers which are possible.

It has been reported[33] that for a series of linear methyl alkyl sulphides the position of the band due to the antisymmetric C-S-C stretch of the *trans* conformer is constant at 720$\pm$1 cm^{-1} for alkyl groups containing five or more carbon atoms. Thus for an unknown substance a band at

Table 3.6: Comparison of Observed and Literature Raman Band Frequencies for Ethyl Methyl Sulphide

Observed (This work)	Hayashi[37]	Sakakibara[38]	Assignments[37,38]
223	218	211	CSC skeletal def (T)
		232	CC tors, CSC bend (G)
274	266	273	CSC skel def (G^{37})(G,T^{38})
355	352	353	CCS skel def (G,T)
658	650	653	S-CH_2 str (G,T^{37})(G^{38})
682	675	678	S-CH_2 str (G^{37})(T^{38})
728	723	725	S-CH_3 str (T^{37})(G,T^{38})
	754	758	CH_2 rock (T^{37})(G^{38})
		785	CH_2 rock (G^{37})(T^{38})
		948	CH_3 rock (G)
		955	CH_3 rock (T)
		960	CH_3 rock (G,T)
975	975	973	C-C str (G,T^{37})(T^{38})
		982	C-C str (G^{38})
1050		1044	CH_3 rock (G,T)
	1058	1060	CH_3 rock
1070	1080	1065	CH_3 rock
1244		1251	CH_2 twist
1269	1260	1267	CH_2 wag
1324	1312	1320	CH_3 sym def
		1377	CH_3 sym def
1430	1416	1427	CH_3 def, CH_2 bend
		1444	CH_3 def
1450	1453	1455	CH_3 degenerate def
2728		CH str	CH str
2836		freq not	CH str
2854		reported	CH str
2876			CH str
2915	2907		CH str
2922	2929		CH str
2967	2958		CH str
	2980		CH str

this position could be a useful indicator of the chain length.

The same workers also noticed that on replacing the α carbon atom of the alkyl group by a large heteroatom such as sulphur this frequency drops to 693±5 cm^{-1}. This is probably due to the removal of one of the two C-S bonds and the resultant disruption of the coupling of the two C-S stretching vibration modes. This band at 693 cm^{-1} is therefore likely to be a pure C-S stretching frequency and as such is a very useful analytical tool for the detection of a CH_3-S group.

On integrating band intensity between 590 and 750 cm^{-1} it can be seen that for the four thioethers studied the intensity is reduced as the alkyl groups attached to sulphur become larger (Table 3.7).

Table 3.7: Integrated C-S Stretching Intensities for Thioethers and Thiols Studied

	I	No. C-S bonds (n)	I/n
$S(CH_3)_2$	96.8	2	48.4
$CH_3SCH_2CH_3$	81.6	2	40.8
$S(CH_2CH_3)_2$	71.6	2	35.8
$CH_3S(CH_2)_2CH_3$	66.4	2	33.2
$HSC(CH_3)_3$	58.3	1	58.3
$HSCH_2CH_3$	77.4	1	77.4

In order to explain this trend let us consider the effects which other parts of the molecule could have on the C-S stretching intensity. The groups adjacent to sulphur in the molecules studied are as follows:

	C-H	C-C	H
$S(CH_3)_2$	6	0	0
$CH_3SCH_2CH_3$	5	1	0
$S(CH_2CH_3)_2$	4	2	0
$CH_3S(CH_2)_2CH_3$	5	1	0
$HSC(CH_3)_3$	0	3	1
$HCCH_2CH_3$	2	1	1

In order to tackle this problem it is necessary to estimate the effect of these adjacent groups on the C-S polarisability derivative. The scattering intensity of the C-S stretching vibration can be expressed as follows:

$$I_{obs} = n_{CS}I_{CS} + n_{\alpha CH}I_{CS(\alpha CH)} + n_{\alpha CC}I_{CS(\alpha CC)} + n_{SH}I_{CS(SH)}$$

(Equation 3.1)

where I_{obs} = observed intensity of C-S stretching bands

n_{CS} ($n_{\alpha CH}$, $n_{\alpha CC}$, n_{SH}) = number of C-S (αCH, αCC, αSH) bonds present

I_{CS} = total C-S stretching intensity per C-S bond

$I_{CS(\alpha CH)}$ ($I_{CS(\alpha CC)}$, $I_{CS(SH)}$) = effect on C-S stretching intensity per αCH (αCC, αSH) bond

Consider the first three thioethers studied. From Equation 3.1:

CH_3SCH_3: $I_{obs} = 2I_{CS} + 6I_{CS(\alpha CH)} = 96.8$ (a)

$CH_3SCH_2CH_3$: $I_{obs} = 2I_{CS} + 5I_{CS(\alpha CH)} + I_{CS(\alpha CC)} = 81.6$ (b)

$S(CH_2CH_3)_2$: $I_{obs} = 2I_{CS} + 4I_{CS(\alpha CH)} + 2I_{CS(\alpha CC)} = 71.6$ (c)

Subtract (c) from (a):

$$2I_{CS(\alpha CH)} - 2I_{CS(\alpha CC)} = 25.2$$

i.e. $I_{CS(\alpha CH)} - I_{CS(\alpha CC)} = 12.6$ (Equation 3.2)

Consider next the thiols:

$HSC(CH_3)_3$: $I_{obs} = I_{CS} + 3I_{CS(\alpha CC)} + I_{CS(SH)} = 58.3$ (d)

$HSCH_2CH_3$: $I_{obs} = I_{CS} + 2I_{CS(\alpha CH)} + I_{CS(\alpha CC)} + I_{CS(SH)}$

$= 77.4$ (e)

Subtract (d) from (e):

$$2I_{CS(\alpha CH)} - 2I_{CS(\alpha CC)} = 19.1$$

i.e. $I_{CS(\alpha CH)} - I_{CS(\alpha CC)} = 9.6$ (Equation 3.3)

From Equations 3.2 and 3.3, the mean value obtained for

$I_{CS(\alpha CH)} - I_{CS(\alpha CC)} = 11.1$ (Equation 3.4)

It is now possible to speculate as to the values of $I_{CS(\alpha CH)}$ and $I_{CS(\alpha CC)}$.

At the limit, $I_{CS} = 0$ and from (a) $6I_{CS(\alpha CH)} = 96.8$

i.e. $I_{CS(\alpha CH)} = 16.1$ and from Equation 3.4, $I_{CS(\alpha CC)} = 5.0$.

This situation is, however, extremely unlikely as it would imply that the change in polarisability during the C-S stretching vibration arises entirely from the effects of the

adjacent groups. It is likely, therefore, that $I_{CS(\alpha CC)}$ is very small or even negative.

Suppose $I_{CS(\alpha CC)} = 0$, then from Equation 3.4,

$I_{CS(\alpha CH)} = 11.1$

From (a): $2I_{CS} + (6 \times 11.1) = 96.8$

i.e. $I_{CS} = 15.1$

From (b): $2I_{CS} + (5 \times 11.1) = 81.6$

i.e. $I_{CS} = 13.1$

From (c): $2I_{CS} + (4 \times 11.1) = 71.6$

i.e. $I_{CS} = 13.6$

From these three results the mean value for I_{CS} is 13.9. Substituting this in (e) gives

$13.9 + (2 \times 11.1) + I_{CS(SH)} = 77.4$

i.e. $I_{CS(SH)} = 41.3$

Alternatively let us assume that $I_{CS(\alpha CC)}$ is negative, say -10. From Equation 3.4, $I_{CS(\alpha CH)}$ will then have a value of 1.1.

From (a): $2I_{CS} + (6 \times 1.1) = 96.8$

i.e. $I_{CS} = 45.1$

From (b): $2I_{CS} + (5 \times 1.1) - 10 = 81.6$

i.e. $I_{CS} = 43.1$

From (c): $2I_{CS} + (4 \times 1.1) - 20 = 71.6$

i.e. $I_{CS} = 43.6$

From these results the mean value for I_{CS} is 43.9.

Substituting this value in (e) gives

$43.9 + (2 \times 1.1) - 10 + I_{CS(SH)} = 77.4$

i.e. $I_{CS(SH)} = 41.3$

We can now attempt to predict the total C-S stretching intensity for t-butane thiol.

Predicted C-S intensity, $I_{pred} = I_{CS} + 3I_{CS(\alpha CC)} + I_{CS(SH)}$

For $I_{CS(\alpha CC)} = 0$, $I_{CS(\alpha CH)} = 11.1$, $I_{CS(SH)} = 41.3$,

$I_{CS} = 13.9$,

$I_{pred} = 13.9 + 0 + 41.3 = 55.2$

For $I_{CS(\alpha CC)} = -10$, $I_{CS(\alpha CH)} = 1.1$, $I_{CS(SH)} = 41.3$,

$I_{CS} = 43.9$,

$I_{pred} = 43.9 - 30 + 41.3 = 55.2$

This predicted C-S stretching intensity (55.2) is very close to that observed experimentally (58.3). However, the fact that two quite different sets of values for $I_{CS(\alpha CH)}$ and $I_{CS(\alpha CC)}$ can give the same results indicates the wide range of values which will satisfy the established relationships, and the need to keep an open mind on the significance of the actual assigned values.

However, of the two cases examined here the second seems to be the one most likely to be close to the real situation. The larger value of I_{CS} and the small value of $I_{CS(\alpha CH)}$ seem more acceptable simply from common sense, since most intensity should originate from the C-S polarisability derivative. The negative contribution of the C-C bonds could be due to the more congested electronic environment around the C-C bond impeding the flow of electrons in the polarising field.

Although it is not possible to ascertain the relative values of I_{CS} and $I_{CS(\alpha CC)}$ it is apparent that the C-S intensity contribution from an adjacent S-H bond is particularly significant. This could stem from the ease of formation of $CS^- H^+$ through the effect of the field.

The large value for $I_{CS(SH)}$ is borne out by the literature[39] which confirms that Raman bands of very strong to strong intensity are seen in the range 590 - 735 cm^{-1} for aliphatic thiols, due to the C-S stretching modes.

Let us attempt to predict the C-S stretching intensity for methyl n-propyl sulphide.

Assume that $I_{CS} = 43.9$, $I_{CS(\alpha CC)} = -10$, $I_{CS(\alpha CH)} = 1.1$

$I_{pred} = 2I_{CS} + 5I_{CS(\alpha CH)} + I_{CS(\alpha CC)}$

i.e. $I_{pred} = 73.3$

The observed C-S intensity was 30.5. Thus the intensity for methyl n-propyl sulphide remains anomalously low. In order to explain this effect there is a clear need for additional data.

3.3.2.2 <u>C-H Bending and Stretching Bands</u>

From Table 3.1 it is apparent that there are several Raman bands due to C-H bending or stretching vibrations which are characteristic of sulphur containing hydrocarbons, some examples of which are shown in Table 3.8.

Table 3.8: Some Characteristic Raman Bands and Intensities Due to C-H Vibrations

Group	Band Frequency (cm^{-1})	Mean Intensity (I_{458} = 100)
$-S-CH_2-$	2731 (±4)	13
$-S-CH_2CH_3$	2932 (±4)	220
$-S-CH_3$	1050 (±2)	8
	2832 (±4)	20
	2986 (±9)	78

The apparent shift of frequency for bands due to C-H vibrations for some C-H bonds adjacent to a sulphur atom arises from the *trans* lone pair effect. This effect is more often seen in molecules containing oxygen. The lone pairs of electrons on oxygen are electron-withdrawing and result in weak C-H bonds in a position *trans* to them. This has the result of producing low frequency C-H stretching bands. The effect of the lone pair of electrons on sulphur is not as significant as with oxygen, but is responsible, for example, for the low frequency C-H stretching bands seen at 2832 (±4) and 2731 (±4) cm^{-1}.

On studying the C-H stretching bands it can be seen that if the total C-H stretching intensity is divided by the number of C-H bonds present for each compound the resulting value is found to be approximately constant (CV = 15%). This value represents the intensity contribution from a single C-H bond (see Table 3.9).

Table 3.9: C-H Stretching Region: Comparison of Calculated Intensity per C-H Bond for Thioethers and Thiols Studied (2700 - 3000 cm^{-1})

Compound	ΣI_{CH}	No. C-H bonds (n)	$\Sigma I_{CH}/n$
$S(CH_3)_2$	469.9	6	78.3
$CH_3SCH_2CH_3$	501.9	8	62.7
$S(C_2H_5)_2$	899.0	10	89.9
$CH_3S(n\text{-}C_3H_7)$	855.7	10	85.6
$HSC(CH_3)_3$	567.0	9	63.0
$HSCH_2CH_3$	398.6	5	79.7

SD = 11.4

CV = 15%

Mean = 76.53

Although the spread of the C-H contribution values is within experimental error it is interesting to note that on plotting the C-H stretching intensity per C-H bond against the number of C-H bonds present, three pairs of values become apparent (see Figure 3.2).

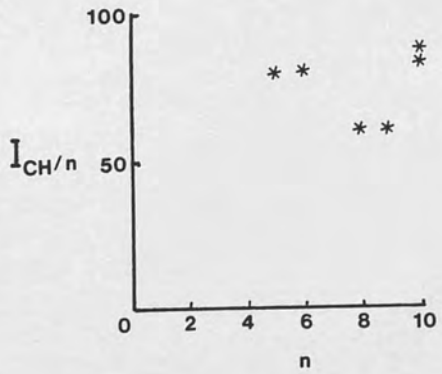

Figure 3.2: Plot of C-H Stretching Intensity *per* C-H Bond *versus* Number of CH_2 Bonds

At first it was thought that perhaps the less volatile compounds produce more intensity per C-H bond than the more volatile compounds which may be more highly polarisable. However, if this were the case then compounds with eight or nine C-H bonds would not produce less intensity than those with five or six. This phenomenon is therefore more likely to be due to the current low accuracy of the experimental system.

The reason for looking at these C-H stretching intensities in this way was to identify any trend relating to C-H bonds adjacent and non-adjacent to sulphur. If such a trend existed then uniform intensity steps would be expected to be seen across the series CH_3SCH_3, $CH_3SCH_2CH_3$, $CH_3SCH_2CH_2CH_3$, $S(CH_2CH_3)_2$. It is evident from Table 3.10 that this is not the case. It can therefore be concluded that there is no significant difference between the polarisability derivative, $\partial\alpha/\partial r$, for C-H bonds adjacent and non-adjacent to sulphur.

Table 3.10: Investigation of C-H Intensity Contribution for Bonds Adjacent and Non-Adjacent to Sulphur

Compound	$\Sigma I/n_{CH}$	n_C	n_S
$S(CH_3)_2$	78.3	6	0
$CH_3SCH_2CH_3$	62.7	5	3
$CH_3S(n\text{-}C_3H_7)$	85.6	5	5
$S(C_2H_5)_2$	89.9	4	6
$HSC(CH_3)_3$	63.0	0	9
HSC_2H_5	79.7	2	3

n_{CH} = total number of C-H bonds
n_S = number of C-H bonds adjacent to sulphur
n_C = number of C-H bonds adjacent to carbon

3.4 Deuterated Dimethyl Sulphide Compared with Dimethyl Sulphide

A comparison of the results obtained for dimethyl sulphide and deuterated dimethyl sulphide can be seen in Table 3.11. The F-sum rule[40] can be applied to infra-red intensities of corresponding transitions for isotopically related molecules as follows:

From

$$F^{-1} = L\Lambda^{-1}L^{t}$$

where F = force constant matrix

L = eigenvector matrix

the following equation can be derived:

$$\sum_{i} \frac{I_i}{\nu_i} = \frac{N\pi}{3c^2} \sum_{jk} \sum_{i} \frac{L_{ji} L_{ki}}{\nu_i^2} \frac{\delta\mu}{\delta R_j} \frac{\delta\mu}{\delta R_k}$$

i.e.

$$\sum_{i} \frac{I_i}{\nu_i} = \frac{4N\pi^3}{3c^2} \sum_{jk} F_{jk}^{-1} \frac{\delta\mu}{\delta R_j} \frac{\delta\mu}{\delta R_k}$$

where I_i = intensity of band due to vibration i

ν_i = frequency of vibration i

$\delta\mu$ = change in dipole moment during vibration

δR = change in bond length during vibration

Therefore, providing that $\delta\mu/\delta R$ is independent of isotopic substitution, $\Sigma(I_i/\nu_i)$ should remain constant. This sum rule should also apply to Raman bands, providing that there is no change in $\delta\alpha/\delta R$ with isotopic substitution. The F-sum rule has been applied to dimethyl sulphide as follows (see also Table 3.12):

For all bands

$S(CH_3)_2$ $\Sigma(I_i/\nu_i)$ = 0.395

$S(CD_3)_2$ $\Sigma(I_i/\nu_i)$ = 0.300

For C-H (C-D) stretching and bending bands only

$S(CH_3)_2$ $\Sigma(I_i/\nu_i)$ = 0.182

$S(CD_3)_2$ $\Sigma(I_i/\nu_i)$ = 0.134

For C-H (C-D) stretching bands only

$C(CH_3)_2$ $\Sigma(I_i/\nu_i) = 0.160$

$C(CD_3)_2$ $\Sigma(I_i/\nu_i) = 0.107$

For summation over the whole spectra the results for the two compounds are of the same order but not as close as would be expected. There must therefore be some other factor causing the non-deuterated dimethyl sulphide to have more scattering intensity than the deuterated form.

Table 3.11: Comparison of Raman Band Frequencies and Intensities for $S(CH_3)_2$ and $S(CD_3)_2$

$S(CH_3)_2$		$S(CD_3)_3$	
$\bar{\nu}$ (cm^{-1})	I	$\bar{\nu}$ (cm^{-1})	I
282	21.4	247	14.9
693	72.7	642	52.0
744	24.1	707	17.8
1333	1.9	822	3.0
1424	11.0	1025	10.4
1444	19.3	1044	13.2
2834	28.6	1998	11.2
2854	45.3	2037	8.1
2914	240.4	2085	21.3
2970	68.9	2126	115.0
2987	86.7	2240	74.7

I refers to the intensity relative to I_{458} for carbon tetrachloride where $I_{458} = 100$.

Table 3.12: F-Sum Rule for Dimethyl Sulphide

$S(CH_3)_2$		$S(CD_3)_2$	
$\bar{\nu}$ (cm^{-1})	$\Sigma(I_i/\nu_i)$	$\bar{\nu}$ (cm^{-1})	$\Sigma(I_i/\nu_i)$
282	0.076	247	0.060
693	0.105	642	0.081
744	0.032	707	0.025
1333	0.001	822	0.004
1424	0.008	1025	0.010
1444	0.013	1044	0.013
2834	0.010	1998	0.006
2854	0.016	2037	0.004
2914	0.082	2085	0.010
2970	0.023	2126	0.054
2987	0.029	2240	0.033

It is unfortunate that the deuterated dimethyl sulphide results cannot be included in this band intensity study due to non-compliance with Crawford's F-sum rule. It would be interesting to investigate the deuterated forms of one or more of the other molecules in the thioether series studied.

3.5 Ethyl Methyl Sulphide Temperature Studies

3.5.1 Introduction

In the liquid state rotation about the carbon-sulphur bond between the ethyl group and sulphur in ethyl methyl sulphide gives rise to *trans* and *gauche* rotational isomers (Figure 3.3).

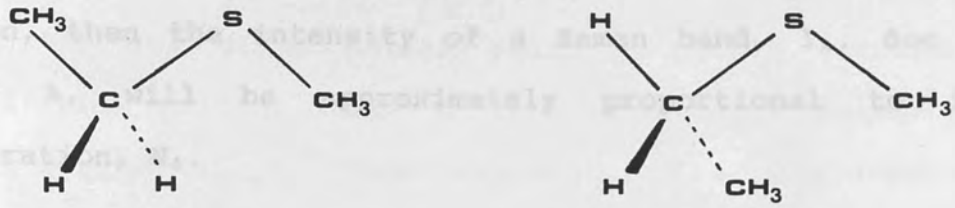

Trans Gauche

Figure 3.3: Rotational Isomers of Ethyl Methyl Sulphide

Normally in cases of rotational isomerism such as this the *trans* isomer would be expected to be the more stable due to steric considerations, and a potential curve would be of the form shown in Figure 3.4.[41]

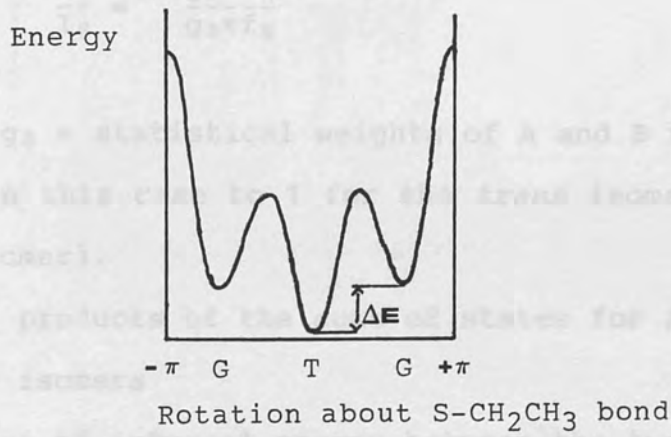

Figure 3.4: Change in Potential Energy with Conformation for Ethyl Methyl Sulphide

In theory it is possible to determine which of these isomers is more stable and to calculate a value for ΔE, the energy difference between the two conformational states, using Raman spectroscopy.[41,42]

If two conformational species, A and B, are present in solution, then the intensity of a Raman band, I_A, due to species A, will be approximately proportional to its concentration, N_A.

i.e. $I_A \propto N_A$

A similar relationship exists for the second species, B. Therefore comparing the band intensities for the two isomers we get:

$$\frac{I_A}{I_B} = \frac{K.N_A}{N_B}$$

where K is a constant which depends on the properties of the spectral lines.

i.e.

$$\frac{I_A}{I_B} = \frac{K.g_A \pi f_A}{g_B \pi f_B}.e^{-\Delta E/RT}$$

where g_A and g_B = statistical weights of A and B respectively (equivalent in this case to 1 for the *trans* isomer and 2 for the *gauche* isomer).

πf_A and πf_B = products of the sums of states for A and B isomers

ΔE = difference of internal energy between the two isomers

R = gas constant, 8.316 $J^{-1}K^{-1}mol^{-1}$

T = temperature (K)

If we take natural logarithms this expression becomes:

$$\ln(I_A/I_B) = \ln(K.g_A \pi f_A / g_B \pi f_B) - \Delta E/RT \quad \text{(Equation 3.5)}$$

From Equation 3.5, a plot of $\ln(I_{gauche}/I_{trans})$ against 1/T for ethyl methyl sulphide should produce a straight line with a slope of $\Delta E/R$ and an intercept of $\ln 2K(\pi f_{gauche}/\pi f_{trans})$. These calculations assume constant volume.

The Raman spectrum of ethyl methyl sulphide exhibits three bands in the C-S stretching region, appearing at 658, 682 and 728 cm^{-1} (Figure 3.5).

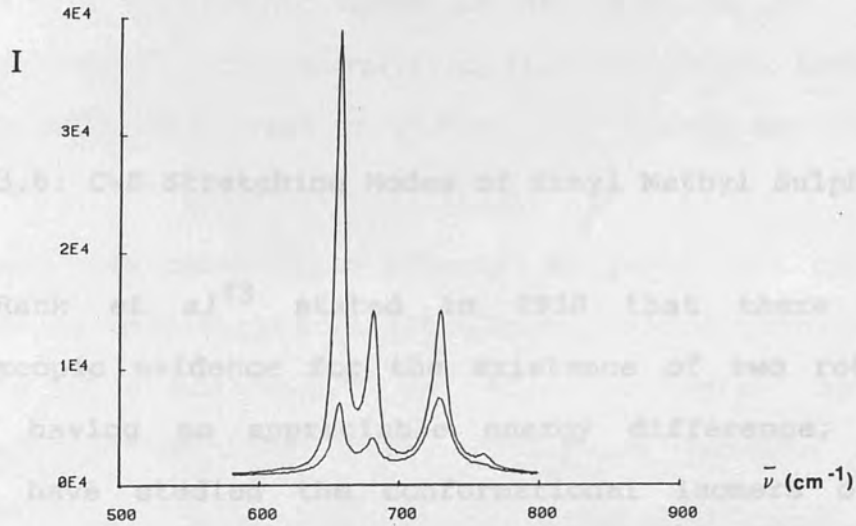

Figure 3.5: C-S Stretching Bands of Ethyl Methyl Sulphide

The small band appearing at 760 cm^{-1} is due to the S-C-H bending motion and is not relevant to these conformational studies.

Since there are two principal C-S stretching modes for ethyl methyl sulphide (see Figure 3.6), it seems likely that one of these three bands is due to both the *trans* and *gauche* isomers, since a total of four bands is to be expected.

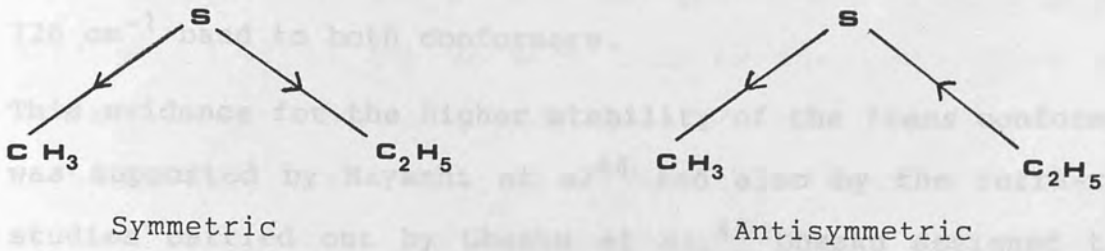

Figure 3.6: C-S Stretching Modes of Ethyl Methyl Sulphide

Since Rank *et al*[43] stated in 1950 that there was no spectroscopic evidence for the existence of two rotational isomers having an appreciable energy difference, several workers have studied the conformational isomers of ethyl methyl sulphide, with the result that there seems to be much controversy over the identity of the more stable isomer.

In 1957 Hayashi *et al*[37] studied ethyl methyl sulphide by Raman spectroscopy and assigned the three observed C-S stretching bands as follows:

650 cm^{-1} *trans* and *gauche*

675 cm^{-1} *gauche*

723 cm^{-1} *trans*

They reported that in the solid state the 675 cm^{-1} band was not present, thus concluding that the *trans* conformer was more stable than the *gauche*.

Similar results have been reported by Sakakibara *et al*[38] who calculated $DE_{(gaseous\ state)}$ between the two conformers to be -30±50 cal/mole. They assigned the 658 cm^{-1} band to the *gauche* conformer, the 682 cm^{-1} band to the *trans* and the 728 cm^{-1} band to both conformers.

This evidence for the higher stability of the *trans* conformer was supported by Hayashi *et al*[44] and also by the infra-red studies carried out by Ohsaku *et al.*[45] Ohsaku assigned the observed C-S stretching bands at 783 and 686 cm^{-1} to the *gauche* conformer, thus suggesting that since the intensities of these bands decreased on cooling the *gauche* conformer was less stable than the *trans*.

There have been conflicting reports, however, that the *gauche* conformer is more stable than the trans, and figures of a few hundredth of a kcal/mole[46] and 46±14 cal/mole[47] have been suggested for ΔE, the energy difference between the two conformers.

Nogami[48] was also amongst those concluding that the *gauche* conformer was the more stable of the two, calculating ΔE to be 0.14 ±0.03 kcal/mole. However, the assignments of the three observed C-S stretching bands were given as:

655 cm^{-1} *gauche*

678 cm^{-1} *trans*

725 cm^{-1} *gauche*

These assignments are not in agreement with those given elsewhere and the disappearance of the 678 cm^{-1} band in the solid state, also seen by Hayashi[37] led to the conclusion that the *gauche* conformer had the higher stability.

3.5.2 Experimental Results

Three bands were observed in the C-S stretching region for ethyl methyl sulphide, at 658, 682 and 728 cm^{-1}. From Tables 3.13 and 3.14 it can be seen that as the temperature was increased the intensity of the 658 cm^{-1} band remained constant relative to the 458 cm^{-1} band of carbon tetrachloride. Relative to the 658 cm^{-1} band the 682 cm^{-1} band intensity decreased while the 728 cm^{-1} band intensity increased.

It has already been shown in Chapter 2 that the relative intensities of the three main bands of carbon tetrachloride do not change with temperature, so it can be assumed that on an absolute scale the 658 cm^{-1} band intensity also remains constant.

From the theoretical calculations carried out on ethyl methyl sulphide which will be discussed in Chapter 4, the assigments for the C-S stretching bands are as follows:

	Freq. No.	$\bar{\nu}$ (cm^{-1})	Intensity (Arbitrary units)	ρ
Gauche	24	728	0.300	0.804
	25	692	0.744	0.159
Trans	24	728	0.433	0.817
	25	711	0.698	0.158

Frequency no. 24 = band arising predominantly from antisymmetric C-S stretch.

Frequency no. 25 = band arising predominantly from symmetric C-S stretch.

Table 3.13: Ethyl Methyl Sulphide: Relative Intensities of the C-S Stretching Bands as a Function of Temperature

$\bar{\nu}$	Temperature (°C)						
(cm^{-1})	-11.0	18.4	42.5	54.5	70.0	80.0	90.0
658	1.000	1.000	1.000	1.000	1.000	1.000	1.000
682	0.284	0.386	0.284	0.278	0.257	0.213	0.214
728	0.638	0.623	0.631	0.719	0.709	0.817	0.836
ΣI	1.922	2.009	1.915	1.997	1.966	2.030	2.050

Table 3.14: Ethyl Methyl Sulphide - Solution in Carbon Tetrachloride: Variation of Relative Intensities of 658 cm^{-1} and 458 cm^{-1} Bands with Temperature

$\bar{\nu}$	Temperature (°C)			
(cm^{-1})	18.4	45.0	64.0	90.0
458 (CCl_4)	1.000	1.000	1.000	1.000
658 ($CH_3SC_2H_5$)	0.388	0.382	0.385	0.389

These calculated frequencies clearly indicate that the band common to both conformers is the band at 728 cm^{-1}. It follows that the band at 682 cm^{-1} is due to the *trans* conformer and that at 658 cm^{-1} is due to the *gauche* conformer. These assignments are consistent with those made by Sakakibara *et al.*[38] They also lead to the conclusion that the *gauche* conformer is the more stable of the two if the 682 cm^{-1} band does disappear in the solid state as reported in the literature.[37,48]

However, this leaves two inconsistencies. Firstly the 658 cm^{-1} band intensity was found experimentally to remain constant with respect to the carbon tetrachloride 458 cm^{-1} band over a range of temperatures, indicating that this might be the band common to both conformers. Secondly, the 682 cm^{-1} band intensity decreased with increasing temperature, contrary to earlier observation[37,48] that it had disappeared in the solid state.

In order to help to clarify these assignments, an attempt was made to obtain a spectrum of frozen ethyl methyl sulphide. This was done by drawing liquid nitrogen through the Coderg temperature cooled unit (see Figure 3.1) using a rotary pump. Unfortunately the lowest temperature achieved without complete frosting of the cell was -11°C, well above the freezing point of ethyl methyl sulphide of -106°C Investigation of band assignments in this way was therefore not possible.

One explanation for these discrepancies could be that since the observed intensity changes were small they may not have been significant compared to experimental error, although a definite trend did appear to be present. Alternatively, since some broadening of bands with increasing temperature was observed, it is possible that this gave rise to inaccuracies in the peak areas, which were calculated using the three band fit routine (see Section 2.3.1).

However, assuming the *ab initio* assignments to be correct, the value of ΔE was calculated by plotting $\ln(I_{658}/I_{682})$ against 1/T. This plot is shown in Figure 3.7 and is seen to be approximately linear (ignoring the -11°C data point, see below). From the gradient of this graph the energy difference between the two conformers was calculated to be 8.5 kJ/mol, in this case the *trans* conformer being the more stable.

The data point obtained at -11°C was not used for this calculation since the spectra produced were of poor quality and the band intensity measurements were subject to error due to the frosting problems.

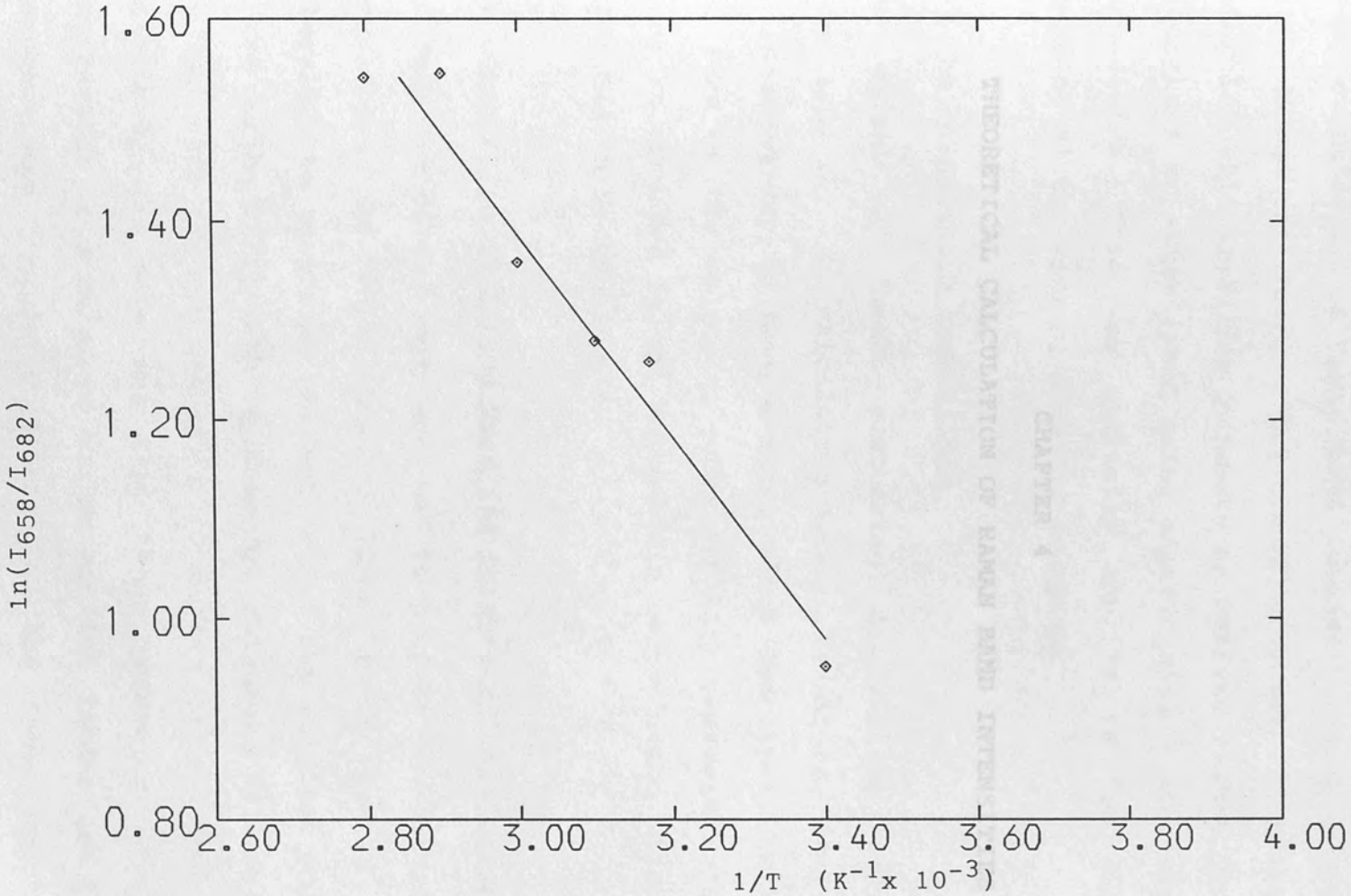

Figure 3.7: Energy Barrier Calculation for Ethyl Methyl Sulphide

CHAPTER 4

THEORETICAL CALCULATION OF RAMAN BAND INTENSITIES

4. THEORETICAL CALCULATION OF RAMAN BAND INTENSITIES

A computer programme has been developed which enables, *inter alia*, calculation of Raman band intensities and frequencies using a set of force constants determined *ab initio* and molecular polarisability parameters, derived either from the literature or established using experimental frequencies and intensities. This was initially applied to the simplest compound of the series, dimethyl sulphide.

4.1 The Wolkenstein Assumptions

The extent of Raman scattering depends on molecular polarisability. In calculating band intensities, therefore, it is necessary to have a model which describes the nature and form of the molecular polarisability parameters. Such a model is provided by the Wolkenstein assumptions, which were described in Section 1.4.4.

4.2 Description of Method Used for Intensity Calculation

The function of the programme was to predict the vibrational frequencies and intensites of Raman bands for a given molecule. The programme was set up for the simplest molecule in the series of thioethers, dimethyl sulphide. In the course of this work it was necessary to derive certain molecular parameters. The hope was that these parameters might be transferable to similar molecules so that future use of the programme may include prediction of the Raman spectra of further molecules in the thioether series.

4.2.1 Input Data for Theoretical Calculation Programme

An example of the data file for dimethyl sulphide, dimethyl sulphide-d6 and ethyl methyl sulphide can be seen in Appendix E. In order to aid explanation, water will be used in this section as an illustration.

The data required for the programme are set out in the following form:

(a) Number of problem, number of atoms, number of internal coordinates, number of isotopes.

e.g. for H_2O 1 3 3 1

(b)Cartesian coordinates for each atom in its equilibrium position.

e.g. for H_2O

	X	Y	Z
O	0.0000	0.0000	0.0000
H	-0.7580	0.5891	0.0000
H	0.7580	0.5891	0.0000

These coordinates were calculated assuming the bond length O-H to be 0.96 Å and the H-O-H angle to be 104.5^{o}.[49]

(c) Internal Coordinates

These describe the nature of the possible molecular vibrations. They are presented as sets of 4, 5 or 6 numbers. The first is a number identifying that particular vibration, the second describes the nature of the vibration, i.e. 1 represents a stretch, 2 a bend, 3 an angle deformation of bond C-D with respect to plane D-E-F, 4 a torsion, 5 an out of plane bend of bond C-D with respect to plane D-E-F and 6 a

bell-type torsion. The remaining numbers denote the atoms taking part in the vibration.

e.g. for H_2O there are 3 internal coordinates:

1	1	1	2		stretch involving atoms 1 and 2
2	1	1	3		stretch involving atoms 1 and 3
3	2	2	1	3	bend involving atoms 2, 1 and 3

(d) Relative atomic masses

e.g. for H_2O

15.9994	1.0079	1.0079
O	H	H

(e) Number of force constants, number of Z matrix tetrads (see (g)).

e.g. for H_2O

4 6

(f) List of force constant values, list of corresponding force constant descriptions.

e.g. for H_2O

7.66	0.703	-0.907	0.0	(Reference 50)
OH STRETCH	HOH BEND	OH/OH	OH/HOH	

(g) Z Matrix

The Z matrix describes the structure of the force constant (F) matrix. The F matrix is of the following form:

			Internal Coordinates 1 R1	2 R2	3 θ
Internal	1	R1	fR1	f(R1/R2)	f(R1/θ)
Coordinates	2	R2	f(R2/R1)	fR2	f(R2/θ)
	2	θ	f(θ/R1)	f(θ/R2)	fθ

where R1 = O-H stretch
R2 = O-H stretch
θ = H-O-H bend

f represents a force constant, e.g. fR1 is the force constant asociated with an O-H stretch and f(R1/R2) is the interaction (OH/OH) force constant.

It can be seen that this matrix is symmetric.

Each force constant is represented by a number (equivalent to its position in the list of force constant values, (f)).

The Z matrix consists of sets of four numbers. The first is the row number of the F matrix, the second the column number, the third the force constant number and the fourth describes the direction in which the force constant acts (+1.00 or -1.00).

For H_2O the Z matrix would be

1	1	1	1.0
1	2	3	1.0
1	3	4	1.0
2	2	1	1.0
2	3	4	1.0
3	3	2	1.0

(h) Static polarisability derivatives and polarisabilities for each bond.

Each bond is described by two atoms, i and j. A third atom, k, attached to j is also given, defining a plane, ijk.

After each bond description the polarisability derivatives, $\partial\alpha_x/\partial r$, $\partial\alpha_y/\partial r$ and $\partial\alpha_z/\partial r$ and the static polarisabilities, α_x, α_y and α_z, for that bond are given.

e.g. for H_2O

	Atoms defining bond		Third atom defining plane	Bond No 1	Bond No 2	Direction
Bond 1	1	2	3	1	2	-1
Bond 2	1	3	2	2	1	-1

For OH

$\partial\alpha_x/\partial r = -1.004$ $\partial\alpha_y/\partial r = \partial\alpha_z/\partial r = 0.223$

$\alpha_x = 0.100$ $\alpha_y = \alpha_z = 0.000$

These polarisability values were based on those given for water vapour by Murphy.[53]

4.2.2 Vibrational Frequency Calculation

Vibrational frequencies are calculated using the Wilson GF matrices method.[52] Molecular vibrational frequencies are related to the atomic masses, bond lengths and the force field, as follows:

$$|GF - \lambda E| = 0 \qquad \text{(Equation 4.1)}$$

where F = the force constant matrix as described above

E = a unit matrix

$\lambda = 4\pi^2\nu^2$, ν being the set of vibrational frequencies

The G matrix, G, is described below.

Equation 4.1 represents the determinant of the vibrational secular equations as shown in Steele.[1]

The G Matrix

The G matrix depends on the relationship between the internal coordinates, r, and the cartesian coordinates, x, as follows:

$$r = Bx$$

where B is a matrix of dimensions 3N-6 (or 3N-5) by 3N (N = the number of atoms in each molecule).

The G matrix is then given as

$$G = BM^{-1}B^{t} \qquad \text{(Equation 4.2)}$$

where M^{-1} is a diagonal matrix containing the inverses of the atomic masses.

It can be seen from Equation 4.2 that the G matrix depends only on the atomic masses and the molecular geometry, and that it is symmetric.

Each G matrix element relates to two internal coordinates and the elements may be tabulated in terms of pairs of coordinates with a given geometrical relationship. Any pair of coordinates with no atoms common produces a zero G matrix element. Thus the G matrix can easily be constructed.

If L_{nj} represents the vibrational displacement of coordinate j for the nth vibration, then Equation 4.1 may be slightly modified to give:

$$|GF - \lambda_n E| L_n = 0 \qquad \text{(Equation 4.3)}$$

where

$$\lambda_n = 4\pi^2\nu_n^2$$

and L_n = column vector containing the amplitudes of motion of the displacement coordinate in the nth vibration.

Since Equation 4.3 describes the vibrational problem in full it is possible to separate the GFL_n and $\lambda_n EL_n$ terms. Thus we obtain the expression:

$$GFL_n = \lambda_n EL_n \qquad \text{(Equation 4.4)}$$

For each n there will be an equivalent expression. These equations can be combined by combining all the eigenvector column matrices L_n into one matrix L and representing $\lambda_n E$ by Λ where

$$\Lambda = \begin{bmatrix} \lambda_1 & 0 & 0 & . & . \\ 0 & \lambda_2 & 0 & . & . \\ 0 & 0 & \lambda_3 & . & . \\ . & . & & & \\ . & . & & & \end{bmatrix}$$

The expression then becomes

$$GFL = L\Lambda$$

In order to evaluate the vibrational frequencies it is necessary to solve the product GF. However, this is not a straightforward procedure since although both F and G are symmetric the product of two symmetric matrices is not necessarily symmetric itself. For this reason another approach to the problem is made.

A new matrix, D, is introduced. D defines the product of B, the matrix relating internal coordinates to cartesian coordinates, with a diagonal matrix containing the reciprocal square roots of the atomic masses. From Equation 4.2 we then get:

$$G = BM^{-1}B^t = DD^t$$

Consider the product D^tFD. If Y and Λ' are the eigenvector and eigenvalue matrices then

$$D^tFDY = \Lambda'Y$$

Premultiplying by D then gives

$$DD^tFDY = DY\Lambda'$$

i.e.

$$GFDY = DY\Lambda'$$

By comparison with Equation 4.4 it can be seen that $\Lambda = \Lambda'$ and $L \propto DY$. Since the matrices L and DY are both related to vibrational amplitude and the energy associated with any vibration is dependent on its amplitude, in order to equate the two there must be a normalisation factor for each column to ensure that the associated energy of vibration is $h\nu$ (where h = Planck's constant). If this normalisation procedure has taken place then L = DY.

It is seen that the product D^tFD has the same eigenvalues as the product GF but since the the former is symmetric it is easier to solve.

Thus the expression

$$|D^tFD - E\lambda| = 0$$

is the vibrational problem in cartesian coordinates (mass weighted) which has been set up using an F matrix defined in internal coordinates. Using a computer the problem is much easier to solve if the data are in this form than if they are in the form of Equation 4.3.

This method has the added advantage that the vibrational problem, when defined by D^tFD, where D is the transformation matrix from internal to mass weighted cartesian coordinates, yields eigenvectors which move with the inertial axes. This overcomes any error which may arise from possible librational motions of the principal polarisability tensor.

4.2.3 Raman Band Intensity Calculation

Following the vibrational frequency determination is the calculation of the cartesian displacement coordinates, and hence the coordinates of the atoms in the deformed state. This is necessary if the band intensities are to be determined. Raman band intensity depends on the change of molecular polarisability which occurs during the course of a vibration. Thus if both the equilibrium and displacement cartesian coordinates are known then the polarisability for both these conditions can be calculated, and hence also the polarisability change.

To carry out this calculation the root mean square amplitudes of vibration are required.

As already stated, the internal coordinates, r, and cartesian coordinates, x, are related as follows:

$$r = Bx \qquad \text{(Equation 4.5)}$$

The reverse relationship between these two sets of coordinates can be expressed as

$$x = Ar \qquad \text{(Equation 4.6)}$$

Substitution of Equation 4.5 into Equation 4.6 gives

$x = ABx$ for the equilibrium state

Therefore $AB = E$, the identity matrix

Using this information and an expression for the root mean square amplitude of vibration, i.e. the distance the atoms move during the course of a vibration, it is possible to calculate the cartesian displacement coordinate matrix, q, simply by replacing x with q for the perturbed state. A relatively straightforward way of carrying out these calculations is to use the expression for q, as follows, which can be derived from Equations 4.2, 4.5 and 4.6.[1]

$$q = M^{-1/2}YQ \qquad \text{(Equation 4.7)}$$

Here Q is a matrix defining the extent of distortion of the atoms for each vibration.

The root mean square displacement for a harmonic oscillator in one direction is

$$[h(v + 1/2)/4\pi^2 m\nu]^{1/2}$$

where m = reduced mass

ν = frequency

v = vibrational quantum number

Thus for mass weighted normal coordinates we get:

$$(\overline{Q_i^2})^{1/2} = [h(\nu_i + {}^1/_2)/4\pi^2\nu_i]^{1/2} \quad \text{(Equation 4.8)}$$

Therefore, using Equations 4.7 and 4.8, the cartesian displacement coordinates may be calculated.

Equation 4.8 assumes that all molecules are in the ground state. If a more accurate determination taking into account the population of excited states is required a correction factor of $(1/2)\coth(h\nu/2kT)$ should be introduced.

The next stage was to form all component polarisability tensors and rotate them to a common laboratory axis. The rotation was required prior to the summing of the component tensors to give the overall molecular polarisability tensor.

This procedure was carried out for the molecule in both the equilibrium and deformed states for each vibration. The difference between the two molecular polarisability tensors was then the tensor containing polarisability changes arising during the course of the vibration.

The form of data required for this part of the calculation is described in Section 4.2.1.(h).

From this information the tensor containing molecular polarisability changes for each vibration was calculated by the following method:

(1)The unit vectors (EMATX, EMATY, EMATZ) along each bond were derived and hence the unit vectors perpendicular to the bond both in the ijk plane (EPLANX, EPLANY, EPLANZ) and perpendicular to the ijk plane (EPERX , EPERY , EPERZ) were also derived.

To achieve this various vector products were used. If e represents a unit vector then

$$e_{ji} = a_1e_x + a_2e_y + a_3e_z \qquad \text{(Equation 4.9)}$$

The dot product of two vectors is equal to the cosine of the angle, θ, between them,

i.e. $e_{ji} \cdot e_{jk} = a_1b_1 + a_2b_2 + a_3b_3 = \cos\theta$ (Equation 4.10)

where a_1b_1, a_2b_2 and a_3b_3 are the x, y and z components of each unit vector.

The cross product of two vectors divided by the sine of the angle between them gives a third unit vector, e_3, which is perpendicular to the original two,

i.e. $e_{ji} \times e_{jk}/\sin ijk = e_3$ (Equation 4.11)

and

$$e_{ji} \times e_{jk} = e_x(a_2b_3 - a_3b_2) + e_y(a_3b_1 - a_1b_3) + e_z(a_1b_2 - a_2b_1)$$

Therefore, combining this information,

From Equation 4.9

$$e_{ji} = a_1e_x + a_2e_y + a_3e_z$$

=> EMATX EMATY EMATZ

The value of $\cos\theta$ could then be calculated from Equation 4.10

$$e_{ji} \cdot e_{jk} = \cos\theta$$

and hence

$$\sin\theta = (1 - \cos^2\theta)^{1/2}$$

Therefore, using Equation 4.11

$$e^{\perp\perp} = \frac{e_{ji} \times e_{jk}}{\sin\theta} \Rightarrow \text{EPERX EPERY EPERZ}$$

and

$$e^{\perp\parallel} = \frac{e_{ji} \times e^{\perp\parallel}}{\sin\theta} = \frac{e_{ji} \times e^{\perp\parallel}}{1} \Rightarrow \text{EPLANX EPLANY EPLANZ}$$

(2) Using the computed unit vector values the x, y and z components of the polarisability of each bond were evaluated. As already stated the polarisability can be written as

$$\begin{bmatrix} \alpha_{xx} & \alpha_{xy} & \alpha_{xz} \\ \alpha_{yx} & \alpha_{yy} & \alpha_{yz} \\ \alpha_{zx} & \alpha_{zy} & \alpha_{zz} \end{bmatrix}$$

Consider α_{xy}:

The static polarisability contribution, α_{xy} can be calculated from:

$$\alpha_{xy} = \alpha_1(e_1e_x)(e_1e_y) + \alpha_2(e_2e_x)(e_2e_y) + \alpha_3(e_3e_x)(e_3e_y)$$

i.e. $\alpha_{xy} = \alpha_1$(ematx ematy) + α_2(eperx epery) +

α_3(eplanx eplany)

Similarly for the polarisability contribution due to reorientation, $(\partial\alpha/\partial R)_{xy}$:

$(\partial\alpha/\partial R)_{xy} = (\partial\alpha/\partial R)_1$(ematx ematy) + $(\partial\alpha/\partial R)_2$(eperx epery)

+ $(\partial\alpha/\partial R)_3$(eplanx eplany)

Therefore overall, $\alpha_{xy} = \alpha_{xy} + (\partial\alpha/\partial R)_{xy}\Delta R$

This calculation was also carried out for α_{xx}, α_{xz}, α_{xy}, α_{yz} and α_{zz} (matrix is symmetric).

The components were then summed over all bonds to produce the equilibrium polarisability tensor.

(3)The procedure was repeated for each vibration using the cartesian coordinates of the atoms in the appropriate deformed state. The equilibrium polarisability tensor was then subtracted from the tensor for the deformed state to give a tensor containing polarisability changes arising from reorientation during each vibration.

(4) The final polarisability tensor could then be used to evaluate the mean polarisability, $\bar{\alpha}$, the anisotropy polarisability squared, γ^2, the intensities I_{VV} and I_{VH} and the depolarisation ratio, ρ, for each vibration from the following expressions:

$$\bar{\alpha} = \frac{1}{3}(\alpha_{xx} + \alpha_{yy} + \alpha_{zz})$$

$$\gamma^2 = \frac{1}{2}[(\alpha_{xx} - \alpha_{yy})^2 + (\alpha_{yy} - \alpha_{zz})^2 + (\alpha_{zz} - \alpha_{xx})^2 + 6(\alpha_{xy}^2 + \alpha_{yz}^2 + \alpha_{zx}^2)]$$

$$I_{VV} = 45\bar{\alpha}^2 + 7\gamma^2$$

$$I_{VH} = 6\gamma^2$$

$$\rho = \frac{6\gamma^2}{45\bar{\alpha}^2 + 7\gamma^2}$$

4.3 *Ab Initio* Calculation of a Force Field for Dimethyl Sulphide

To allow the accurate determination of vibrational frequencies it is necessary to have available a representative force field for the molecule in question. For dimethyl sulphide and, in fact, thioethers and thiols in

general, there are very few force field data available, particularly corresponding to interaction terms.

For this reason a force field was calculated *ab initio* using the Gaussian 82 package available on the University of London Cray system. In doing this it was hoped that individual force constants would be transferable to other molecules in the series. There is evidence to suggest that this transferability is feasible as several earlier workers using other series of compounds have found this to be so.[51,53-57]

Many workers who have evaluated force constants have derived them from vibrational frequency data.[51,53,54,57-61] This method was used following the *ab initio* force field calculation to optimise force constant scaling factors.

4.3.1 <u>The Gaussian 82 Package</u>

Gaussian 82 is based on the LCAO (Linear Combination of Atomic Orbitals) method. A molecular wavefunction, ϕ can be assumed to consist of the sum of separate atomic wavefunctions, i.e.

$$\phi = \sum_i a_i \psi_i$$

where ψ = atomic wavefunction

a = variable parameter

The various ψ_is are collectively known as the basis set of atomic orbitals.

One application of the Gaussian 82 programme is to calculate the structure for which the energy, that is the nuclear-

nuclear, nuclear-electron and electron-electron energy is at a minimum.

Molecular structure calculations are usually very tedious due to the complexity of many of the electron-electron interaction energy integrals which must be calculated.

In a Self-Consistent Field[62] calculation (see Appendix F) many of the integrals involve atomic orbitals based on more than one centre. These are complicated and very time consuming to evaluate.

In general an atomic orbital, for instance the s orbital of a hydrogen atom, can be represented by

$$f(x) = x^n \exp(-ar_i)$$

where a = variable parameter

r = distance from centre

This is a Slater type of atomic orbital. A simplification, however, is to express the atomic orbital in the form of a Gaussian function

$$\exp(-a_i r^2)$$

However, since an atomic orbital is not well represented by a simple Gaussian function, each is expressed as the sum of three Gaussians

$$\sum_i b_j \exp(-a_i r^2)$$

where b = variable parameter

The advantage of this method is that the product of two Gaussians based on different centres is itself a Gaussian based on a point lying between the two centres. Thus a

complicated 3 or 4-centred integral can be reduced to a simpler 2-centred integral. So, taking into account the fact that the Gaussian function representing each atomic orbital is already the sum of three Gaussians, each is relatively simple and so the whole procedure is overall less time-consuming than with the Slater Type Orbitals.

In Gaussian 82, in calculating a molecular orbital from the component atomic orbitals the three Gaussians for each atomic orbital are partitioned into a pair plus one. Therefore the pair of functions and the single function are allowed to vary independently in the molecular wavefunction, ϕ. Thus the calculation is denoted 3-21G. In this case an s orbital is represented by

$$a_1\exp(-b_1r^2) + a_2\exp(-b_2r^2) + a_3\exp(-b_3r^2)$$

and a p orbital by

$$d_1x\exp(-f_1x^2) + d_2x\exp(-f_2x^2) + d_3x\exp(-f_3x^2)$$

where a_1 and a_2, and d_1 and d_2 are held relative to one another at the optimised values for atoms, but a_3 and d_3 can vary independently.

The notations n-21 and n-31 (if the atomic orbital is represented by four Gaussians) limit the calculations to s and p type wavefunctions only. If *d* orbitals are to be included the calculation must be denoted n-21*.

An input for a Gaussian 82 calculation consists of a description of the molecule geometry followed by values of various bond angles and bond lengths. An example of the data input for dimethyl sulphide can be seen in Appendix G.

4.3.2 Experimental Procedure for Dimethyl Sulphide

As mentioned previously (Section 4.3.1) part of the Gaussian 82 procedure is to calculate the wavefunction for which the molecular energy is at a minimum (see Figure 4.1). The energy is minimised by varying coordinates, thereby establishing the structure for the chosen basis.

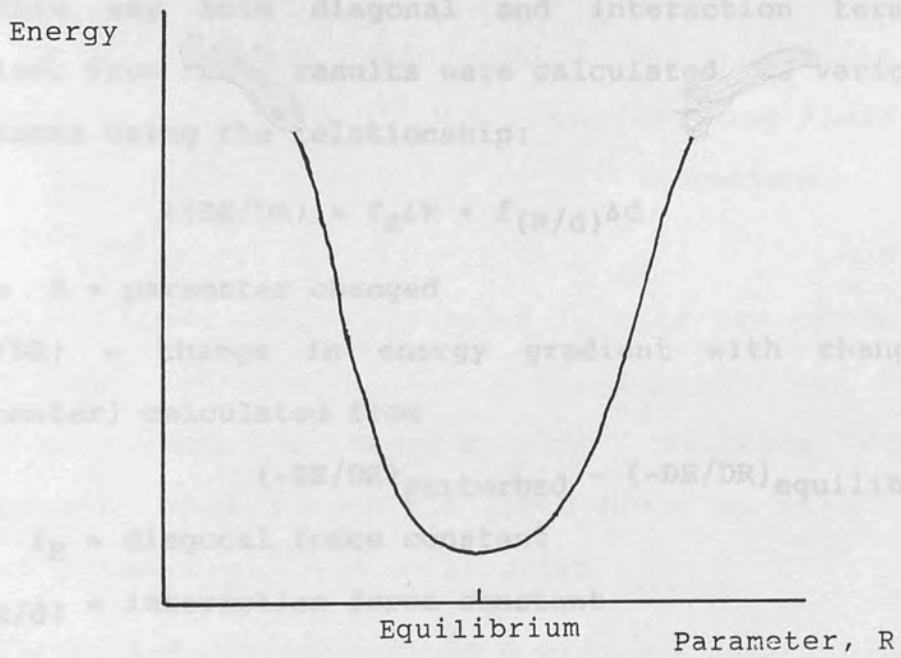

Figure 4.1: Molecular Energy Curve

In doing this, by estimating new molecular parameter values, the programme can calculate values of -DE/DR, the change in total molecular energy with respect to parameter change. The value of the total molecular energy, E(RHF), is also given.

The first step in the force constant calculation involved varying the molecular parameters, using those suggested by the programme as a guide, until they were found to correspond to the equilibrium position of the molecule. At this point each value of -DE/DR was ideally zero and E(RHF) was at a minimum.

On reaching equilibrium the next stage was to vary each parameter in turn by a predetermined quantity, noting the resulting energy gradient changes for all parameters in each case. Bond lengths were changed by 0.01 Å and angles by 1°. In this way both diagonal and interaction terms could studied. From these results were calculated the various force constants using the relationship:

$$\Delta(DE/DR) = f_R \Delta R + f_{(R/d)} \Delta d$$

where R = parameter changed

$\Delta(DE/DR)$ = change in energy gradient with change in R (parameter) calculated from

$$(-DE/DR)_{perturbed} - (-DE/DR)_{equilibrium}$$

f_R = diagonal force constant

$f_{(R/d)}$ = interaction force constant

The force constants thus calculated were bond weighted. This was applied to any force constant which involved a bend as follows:

Diagonal force constant $f'_\alpha = \frac{f_\alpha}{r_1 r_2}$ (bend)

where f'_α = bond weighted force constant

f_α = original force constant

r_1 and r_2 are the bond lengths making up angle α

Interaction force constant $f'_{(R1/\alpha)} = \frac{f_{(R1/\alpha)}}{r_1 r_2}$ (stretch/bend)

$$f'_{(\alpha/\beta)} = \frac{f_{(\alpha/\beta)}}{(r_1 r_2 r_3 r_4)^{1/2}} \quad \text{(bend/bend)}$$

where r_1 and r_2 are the bond lengths making up angle α and r_3 and r_4 are the bond lengths making up angle β.

With a restricted Hartree-Fock basis the potential minima are too steep and hence the force constants are too large. For 3-21* basis the errors are 10 - 25%. Fortunately these errors are reasonably consistent between different molecules and may be corrected by reference to previously studied systems.

The force constants were scaled using scaling factors provided by Pulay et al.[59] The completed force field was then used as input data for the vibrational frequency calculations.

The first force field calculated in this way was based on a 3-21G basis set; that is, only s and p orbitals were taken into consideration. However, the resulting vibrational frequencies, although of the right order of magnitude, were not as accurate as would be expected.

One reason for this is that in a dimethyl sulphide molecule a significant amount of d-orbital around the sulphur atom is likely to be occupied. This would vastly increase the strength of the C-S bonds, and hence the associated force constants. The corresponding vibrational frequencies would also increase. The decision was made, therefore, to repeat the calculations using a 3-21* basis set, introducing d-orbitals.

4.3.3 Force Field Results

The molecular parameters for dimethyl sulphide (Figure 4.2) were initially set for the Gaussian 82 programme as follows:[51]

R = 1.82 Å

RH1 = 1.10 Å

RH2 = 1.10 Å

θ = 98°52'

$\beta 1$ = 109.5°

$\beta 2$ = 109.5°

$\alpha 1$ = 109.5°

$\alpha 2$ = 109.5°

τ = 180.0° (torsion)

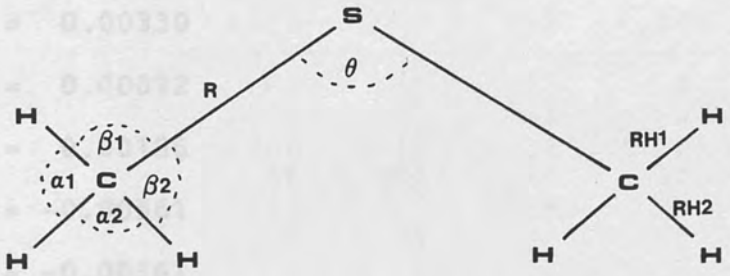

Figure 4.2: Dimethyl Sulphide Molecule

It can be seen that the atoms around each carbon atom were assumed to be in a tetrahedral configuration. However, on optimisation, the equilibrium values of these parameters proved that this was not the case and that one hydrogen atom on each carbon was unique with respect to the other two. For equilibrium (minimum energy) these values become:

R.H.B.N.C.
LIBRARY

R = 1.8158 Å

RH1 = 1.0812 Å

RH2 = 1.0815 Å

θ = 99.4°

$\beta 1$ = 107.6°

$\beta 2$ = 110.6°

$\alpha 1$ = 109.43°

$\alpha 2$ = 109.43°

τ = 180.0° (torsion)

Under these conditions E(RHF) = -474.456927341 AU and the -DE/DR values were (units Hartree/Bohr):

R = 0.00346

RH1 = 0.00055

RH2 = 0.00192

θ = 0.00330

$\beta 1$ = 0.00072

$\beta 2$ = 0.00136

$\alpha 1$ = -0.00561

$\alpha 2$ = -0.00561

τ = 0.00000

On varying each parameter in turn changes in the values of -DE/DR were observed, as shown in Table 4.1. These -DE/DR values were then used to calculate the corresponding force constants using Equation 4.11. The values of change of -DE/DR associated with parameters not listed above were determined by symmetry for the equilibrium position. To simplify this calculation conversion factors were derived for each type of force constant. Each -DE/DR value was then simply multiplied to take into

account the fact that in Equation 4.11 all energy is expressed in Hartrees per Bohr but which, for the purposes of this work, must be converted into mdyne $Å^{-1}$.

These conversion factors were calculated as:

stretch/stretch $f_R = 82389x$

stretch/bend $f_R = 43600x$

bend /stretch $f_R = 47205x$

bend/bend $f_R = 24981x$

where f_R = force constant

$x = \Delta(DE/DR)$

The resulting force constants can be seen in Table 4.2.

Table 4.1: Rate of Change of (-DE/DR) with Change in Molecular Parameter, R, for Dimethyl Sulphide

Molec. Param.	Parameter Changed R1	β1	β2	RH1	RH2	α1	θ
R1	-431	-68	-85	-10	-12	3	-28
R2	6	-12	3	11	-3	-4	-28
θ	-3	-88	33	-10	4	0	-410
RH1	-10	-30	-1	-702	-5	-37	-9
RH2	-12	40	23	-6	-759	5	3
RH3	-12	40	38	-6	-8	41	3
RH4	1	-2	1	1	1	0	-9
RH5	-4	1	0	0	-1	0	3
RH6	-4	1	-4	0	0	1	3
β1	-74	-603	-277	-33	43	-279	-89
β2	-93	-281	-589	-2	24	-272	33
β3	-93	-281	-258	-2	41	-254	33
β4	-13	-21	4	-3	1	0	89
β5	3	4	-3	1	0	0	33
β6	3	4	-6	1	-4	-3	33
α1	4	-282	-272	-41	5	-545	-1
α2	4	-282	-254	-41	55	-261	-1
α3	-4	0	0	-1	1	-1	-1
α4	-4	0	-3	-1	2	-1	-1
τ1	0	0	14	0	-1	16	0
τ2	0	0	-5	0	0	0	0

All Δ(-DE/DR) values are multiplied by 10^5.

Table 4.2: Non-Scaled *Ab Initio* Force Field for Dimethyl Sulphide

Molec. Param.	Parameter Changed R1	β1	β2	RH1	RH2	α1	θ
R1	3.551	0.032	0.401	0.082	0.099	-0.014	0.132
R2	-0.049	0.057	-0.014	-0.091	0.025	0.019	0.132
θ	0.013	0.082	-0.082	0.044	-0.017	0.0	1.274
RH1	0.082	0.142	0.005	5.784	0.041	0.175	0.042
RH2	0.010	-0.189	-0.109	0.049	6.253	-0.024	-0.014
RH3	0.010	-0.189	-0.179	0.049	0.066	-0.194	-0.014
RH4	-0.008	0.009	-0.005	-0.008	-0.008	0.0	0.042
RH5	0.033	-0.005	0.0	0.0	0.008	0.0	-0.014
RH6	0.033	-0.005	0.019	0.0	0.0	-0.005	-0.014
β1	0.323	1.506	0.692	0.144	-0.187	0.697	0.222
β2	0.410	0.702	1.471	0.009	-0.105	0.679	-0.082
β3	0.410	0.702	0.644	0.009	-0.179	0.635	0.082
β4	0.057	0.052	-0.010	0.013	-0.004	0.0	0.222
β5	-0.013	-0.010	0.007	-0.004	0	0.0	-0.082
β6	-0.013	-0.010	0.015	-0.004	0.017	0.007	-0.082
α1	-0.013	0.704	0.679	0.179	-0.022	1.361	0.004
α2	-0.013	0.704	0.635	0.179	-0.240	0.652	0.004
α3	0.013	0.0	0	0.004	-0.004	0.004	0.004
α4	0.013	0.0	0.007	0.004	-0.008	0.004	0.004
τ1	0.0	0.0	-0.035	0.0	0.004	-0.040	0.0
τ2	0.0	0.0	0.012	0.0	0.0	0.0	0.0

Due to molecular geometry, several of the parameters listed in the first column are equivalent. For example, β1 = β4, β2 = β5, RH1 = RH4 and for this reason it was not necessary to vary all the parameters listed.

These force constants were then bond-weighted, as described in Section 4.3.2 and scaled using scaling factors based on those suggested by Pulay.[61]

Pulay's proposed force constant scaling factors were:

C-H stretching	0.8677 (11)
C=C stretching	0.8657 (46)
C-C stretching	0.9215 (87)
C=O stretching	0.8264 (30)
CCC, CCH in plane deformation	0.8025 (23)
C-C=O, C-H formyl deformation	0.8361 (31)
C-H, CH2 wagging	0.7217 (28)
C-H formyl wagging	0.7867 (31)
C=C torsion	0.7837 (48)

The numbers in brackets represent the coefficients of variation.

Since Pulay did not consider sulphur-containing molecules, the scaling factors for modes involving sulphur were estimated using Pulay's work as a guide. Thus the set of scaling factors used initially for this work was as follows:

C-H stretching	0.868
CH2 bending	0.722
C-S-C bending	0.800
H-C-S bending	0.800
C-S stretching	0.800
HCSC torsion	0.750

The completed force field is shown in Table 4.3.

Table 4.3: Scaled Force Constants for Dimethyl Sulphide (Scaling Factors Based on Pulay's Values)

1.	CS	2.841	34.	(SCH1/SCH4)	0.022
2.	CSC	0.250	35.	(SCH1/SCH5)	-0.003
3.	CH1	5.009	36.	(SCH2/SCH3)	0.264
4.	CH2	5.413	37.	(SCH2/SCH5)	-0.003
5.	SCH1	0.616	38.	HCH	0.852
6.	SCH2	0.602	39.	T	0.000
7.	(CS/CS)	-0.039	40.	(HCH1/HCH2)	0.409
8.	(CS/CSC)	0.006	41.	(HCH1/HCH3)	0.002
9.	(CS/CH1)	0.068	42.	(HCH1/HCH4)	0.002
10.	(CS/CH2)	0.008	43.	(HCH1/T)	0.000
11.	(CS/CH4)	-0.007	44.	(HCH1/CS1)	-0.100
12.	(CS/CH5)	-0.027	45.	(HCH1/CS2)	0.014
13.	(CS/SCH1)	0.185	46.	(HCH/CSC)	0.000
14.	(CS/SCH2)	0.234	47.	(HCH1/CH1)	0.123
15.	(CS/SCH4)	0.033	48.	(HCH1/CH2)	-0.017
16.	(CS/SCH5)	-0.007	49.	(HCH1/CH3)	-0.142
17.	(CSC/CH1)	0.019	50.	(HCH1/CH3)	0.000
18.	(CSC/CH2)	-0.007	51.	(HCH1/CH6)	-0.004
19.	(CSC/SCH1)	0.070	52.	(HCH1/SCH1)	0.353
20.	(CSC/SCH2)	-0.026	53.	(HCH1/SCH2)	0.344
21.	(CH1/CH2)	0.042	54.	(HCH1/SCH3)	0.322
22.	(CH1/CH4)	-0.007	55.	(HCH1/SCH6)	0.004
23.	(CH1/SCH1)	0.086	56.	(T/R1)	0.000
24.	(CH1/SCH2)	0.005	57.	(T/CSC)	0.000
25.	(CH1/SCH4)	0.007	58.	(T1/CH2)	0.000
26.	(CH1/SCH5)	-0.002	59.	(T1/CSH2)	0.000
27.	(CH2/CH3)	0.057	60.	(T1/CSH3)	0.000
28.	(CH2/SCH1)	-0.112	61.	HCH3	0.000
29.	(CH2/SCH2)	-0.062	62.	T	0.000
30.	(CH2/SCH3)	-0.107	63.	(T1/SCH6)	0.000
31.	(CH2/SCH5)	0.000	64.	(T1/CH3)	0.000
32.	(CH2/SCH6)	0.010	65.	(HCH1/T1)	0.000
33.	(SCH1/SCH2)	0.185			

The assumption was made that all the force constants involving torsions were equal to zero. All torsion terms actually had values which were either zero or very near zero so this action would have very little efffect on the calculated vibrational frequencies.

It is also noticed that the third H-C-H angle associated with each carbon atom has not been included in the calculation. When establishing a force field, if a redundant angle is

ignored when defining coordinates then all associated terms in the force constant matrix are increased by the value of the force constant of that angle.[63] This results in very large interaction constants, but is a convenient way of simplifying procedures since calculated vibrational frequencies are unaffected.

4.4 Polarisability Data for Dimethyl Sulphide

Of the band polarisability data reported in the literature, very few concern sulphur-containing compounds. A summary of the data available involving simple hydrocarbons is shown in Table 4.4.

Table 4.4: Examples of Bond Polarisabilities and Polarisability Derivatives for Some Simple Hydrocarbons (cm^3)

		$\partial\alpha_x/\partial r$	α_x	α_y	Reference
CH_4	C-H	1.04			1
			0.858	0.546	9
			0.79	0.58	9
C_2H_6 (I)	C-H	1.08			1
	C-C	0.92			1
C_2H_6 (II)	C-H	1.10			1
		1.08			10
	C-C	1.37			1
		1.37			10
$CHCl_3$	C-Cl	0.93			10
			0.118		21
CCl_4	C-Cl	2.08			10

As a first approximation of the molecular polarisability data for the dimethyl sulphide intensity calculations the values given in Table 4.5 were used:

Table 4.5: Initial Polarisability Values Used in DMS Calculations (cm^3)

	$\partial\alpha_x/\partial r$	$\partial\alpha_y/\partial r$	$\partial\alpha_z/\partial r$	α_x	α_y	α_z
C-S	2.000	0.200	0.200	0.800	0.080	0.080
C-H	1.040	0.104	0.104	0.550	0.055	0.055

4.5 Optimisation of Data for Dimethyl Sulphide

4.5.1 Force Field

Since some of the force constant scaling factors were estimated a routine was added to the theoretical calculation programme which enabled these parameters to be optimised. This optimisation was carried out for dimethyl sulphide in the hope that the parameters derived could be transferred to other molecules in the thioether series.

The experimental frequencies observed for dimethyl sulphide (see Chapter 3) were included in the dimethyl sulphide input data file.

The original set of input data was used to generate a theoretical set of vibrational frequencies and these data were then compared with the experimental data and by making use of the Jacobian method, as described in Section 2.3.1, appropriate changes to the original data were calculated. Thus an optimised set of force constant scaling factors was produced. These are as follows:

C-H' stretching	0.822
C-H stretching	0.778
CH2 bending	0.769
C-S-C bending	0.834
H-C-S bending	0.892
C-S stretching	0.894
HCSC torsion	Not Determined

The complete, optimised force field is shown in Table 4.6. This final force field includes allowance for the redundant HCH bending force constant which was previously set to zero for ease of calculation. This involves setting the diagonal force constant for this HCH bend to a suitable value (0.3959 in this case) and subtracting this value from the force constants of all associated modes, as described in Section 4.3.3. This action has no effect on the resulting frequency calculation, but reduces the deceptively high interaction force constant terms to realistic values.

4.5.2 Polarisability Data

In order to optimise the polarisability data the experimentally observed intensities (relative to the intensity of the 458 cm^{-1} band of carbon tetrachloride) were compared with those produced theoretically. Polarisability values were then altered on a trial and error basis until the theoretical values produced were as close as possible to the experimental. The polarisability values which were found to

Table 4.6: Optimised Force Field for Dimethyl Sulphide

1.	CS	3.176	34.	(SCH1/SCH4)	0.020
2.	CSC	0.373	35.	(SCH1/SCH5)	-0.004
3.	CH1	4.754	36.	(SCH2/SCH3)	0.020
4.	CH2	4.868	37.	(SCH2/SCH5)	-0.003
5.	SCH1	0.346	38.	HCH	0.502
6.	SCH2	0.333	39.	T	0.000
7.	(CS/CS)	0.000	40.	(HCH1/HCH2)	0.034
8.	(CS/CSC)	0.063	41.	(HCH1/HCH3)	0.003
9.	(CS/CH1)	0.070	42.	(HCH1/HCH4)	0.003
10.	(CS/CH2)	0.008	43.	(HCH1/T)	0.000
11.	(CS/CH4)	-0.007	44.	(HCH1/CS1)	-0.011
12.	(CS/CH5)	0.028	45.	(HCH1/CS2)	0.015
13.	(CS/SCH1)	0.189	46.	(HCH/CSC)	0.000
14.	(CS/SCH2)	0.240	47.	(HCH1/CH1)	0.129
15.	(CS/SCH4)	0.033	48.	(HCH1/CH2)	-0.017
16.	(CS/SCH5)	-0.008	49.	(HCH1/CH3)	-0.139
17.	(CSC/CH1)	0.020	50.	(HCH1/CH3)	0.000
18.	(CSC/CH2)	-0.006	51.	(HCH1/CH6)	-0.004
19.	(CSC/SCH1)	0.071	52.	(HCH1/SCH1)	0.049
20.	(CSC/SCH2)	0.026	53.	(HCH1/SCH2)	0.040
21.	(CH1/CH2)	0.081	54.	(HCH1/SCH3)	0.018
22.	(CH1/CH4)	0.007	55.	(HCH1/SCH6)	0.004
23.	(CH1/SCH1)	0.081	56.	(T/R1)	0.000
24.	(CH1/SCH2)	0.005	57.	(T/CSC)	0.000
25.	(CH1/SCH4)	0.007	58.	(T1/CH2)	0.000
26.	(CH1/SCH5)	-0.002	59.	(T1/CSH2)	0.000
27.	(CH2/CH3)	0.051	60.	(T1/CSH3)	0.000
28.	(CH2/SCH1)	-0.102	61.	HCH3	0.396
29.	(CH2/SCH2)	-0.057	62.	T	0.000
30.	(CH2/SCH3)	-0.098	63.	(T1/SCH6)	0.000
31.	(CH2/SCH5)	0.000	64.	(T1/CH3)	0.000
32.	(CH2/SCH6)	0.009	65.	(HCH1/T1)	0.000
33.	(SCH1/SCH2)	0.031			

give the best fit between calculated and observed intensities are given in Table 4.7.

Table 4.7: Optimised Polarisability Values for Dimethyl Sulphide (cm^3)

	$\partial\alpha_x/\partial r$	$\partial\alpha_y/\partial r$	$\partial\alpha_z/\partial r$	α_x	α_y	α_z
C-S	2.350	0.205	0.205	1.500	0.080	0.080
C-H	1.700	0.104	0.104	0.550	0.055	0.055

4.6 Results

Tables of frequency and intensity results given by the theoretical calculation programme for dimethyl sulphide, dimethyl sulphide-d6 and ethyl methyl sulphide are shown in Appendix H.

4.6.1 Water

The molecule used as a test for the theoretical calculation was water. The results obtained using the data described in Section 4.2.1 were as follows:

FREQUENCY	ALPHA	BETA SQ.	PAR. INT	PER. INT	P
0.3754162E+04	0.000000	0.040910	0.286373	0.245462	0.857143
0.3653749E+04	0.036427	0.017418	0.181638	0.104509	0.575372
0.1595047E+04	0.000745	0.002377	0.016661	0.014259	0.855859

The positions of the Raman bands to be expected are at 1595.0 cm^{-1}, due to the H-O-H bending motion, 3654.5 cm^{-1} due to the symmetric O-H stretching motion and 3651.7 cm^{-1} due to the anti-symmetric O-H stretching motion.[50]

It can therefore be seen that the vibrational frequencies calculated are very close to those observed experimentally.

The symmetry of each vibration is indicated by its depolarisation ratio. A value of 0.857 (=6/7) indicates an anti-symmetric vibration whilst a ratio less than this indicates symmetry.

4.6.2 Dimethyl sulphide

Agreement between theoretical and experimental Raman band frequencies is very good (Table 4.8), implying that the optimised *ab initio* force field must be fairly representative

of the true force field. The derived force constant scaling factors should, therefore, be transferable to other *ab initio* fields calculated for similar molecules.

There were, however, a few bands observed experimentally which did not appear in the theoretical calculations, notably in the 2800 - 2900 cm^{-1} region. These bands could be overtones of the C-H bending band positioned around 1400 cm^{-1}, or due to Fermi resonance. The presence of such bands makes confident assignment of bands in the C-H stretching region in particular very difficult.

Table 4.8: Dimethyl Sulphide: Comparison of Theoretical and Experimental Vibrational Frequencies

Vibn No.	Vibrational Mode	Vibrational Frequencies (cm^{-1}) Theory	Exptl (Lit)[64]	Exptl (This work)
1	CH' B_1	2995	2998	2987
2	CH' A_1	2994	2998	2987
3	HCS B_2	2962		
4	CH A_2	2959	2970	2970
5	CH B_1	2925	2930	2914
6	CH A_1	2922	2930	2914
7	HCS/HCH A_2	1466	1438	1444
8	HCH B_2	1461	1438	1444
9	H'CH A_1	1436	1438	1424
10	H'CH B_1	1426	1438	1424
11	HCS/HCH A_1	1353	1331	1333
12	HCS/HCH B_1	1348	1315	
13	H'CS A_1	1015	1030	
14	HCS B_2	970	973	
15	HCS A_2	957	950	
16	H'CS B_1	922	902	
17	CS B_1	747	742	744
18	CS A_1	685	694	693
19	CSC A_1	303	282	282

The scaled force constants have been tested for transferability to ethyl methyl sulphide (*trans* and *gauche*) and these results are discussed in Section 4.6.4.

Comparison of the theoretical band intensities with the experimental (Table 4.9) shows the improved set of polarisability data to be also quite satisfactory. However, a routine such as that used for the force field data would be useful in optimising these values in a more complete way, producing the type of 'fine tuning' that is not possible by hand calculations.

Table 4.9: Dimethyl Sulphide: Comparison of Theoretical and Experimental Raman Band Intensities and Depolarisation Ratios

Vibration Number	Relative Band Intensity Theory	Relative Band Intensity Exptl	Depolarisation Ratio Theory	Depolarisation Ratio Exptl
1	94.4	86.7	0.857	0.87
2	00.6		0.857	
3	11.1	68.9	0.857	0.83
4	110.1		0.347	
5	38.2	240.4	0.857	0.19
6	176.8		0.032	
7	2.1	19.3	0.857	0.91
8	9.7		0.841	
9	11.7	11.0	0.856	0.91
10	1.3		0.857	
11	1.0	1.9	0.855	0.48
12	2.6		0.856	
13	14.6		0.848	
14	8.5		0.584	
15	7.6		0.857	
16	1.2		0.857	
17	33.7	24.1	0.857	0.85
18	72.7	72.7	0.128	0.20
19	22.4	21.4	0.032	0.82

Data normalised to 685 cm^{-1} (693 cm^{-1}) band

4.6.3 Dimethyl Sulphide-d6

The optimised force field for dimethyl sulphide was tested for deuterated dimethyl sulphide. The resulting band frequencies, along with the experimental frequencies, can be seen in Table 4.10.

Table 4.10: Dimethyl Sulphide-d6: Comparison of Theoretical and Experimental Vibrational Frequencies and Relative Band Intensities

Vibn No.	Vibrational Frequency (cm^{-1}) Theory	Exptl	Relative Band Intensity Theory	Exptl
1	2221	2240	53.5	74.7
2	2220	2240	6.3	
3	2192	2126	13.1	115.0
4	2191	2126	43.0	
5	2098	2085	1.8	21.3
6	2096	2085	119.3	
7	1062	1044	3.2	13.2
8	1060	1044	3.9	
9	1045	1025	5.7	10.4
10	1034	1025	1.9	
11	1030	822	12.2	3.0
12	1029	-	0.0	
13	796	-	16.8	
14	733	-	8.1	
15	714	-	7.4	
16	711	-	22.5	
17	690	707	4.5	17.8
18	630	642	52.9	52.9
19	264	247	15.3	14.9

Study of Table 4.10 again reveals good agreement between results. This is to be expected since the force field of any molecule should be the same for the deuterated and non-deuterated forms. Nevertheless it is useful to carry out a cross check such as this to reinforce the accuracy of the force field.

Also shown in Table 4.10 is a comparison between theoretical and experimental intensities. As with the force field data the polarisability values are also the same for deuterated and non-deuterated molecules. Thus, since the polarisability data were optimised for dimethyl sulphide, the theoretical intensities for the deuterated form would be expected to be close to the experimental. This is the case for many of the

bands. However, inconsistencies seem to arise due to uncertainties in vibrational assignment, particularly in the C-H stretching region. This is illustrated in Table 4.10 by the band at 2126 cm^{-1} (experimental). The intensity of this band is very close to that of the theoretical band at 2096 cm^{-1}. It is likely, therefore, that these intensities refer to the same band. However, it is difficult to assign the bands in the C-H stretching regions owing to the appearance of additional bands in this region, these being either combination bands or bands due to Fermi resonance.

4.6.4 Ethyl Methyl Sulphide

The theoretical and experimental band frequencies for ethyl methyl sulphide, for both the *trans* and *gauche* conformers are given in Table 4.11. Again some bands observed experimentally do not appear amongst the theoretical bands for the same reasons given for dimethyl sulphide (Section 4.6.2).

On comparing the two sets of frequencies it can be seen that agreement for both conformers is very pleasing, although not all frequencies are as close as for dimethyl sulphide. This is not surprising given that for the additional bonds of ethyl methyl sulphide additional force constants had to be taken from the literature.[51] It is also possible that for some bonds whose characteristics have been assumed to remain constant on moving to a different molecule this is not the case. This is borne out by the many non-zero interaction force constants which have been derived.

Table 4.11: Ethyl Methyl Sulphide: Comparison of Theoretical and Experimental Vibrational Frequencies

Vibration Number	Vibrational Frequency (cm^{-1}) Theory (*trans*)	Theory (*gauche*)	Experimental
1	3010	3011	
2	3006	3006	
3	3002	3002	
4	2999	2999	
5	2998	2998	
6	2960	2963	2967
7	2921	2921	2922
8	2911	2913	2915
9	1447	1446	1450
10	1445	1445	1450
11	1438	1438	1430
12	1438	1411	1430
13	1382	1381	1324
14	1366	1371	1269
15	1322	1322	
16	1294	1289	
17	1143	1143	1244
18	1001	997	1070
19	968	968	1050
20	948	956	
21	946	943	
22	913	908	975
23	732	749	
24	728	727	728
25	710	689	658/682
26	312	334	355/274
27	230	229	223

One very useful result arising from these calculations is the ability to assign bands to the *trans* or *gauche* form. Of particular interest in this case were the bands in the C-S stretching region. As explained in Chapter 3, there is much controversy about the assignment of the three C-S stretching bands to the *trans* and *gauche* conformers.

From the theoretical calculations it is immediately obvious that the highest frequency band at 728 cm^{-1} is due to both conformers. The 682 cm^{-1} band (calculated at 710 cm^{-1}) is due

to the *trans* conformer whilst the band at 658 cm^{-1} (calculated at 689 cm^{-1}) is due to the *gauche* conformer. This information was used to calculate the energy difference between the two conformations (see Chapter 3).

Theoretical and experimental intensity results for ethyl methyl sulphide are given in Table 4.12. Agreement between the experimental and theoretical intensities is quite good, although again not as good as for dimethyl sulphide. This is probably for the same reasons that the frequencies were not as accurate. It must also be remembered that for bands due to just one conformer the theoretical intensities will differ from the experimental results as theoretical calculations will assume 100% of one form, whilst experimentally only a precentage of the sample will be in that form.

Overall, however, the conclusions are that both force field data and polarisability data are transferable between similar thioether molecules, and that theoretical calculations of the type described in this Chapter can be very useful for the prediction of spectra and for spectral analysis.

Table 4.12: Ethyl Methyl Sulphide: Comparison of Theoretical and Experimental Raman Band Intensities and Depolarisation Ratios

Vibration No.	Raman Band Intensity *Trans*	*Gauche*	Exptl	Depolarisation Ratio *Trans*	*Gauche*	Exptl
1	81.6	78.7		0.857	0.857	
2	48.9	48.7		0.857	0.857	
3	20.1	22.8		0.857	0.857	
4	62.5	59.5		0.695	0.696	
5	51.6	54.3		0.759	0.745	
6	99.8	98.5	138.3	0.202	0.202	0.86
7	114.3	114.3	114.3	0.117	0.116	0.48
8	121.5	119.9	163.8	0.123	0.128	0.32
9	8.9	8.1	23.9	0.857	0.855	0.93
10	8.0	7.8		0.857	0.857	
11	1.8	3.0	11.7	0.702	0.808	0.79
12	7.7	7.8		0.857	0.767	
13	9.9	9.0	1.5	0.812	0.774	0.83
14	8.0	7.8	2.8	0.723	0.857	0.41
15	2.8	3.0		0.270	0.332	
16	2.6	2.0		0.813	0.681	
17	7.9	9.2	3.0	0.857	0.850	0.74
18	15.5	9.1	5.3	0.368	0.237	0.41
19	11.1	10.1	5.5	0.857	0.856	0.49
20	6.8	11.4		0.833	0.820	
21	6.1	5.3		0.857	0.851	
22	5.5	7.5	12.6	0.741	0.696	0.88
23	3.4	16.6		0.857	0.679	
24	40.2	27.7	26.9	0.817	0.804	0.75
25	64.8	68.7	38.6/16.1	0.158	0.159	0.35/0.47
26	24.0	22.8	6.9/12.8	0.735	0.832	0.07/0.61
27	7.4	16.2	4.4	0.777	0.809	0.74

CHAPTER 5

USE OF INFRA-RED BAND INTENSITIES IN STRUCTURAL ANALYSIS

5. THE USE OF INFRA-RED BAND INTENSITIES IN STRUCTURAL ANALYSIS

5.1 Introduction

The main use of vibrational spectroscopy is in the elucidation of structure. However, as with Raman spectroscopy, infra-red spectroscopic studies are largely restricted to vibrational frequencies; intensities, where reported, are often limited to indications of band strength with no scale given. The addition of band intensity data would very much increase the amount of information which could be deduced from spectra.

In the past considerable work has been carried out on infra-red intensities, much more so than on Raman intensities. A review of such work related to the intensities of group vibration up to 1967 is given by Wexler.[65] Since then, however, infra-red intensity studies seem to have tailed off. Initially this was due to a lack of reliable force constant data and problems in defining a representative bond dipole model.

It is therefore surprising that with the introduction in recent years of ab-initio force field calculations, vastly improved data handling facilities and the advancement of molecular dipole studies,[66,67] that few workers have pursued in much depth infra-red band intensities for the purpose of structural analysis.

Some recent work by Steele *et al*[68] consisted of a systematic investigation of group absorption band intensities of n-alkanes and methyl n-alkyl ketones. For given regions intensity contributions from each structural group were calculated. The results obtained were then used to predict the infra-red band intensities of three further molecules of related structure. A brief review of these studies is given in this Chapter. A continuation of these investigations has been carried out by Steele[69] to cover n-aldehydes.

The present studies comprised an extension of this work to include some thioethers. The aim of the work was to develop a simple analytical procedure in which the need to separate individual bands is eliminated. The breaking down of a spectrum into component bands introduces errors due to uncertainties in the number of components and band contours. Therefore the ability to avoid such errors would be an advantage.

5.2 Measurement of Infra-red Band Intensities

As with Raman spectroscopy, the accurate measurement of Infra-red band intensities may be hindered by several factors. For example, temperature may affect the bandwidth and intensity, as may various solvents. Intensity changes have also been attributed to various inter and intramolecular forces which are present on transition from the vapour to the liquid to the solid state.

Other factors which have been recognised include uncertainty in baselines caused by drift, cell window reflection losses and difficulties incurred in the measurement of the thickness of very thin sample films.

Thus these factors, where applicable, must be taken into account in cases where accurate infra-red band intensities are required.

For accurate intensity measurements two experimental conditions must be met, namely

(1) The energy which reaches the detector should be as monochromatic as possible; that is, the frequency spread should be small compared with the half band width of the band being measured. The half band width is defined as the frequency difference between the two points where the extinction coefficient, E, has a value of half its maximum (see Figure 5.1).

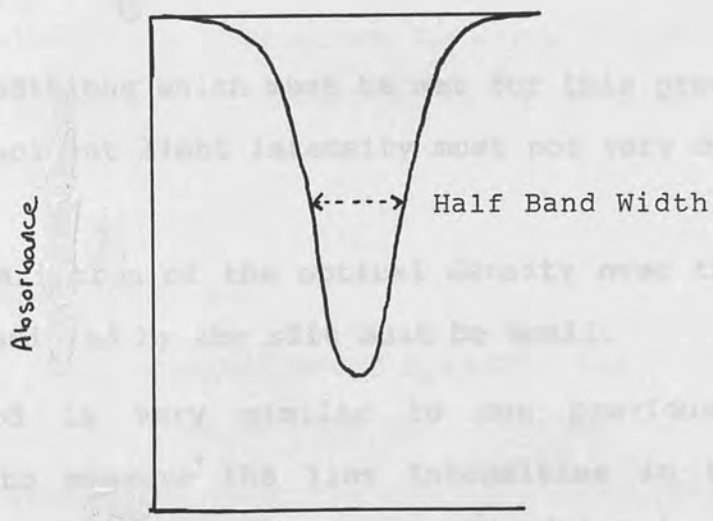

Figure 5.1: Half Band Width

(2) The signal recorded by the detector must be directly proportional to the energy falling on the detector.

In general it is the first of these two conditions which is most difficult to meet, since the second is usually not a problem with most modern spectrophotometers.

The failure to meet the first condition usually arises from the fact that finite slit widths give low values for integrated intensities. This effect is particularly apparent for narrow bands such as are produced by solids and gases.

Several methods have been developed to overcome this problem. One such method is that of Wilson and Wells[70] in which the integrated optical intensity $\int[\log(I_0/I)_\nu d\ln\nu]/c$ is plotted against c

where I_0 = observed incident light intensity

I = observed transmitted intensity

ν = frequency

c = concentration of sample

The plot is then extrapolated to c = 0 to give the true value of I_0/I.

The two conditions which must be met for this procedure are:

(1) The incident light intensity must not vary over the slit width

(2) The variation of the optical density over the frequency range transmitted by the slit must be small.

This method is very similar to one previously used by Bourgin[71] to measure the line intensities in the hydrogen chloride fundamental band. Here $\int(I_0/I)_\nu d\nu/c$ was plotted against c and the same procedure then followed. In Bourgin's case, however, low accuracy results were obtained due to the low resolving power of the instrument used.

Another method which can be used to eliminate the finite slit width error is that known as the 'curve of growth' method.[1] This procedure involves the assumption of a certain band shape, for example, Lorentzian, and the measurement of spectra being made at varying path lengths. In this way the true integral over frequency of the fraction of energy absorbed is equal to that observed.

It can be shown that the intensity of an individual absorption band is given by:

$$I = \frac{N\pi}{3c\nu_i}\left(\frac{\partial\mu}{\partial Q_i}\right)^2$$

where N = total no. of molecules per unit volume

ν_i = transition frequency

μ = molecular dipole

Q = displacement coordinate

This equation does not take into account any collisionally induced contribution, but since this would have very little effect on the resulting intensity it is assumed adequate for most purposes.

5.3 Experimental Details

All spectra were measured using a Perkin Elmer 983 infra-red spectrophotometer, the data being collected and processed by a Perkin Elmer 3600 data station. The cell pathlength was 0.103 mm and spectral resolution varied from 3.6 cm^{-1} at 3000 cm^{-1} to 2.1 cm^{-1} at 1200 cm^{-1}.

It was necessary for the conditions for each spectrum to be identical. To ensure that this was the case samples were investigated as solutions in carbon tetrachloride at concentrations between 3 and 20%.

To correct for cell background and carbon tetrachloride absorptions the following method was used:

(1) Available in memory were three spectra of carbon tetrachloride, one recorded using a cell of path length 0.103 mm, one using a cell of path length 0.025 mm and a third in absorbance units obtained by ratioing the first two, thereby eliminating cell backgrounds.

(2) The spectrum of a sample in carbon tetrachloride (known percentage volume) was recorded. The spectral bands of carbon tetrachloride were then eliminated using the following procedure:

(a) The solution spectrum was stored in one memory, e.g. X.

(b) The carbon tetrachloride spectrum obtained with the same path length cell (in all cases 0.103 mm) was stored in a second memory, e.g. Y.

(c) The carbon tetrachloride spectrum was subtracted from the solution spectrum, the resultant spectrum being stored in a third memory, e.g. Z.

(d) The spectrum in Z was corrected for carbon tetrachloride but by an excess amount equal to the volume fraction of sample in solution.

(e) The absorbance spectrum in carbon tetrachloride was retrieved and multiplied by the appropriate factor and added to the overcorrected sample spectrum stored in Z. This gave the corrected spectrum.

Seven thioethers were studied, the spectra being measured between 4000 and 450 cm-1. for each sample three solutions were prepared in carbon tetrachloride, typically 5%, 10% and 20% v/v. The spectrum for each solution was then obtained and the results for two or three spectral regions were checked for adherence to the Beer-Lambert Law.

The Beer-Lambert Law states that

$$c \propto \log(1/T)$$

or $c \propto A$

where c = concentration

T = transmittance

A = absorbance

Having established that this was the case for each sample the 5% solution was analysed in detail by calculating the integral absorbance for each 25 cm^{-1} region. The intensities of the appropriate sections could then be summed to give the total intensities over the regions of interest. These intensities were corrected for molar concentration.

5.4 Results

5.4.1 Review of Studies of n-Alkanes and Methyl n-Alkyl Ketones

In previous studies[68] the infra-red band intensities of various n-alkanes and methyl n-alkyl ketones have been measured. In these studies the C-H stretching and C-H deformation regions were subdivided at frequencies at which absorption minima occured in the higher n-alkanes.

Plots of intensities in these regions against the number of CH2 units for each of the alkanes and methyl n-alkyl groups produced straight lines, the gradients for the two groups differing only within experimental error.

The two exceptions to this straight line trend were propanone and butanone. These deviations were presumed to be due to the weakening of the C-H bonds alpha and beta to the carbonyl group.

The data were fitted by least squares analysis to:

Intensity = mN + c

where N = number of CH_2 units

m = gradient, equivalent to the intensity contribution per CH_2 unit

c = intercept on the y axis

From the information gathered from this work the corresponding intensities for cyclohexane were predicted. On comparison with the observed intensities these predictions looked very promising. Satisfactory predictions were also carried out for cycloheptanone by making allowances for the C-H weakening effect caused by the carbonyl group.

5.4.2 Thioethers - Infra-red Intensity Results

To ensure adherence to the Beer-Lambert Law the total intensity in the region 3000 - 2800 cm^{-1} was plotted against concentration (see Figure 5.2). This was carried out for each of the four compounds dimethyl sulphide, ethyl methyl sulphide, diethyl sulphide and methyl n-propyl sulphide. The intensity values are shown in Table 5.1.

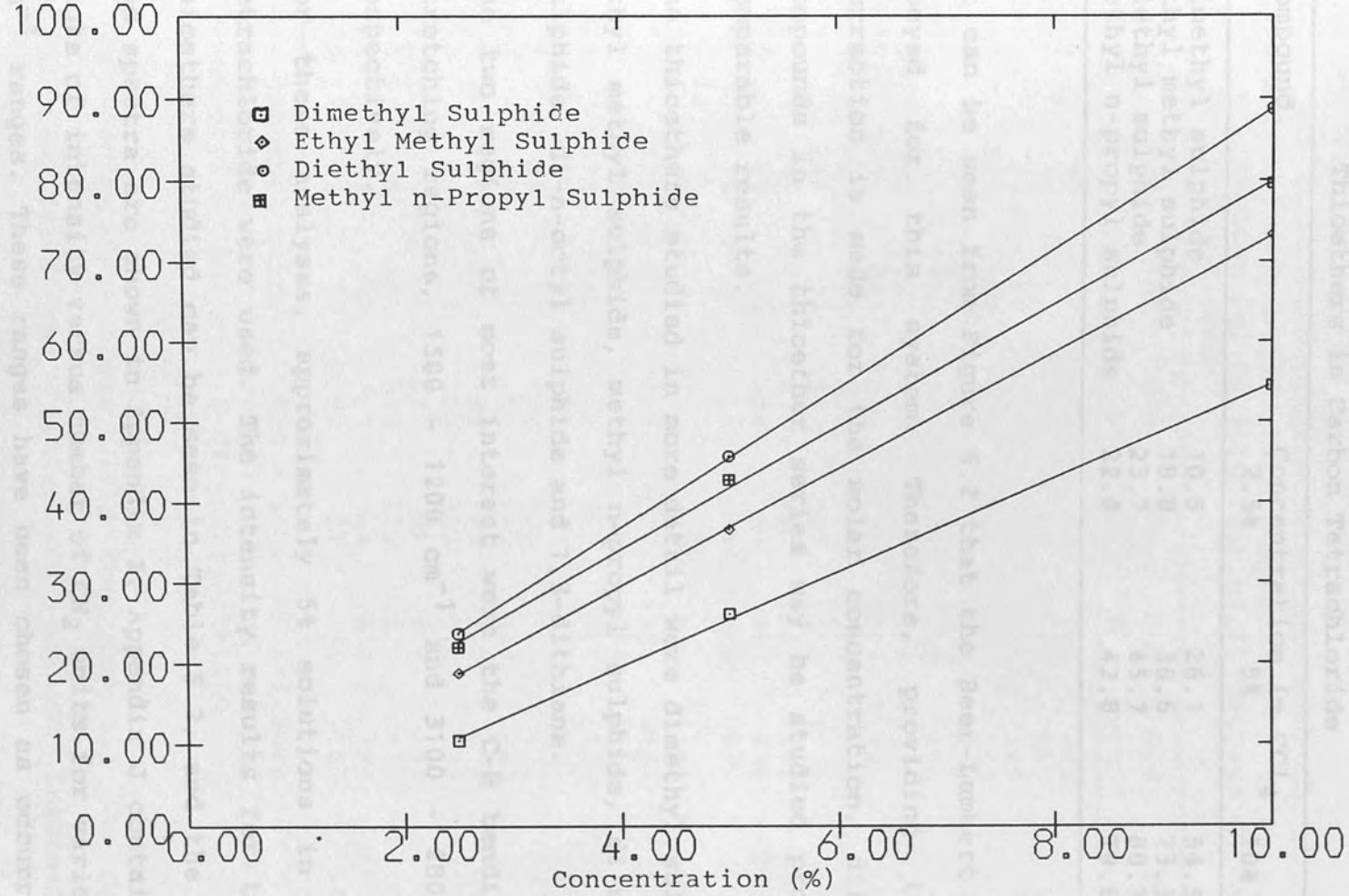

Figure 5.2: Plot of Intensity versus Concentration for Thioethers

Table 5.1: Infra-red Intensities in the Region 3000 - 2800 cm^{-1} for Varying Concentrations of Thioethers in Carbon Tetrachloride

Compound	Concentration in CCl_4 2.5%	5%	10%
Dimethyl sulphide	10.5	26.1	54.5
Ethyl methyl sulphide	18.8	36.6	73.3
Diethyl sulphide	23.7	45.7	88.7
Methyl n-propyl sulphide	22.0	42.8	79.6

It can be seen from Figure 5.2 that the Beer-Lambert Law is obeyed for this system. Therefore, providing that a correction is made for the molar concentration, different compounds in the thioether series may be studied producing comparable results.

The thioethers studied in more detail were dimethyl sulphide, ethyl methyl sulphide, methyl n-propyl sulphide, di-n-hexyl sulphide, di-n-octyl sulphide and 1,3-dithiane.

The two regions of most interest were the C-H bending and stretching regions, 1500 - 1200 cm^{-1} and 3100 - 2800 cm^{-1} respectively.

For these analyses, approximately 5% solutions in carbon tetrachloride were used. The intensity results for the six thioethers studied can be seen in Table 5.2, and the infra-red spectra are shown in Appendix I. Appendix J contains the plots of intensity versus number of CH_2 units for various 25 cm^{-1} ranges. These ranges have been chosen as occurring in regions of band maxima, ie where there is no band overlap. This should eliminate the possibility of intensity migration from one region to another between different compounds. Also

shown are the intensity results for alkanes over the same frequency ranges.

Table 5.2: Infra-Red Absorption Intensities of 25 cm^{-1} Regions for 5% Solutions of Thioethers in Carbon Tetrachloride

$\bar{\nu}$ upper (cm^{-1})	DMS	EMS	DES	MPS	DHS	DOS	1,3-DT
3100	34	57	70	50	146	203	39
3075	38	65	82	63	184	251	34
3050	56	91	123	93	256	344	37
3025	137	199	246	202	432	555	53
3000	507	1098	1556	947	1212	1414	166
2975	586	1424	2454	2602	6731	7730	767
2950	389	1102	1974	1917	10078	15312	895
2925	1194	1465	1596	1989	7201	11392	1433
2900	192	498	826	904	3113	4360	1470
2875	246	533	912	887	5013	7745	282
2850	341	376	376	490	1817	2812	383
2825	69	105	134	168	483	679	255
2800	26	39	55	70	228	329	40
1500	63	93	119	109	223	280	39
1475	127	375	641	628	1924	2484	55
1450	812	834	752	790	936	1134	418
1425	315	330	255	360	371	436	732
1400	78	192	316	229	425	465	233
1375	49	142	244	138	326	471	52
1350	63	70	74	118	257	340	43
1325	216	121	89	149	326	409	44
1300	58	111	222	300	512	573	312
1275	36	726	1029	71	422	541	278
1250	25	129	378	372	379	431	347
1225	23	43	61	64	250	284	181
1200	22	30	39	27	145	182	194

DMS = Dimethyl Sulphide EMS = Ethyl Methyl Sulphide
MPS = Methyl n-Propyl Sulphide DHS = Di-n-Hexyl Sulphide DOS = Di-n-octyl Sulphide 1,3-DT = 1,3-Dithiane

It is evident from these plots that for all the spectral ranges considered the relationship between intensity and number of CH_2 units is approximately linear for the thioethers, although there is some deviation from linearity for the smaller molecules. This deviation is probably due to the weakening effect of the sulphur atom on neighbouring C-H

bonds. This effect has also been observed for the alk-2-ones and n-aldehydes.[68,69]

From the line curvature occurring for low CH_2 unit numbers it appears that the effect of the sulphur atom on intensity is most significant for C-H bonds in the position alpha to the sulphur. Bonds in the beta position are also affected but to a lesser degree.

In a study such as this it would have been useful to have investigated many more compounds in the series, and this could be an area for future work.

It is important to note that the linear portions of the graphs are approximately parallel to the equivalent lines for the n-alkanes, indicating normal alkane character remote from the sulphur site (see Appendix J).

From least squares analysis the equations of the linear portions of the thioether lines in the regions considered are as follows:

$\bar{\nu}$ range (cm^{-1})	
3000 - 2976	Y = 38.2X + 862.1
2950 - 2926	Y = 1092.3X - 325.5
2925 - 2901	Y = 1047.8X - 3276.5
2875 - 2851	Y = 558.0X - 266.4
2850 - 2826	Y = 248.8X - 670.5
1475 - 1426	Y = 155.7X + 329.4
1425 - 1401	Y = 16.3X + 208.5

Let us consider the meaning of these figures. All the larger molecules contain two CH_2 units adjacent to the sulphur atom, two CH_2 units in the beta position and two CH_2 units at some 'distance' from the sulphur, ie having behaviour independent of sulphur. Therefore, as the molecular size is increased, alkane type CH_2 units are added and the intensity increase will be the same as for an n-alkane. Thus the gradients of the n-alkane and thioether intensity versus CH_2 units lines will be equivalent and equal to the intensity contributed by one n-alkane type unit. The reason for the displacement of the thioether line to lower intensity is because in all the thioether molecules there is a lower intensity contribution from the C-H bonds α and β to sulphur.

Thus if the linear portion of the thioether plot is extrapolated the intercept is equivalent to the intensity due to the two terminal CH_3 groups plus the negative contribution exerted by the sulphur atom on nearby C-H bonds.

One inconsistency seen in the intensity plots (Appendix J) is that the line curvature seems to tend towards the alkane line rather than away. The only possible explanation for this is that the sulphur has a smaller intensity reducing effect on an adjacent methyl group than on a CH_2 group in the same position. In the cases where the thioether line actually crosses the alkane line the implication is that the sulphur atom exerts a positive intensity effect on a methyl group in the alpha position, resulting in greater intensity compared to an alkane type methyl group.

5.5 Prediction of Infra-red Intensities

Using these results it is possible to predict the intensity of an n-alkyl sulphide C-H bond for a given 25 cm^{-1} range, providing both alkyl portions of the molecule are propyl or larger. To make predictions for molecules containing ethyl or methyl groups adjacent to sulphur the actual effect which sulphur has on α and β C-H bonds must be quantified.

5.5.1 Stretching Intensities

5.5.1.1 Calculation of S Effect on α and β CH_2 Group Intensities

Consider the region 2950 - 2925 cm^{-1}:

For alkanes the equation of the plot of intensity versus no. of CH_2 units is[69]

$$Y = 1140X + 520$$

i.e. $2I(CH_3)_{alkane} = 520$ (Equation 5.1)

and $I(CH_2)_{alkane} = 1140$

where $I(CH_3)_{alkane}$ = intensity due to an alkyl CH_3 group

$I(CH_2)_{alkane}$ = intensity due to an alkyl CH_2 group

For thioethers the equation of the corresponding line is

$$Y = 1092X - 326$$

i.e. $2I(CH_3)_{alkane}$ + intensity contribution from S = -326 (Equation 5.2)

and $I(CH_2)_{alkane} = 1092$

Therefore from Equations 5.1 and 5.2, the sulphur intensity contribution to the α and β CH_2 groups is -846.

i.e. $2I\alpha + 2I\beta = -846$ (Equation 5.3)

In order to determine the individual intensity values for α and β CH_2 groups it is necessary to have results for a compound containing differing numbers of α and β CH_2 units. The only such compound studied here was 1,3-dithiane, which has the structure:

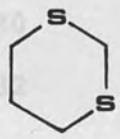

However, 1,3-dithiane is a more complicated case as the CH_2 in the 2 position will be affected by both sulphur atoms, as will the β CH_2.

Therefore, for the region 2950 - 2926 cm^{-1}:

$895 = 4I(CH_2)_{alkane} + 4I\alpha + 2I\beta$

i.e. $895 = 4368 + 4I\alpha + 2I\beta$ (Equation 5.4)

where $I\alpha$ = intensity contribution from S to an α CH_2 group

$I\beta$ = intensity contribution from S to a β CH_2 group

From Equations 5.3 and 5.4:

$4368 + 2I\alpha = 1741$

$-2627 = 2I\alpha$

i.e $I\alpha = -1313.5$ and $I\beta = 890.5$

This result implies that the sulphur atom will decrease the intensity of an α CH_2 group by 1313.5 units in this region, but will increase the intensity of a β CH_2 group by 890.5,

i.e. $I(CH_2)_\alpha = -221.5$

$I(CH_2)_\beta = 1982.5$

Applying the same procedure to the region 2850 - 2826 cm^{-1}:
The equation of the line produced from the plot of intensity versus number of CH_2 units for alkanes is[69]

$Y = 232X - 20$

i.e. $2I(CH_3)_{alkane} = -20$ (Equation 5.5)

$I(CH_2)_{alkane} = 232$

The equation of the equivalent line for thioethers is

$Y = 249X - 671$

i.e. $2(ICH_3)_{alkane}$ + total intensity contribution from S

$= -671$ (Equation 5.6)

and $I(CH_2)_{alkane} = 249$

From Equations 5.5 and 5.6 the sulphur intensity contribution to the α and β CH_2 groups is -651.

i.e. $2I\alpha + 2I\beta = -651$ (Equation 5.7)

Over the same region the observed intensity for 1,3-dithianes was 383.

i.e. $4I(CH_2)_{alkane} + 4I\alpha + 2I\beta = 383$

and $996 + 4I\alpha + 2I\beta = 383$ (Equation 5.8)

From Equations 5.7 and 5.8

$996 + 2I\alpha = 1034$

i.e. $I\alpha = 19$

$I\beta = -344.5$

This result implies that the sulphur atom will increase the intensity of an α CH_2 group by 19 units in this region, but will decrease the intensity of a β CH_2 group by 344.5.

i.e. $I(CH_2)_\alpha = 268$

$I(CH_2)_\beta = -95.5$

5.5.1.2 Prediction of Infra-red Intensity for Methyl n-Propyl Sulphide

The total intensity, I, for methyl n-propyl sulphide in any region of interest can be expressed as follows:

$$I = I(CH_3)_\alpha + I(CH_2)_\alpha + I(CH_2)_\beta + I(CH_3)_{alkane}$$

where $I(CH_3)_\alpha$ = intensity due to an α CH_3 group.

(a) Intensity in the region 2950 - 2926 cm^{-1}

From the intensity observed for dimethyl sulphide (Table 5.2)

$I(CH_3)_\alpha = 389/2 = 194.5$

Therefore for methyl n-propyl sulphide, using values derived in Section 5.5.1.1,

Predicted intensity, $I_{pred} = 194.5 - 221.5 + 1982.5 + 260$

$= 2215.5$

The intensity observed was 1917.

(b) Intensity in the region 2850 - 2826 cm^{-1}

From the observed dimethyl sulphide data (Table 5.2)

$I(CH_2)_\alpha = 341/2 = 170.5$

Therefore for methyl n-propyl sulphide, using values derived in Section 5.5.1.1,

$I_{pred} = 170.5 + 268 - 95.5 - 10 = 333$

The intensity observed was 490.

These predictions seem very promising. In order to carry out more accurate calculations for the intensity values of α and β CH_2 groups it would be necessary to study more molecules in the thioether series, particularly smaller molecules. It must be remembered that 1,3-dithiane is a cyclic molecule and therefore may have properties which differ from those of an n-alkyl sulphide molecule.

It is evident from the study of these two regions that there is conflicting information as to whether the sulphur atom provides a positive or negative intensity contribution to α and β CH_2 groups. One explanation for this could be that the sulphur atom has different effects on different vibrational modes. Alternatively, any band shifts between molecules could explain such observations. Obviously this varies from region to region. In each case, however, the overall effect of this is to reduce the observed intensity compared with that of the corresponding alkane.

5.5.2 Bending Intensities

In the C-H bending region there appeared to be more mixing of intensities between the 25 cm^{-1} regions than in the C-H stretching region. It was therefore considered appropriate to use a slightly different method to analyse these data.

The C-H bending intensities are given in Table 5.2. If we consider molecules which differ in size by one CH_2 unit it is possible to calculate the intensity attributed to that CH_2 unit by subtraction.

This procedure was carried out for each 25 cm^{-1} region between 1350 and 1500 cm^{-1} as shown in Table 5.3. From Table 5.3 it can be seen that for the regions 1500 - 1476 cm^{-1} and 1475 - 1451 cm^{-1} agreement between different calculated values for CH_2 intensity contributions is good.

From these results, however, it is evident that the presence of a sulphur atom increases the intensity of any bending bonds arising from neighbouring CH_2 groups. This effect is only significant as far as the beta position. This is borne out by the fact that the addition of four CH_2 units to dihexyl sulphide to form dioctyl sulphide is essentially equivalent to the addition of four alkane CH_2 units, as seen in Table 5.3.

Table 5.3: Infra-Red Intensities per CH_2 or CH_3 Unit over 25 cm^{-1} Regions between 1500 and 1350 cm^{-1}

	Upper $\bar{\nu}$ limit (cm^{-1})							
	1500	1475	1450	1425	1400	1375	1350	Σ
EMS - DMS	30	248	22	15	114	94	7	530
MPS - EMS	16	253	-44	30	37	-4	48	336
DES - EMS	26	266	-82	-75	124	102	4	365
(DOS - DHS)/4	14	140	50	16	10	36	21	287
$(CH_2)_{alkane}$	11	136	49	10	12	37	16	271
$(CH_3)_{alkane}$	60	293	60	33	134	13	10	603
$(CH_3)_{\alpha}$ (DMS/2)	32	64	406	158	39	25	32	756

EMS = Ethyl Methyl Sulphide DMS = Dimethyl Sulphide
MPS = Methyl n-Propyl Sulphide DES = Diethyl Sulphide
DHS = Dihexyl Sulphide DOS = Dioctyl Sulphide

Table 5.4: Bending Intensities for α and β CH_2 Units over 25 cm^{-1} Regions Determined for Thioethers

	Upper $\bar{\nu}$ limit (cm^{-1})							
	1500	1475	1450	1425	1400	1375	1350	Σ
$(CH_2)_{\alpha}$ + $(CH_3)_{\beta}$	60	321	376	128	158	123	38	1204
$(CH_2)_{\beta}$ - $(CH_3)_{\beta}$	-44	-40	-104	-3	- 97	-17	38	-267
$(CH_2)_{\alpha}$ + $(CH_2)_{\beta}$	16	281	272	125	61	106	76	937

Table 5.5: Comparison of Predicted and Observed Infra-Red Intensities over 25 cm^{-1} Regions for Dihexyl Sulphide and Dioctyl Sulphide

	Upper $\bar{\nu}$ limit (cm^{-1})							
	1500	1475	1450	1425	1400	1375	1350	Σ
DHS predict.	218	1964	958	376	462	460	268	4706
DHS observed	223	1924	936	371	425	326	251	4456
DOS predict.	262	2508	1154	416	510	608	332	5790
DOS observed	280	2484	1134	436	465	471	340	5610

DHS = Dihexyl Sulphide DOS = Dioctyl Sulphide

The region of 1500 - 1451 cm^{-1} is one of fairly high intensity in all the spectra studied. However, between 1450 and 1326 cm^{-1} there is more intensity distribution between 25 cm^{-1} regions. In this instance, therefore, it is also useful to consider total intensities.

The sums of the individual intensities for the systems studied between 1500 and 1326 cm^{-1} are also given in Table 5.3. These total intensities confirm that the sulphur atom has the effect of increasing intensity in the C-H bending region for those CH_2 and CH_3 groups situated close to it.

Let us attempt to quantify the intensities due to α and β CH_2 groups. Consider the group differences between molecules.

$$EMS - DMS = (CH_3)_\beta + (CH_2)_\alpha - (CH_3)_\alpha \qquad \text{(Equation 5.9)}$$

$$DES - EMS = (CH_3)_\beta + (CH_2)_\alpha - (CH_3)_\alpha \qquad \text{(Equation 5.10)}$$

$$MPS - EMS = (CH_2)_\beta + (CH_3)_{alkane} - (CH_3)_\beta \qquad \text{(Equation 5.11)}$$

From Equations 5.9 and 5.10

$$(DES - EMS)/2 + (EMS - DMS)/2 + (CH_3)_\alpha = (CH_3)_\beta + (CH_2)_\alpha \qquad \text{(Equation 5.12)}$$

From Equation 5.11

$$(MPS - EMS) - (CH_3)_{alkane} = (CH_2)_\beta - (CH_3)_\beta \qquad \text{(Equation 5.13)}$$

Adding Equations 5.12 and 5.13 therefore allows the determination of $(CH_2)_\alpha + (CH_2)_\beta$ (see Table 5.4).

5.5.2.1 Prediction of Infra-Red Intensities for Dihexyl Sulphide and Dioctyl Sulphide

A prediction of the infra-red intensities in the C-H bending region was made for dihexyl sulphide and dioctyl sulphide by considering the individual groups which each molecule contains as follows:

Dihexyl sulphide,

$$DHS = 2(CH_3)_{alkane} + 6(CH_2)_{alkane} + 2(CH_2)_{\alpha} + 2(CH_2)_{\beta}$$

Dioctyl sulphide,

$$DOS = 2(CH_3)_{alkane} + 10(CH_2)_{alkane} + 2(CH_2)_{\alpha} + 2(CH_2)_{\beta}$$

Since values for the intensities of all these groups have been determined (Tables 5.3 and 5.4) it was possible to predict the total intensity for each 25 cm^{-1} region as shown in Table 5.5.

A study of Table 5.5 shows that for both dihexyl sulphide and dioctyl sulphide the predicted and observed intensities are very close. Thus the prospect of group transferability between molecules for the prediction of spectra is very encouraging.

CHAPTER 6

CONCLUSIONS AND SUGGESTIONS FOR FURTHER WORK

6. CONCLUSIONS AND SUGGESTIONS FOR FURTHER WORK

Chapter 1 set out the five main aims of this work. These were:

(1) To set up an experimental system for the accurate measurement of absolute Raman band intensities.

(2) To measure the Raman band intensities of various thioethers and thiols and to evaluate the results in terms of potential quantitative applications.

(3) To establish a set of molecular parameters that would allow prediction and analysis of Raman spectra of thioethers, and to study their transferability between molecules.

(4) To calculate theoretical Raman band intensities using a model based on the Wolkenstein assumptions.

(5) To carry out a brief study of the infra-red band intensities of some thioethers.

6.1 Experimental System for the Measurement of Raman Band Intensities

An experimental system has been successfully set up around a Coderg PHO Raman spectrometer. Additions to the spectrometer include a photocell, which accounts for variations in laser power, and a Pockels cell, which allows accurate determination of depolarisation ratios. The spectrometer is controlled with a microprocessor using a BASIC programme written specifically for the purpose. The programme also allows data manipulation and includes options for correcting scattering intensity for variation in frequency (including the instrument calibration) and temperature, and for calculation of band intensities.

Carbon tetrachloride was studied extensively for use as an internal standard and was found to be suitable for the series of compounds being studied. Relative band intensities were measured for several different exciting frequencies. A small trend was seen across the frequencies used. It is therefore important to specify the exciting line used when quoting intensities. The only small anomaly seen was for a 501.7 nm exciting line. However, this result was not a problem in the present work, since this exciting frequency was not used, but it could be the subject of further investigation. Carbon tetrachloride relative band intensities were found not to vary with temperature.

Initial studies on diphenyl acetylene have indicated that this compound could also be useful as a standard, although further work needs to be done before it is used as such.

6.2 Raman Band Intensity Measurements of Thioethers and Thiols

The Raman band intensities of five thioethers and two thiols have been measured. The main problem in carrying out this type of work with these compounds is their volatility. Care must be taken during sample preparation to ensure minimum error. The overall experimental error including sample preparation and variation between replicates has been calculated as 11%.

On the whole the measurement of Raman band intensities looks very promising as a potential analytical method for thioethers and thiols.

In the C-S stretching region the intensity appears to be closely related to the length of the alkyl chain attached to sulphur. Intensity contribution values have been estimated for different parts of the molecule, resulting in a successful prediction of the C-S stretching intensity for t-butane thiol.

However, there is a need for further study in order to understand fully the nature of the factors which affect the intensities of the C-S stretching bands and to quantify them accurately. Work on molecules containing alkyl groups propyl and larger would be particularly useful. Thus it may be possible to explain the low C-S stretching band intensity obtained for methyl propyl sulphide.

The C-H bending and stretching regions in particular show potential for analytical applications since there are several bands which are characteristic of sulphur containing hydrocarbons. Also, the value given by the division of the total intensity by the number of CH groups present has been found to remain constant (CV = 15%) across the series of compounds. This provides a useful method of determining the approximate sizes of the alkyl groups in a molecule.

The only deuterated compound studied was dimethyl sulphide. The intensity results from this and dimethyl sulphide did not appear to comply with Crawford's F-Sum Rule. It would therefore be interesting to carry out a similar procedure for the deuterated compounds of the other thioethers studied.

The results from the methyl ethyl sulphide conformational studies confirm that there is only a very small energy barrier between the *trans* and *gauche* conformers.

Difficulty arose here in the assignment of the three C-S stretching bands. Experimental observations combined with assignments produced by the theoretical calculation programme were not consistent with results reported in the literature. In order to clarify the situation it would be necessary to conduct further investigations, including the measurement of the band intensities of ethyl methyl sulphide in the solid state.

Assuming the theoretical assignments to be correct the energy difference between the two conformers has been calculated as being 8.5 kJ mol^{-1}, *trans* being the more stable conformer.

6.3 Theoretical Calculation of Raman Band Intensities

A programme has been developed which allows the theoretical calculation of Raman band frequencies and intensities.

For the simplest thioether, dimethyl sulphide, a set of molecular parameters has been derived as data for this programme. This includes a force field calculated *ab initio* and molecular polarisability values.

The programme has been tested on deuterated dimethyl sulphide and ethyl methyl sulphide (*trans* and *gauche*) for transferability of molecular parameters between molecules of the same series. The results were quite encouraging, implying that transferability is possible. Discrepancies between theoretical and experimental results for ethyl methyl

sulphide could be due to the necessary addition of some force constants from the literature which were not applicable to dimethyl sulphide.

One area for further work, therefore, could be to establish an *ab initio* force field for a slightly larger molecule in the series, such as ethyl methyl sulphide or methyl propyl sulphide, since dimethyl sulphide differs in that it has no CH_2 groups or C-C bonds.

6.4 Infra-red Band Intensities of Thioethers

A short study has been made of the infra-red band intensities of various thioethers using an approach to the band intensity analysis different from that normally employed. This was an extension of some earlier work.[68,69]

The thioether studies produced results similar to those obtained previously for n-alkanes, alk-2-ones and n-aldehydes. Thus it appears possible that this method of measuring band intensities over 25 cm^{-1} regions, avoiding the necessity for band separation, could provide a technique for thioether analysis.

On investigating the C-H bending and stretching regions it was found that the sulphur atom has an effect on the C-H bands to at least the beta position. An attempt was made to quantify the effects of a sulphur atom on the stretching and bending band intensities of C-H bonds in the alpha and beta positions. Successful predictions of band intensities have resulted from these calculations. Such studies could

therefore be very useful in the prediction and analysis of infra-red spectra of thioethers.

In order to produce the accurate data necessary for analytical application the study would need to be extended to a much wider range of thioethers, including in particular those with larger (greater than four carbons) alkyl groups.

6.5 Conclusions

This work indicates that Raman spectroscopy has much potential as a quantitative analytical technique for thioethers and thiols, especially if used in conjunction with theoretical calculations such as those described here. Infra-red band intensity measurements could also provide a good complimentary or alternative analytical method. In carrying out this work many areas for further study became apparent. Hopefully it will be possible for the work to continue in the future.

CHAPTER 7

REFERENCES

REFERENCES

1. D. Steele in '*Theory of Vibrational Spectroscopy*', W.B. Saunders Company, 1971.

2. C.N. Banwell in '*Fundamentals of Molecular Spectroscopy*', McGraw-Hill Book Company (UK) Ltd., 1972.

3. J. Loader in '*Basic Laser Raman Spectroscopy*', Heyden and Son Ltd., 1970.

4. W.F. Murphy, W. Holzer and H.J. Bernstein, *Appl. Spectrosc.*, **23** (3), 211-218, 1969.

5. H.J. Bernstein and G. Allen, *J. Opt. Soc. Am.*, **45** (4), 237-249, 1955.

6. T. Yoshino and H.J. Bernstein, *J. Mol. Spectrosc.*, **2**, 213-240, 1958.

7. D.M. Golden and B. Crawford Jr., *J. Chem. Phys.*, **36** (6), 1654-1661, 1962.

8. H.W. Schrotter and H.J. Bernstein, *J. Mol. Spectrosc.*, **12**, 1-17, 1964.

9. G.W. Chantry in '*The Raman Effect*', Vol. 1, Chapter 2, A. Anderson ed., Marcel Dekker Inc., New York, 1971.

10. R.E. Hester in '*Specialist Periodical Reports, Molecular Spectroscopy* ', Vol. 2, 439-465, The Chemical Society, 1974.

11. G. Placzek in '*Handbuch der Radiologie*', Vol 6, E. Merk ed., Akademische Verlagsgesellschaft, Leipzig, 1934.

12. P.P. Shorygin, *Russian Chemical Reviews*, **40** (4), 367-389, 1971.

13. J.R. Nestor and E.R. Lippincott, *J. Raman Spectrosc.*, **1**, 305-318, 1973.

14. K.A. Rooney in '*Determination of Absolute Intensities in the Raman Effect for some Organic Liquids*', Chapter 3, Fordham Univ., New York, 1970.

15. L.A. Woodward and J.H.B. George, *Nature*, **167**, 193, 1951.

16. H.W. Schrotter and H.W. Klockner in '*Raman Spectroscopy of Gases and Liquids*', Chapter 4, A. Weber ed., Springer-Verlag, Berlin, Heidelberg, New York, 1979.

17. R.J.H. Clark and P.D. Mitchell, *J. Chem. Soc., Faraday Trans.* II, **71**, 515-524, 1975.

18. G. Eckhart and W.G. Wagner, *J. Mol. Spectrosc.*, **19**, 407-411, 1966.

19. J.C. Evans and H.J. Bernstein, *Can. J. Chem.*, **34**, 1127-1133, 1956.

20. P. Mirone, *Chem. Phys. Lett.*, **4** (6), 323-326, 1969.

20a. D Steele, J.A. Stevens*, D.L. Gerard and W.F. Maddams, *J. Raman Spectrosc.*, **18**, 373-374, 1987.

21. D.A. Long, R.B. Gravenor, D.C. Milner, *Trans. Faraday Soc.*, **59**, 46, 1963.

22. S. Montero, D. Bermejo and W. Klockner, *Mol. Phys.*, **33** (4), 1029-1037, 1977.

23. J. Brandmuller and H. Schrotter, *Ztg. Phys.*, **149**, 131, 1957.

24. D.A. Bahnick and W.B. Person, *J. Chem. Phys.*, **48** (3), 1251-1261, 1968.

25. G.L. Squires in '*Practical Physics*', McGraw-Hill, London, 1968.

26. H. Siebert, *Ztg. anorg. allg. Chem.*, **271**, 65-75, 1952.

27. V.N. Thatte and A.S. Ganesan, *Nature*, **127**, 306, 1931.

28. P. Donzelot and M. Chaix, *Compte Rendu*, **202**, 851-852, 1936.

29. J.R. Durig, M.R. Jalilian, J.F. Sullivan and D.A.C. Compton, *J. Chem. Phys.*, **75** (10), 4833-4839, 1981.

30. K.W.F. Kohlrausch, *Mon. heft. Chem.*, **68**, 349-358, 1936.

31. R.S. Cataliotti, G. Paliano and S. Santini, *Can. J. Phys.*, **64**, 100-106, 1986.

32. M. Ohta, Y. Ogawa, H. Matsuura, I. Harada and T. Shimanouchi, *Bull. Chem. Soc. Jpn.*, **50** (2), 380-390, 1977.

33. S.K. Freeman and D.W. Mayo, *Appl. Spectrosc.*, **27** (4), 286- 287, 1973.

34. J.R. Allkins and P.J. Hendra, *Spectrochim. Acta*, **22**, 2075-2081, 1966.

35. R. Fonteyne, *J. Chem. Phys.*, **8**, 60-62, 1940.

36. G. Geisler and G. Hanschmann, *J. Mol. Struct.*, **8**, 293-306, 1971.

* now Ellwood

37. M. Hayashi, T. Shimanouchi and S. Mizushima, *J. Chem. Phys.*, **26** (3), 608-612, 1957.

38. M. Sakakibara, H. Matsuura, I. Harada and T. Shimanouchi, *Bull. Chem. Soc. Jpn.*, **50** (1), 111-115, 1977.

39. F.R. Dollish, W.G. Fateley and F.F. Bentley in '*Characteristic Raman Frequencies of Organic Compounds*', Chapter 5, Wiley-Interscience.

40. B. Crawford Jr., *J. Chem. Phys.*, **20** (6), 977-981, 1952.

41. M.M. Sushchinskii in '*Raman Spectra of Molecules and Crystals*', Israel Program for Scientific Translations Ltd., 1972.

42. S-I. Mizushima in '*Structure of Molecules and Internal Rotation*', Academic Press Inc., New York, 1954.

43. D.H. Rank, E.R. Shull and D.W.E. Axford, *J. Chem. Phys.*, **18**, 392, 1950.

44. M. Hayashi, M. Adachi and J. Nakagawa, *J. Mol. Spectrosc.*, **86**, 129-135, 1981.

45. M. Ohsaku, Y. Shiro and H. Murata, *Bull. Chem. Soc. Jpn.*, **46**, 1399-1407, 1973.

46. M. Ohsaku and A. Imamura, *Mol. Phys.*, **55** (2), 331-339, 1985.

47. J.R. Durig, D.A.C. Compton and M.R. Jalilian, *J. Phys. Chem.*, **83** (4), 511-515, 1979.

48. N. Nogami, H. Sugeta and T. Miyazawa, *Bull. Chem. Soc. Jpn.*, **48** (12), 3573-3575, 1975.

49. *CRC Handbook of Chemistry and Physics*, R.C. West ed., CRC Press Inc., Florida.

50. G. Herzberg in '*Molecular Spectra and Molecular Structure, II, Infra-red and Raman Spectra of Polyatomic Molecules*', D. Van Nostrand Co. Inc., 1945.

51. D.W. Scott and M.Z. El-Sabban, *J. Mol. Spectrosc.*, 30 (2), 317-337, 1969.

52. W.F. Murphy, *Mol. Phys.*, **33** (6), 1701-1714, 1977.

53. J.C. Decius, *J. Chem. Phys.*, **16** (3), 214-223, 1948.

54. J.H. Schachtschneider and R.G. Snyder, *Spectrochim. Acta*, **19**, 117-168, 1963.

55. R.G.Snyder and G Zerbi, *Spectrochim. Acta*, **23A**, 391-437, 1967.

56. R.G. Snyder and J.H. Schachtschneider, *J. Mol. Spectrosc.*, **30**, 290-309, 1969.

57. R.G. Snyder and J.H. Schachtschneider, *Spectrochim. Acta*, **19**, 85-116, 1963.

58. J. Heckly, Y. Repelin and Nguyen Quy Dao, *Spectrochim. Acta*, **41A** (5), 743-750, 1985.

59. A. Santucci, G Paliani and R.S. Cataliotti, *Spectrochim. Acta*, **41A**, 679-685, 1985.

60. H. Weiser, P.J. Krueger, E. Muller and J.B. Hyne, *Can. J. Chem.*, **47** (10), 1633-1637, 1969.

61. P. Pulay, G. Fogarassi, G. Pongor, J.E. Boggs and A. Vargha, *J. Am. Chem. Soc.*, **105**, 7037-7047, 1985.

62. P.W. Atkins in '*Quanta, A Handbook of Concepts*', Clarendon Press, Oxford, 1974.

63. D. Steele and A. Quartermain, *Spectrochim. Acta*, **43A** (6), 781-789, 1987.

64. G. Geisler and G. Hanschmann, *J. Mol. Struct.*, **11**, 283, 1972.

65. A.S. Wexler, *Applied Spectroscopy Reviews*, **1** (1), 29-98, 1967.

66. W.T. King, G.B. Mast and P.P. Blanchett, *J. Chem. Phys.*, **56** (9), 4440-4447, 1972.

67. W.B. Person and D. Steele in '*Specialist Periodical Reports, Molecular Spectroscopy*, Vol. 2, 357-438, The Chemical Society, 1974.

68. D. Steele, K. Hamilton and J. Stevens*, *Croat. Chem. Acta*, **61** (3), 551-567, 1988.

69. D. Steele, *Spectrochim. Acta*, **44A** (12), 1255-1266, 1988.

70. E. Bright Wilson Jnr. and A.J. Wells, *J. Chem. Phys.*, **14** (10), 578-580, 1946.

71. D.G Bourgin, *Phys. Rev.*, **29**, 794-816, 1927.

72. J. Wilson and J.F.B. Hawkes in '*Optoelectronics: An Introduction*', Prentice-Hall International Inc., 1983.

73. P.W. Atkins in '*Physical Chemistry*', Oxford University Press, 1978.

* now Ellwood

APPENDIX A

Appendix A

Theory of the Pockels Cell

The Pockels Cell[62,72] makes use of Pockels' electro-optic effect which occurs in certain crystals. This effect is a change in the birefringence of a material in the presence of an electric field. Birefringence of a material denotes the presence of different refractive indices for the two polarisation components of a beam of light. This is due to distortion of the electron distribution within the optical medium such that the polarisability and hence the refractive index change anisotropically. This change is a function of the applied field.

If a Pockels cell is used in light which is linearly polarised in the direction for which the refractive index is voltage dependent then it is possible to control directly the phase of the emergent light. Thus, by applying the appropriate voltage, the plane of polarisation may be rotated by 90°.

Examples of useful electro-optic crystals are ammonium dihydrogen phosphate (ADP), potassium dihydrogen phosphate (KDP) and its deuterated isomorph (KD*P) and lithium niobate.

APPENDIX B

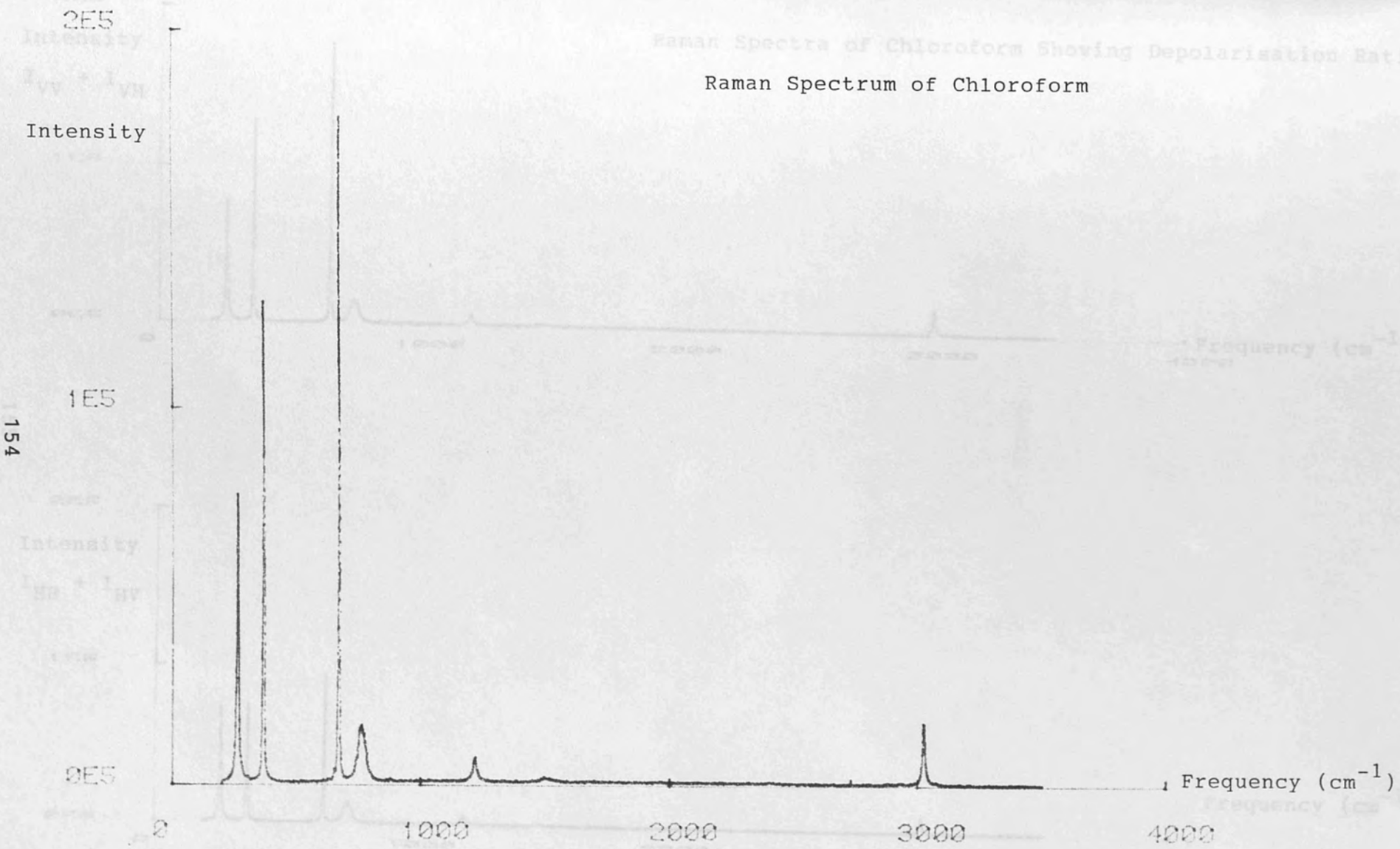
Raman Spectrum of Chloroform
Intensity
2E5
1E5
0E5
0
1000
2000
3000
4000
Frequency (cm^{-1})

Raman Spectra of Chloroform Showing Depolarisation Ratios

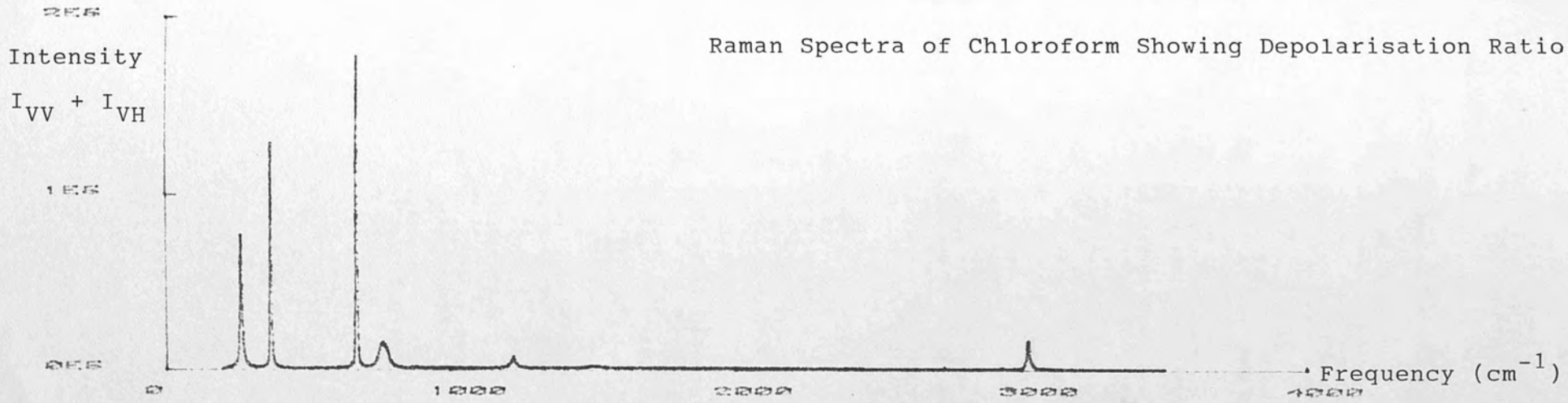

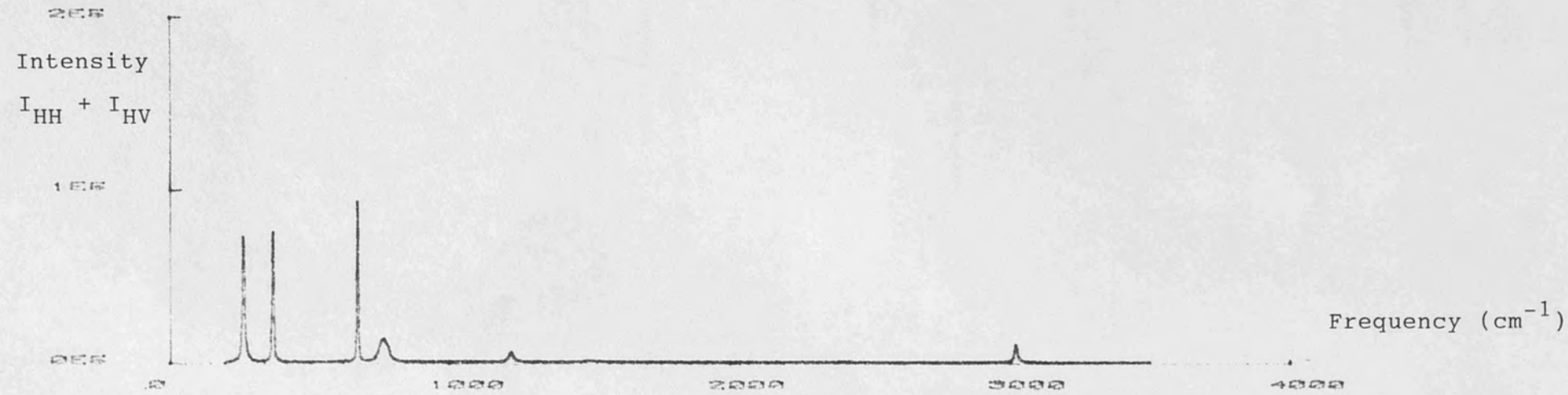

APPENDIX C

Appendix C

Programme for Polynomial Fit Calculations

```
c       this version requires input of frequencies
        implicit real*8(a-h,o-z)
        dimension aint(200),apar(10),cint(200),erR(200),EJAC(200,40)
        DIMENSION AJTJ(45,45),DE(45,45),BJ(40,130),DB(45),DISP(10)
        DIMENSION AINJ(45,45),WS(45),FREQ(200)
        character*13 fred
        write (6,199)
 199    format (' input file name to be processed')
        read (5,200) fred
 200    format (a13)
        writE(6,200) fred
        open(1,file=freq,status='old')
        nc=0
c       on file we should have n0=number of points,frequency 0,reference
c       frequency, frequencies,points to be fitted to polynomial
        read (1,*)n0,v0,v2,((freq(i),aint(i)),i=1,n0)
        writE(8,403)n0,v0,v2,((freq(i),aint(i)),i=1,n0)
 403    format (3x,'n0=',i3,'starting freq.=',f9.1,
       q'ref. freq.=',f9.1,/,(2X,5E10.2,/))
        do 415 i=1,n0
 415    freq(i)=freq(i)/1000
        v2=v2/1000
        v0=v0/1000
        write (6,201)
 201    format ('input number of parameters; ie power of polynomial + 1,
       qfollowed by initial guesses')
        read (5,*) np
        read (5,*)(apar(i),i=1,np)
c       apar contains the current parameter list
c       cint contains the calculated intensities
        IX=N0
        IY=NP
  99    Do 203 i=1,IX
        cint(i)=apar(1)
        do 202 j=2,IY
 202    cint(i)=cint(i)+apar(j)*(FREQ(I)-V2)**(j-1)
 203    err(i)=aint(i)-cint(i)
        ESUM=0.0
        DO 406 I=1,IX

 406    ESUM=ESUM+ABS(ERR(I))
 404    Format (' FREQ/1000=',F9.3,' OBS. int.=',F10.3,'CALC. INT.='
       Q,F10.3,' ERROR=',F10.3,/)
        writE(8,404)((FREQ(i),aint(i),cint(i),err(i)),i=1,IX)
        do 410 i=1,IX
        ejac (i,1)=1.0
        do 410 j=2,IY
        k=j-1
 410    ejac (i,j)=(freq(i)-v2)**k
        WRITE (8,504) (N0,NP,IX,IY)
        do 13 j=1,IY
        do 13 i=1,IY
        ajtj(i,j)=0.0
        do 14 k=1,IX
  14    ajtj(i,j)=ajtj(i,j)+ejac(k,i)*ejac(k,j)
  13    de(i,j)=ajtj(i,j)
        ifail=0.0
        dete=0.0
        WRITE (8,505)(N0,NP,IX,IY)
        NP=IY
```

```
      call f03aaf(de,45,np,dete,ws,ifail)
      WRITE (8,507)(NO,NP,IX,IY)
      WRITE (8,304) dete
304   format (3x,'dete=',e14.6)
      call f01abf(ajtj,45,np,ainj,45,ws,ifail)
      WRITE (8,506)(NO,NP,IX,IY)

      efac=(Esum/(IX-IY))**2
      EFAC=EFAC**0.25
      IZ=IX-IY
      WRITE (8,501),EFAC,ESUM,IZ,IX,IY
501   FORMAT (3X'EFAC=',F14.6,'ESUM=',F14.6,'NO-NP=',(I5),' NO=',(I5),
     Q'NP=',(I5))
      do 125 i=1,IY
      do 125 j=1,i
      ip=i+1
      ajtj(i,j)=ajtj(ip,j)
125   ajtj(j,i)=ajtj(i,j)
303   format (3x,4e14.6)
      do 126 i=1,IY
      do 126 j=1,IX
      BJ(I,J)=0.0
      do 126 k=1,IY
126   bj(i,j)=bj(i,j)+ajtj(i,k)*ejac(j,k)
      do 127 k=1,IY
      db(k)=0.0
      do 127 j=1,IX
127   db(k)=db(k)+bj(k,j)*ERR(j)
      writE(8,411)(db(k),k=1,IY)
411   format (3x,'parameter corr',/,(3(f12.3,2x),/))
      do 412 i=1,IY
      AJTJ(I,I)=ABS(AJTJ(I,I))
      DISP(I)=EFAC*AJTJ(I,I)**0.5
412   apar(i)=apar(i)+db(i)
      WRITE (8,413)((APAR(I),DISP(I)),I=1,IY)
413   FORMAT (' PAR=',F12.3,'  ST. DEV.=',F12.3,/)
      nc=nc+1
      if (nc.ne.4) goto 99
500   FORMAT (3X,'EJAC',/,((3E14.6),/))
502   FORMAT (3X,'JTJ INVERSE',((3E14.6),/))
503   FORMAT (3X,'(JTJ)-1*JT',((3E14.6),/))
504   FORMAT (3X,'NO=',i5,' NP=',i5,' IX=',i5,' IY=',i5)
505   FORMAT (3X,'NO=',I5,' NP=',I5,' IX=',I5,' IY=',I5)
506   FORMAT (3X,'NO=',I5,' NP=',I5,' IX=',I5,' IY=',I5)
507   FORMAT (3X,'NO=',I5,' NP=',I5,' IX=',I5,' IY=',I5)
      end
```

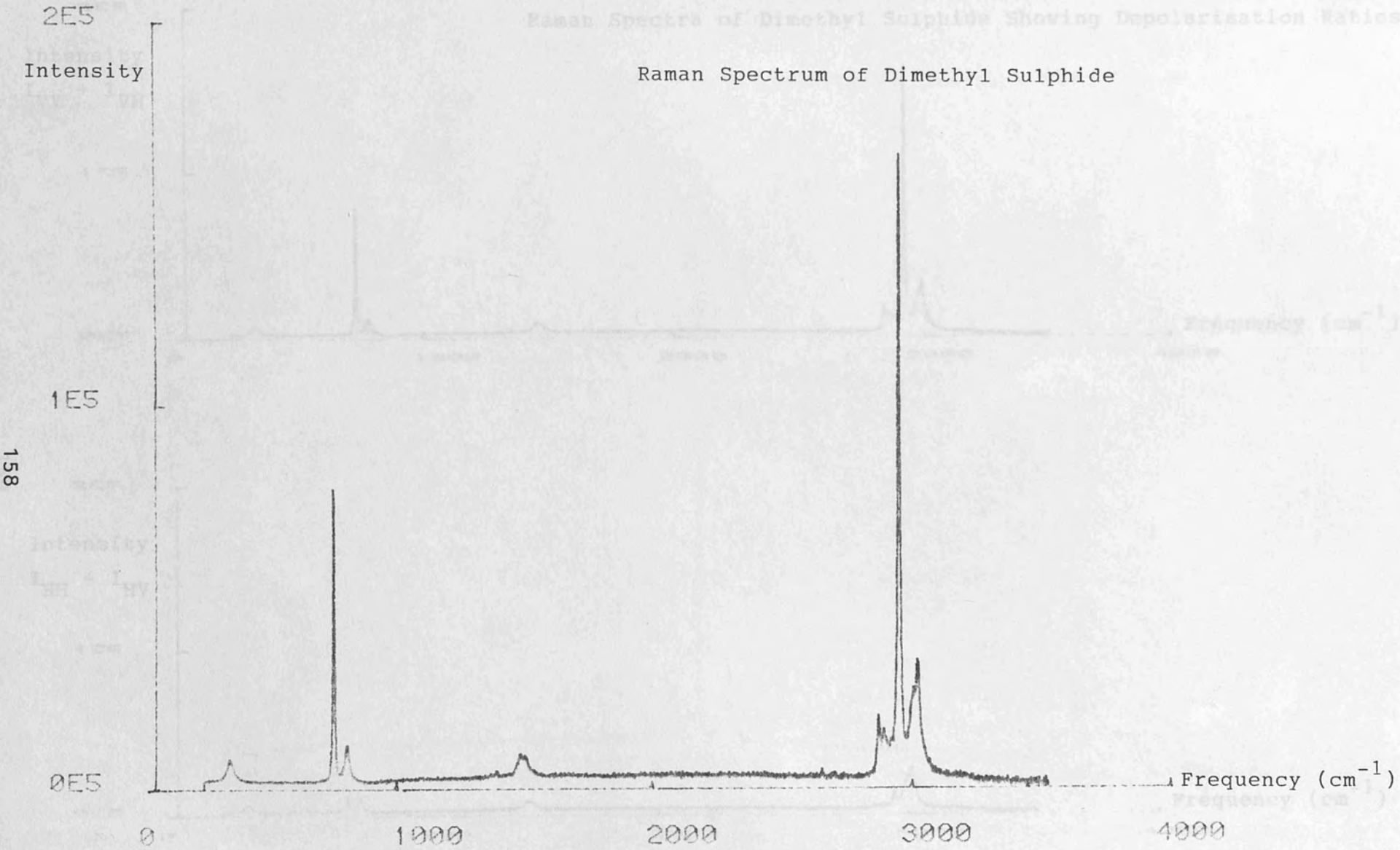
Raman Spectrum of Dimethyl Sulphide
2E5
Intensity
1E5
0E5
0
1000
2000
3000
4000
Frequency (cm^{-1})

Raman Spectra of Dimethyl Sulphide Showing Depolarisation Ratios

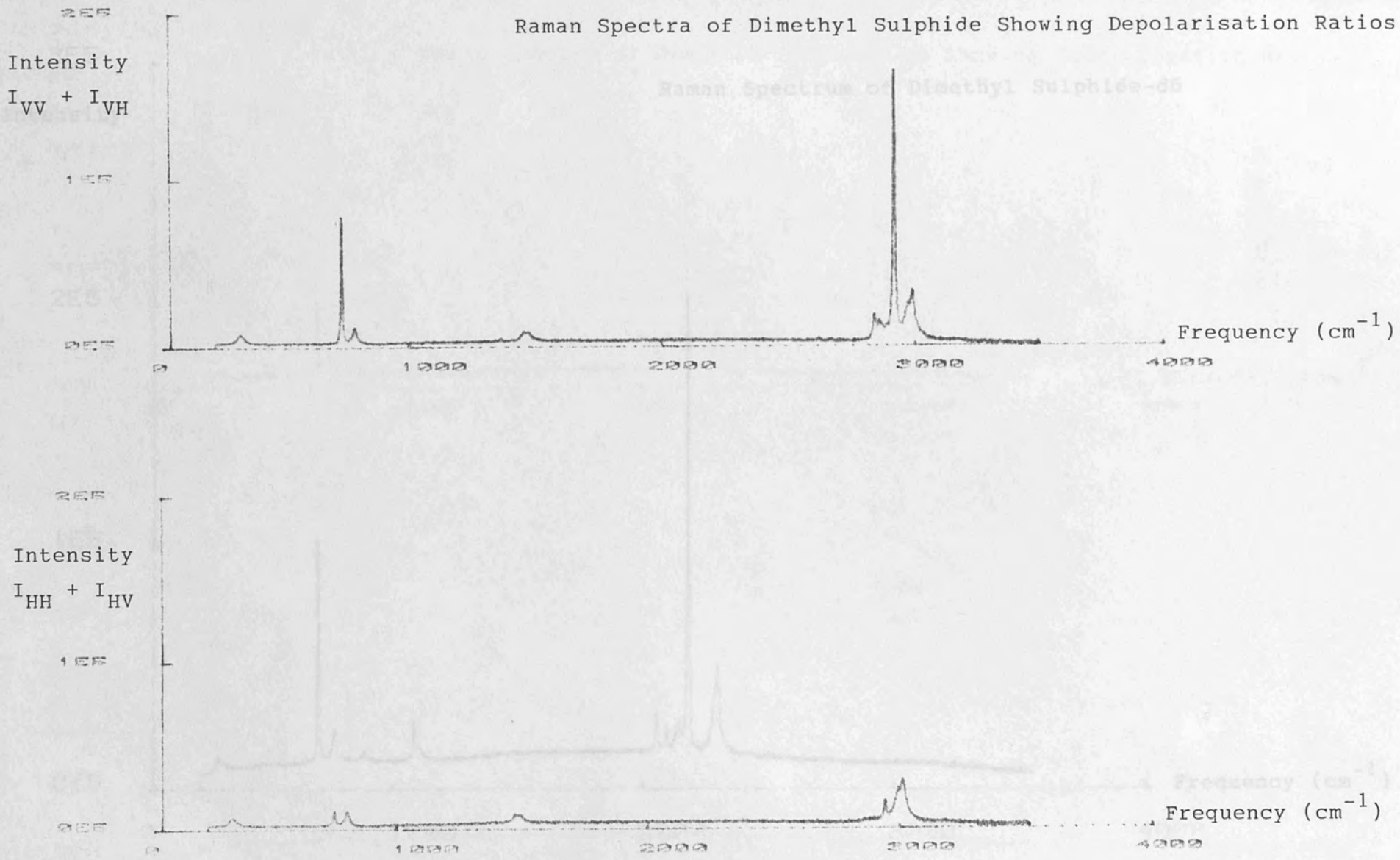

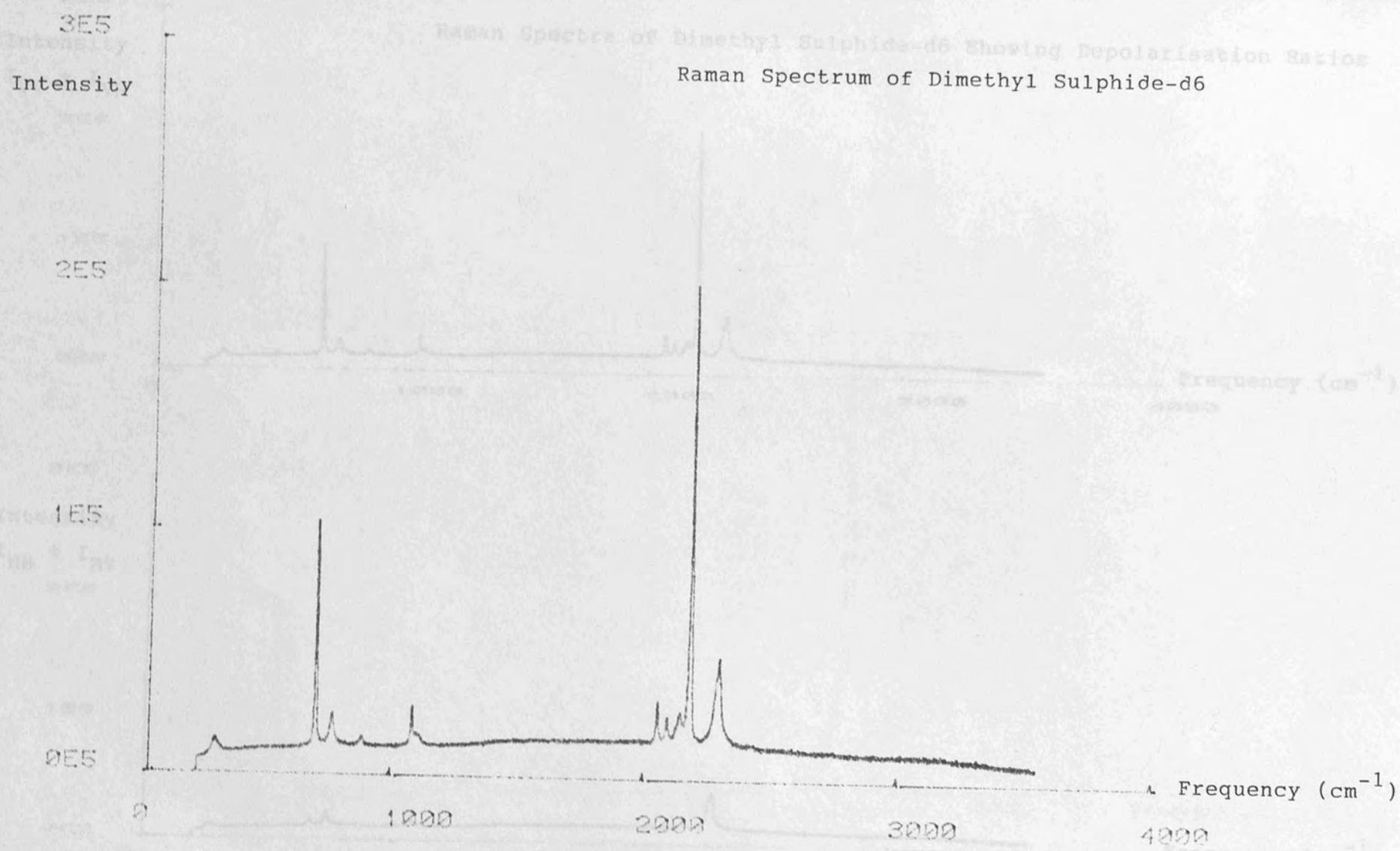
Raman Spectrum of Dimethyl Sulphide-d6
Intensity
3E5
2E5
1E5
0E5
0
1000
2000
3000
4000
Frequency (cm^{-1})

Raman Spectra of Dimethyl Sulphide-d6 Showing Depolarisation Ratios

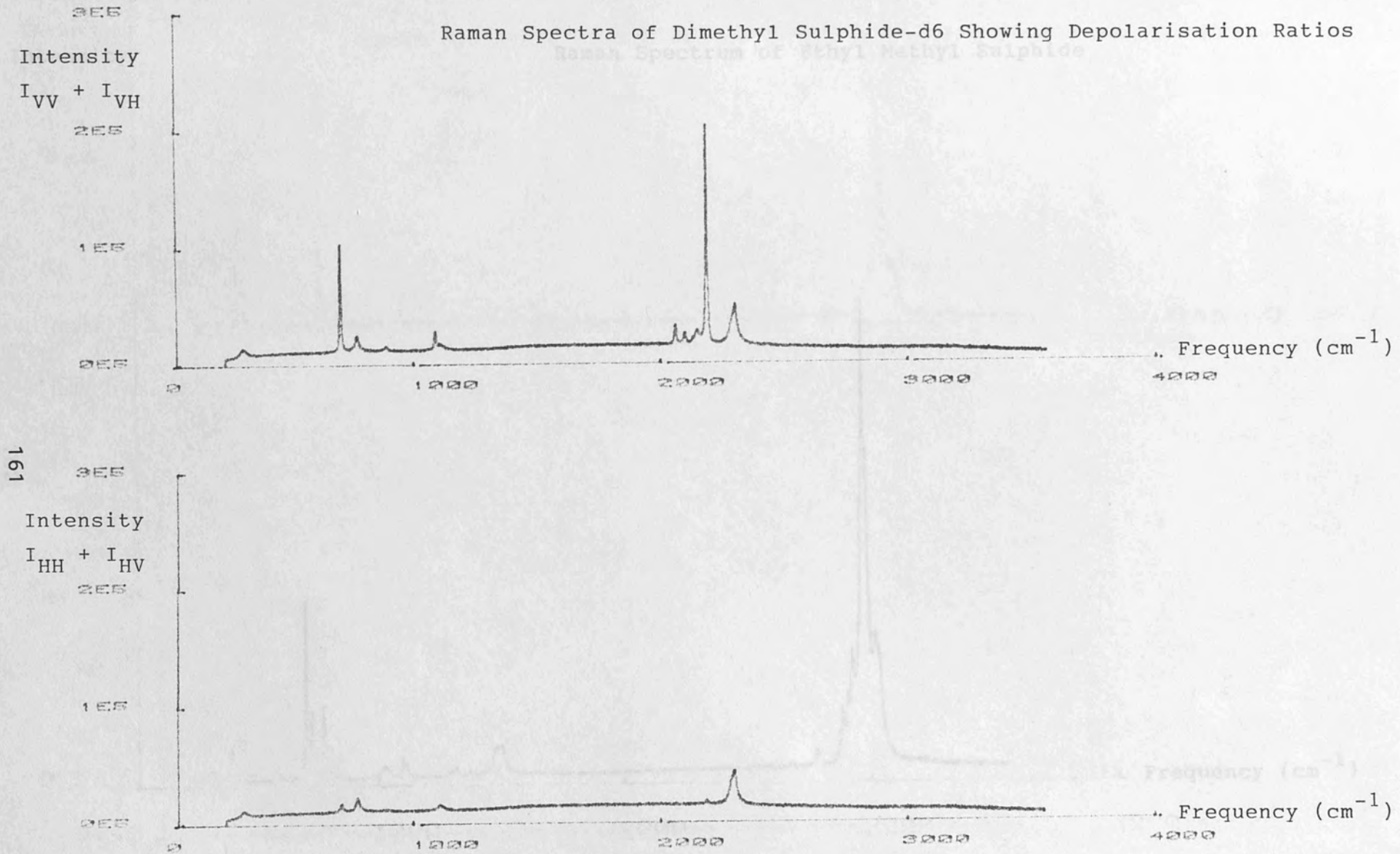

Raman Spectrum of Ethyl Methyl Sulphide

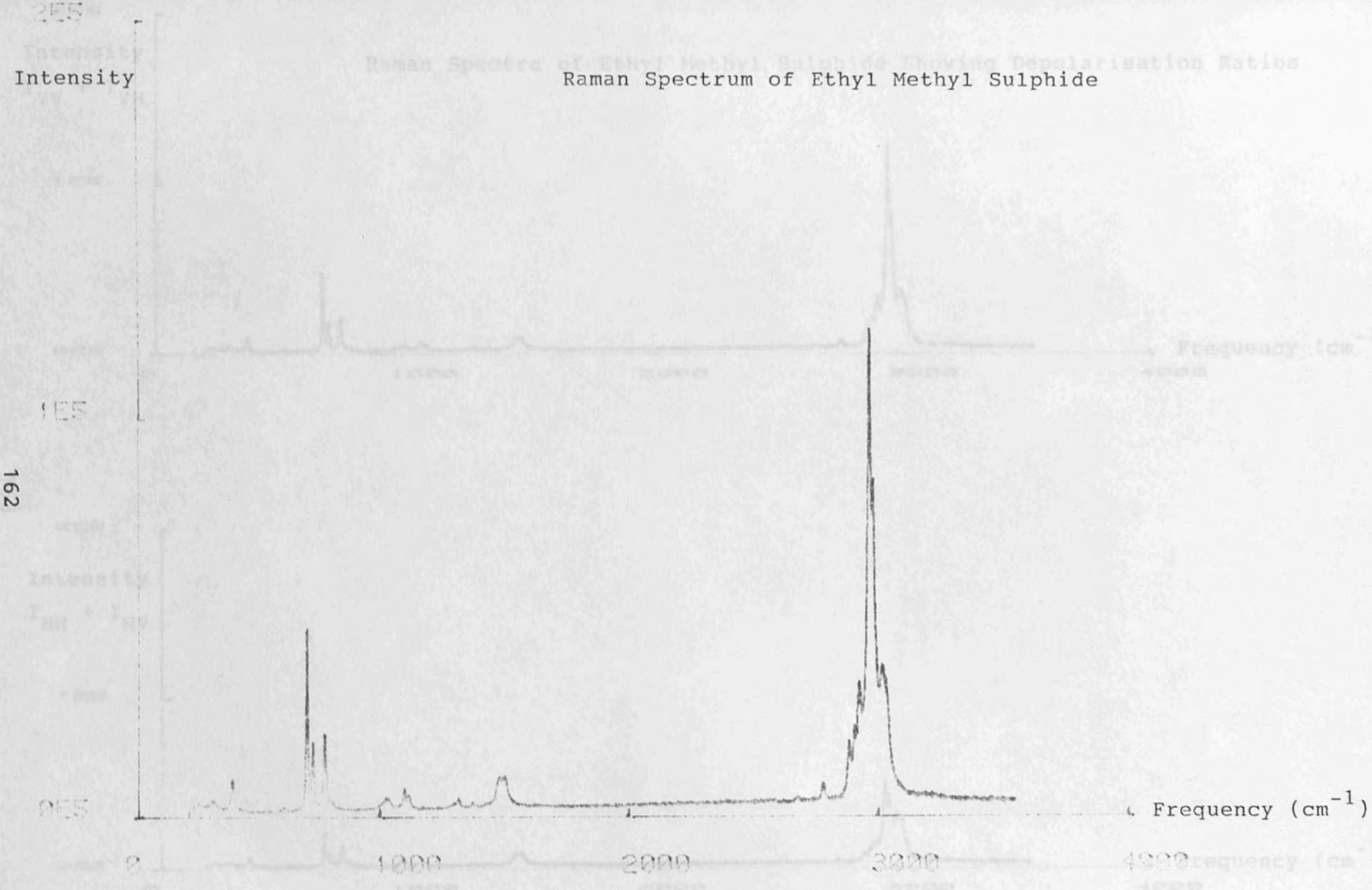

Raman Spectra of Ethyl Methyl Sulphide Showing Depolarisation Ratios

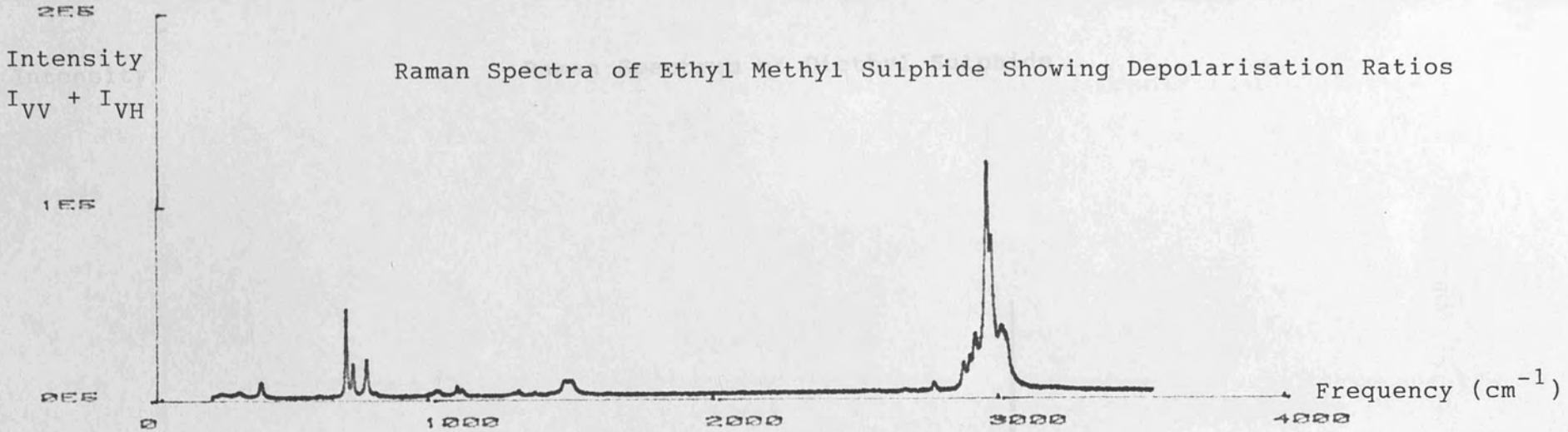

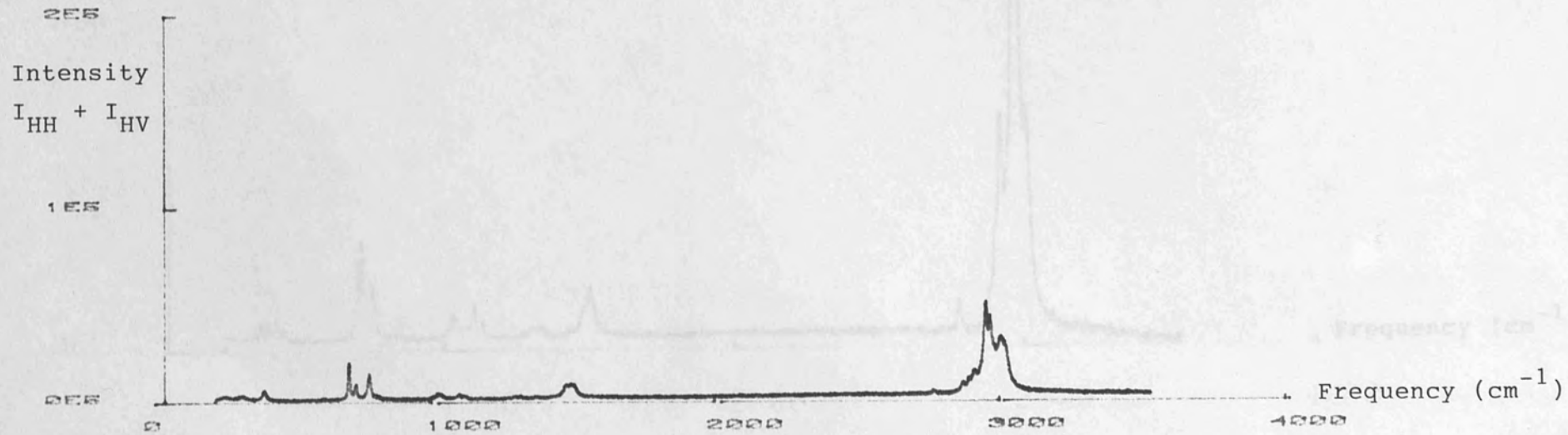

Raman Spectrum of Diethyl Sulphide

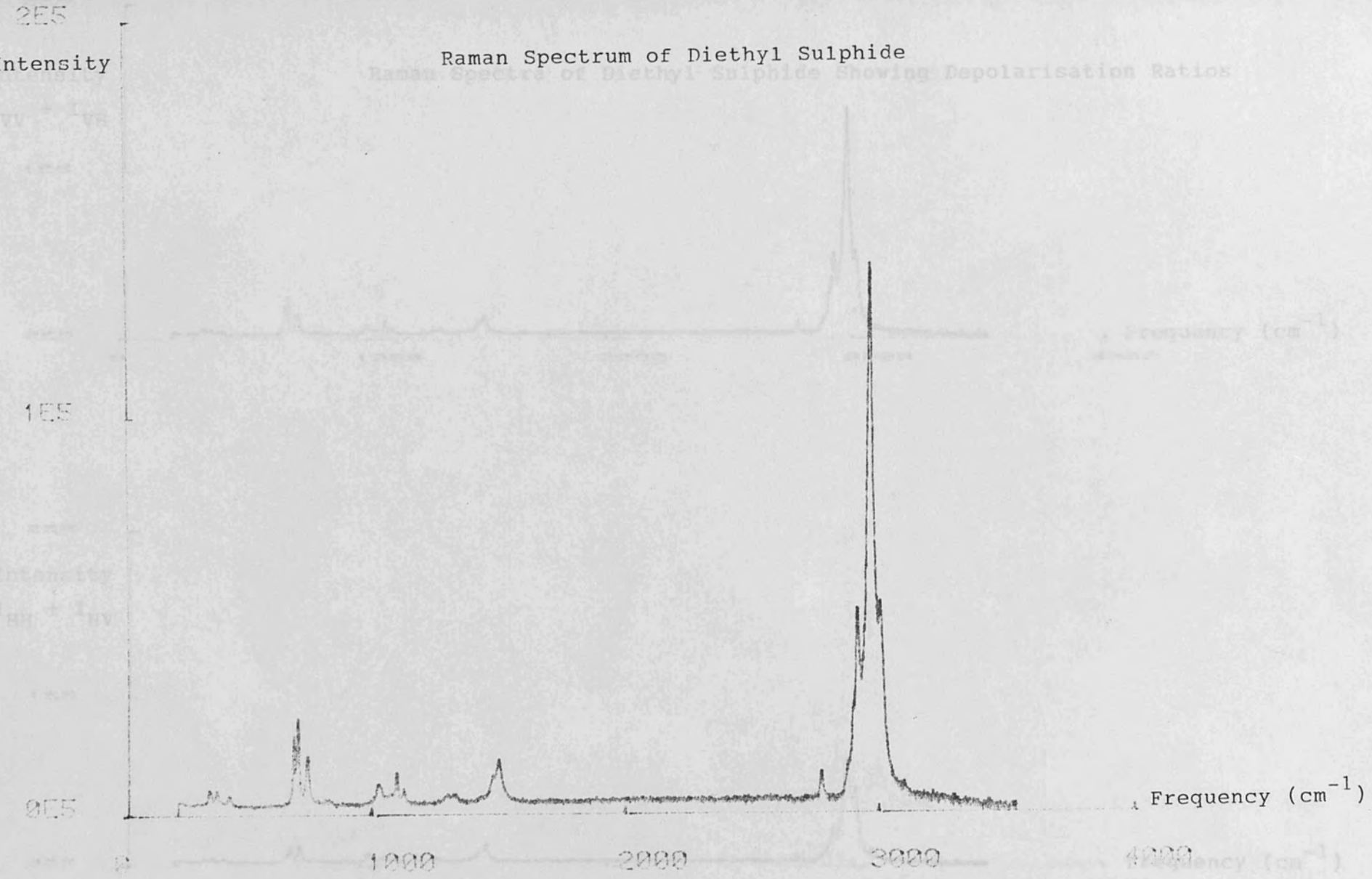

Raman Spectra of Diethyl Sulphide Showing Depolarisation Ratios

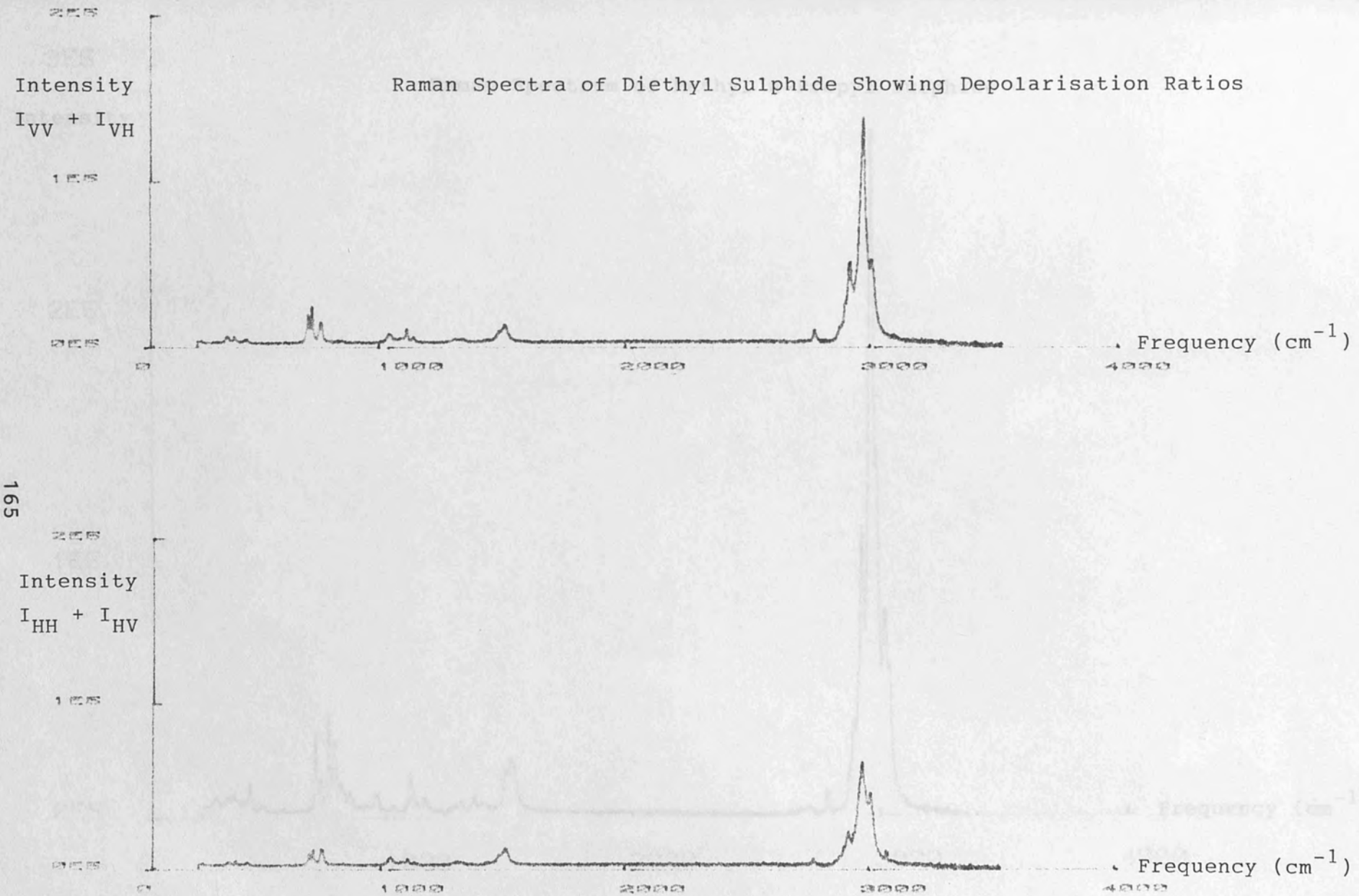

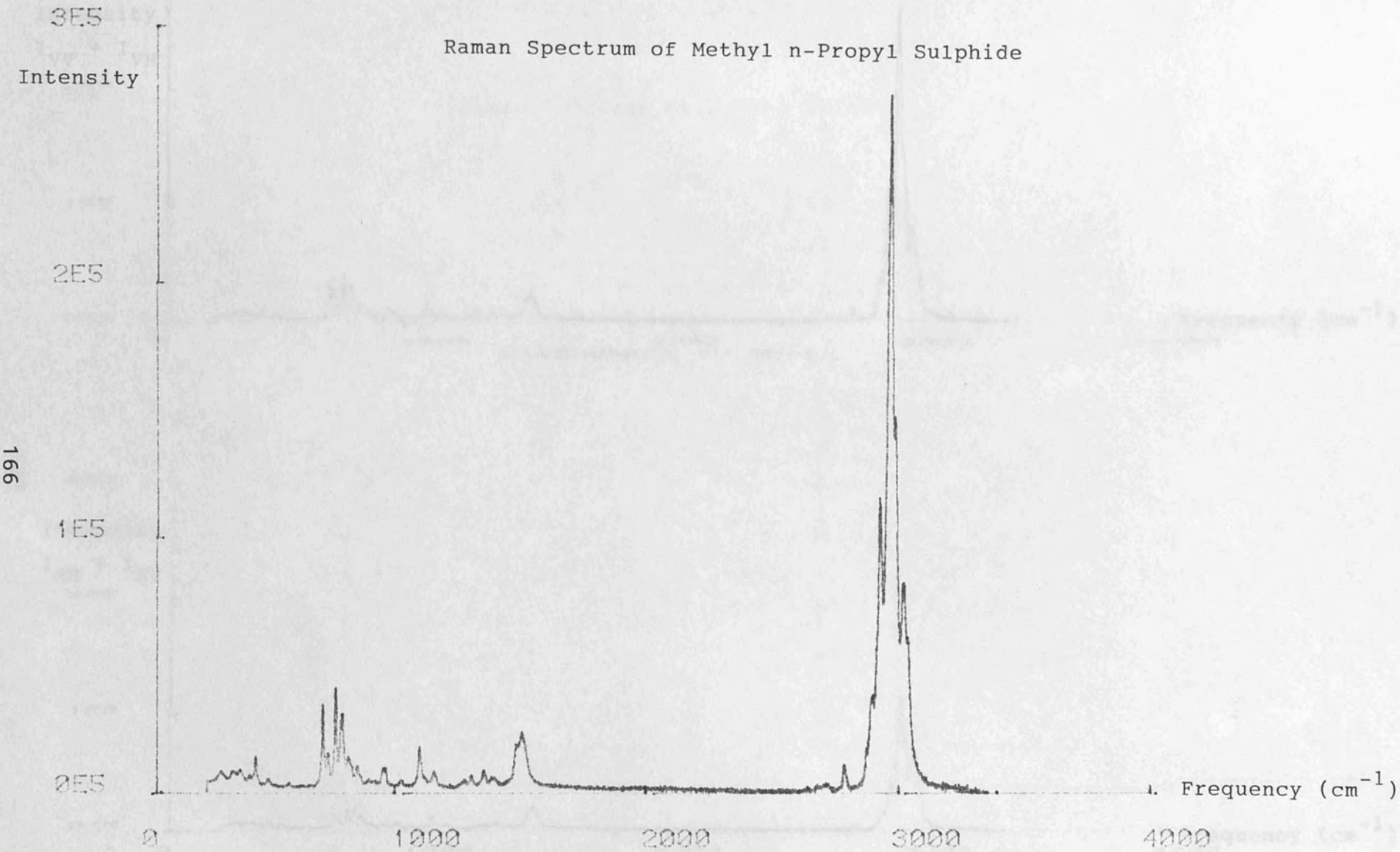
Raman Spectrum of Methyl n-Propyl Sulphide
Intensity
3E5
2E5
1E5
0E5
0
1000
2000
3000
4000
Frequency (cm^{-1})

Raman Spectra of Methyl n-Propyl Sulphide Showing Depolarisation Ratios

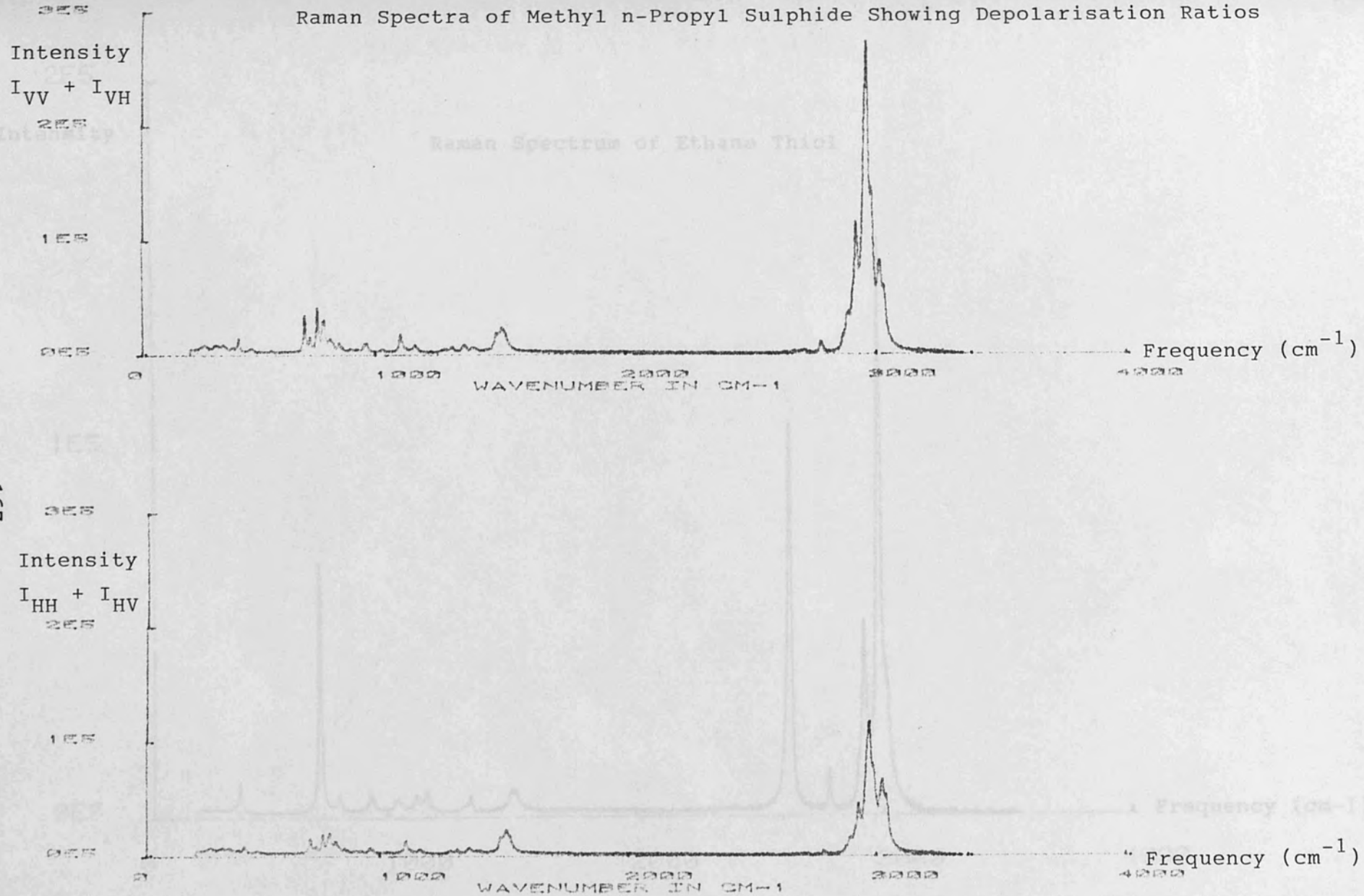

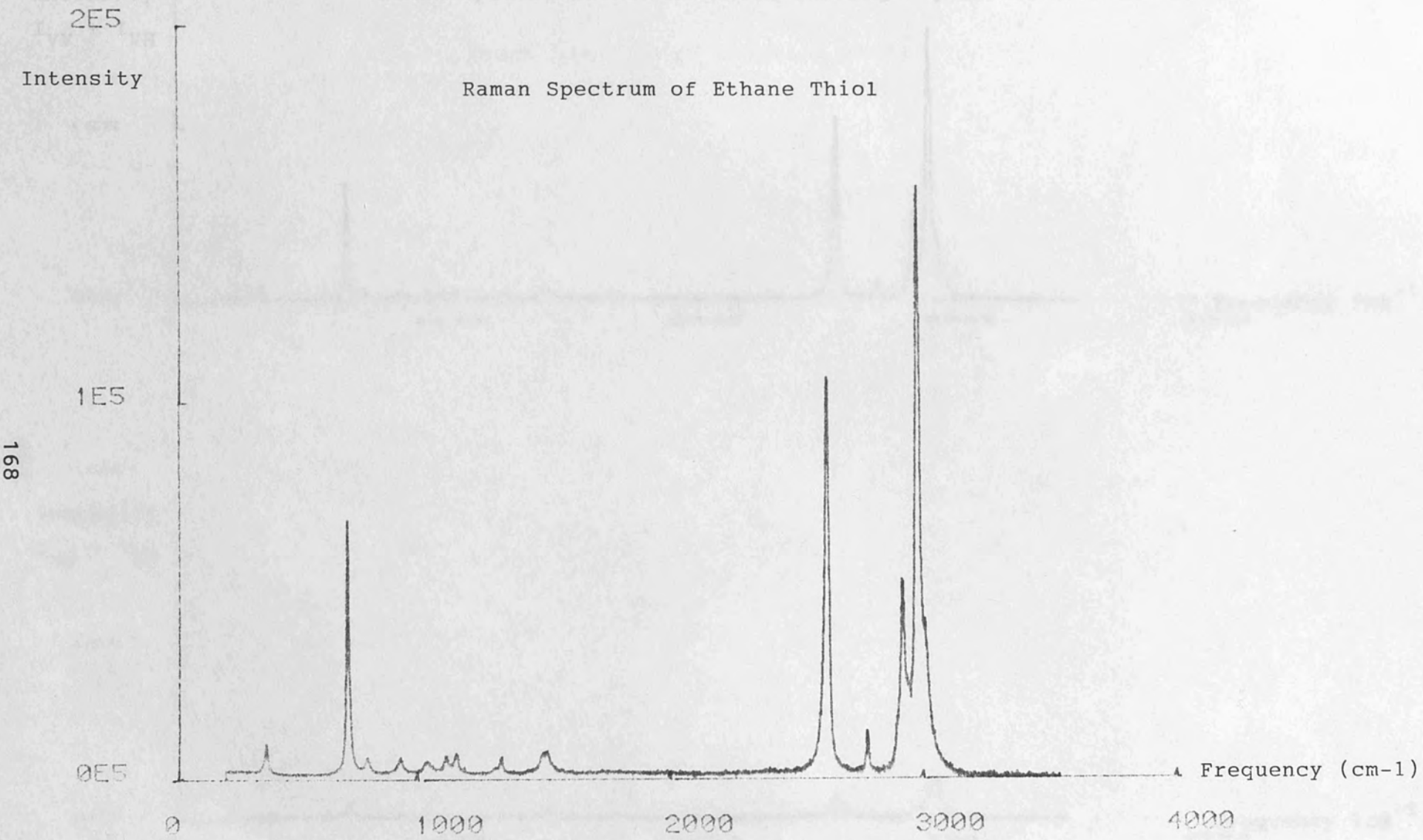
Raman Spectrum of Ethane Thiol
Intensity
2E5
1E5
0E5
0
1000
2000
3000
4000
Frequency (cm-1)

Raman Spectra of Ethane Thiol Showing Depolarisation Ratios

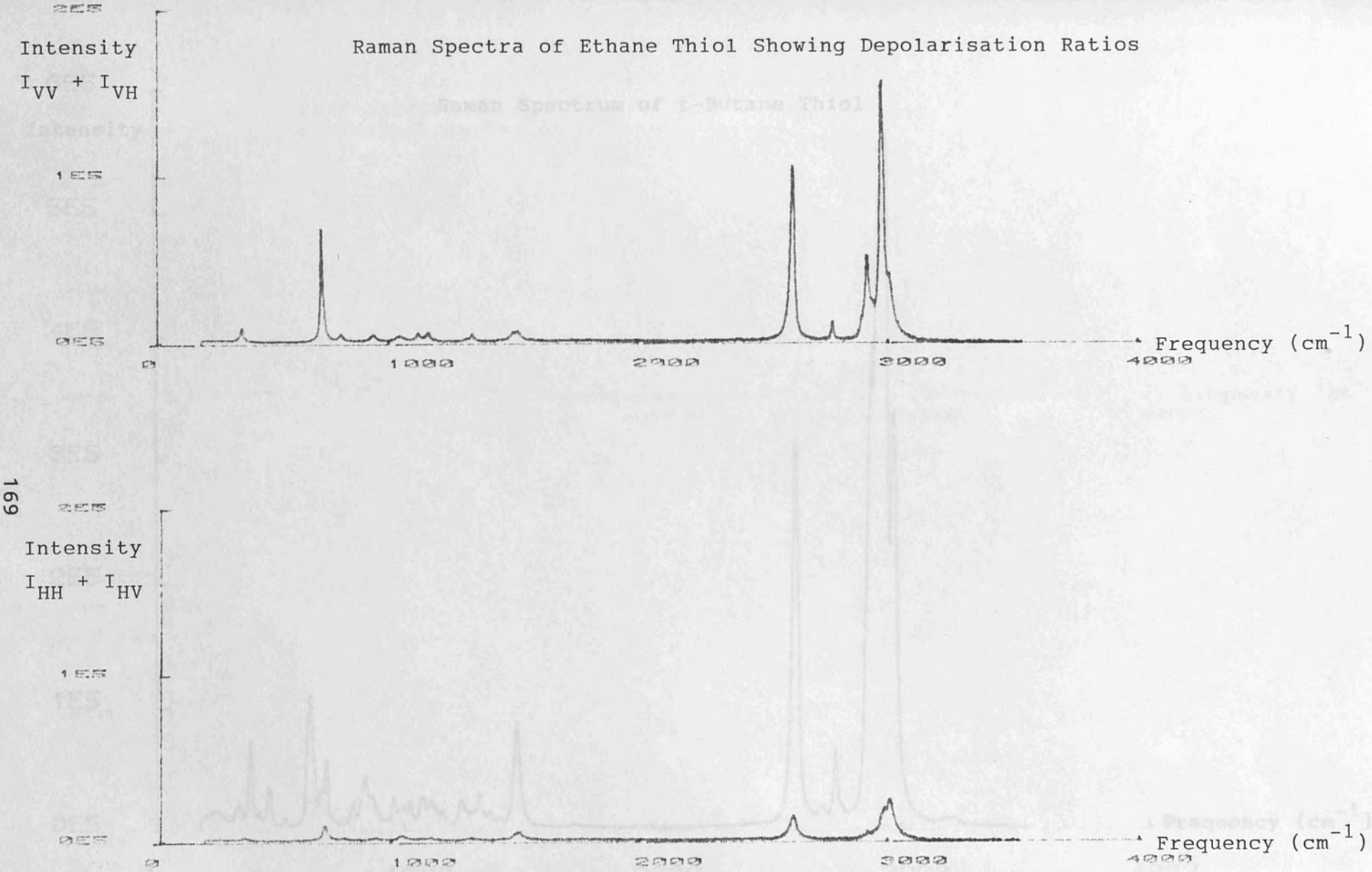

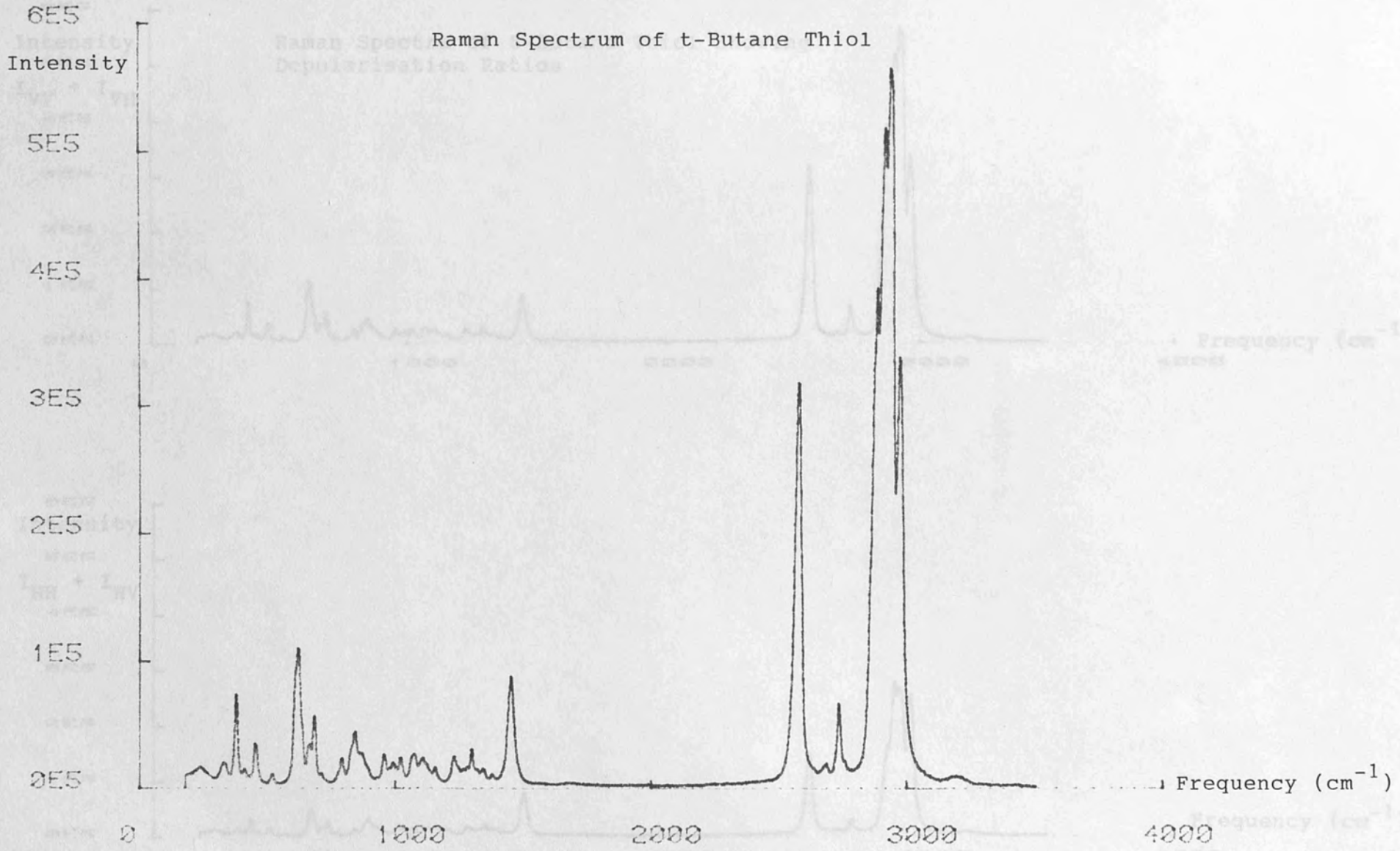
Raman Spectrum of t-Butane Thiol
Intensity
6E5
5E5
4E5
3E5
2E5
1E5
0E5
0
1000
2000
3000
4000
Frequency (cm^{-1})

Raman Spectra of t-Butane Thiol Showing Depolarisation Ratios

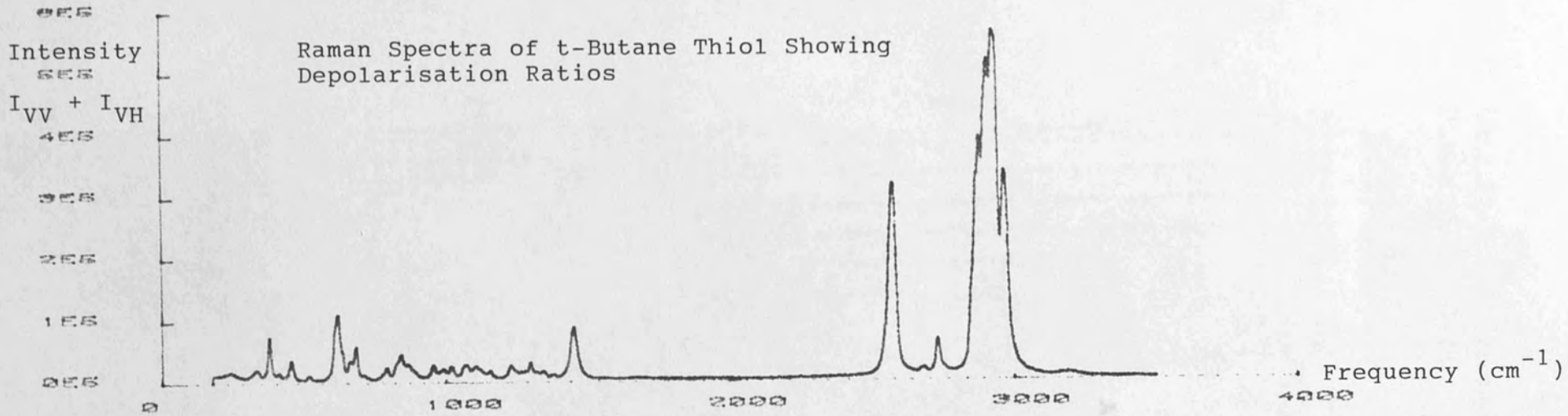

APPENDIX E

Data File for Theoretical Calculation Programme

Dimethyl Sulphide

```
 DIMETHYL SULPHIDE
 1 9 27 1
0.00000  0.00000  0.00000  -1.44400  0.00000  1.10800
1.44400  0.00000  1.10800  -2.35800  0.00000  0.51390
-1.41950  -0.88700  1.73700  -1.41950  0.88700  1.73700
2.35800  0.00000  0.51390  1.41950  -0.88700  1.73700
1.41950  0.88700  1.73700
 1  1  1  2
 2  1  1  3
 3  1  2  4
 4  1  2  5
 5  1  2  6
 6  1  3  7
 7  1  3  8
 8  1  3  9
 9  2  2  1  3
10  2  4  2  1
11  2  5  2  1
12  2  6  2  1
13  2  4  2  5
14  2  4  2  6
15  2  5  2  6
16  2  7  3  1
17  2  8  3  1
18  2  9  3  1
19  2  7  3  8
20  2  7  3  9
21  2  8  3  9
22  4  4  2  1  3
23  4  5  2  1  3
24  4  6  2  1  3
25  4  7  1  3  2
26  4  8  3  1  2
27  4  9  3  1  2
32.06  12.011  12.011  1.0079  1.0079
1.0079  1.0079  1.0079  1.0079
65  196
3.1758  0.3728  4.7535  4.8679  0.3455  0.3325  0.0  0.063  0.0703
0.0083 -0.0069  0.0275  0.1886  0.2396  0.0333  -0.0075  0.0198
-0.0064  0.0714  0.0264  0.0806  -0.0056  0.0806  0.005  0.0073
-0.0022  0.0514  -0.1019  -0.057  -0.0976  0.0  0.0093  0.0305  0.0198
-0.0038  0.0195 -0.0027  0.5021  0.0  0.0343  0.0027  0.0027  0.0
-0.0107  0.0146  0.0  0.1289  -0.017  -0.139  0.0  -0.0036  0.0486
0.0396  0.0176  0.0035  0.0  0.0  0.0  0.0  0.0  0.3959  0.0  0.0
0.0  0.0
CS STR
CSC
CH1 STR
CH2 STR
SCH1
SCH2
CS/CS
CS/CSC
CS/CH1
CS/CH2
CS/CH4
CS/CH5
CS/SCH1
CS/SCH2
CS/SCH4
CS/SCH5
CSC/CH1
CSC/CH2
CSC/SCH1
CSC/SCH2
CH1/CH2
CH1/CH4
CH1/SCH1
CH1/SCH2
CH1/SCH4
CH1/SCH5
CH2/CH3
CH2/SCH1
CH2/SCH2
CH2/SCH3
CH2/SCH5
CH2/SCH6
SCH1/SCH2
SCH1/SCH4
```

```
SCH1/SCH5
SCH2/SCH3
SCH2/SCH5
HCH
TORSION
HCH1/HCH2
HCH1/HCH3
HCH1/HCH4
HCH1/TORSION1
HCH1/CS1
HCH1/CS2
HCH/CSC
HCH1/CH1
HCH1/CH2
HCH1/CH3
HCH1/CH5
HCH1/CH6
HCH1/SCH1
HCH1/SCH2
HCH1/SCH3
HCH1/SCH6
T1/CS1
T/CSC
T1/CH2
T1/SCH2
T1/SCH5
HCH3/HCH3
TORSION
T1/SCH6
T1/CH3
T1/HCH1
1  1  1  1.0
1  2  7  1.0
1  3  9  1.0
1  4  10  1.0
1  5  10  1.0
1  6  11  1.0
1  7  12  1.0
1  8  12  1.0
1  9  8  1.0
1  10  13  1.0
1  11  14  1.0
1  12  14  1.0
1  13  44  1.0
1  14  44  1.0
1  16  15  1.0
1  17  16  1.0
1  18  16  1.0
1  19  45  1.0
1  20  45  1.0
2  2  1  1.0
2  3  11  1.0
2  4  12  1.0
2  5  12  1.0
2  6  9  1.0
2  7  10  1.0
2  8  10  1.0
2  9  8  1.0
2  10  15  1.0
2  11  16  1.0
2  12  16  1.0
2  13  45  1.0
2  14  45  1.0
2  16  13  1.0
2  17  14  1.0
2  18  14  1.0
2  19  44  1.0
2  20  44  1.0
3  3  3  1.0
3  4  21  1.0
3  5  21  1.0
3  6  22  1.0
3  9  17  1.0
3  10  23  1.0
3  11  24  1.0
3  12  24  1.0
3  13  47  1.0
3  14  47  1.0
3  16  25  1.0
3  17  26  1.0
3  18  26  1.0
4  4  4  1.0
4  5  27  1.0
4  9  18  1.0
4  10  28  1.0
4  11  29  1.0
4  12  30  1.0
4  13  48  1.0
4  14  49  1.0
4  17  31  1.0
```

4	18	32	1.0
4	19	50	1.0
4	20	51	1.0
4	22	58	1.0
5	5	4	1.0
5	9	18	1.0
5	10	28	1.0
5	11	30	1.0
5	12	29	1.0
5	13	49	1.0
5	14	48	1.0
5	17	32	1.0
5	18	31	1.0
5	19	51	1.0
5	20	50	1.0
5	22	64	1.0
6	6	3	1.0
6	7	21	1.0
6	8	21	1.0
6	9	17	1.0
6	10	25	1.0
6	11	26	1.0
6	12	26	1.0
6	16	23	1.0
6	17	24	1.0
6	18	24	1.0
6	19	47	1.0
6	20	47	1.0
7	7	4	1.0
7	8	27	1.0
7	9	18	1.0
7	11	31	1.0
7	12	32	1.0
7	13	50	1.0
7	14	51	1.0
7	16	28	1.0
7	17	29	1.0
7	18	30	1.0
7	19	48	1.0
7	20	49	1.0
7	25	58	1.0
8	8	4	1.0
8	9	18	1.0
8	11	32	1.0
8	12	31	1.0
8	13	51	1.0
8	14	50	1.0
8	16	28	1.0
8	17	30	1.0
8	18	29	1.0
8	19	49	1.0
8	20	48	1.0
8	25	64	1.0
9	9	2	1.0
9	10	19	1.0
9	11	20	1.0
9	12	20	1.0
9	13	46	1.0
9	14	46	1.0
9	16	19	1.0
9	17	20	1.0
9	18	20	1.0
9	19	46	1.0
9	20	46	1.0
9	22	57	1.0
9	25	57	1.0
10	10	5	1.0
10	11	33	1.0
10	12	33	1.0
10	13	52	1.0
10	14	52	1.0
10	16	34	1.0
10	17	35	1.0
10	18	35	1.0
11	11	6	1.0
11	12	36	1.0
11	13	53	1.0
11	14	54	1.0
11	16	35	1.0
11	17	37	1.0
11	18	37	1.0
11	20	55	1.0
11	22	59	-1.0
11	25	60	1.0

```
12  12  6  1.0
12  13  54  1.0
12  14  53  1.0
12, 16  35  1.0
12  17  37  1.0
12  18  37  1.0
12  19  55  1.0
12  22  59  1.0
12  25  60  -1.0
13  13  38  1.0
13  14  40  1.0
13  18  55  1.0
13  19  41  1.0
13  20  42  1.0
13  22  43  -1.0
13  25  65  -1.0
14  14  38  1.0
14  17  55  1.0
14  19  42  1.0
14  20  41  1.0
14  22  43  1.0
14  25  65  1.0
15  15  61  1.0
16  16  5  1.0
16  17  33  1.0
16  18  33  1.0
16  19  52  1.0
16  20  52  1.0
17  17  6  1.0
17  18  36  1.0
17  19  53  1.0
17  20  54  1.0
17  22  60  1.0
17  25  59  -1.0
18  18  6  1.0
18  19  54  1.0
18  20  53  1.0
18  22  60  -1.0
18  25  59  1.0
19  19  38  1.0
19  20  40  1.0
19  22  65  -1.0
19  25  43  -1.0
20  20  38  1.0
20  22  65  1.0
20  25  43  1.0
21  21  61  1.0
22  22  39  1.0
23  23  62  1.0
24  24  62  1.0
25  25  39  1.0
26  26  62  1.0
27  27  62  1.0
-1  -1
1  2  3  1  2  -1
2.35  0.205  0.205  1.50  0.08  0.08
1  3  2  2  1  -1
2.35  0.205  0.205  1.50  0.08  0.08
2  4  1  3  1  -1
1.7  0.104  0.104  0.28  0.055  0.055
2  5  1  4  1  -1
1.7  0.104  0.104  0.28  0.055  0.055
2  6  1  5  1  -1
1.7  0.104  0.104  0.28  0.055  0.055
3  7  1  6  2  -1
1.7  0.104  0.104  0.28  0.055  0.055
3  8  1  7  2  -1
1.7  0.104  0.104  0.28  0.055  0.055
3  9  1  8  2  -1
1.7  0.104  0.104  0.28  0.055  0.055

999
```

Data File for Theoretical Calculation Programme

Dimethyl Sulphide-d6

```
 DIMETHYL SULPHIDE
 1 9 27 1
0.00000  0.00000  0.00000  -1.44400  0.00000  1.10800
1.44400  0.00000  1.10300  -2.35300  0.00000  0.51390
-1.41950  -0.88700  1.73700  -1.41950  0.88700  1.73700
2.35800  0.00000  0.51390  1.41950  -0.88700  1.73700
1.41950  0.88700  1.73700
  1  1  1  2
  2  1  1  3
  3  1  2  4
  4  1  2  5
  5  1  2  6
  6  1  3  7
  7  1  3  8
  8  1  3  9
  9  2  2  1  3
 10  2  4  2  1
 11  2  5  2  1
 12  2  6  2  1
 13  2  4  2  5
 14  2  4  2  6
 15  2  5  2  6
 16  2  7  3  1
 17  2  8  3  1
 18  2  9  3  1
 19  2  7  3  8
 20  2  7  3  9
 21  2  8  3  9
 22  4  4  2  1  3
 23  4  5  2  1  3
 24  4  6  2  1  3
 25  4  7  1  3  2
 26  4  8  3  1  2
 27  4  9  3  1  2
32.06  12.011  12.011  2.0158  2.0158
2.0158  2.0158  2.0158  2.0158
65  196
3.1758  0.3728  4.7535  4.8679  0.3455  0.3325  0.0  0.063  0.0703
0.0083 -0.0069  0.0275  0.1886  0.2396  0.0333  -0.0075  0.0198
-0.0064  0.0714  0.0264  0.0806  -0.0056  0.0806  0.005  0.0073
-0.0022  0.0514  -0.1019  -0.057  -0.0976  0.0  0.0093  0.0305  0.0198
-0.0038  0.0195 -0.0027  0.5021  0.0  0.0343  0.0027  0.0027  0.0
-0.0107  0.0146  0.0  0.1289  -0.017  -0.139  0.0  -0.0036  0.0486
0.0396  0.0176  0.0035  0.0  0.0  0.0  0.0  0.0  0.3959  0.0  0.0
0.0  0.0
CS STR
CSC
CH1 STR
CH2 STR
SCH1
SCH2
CS/CS
CS/CSC
CS/CH1
CS/CH2
CS/CH4
CS/CH5
CS/SCH1
CS/SCH2
CS/SCH4
CS/SCH5
CSC/CH1
CSC/CH2
CSC/SCH1
CSC/SCH2
CH1/CH2
CH1/CH4
CH1/SCH1
CH1/SCH2
CH1/SCH4
CH1/SCH5
CH2/CH3
CH2/SCH1
CH2/SCH2
CH2/SCH3
CH2/SCH5
CH2/SCH6
SCH1/SCH2
SCH1/SCH4
SCH1/SCH5
SCH2/SCH3
SCH2/SCH5
HCH
TORSION
```

```
HCH1/HCH2
HCH1/HCH3
HCH1/HCH4
HCH1/TORSION1
HCH1/CS1
HCH1/CS2
HCH/CSC
HCH1/CH1
HCH1/CH2
HCH1/CH3
HCH1/CH5
HCH1/CH6
HCH1/SCH1
HCH1/SCH2
HCH1/SCH3
HCH1/SCH6
T1/CS1
T/CSC
T1/CH2
T1/SCH2
T1/SCH5
HCH3/HCH3
TORSION
T1/SCH6
T1/CH3
T1/HCH1
1  1  1  1.0
1  2  7  1.0
1  3  9  1.0
1  4  10  1.0
1  5  10  1.0
1  6  11  1.0
1  7  12  1.0
1  8  12  1.0
1  9  8  1.0
1  10  13  1.0
1  11  14  1.0
1  12  14  1.0
1  13  44  1.0
1  14  44  1.0
1  16  15  1.0
1  17  16  1.0
1  18  16  1.0
1  19  45  1.0
1  20  45  1.0
2  2  1  1.0
2  3  11  1.0
2  4  12  1.0
2  5  12  1.0
2  6  9  1.0
2  7  10  1.0
2  8  10  1.0
2  9  8  1.0
2  10  15  1.0
2  11  16  1.0
2  12  16  1.0
2  13  45  1.0
2  14  45  1.0
2  16  13  1.0
2  17  14  1.0
2  18  14  1.0
2  19  44  1.0
2  20  44  1.0
3  3  3  1.0
3  4  21  1.0
3  5  21  1.0
3  6  22  1.0
3  9  17  1.0
3  10  23  1.0
3  11  24  1.0
3  12  24  1.0
3  13  47  1.0
3  14  47  1.0
3  16  25  1.0
3  17  26  1.0
3  18  26  1.0
4  4  4  1.0
4  5  27  1.0
4  9  18  1.0
4  10  28  1.0
4  11  29  1.0
4  12  30  1.0
4  13  48  1.0
4  14  49  1.0
4  17  31  1.0
4  18  32  1.0
4  19  50  1.0
4  20  51  1.0
4  22  58  1.0
```

```
5   5   4   1.0
5   9   18   1.0
5   10   28   1.0
5   11   30   1.0
5   12   29   1.0
5   13   49   1.0
5   14   48   1.0
5   17   32   1.0
5   18   31   1.0
5   19   51   1.0
5   20   50   1.0
5   22   64   1.0
6   6   3   1.0
6   7   21   1.0
6   8   21   1.0
6   9   17   1.0
6   10   25   1.0
6   11   26   1.0
6   12   26   1.0
6   16   23   1.0
6   17   24   1.0
6   18   24   1.0
6   19   47   1.0
6   20   47   1.0
7   7   4   1.0
7   8   27   1.0
7   9   18   1.0
7   11   31   1.0
7   12   32   1.0
7   13   50   1.0
7   14   51   1.0
7   16   28   1.0
7   17   29   1.0
7   18   30   1.0
7   19   48   1.0
7   20   49   1.0
7   25   58   1.0
8   8   4   1.0
8   9   18   1.0
8   11   32   1.0
8   12   31   1.0
8   13   51   1.0
8   14   50   1.0
8   16   28   1.0
8   17   30   1.0
8   18   29   1.0
8   19   49   1.0
8   20   48   1.0
8   25   64   1.0
9   9   2   1.0
9   10   19   1.0
9   11   20   1.0
9   12   20   1.0
9   13   46   1.0
9   14   46   1.0
9   16   19   1.0
9   17   20   1.0
9   18   20   1.0
9   19   46   1.0
9   20   46   1.0
9   22   57   1.0
9   25   57   1.0
10   10   5   1.0
10   11   33   1.0
10   12   33   1.0
10   13   52   1.0
10   14   52   1.0
10   16   34   1.0
10   17   35   1.0
10   18   35   1.0
11   11   6   1.0
11   12   36   1.0
11   13   53   1.0
11   14   54   1.0
11   16   35   1.0
11   17   37   1.0
11   18   37   1.0
11   20   55   1.0
11   22   59   -1.0
11   25   60   1.0
12   12   6   1.0
12   13   54   1.0
12   14   53   1.0
12   16   35   1.0
```

```
12  17  37  1.0
12  18  37  1.0
12  19  55  1.0
12  22  59  1.0
12  25  60  -1.0
13  13  38  1.0
13  14  40  1.0
13  18  55  1.0
13  19  41  1.0
13  20  42  1.0
13  22  43  -1.0
13  25  65  -1.0
14  14  38  1.0
14  17  55  1.0
14  19  42  1.0
14  20  41  1.0
14  22  43  1.0
14  25  65  1.0
15  15  61  1.0
16  16  5  1.0
16  17  33  1.0
16  18  33  1.0
16  19  52  1.0
16  20  52  1.0
17  17  6  1.0
17  18  36  1.0
17  19  53  1.0
17  20  54  1.0
17  22  60  1.0
17  25  59  -1.0
18  18  6  1.0
18  19  54  1.0
18  20  53  1.0
18  22  60  -1.0
18  25  59  1.0
19  19  38  1.0
19  20  40  1.0
19  22  65  -1.0
19  25  43  -1.0
20  20  38  1.0
20  22  65  1.0
20  25  43  1.0
21  21  61  1.0

22  22  39  1.0
23  23  62  1.0
24  24  62  1.0
25  25  39  1.0
26  26  62  1.0
27  27  62  1.0
-1  -1
1  2  3  1  2  -1
2.35  0.205  0.205  1.50  0.08  0.08
1  3  2  2  1  -1
2.35  0.205  0.205  1.50  0.08  0.08
2  4  1  3  1  -1
1.7  0.104  0.104  0.28  0.055  0.055
2  5  1  4  1  -1
1.7  0.104  0.104  0.28  0.055  0.055
2  6  1  5  1  -1
1.7  0.104  0.104  0.28  0.055  0.055
3  7  1  6  2  -1
1.7  0.104  0.104  0.28  0.055  0.055
3  8  1  7  2  -1
1.7  0.104  0.104  0.28  0.055  0.055
3  9  1  8  2  -1
1.7  0.104  0.104  0.28  0.055  0.055

999
```

Data File for Theoretical Calculation Programme

Ethyl Methyl Sulphide - Gauche

```
METHYL ETHYL SULPHIDE (GAUCHE)
1  12  33  1
0.0000  0.0000  0.0000  0.0000  0.0000  1.8040
1.7818  0.0000  -0.2822  2.4308  -1.2365  0.3390
-1.0430  0.0000  2.1173  0.5094  0.8823  2.1914
0.5094  -0.8823  2.1914  1.9281  0.0000  -1.3613
2.2471  0.8880  0.1632  3.5041  -1.2354  0.1671
1.9989  -2.1494  -0.0809  2.2354  -1.2763  1.4127
1  1  1  2
2  1  1  3
3  1  2  5
4  1  2  6
5  1  2  7
6  1  3  8
7  1  3  9
8  1  3  4
9  1  4  10
10  1  4  11
11  1  4  12
12  2  2  1  3
13  2  5  2  1
14  2  6  2  1
15  2  7  2  1
16  2  8  3  1
17  2  9  3  1
18  2  4  3  1
19  2  10  4  3
20  2  11  4  3
21  2  12  4  3
22  2  5  2  6
23  2  5  2  7
24  2  6  2  7
25  2  4  3  9
26  2  4  3  8
27  2  8  3  9
28  2  11  4  10
29  2  11  4  12
30  2  10  4  12
31  4  5  2  1  3
32  4  6  2  1  3
33  4  7  2  1  3
34  4  8  3  1  2
35  4  9  3  1  2
36  4  10  4  3  1
37  4  11  4  3  1
38  4  12  4  3  1
32.06  12.011  12.011  12.011  1.0079  1.0079
1.0079  1.0079  1.0079  1.0079  1.0079  1.0079
52  107
3.1758  4.7535  4.8679  4.1642  0.348  0.3436  0.3303
0.246  0.321  0.321  0.4925  0.4925  0.321  0.0303  0.0165
0.048  0.0173  0.0391  0.1881  0.2388  0.0332  0.0196
-0.0106  -0.0106  0.0145  0.0145  0.0  0.0337  0.0337
0.0438  0.063  0.020  -0.0062  0.0  0.0435  -0.2  -0.2
-0.2  -0.021  -0.021  0.0  0.0  0.0  0.0  0.0703  0.0083
0.0392  0.0514  0.512  0.048  0.0173  0.451
CS
CH1
CH
CC
CSC
HCS1
HCS
CCS
CCH1
CCH
HCH
HCH1
CCH
HCH1/SCH2
SCH2/SCH3
SCH1/SCH
SCH1/HCH1
SCH1/HCH1
CS/SCH1
CS/HCH2
CS2/SCH1
```

```
CS2/SCH2
CS/HCH2
CS/HCH1
CS2/HCH2
CS2/HCH1
HCH/CCS
HCH2/HCH3
HCH2/HCH1
CS/CS
CS/CSC
CSC/CH1
CSC/CH2
CSC/CC
CC/HCS
CC/HCH
CC/HCH
CC/HCH1
HCC1/HCC2
HCC2/HCC3
HCC1/HCH
HCS1/HCH1
HCC/HCH
HCC/HCH1
CS/CH1
CS/CH2
CH1/CH2
CH2/CH3
CS2/CC
HCS/HCH1
HCS1/HCH2
HCH(ALKYL)
1  1  1  1.0
1  2  30  1.0
1  3  45  1.0
1  4  46  1.0
1  5  46  1.0
1  12  31  1.0
1  13  19  1.0
1  14  20  1.0
1  15  20  1.0
1  16  22  1.0
1  17  22  1.0
1  22  23  1.0
1  23  23  1.0
1  24  24  1.0
2  2  1  1.0
2  6  46  1.0
2  7  46  1.0
2  8  49  1.0
2  12  31  1.0
2  13  21  1.0
2  14  22  1.0
2  15  22  1.0
2  16  20  1.0
2  17  20  1.0
2  22  25  1.0
2  23  25  1.0
2  24  26  1.0
3  3  2  1.0
3  4  47  1.0
3  5  47  1.0
3  12  32  1.0
4  4  3  1.0
4  5  48  1.0
4  12  33  1.0
5  5  3  1.0
5  12  33  1.0
6  6  3  1.0
6  7  48  1.0
6  12  33  1.0
7  7  3  1.0
7  12  33  1.0
8  8  4  1.0
8  12  34  1.0
8  16  35  1.0
8  17  35  1.0
8  27  36  1.0
8  28  37  1.0
8  29  38  1.0
8  30  37  1.0
9  9  2  1.0
9  10  47  1.0
9  11  47  1.0
10  10  3  1.0
10  11  48  1.0
11  11  3  1.0
12  12  5  1.0
13  13  6  1.0
13  14  14  1.0
13  15  14  1.0
```

```
13  22  16  1.0
13  23  16  1.0
13  24  17  1.0
14  14  7  1.0
14  15  15  1.0
14  22  18  1.0
14  23  51  1.0
14  24  50  1.0
15  15  7  1.0
15  22  51  1.0
15  23  18  1.0
15  24  50  1.0
16  16  7  1.0
16  27  18  1.0
17  17  7  1.0
17  27  18  1.0
18  18  8  1.0
18  27  27  1.0
19  19  9  1.0
19  20  39  1.0
19  21  40  1.0
19  28  41  1.0
19  29  42  1.0
19  30  41  1.0
20  20  10  1.0
20  21  41  1.0
20  28  43  1.0
20  29  44  1.0
20  30  43  1.0
21  21  10  1.0
21  28  43  1.0
21  29  44  1.0
21  30  43  1.0
22  22  11  1.0
22  23  28  1.0
22  24  29  1.0
23  23  11  1.0
23  24  29  1.0
24  24  12  1.0
25  25  13  1.0
26  26  13  1.0
27  27  12  1.0
28  28  52  1.0
28  29  29  1.0
28  30  30  1.0
29  29  52  1.0
29  30  29  1.0
30  30  52  1.0
-1  -1
1  2  3  1  2  -1
2.35  0.205  0.205  1.5  0.08  0.08
1  3  2  2  1  -1
2.35  0.205  0.205  1.5  0.08  0.08
2  5  1  3  1  -1
1.7  0.104  0.104  0.28  0.055  0.055
2  6  1  4  1  -1
1.7  0.104  0.104  0.28  0.055  0.055
2  7  1  5  1  -1
1.7  0.104  0.104  0.28  0.055  0.055
3  8  1  6  2  -1
1.7  0.104  0.104  0.28  0.055  0.055
3  9  1  7  2  -1
1.7  0.104  0.104  0.28  0.055  0.055
4  3  1  8  2  -1
0.92  0.092  0.092  0.322  0.0322  0.0322
10  4  11  9  10  -1
1.7  0.104  0.104  0.28  0.055  0.055
11  4  12  10  11  -1
1.7  0.104  0.104  0.28  0.055  0.055
12  4  10  11  9  -1
1.7  0.104  0.104  0.28  0.055  0.055

999
```

Data File for Theoretical Calculation Programme

Ethyl Methyl Sulphide - Trans

```
METHYL ETHYL SULPHIDE (TRANS)
1  12  38  1
0.0000  0.0000  0.0000  0.0000  0.0000  1.8040
1.7818  0.0000  -0.2822  2.0952  0.0000  -1.7798
-1.0430  0.0000  2.1173  0.5094  0.8823  2.1914
0.5094  -0.8823  2.1914  2.2100  -0.8956  0.1735
2.2100  0.8956  0.1735  3.1694  0.0000  -1.9462
1.6530  0.8730  -2.2643  1.6530  -0.8730  -2.2643
1  1  1  2
2  1  1  3
3  1  2  5
4  1  2  6
5  1  2  7
6  1  3  8
7  1  3  9
8  1  3  4
9  1  4  10
10  1  4  11
11  1  4  12
12  2  2  1  3
13  2  5  2  1
14  2  6  2  1
15  2  7  2  1
16  2  8  3  1
17  2  9  3  1
18  2  4  3  1
19  2  10  4  3
20  2  11  4  3
21  2  12  4  3
22  2  5  2  6
23  2  5  2  7
24  2  6  2  7
25  2  4  3  9
26  2  4  3  8
27  2  8  3  9
28  2  11  4  10
29  2  11  4  12
30  2  10  4  12
31  4  5  2  1  3
32  4  6  2  1  3
33  4  7  2  1  3
34  4  8  3  1  2
35  4  9  3  1  2
36  4  10  4  3  1
37  4  11  4  3  1
38  4  12  4  3  1
32.06  12.011  12.011  12.011  1.0079  1.0079
1.0079  1.0079  1.0079  1.0079  1.0079  1.0079
52  107
3.1758  4.7535  4.8679  4.1643  0.3728  0.3436  0.3303  0.246
0.321  0.321  0.4925  0.4925  0.321  0.0303  0.0165  0.048  0.0173
0.0391  0.1881  0.2388  0.0332  0.0196  -0.0106  -0.0106
0.0145  0.0145  0.0  0.0337  0.0337  0.0  0.063  0.02
-0.0062  0.0  0.0435  -0.2  -0.2  -0.2  -0.021  -0.021
0.0  0.0  0.0  0.0  0.0703  0.083  0.0392  0.0514  0.512
0.0480  0.0173  0.451
CS
CH1
CH
CC
CSC
HCS1
HCS
CCS
CCH1
CCH
HCH
HCH1
CCH
HCH1/SCH2
SCH2/SCH3
SCH1/SCH
SCH1/HCH1
SCH1/HCH1
CS/SCH1
```

```
CS/HCH2
CS/HCH1
CS2/HCH2
CS2/HCH1
HCH/CCS
HCH2/HCH3
HCH2/HCH1
CS/CS
CS/CSC
CSC/CH1
CSC/CH2
CSC/CC
CC/HCS
CC/HCH
CC/HCH
CC/HCH1
HCC1/HCC2
HCC2/HCC3
HCC1/HCH
HCS1/HCH1
HCC/HCH
HCC/HCH1
CS/CH1
CS/CH2
CH1/CH2
CH2/CH3
CS2/CC
HCS/HCH1
HCS1/HCH2
HCH(ALKYL)
1  1  1  1.0
1  2  30  1.0
1  3  45  1.0
1  4  46  1.0
1  5  46  1.0
1  12  31  1.0
1  13  19  1.0
1  14  20  1.0
1  15  20  1.0
1  16  22  1.0
1  17  22  1.0
1  22  23  1.0
1  23  23  1.0
1  24  24  1.0
2  2  1  1.0
2  6  46  1.0
2  7  46  1.0
2  8  49  1.0
2  12  31  1.0
2  13  21  1.0
2  14  22  1.0
2  15  22  1.0
2  16  20  1.0
2  17  20  1.0
2  22  25  1.0
2  23  25  1.0
2  24  26  1.0
3  3  2  1.0
3  4  47  1.0
3  5  47  1.0
3  12  32  1.0
4  4  3  1.0
4  5  48  1.0
4  12  33  1.0
5  5  3  1.0
5  12  33  1.0
6  6  3  1.0
6  7  48  1.0
6  12  33  1.0
7  7  3  1.0
7  12  33  1.0
8  8  4  1.0
8  12  34  1.0
8  16  35  1.0
8  17  35  1.0
8  27  36  1.0
8  28  37  1.0
8  29  38  1.0
8  30  37  1.0
9  9  2  1.0
9  10  47  1.0
9  11  47  1.0
10  10  3  1.0
10  11  48  1.0
11  11  3  1.0
12  12  5  1.0
13  13  6  1.0
13  14  14  1.0
13  15  14  1.0
13  22  16  1.0
```

```
13  22  16  1.0
13  23  16  1.0
13  24  17  1.0
14  14  7  1.0
14  15  15  1.0
14  22  18  1.0
14  23  51  1.0
14  24  50  1.0
15  15  7  1.0
15  22  51  1.0
15  23  18  1.0
15  24  50  1.0
16  16  7  1.0
16  27  18  1.0
17  17  7  1.0
17  27  18  1.0
18  18  8  1.0
18  27  27  1.0
19  19  9  1.0
19  20  39  1.0
19  21  40  1.0
19  28  41  1.0
19  29  42  1.0
19  30  41  1.0
20  20  10  1.0
20  21  41  1.0
20  28  43  1.0
20  29  44  1.0
20  30  43  1.0
21  21  10  1.0
21  28  43  1.0
21  29  44  1.0
21  30  43  1.0
22  22  11  1.0
22  23  28  1.0
22  24  29  1.0
23  23  11  1.0
23  24  29  1.0
24  24  12  1.0
25  25  13  1.0
26  26  13  1.0
27  27  12  1.0
28  28  52  1.0
28  29  29  1.0
28  30  30  1.0
29  29  52  1.0
29  30  29  1.0
30  30  52  1.0
-1  -1
1  2  3  1  2  -1
2.35  0.205  0.205  1.50  0.08  0.08
1  3  2  2  1  -1
2.35  0.205  0.205  1.50  0.08  0.08
2  5  1  3  1  -1
1.7  0.104  0.104  0.28  0.055  0.055
2  6  1  4  1  -1
1.7  0.104  0.104  0.28  0.055  0.055
2  7  1  5  1  -1
1.7  0.104  0.104  0.28  0.055  0.055
3  8  1  6  2  -1
1.7  0.104  0.104  0.28  0.055  0.055
3  9  1  7  2  -1
1.7  0.104  0.104  0.28  0.055  0.055
4  3  1  8  2  -1
0.92  0.092  0.092  0.322  0.0322  0.0322
10  4  11  9  10  -1
1.7  0.104  0.104  0.28  0.055  0.055
11  4  12  10  11  -1
1.7  0.104  0.104  0.28  0.055  0.055
12  4  10  11  9  -1
1.7  0.104  0.104  0.28  0.055  0.055

999
```

APPENDIX F

Appendix F

Self Consistent Field Method[62,73]

This is a method of solving the Schroedinger equation for a many electron system. It was originated by Hartree but later modified by Fock to take into account the fact that it is impossible to differentiate between individual electrons.

The basis of the method is to estimate the wavefunctions for all the electrons in the system. One electron is then considered and its wavefunction is calculated by assuming that the attractive and repellant forces to which it is subjected arise from all the other electrons, which for this purpose are 'frozen'.

With this new wavefunction the next electron is treated in the same way and so on until all the electrons have been considered and a new set of wavefunctions has been derived.

The whole process is then repeated using the new set of wavefunctions to generate a further set of wavefunctions. This cycle continues until a new wavefunction set does not differ significantly from the previously calculated set.

APPENDIX G

Appendix G

Gaussian 82 Data File for Dimethyl Sulphide

```
JOB,US=UHCA103,MFL=290000,T=99.
ACCESS,DN=GAUS82,ID=TRIAL.
MEMORY,FL=140000,USER.
GAUS82.
/EOF
£P  3-21G* RHF FORCE

DIMETHYL SULPHIDE

O  1
S
C  1  R1
H  2  RH1  1  BETA1
H  2  RH2  1  BETA2  3  ALP1   1
H  2  RH3  1  BETA3  3  ALP2  -1
C  1  R2   2   TH    3  TOR1   0
H  6  RH4  1  BETA4  2  TOR2   0
H  6  RH5  1  BETA5  7  ALP3  1
H  6  RH6  1  BETA6  7  ALP4  -1

R1=1.8158
R2=1.8158
TH=99.40
RH1=1.0812
RH2=1.0815
RH3=1.0815
RH4=1.0812
RH5=1.0815
RH6=1.0815
BETA1=107.60
BETA2=110.60
BETA3=110.60
BETA4=107.60
BETA5=110.60
BETA6=110.60
ALP1=109.43
ALP2=109.43
ALP3=109.43
ALP4=109.43
TOR1=180.0
TOR2=180.0

/EOF
```

APPENDIX H

Theoretical Calculation Results

Dimethyl Sulphide

2-SIDED POLARISABILITY TENSOR

NO.	FREQUENCY	ALPHA	BETA SQ.	PAR. INT	PER. INT	P
1	0.2994790E+04	0.000000	0.151840	1.062878	0.911039	0.857143
2	0.2993752E+04	0.000000	0.001052	0.007363	0.006311	0.857143
3	0.2962383E+04	0.000000	0.017834	0.124838	0.107004	0.857143
4	0.2959205E+04	0.093059	0.121533	1.240427	0.729199	0.587861
5	0.2925040E+04	0.000000	0.061468	0.430277	0.368809	0.857143
6	0.2921593E+04	0.210094	0.000857	1.992274	0.005141	0.002580
7	0.1465893E+04	0.000000	0.003498	0.024488	0.020990	0.857143
8	0.1460775E+04	0.000000	0.015591	0.109136	0.093545	0.857143
9	0.1436407E+04	0.003959	0.018755	0.131992	0.112532	0.852563
10	0.1425545E+04	0.000000	0.002085	0.014595	0.012510	0.857143
11	0.1353256E+04	0.000000	0.001521	0.010645	0.009125	0.857143
12	0.1347909E+04	0.022659	0.000909	0.029467	0.005454	0.185078
13	0.1015469E+04	0.018212	0.021442	0.165020	0.128653	0.779617
14	0.9700277E+03	0.000000	0.013686	0.095800	0.082114	0.857143
15	0.9575167E+03	0.000000	0.012224	0.085566	0.073342	0.857143
16	0.9218236E+03	0.000000	0.001799	0.012590	0.010791	0.857143
17	0.7472070E+03	0.000000	0.053564	0.374947	0.321383	0.857143
18	0.6853494E+03	0.122538	0.020415	0.818607	0.122487	0.149629
19	0.3031789E+03	0.009661	0.035387	0.251911	0.212324	0.842853
20	0.0000000E+00	0.000000	0.000000	0.000000	0.000000	INDETERMINATE
21	0.0000000E+00	0.000000	0.000000	0.000000	0.000000	INDETERMINATE

Theoretical Calculation Results

Dimethyl Sulphide-d6

2-SIDED POLARISABILITY TENSOR

NO.	FREQUENCY	ALPHA	BETA SQ.	PAR. INT	PER. INT	P
1	0.2220934E+04	0.000000	0.101211	0.708476	0.607265	0.857143
2	0.2219855E+04	0.000000	0.001412	0.009884	0.008472	0.857143
3	0.2191886E+04	0.000000	0.024730	0.173108	0.148378	0.857143
4	0.2190587E+04	0.020698	0.078590	0.569410	0.471541	0.828123
5	0.2097878E+04	0.000000	0.034008	0.238055	0.204047	0.857143
6	0.2095863E+04	0.184990	0.005640	1.579434	0.033838	0.021424
7	0.1062284E+04	0.000000	0.006010	0.042072	0.036061	0.857143
8	0.1059901E+04	0.000000	0.007436	0.052053	0.044617	0.857143
9	0.1044546E+04	0.023336	0.007304	0.075631	0.043821	0.579414
10	0.1034290E+04	0.000000	0.003535	0.024744	0.021209	0.857143
11	0.1029856E+04	0.053378	0.004885	0.162406	0.029308	0.180460
12	0.1029363E+04	0.000000	0.000043	0.000302	0.000259	INDETERMINATE
13	0.7958514E+03	0.030969	0.025569	0.222142	0.153414	0.690611
14	0.7330126E+03	0.000000	0.015216	0.106511	0.091295	0.857143
15	0.7137907E+03	0.000000	0.013991	0.097939	0.083948	0.857143
16	0.7105699E+03	0.000000	0.042622	0.298353	0.255731	0.857143
17	0.6898592E+03	0.000000	0.008363	0.058538	0.050175	0.857143
18	0.6296156E+03	0.111288	0.020372	0.699933	0.122230	0.174631
19	0.2642837E+03	0.008641	0.028486	0.202763	0.170917	0.842938
20	0.0000000E+00	0.000000	0.000000	0.000000	0.000000	INDETERMINATE
21	0.0000000E+00	0.000000	0.000000	0.000000	0.000000	INDETERMINATE

Theoretical Calculation Results

Ethyl Methyl Sulphide - Gauche

2-SIDED POLARISABILITY TENSOR

NO.	FREQUENCY	ALPHA	BETA SQ.	PAR. INT	PER. INT	P
1	0.3010788E+04	0.000790	0.121735	0.852171	0.730408	0.857115
2	0.3006492E+04	0.000020	0.075413	0.527890	0.452477	0.857143
3	0.3001892E+04	0.000382	0.035338	0.247374	0.212029	0.857120
4	0.2999087E+04	0.051855	0.074719	0.644035	0.448312	0.696100
5	0.2998432E+04	0.041400	0.073030	0.588339	0.438179	0.744773
6	0.2962794E+04	0.134646	0.035912	1.067214	0.215471	0.201901
7	0.2920757E+04	0.154241	0.023972	1.238365	0.143831	0.116146
8	0.2913243E+04	0.156737	0.027642	1.298987	0.165851	0.127677
9	0.1446335E+04	0.002411	0.012527	0.087954	0.075165	0.854594
10	0.1444919E+04	0.000054	0.012212	0.085485	0.073273	0.857142
11	0.1438425E+04	0.006410	0.004318	0.032077	0.025910	0.807742
12	0.1411068E+04	0.014054	0.010761	0.084217	0.064568	0.766685
13	0.1380517E+04	0.014435	0.012465	0.096634	0.074792	0.773972
14	0.1371133E+04	0.000162	0.012056	0.084395	0.072337	0.857131
15	0.1322244E+04	0.021444	0.001870	0.033784	0.011220	0.332114
16	0.1288863E+04	0.010029	0.002496	0.021998	0.014976	0.680793
17	0.1142611E+04	0.004425	0.014099	0.099575	0.084595	0.849559
18	0.9967350E+03	0.039970	0.003918	0.099319	0.023509	0.236702
19	0.9682690E+03	0.001663	0.015529	0.108828	0.093174	0.856163
20	0.9560017E+03	0.010874	0.016906	0.123665	0.101437	0.820259
21	0.9425893E+03	0.003111	0.008072	0.056942	0.048434	0.850589
22	0.9076304E+03	0.018379	0.009402	0.081012	0.056410	0.696322
23	0.7489289E+03	0.028858	0.020348	0.179910	0.122086	0.678595
24	0.7266153E+03	0.020429	0.040189	0.300104	0.241134	0.803502
25	0.6893014E+03	0.116112	0.019677	0.744428	0.118059	0.158591
26	0.3344961E+03	0.012635	0.034207	0.246634	0.205243	0.832178
27	0.2289606E+03	0.014767	0.023626	0.175192	0.141754	0.809134
28	0.0000000E+00	0.000000	0.000000	0.000000	0.000000	INDETERMINATE
29	0.0000000E+00	0.000000	0.000000	0.000000	0.000000	INDETERMINATE
30	0.0000000E+00	0.000000	0.000000	0.000000	0.000000	INDETERMINATE

Theoretical Calculation Results

Ethyl Methyl Sulphide - Trans

2-SIDED POLARISABILITY TENSOR

NO.	FREQUENCY	ALPHA	BETA SQ.	PAR. INT	PER. INT	P
1	0.3010120E+04	0.000000	0.125627	0.879387	0.753760	0.857143
2	0.3006492E+04	0.000000	0.075234	0.526638	0.451404	0.857143
3	0.3002157E+04	0.000000	0.031036	0.217251	0.186215	0.857143
4	0.2999029E+04	0.053270	0.078012	0.673780	0.468074	0.694698
5	0.2997674E+04	0.037633	0.070360	0.556250	0.422159	0.758937
6	0.2960242E+04	0.135143	0.036252	1.075629	0.217514	0.202220
7	0.2920573E+04	0.153737	0.024043	1.231877	0.144260	0.117106
8	0.2911386E+04	0.157888	0.026954	1.310463	0.161723	0.123409
9	0.1446555E+04	0.000152	0.013694	0.095856	0.082162	0.857134
10	0.1444919E+04	0.000000	0.012255	0.085783	0.073529	0.857143
11	0.1438268E+04	0.008816	0.002267	0.019363	0.013600	0.702340
12	0.1438074E+04	0.000000	0.011876	0.083130	0.071254	0.857143
13	0.1381907E+04	0.011226	0.014512	0.107252	0.087070	0.811824
14	0.1365935E+04	0.017271	0.010359	0.085933	0.062151	0.723249
15	0.1321939E+04	0.021443	0.001359	0.030207	0.008156	0.269996
16	0.1293993E+04	0.005714	0.003826	0.028251	0.022956	0.812565
17	0.1142891E+04	0.000000	0.012123	0.084862	0.072739	0.857143
18	0.1000847E+04	0.046074	0.010247	0.167255	0.061483	0.367599
19	0.9684403E+03	0.000000	0.017203	0.120420	0.103217	0.857143
20	0.9478684E+03	0.006745	0.010076	0.072578	0.060454	0.832963
21	0.9456729E+03	0.000000	0.009386	0.065705	0.056319	0.857143
22	0.9128314E+03	0.013270	0.007251	0.058679	0.043505	0.741400
23	0.7324802E+03	0.000000	0.005341	0.037386	0.032045	0.857143
24	0.7278450E+03	0.021303	0.058914	0.432822	0.353486	0.816701
25	0.7108550E+03	0.112471	0.018392	0.697976	0.110351	0.158102
26	0.3115192E+03	0.028618	0.031669	0.258533	0.190011	0.734959
27	0.2308036E+03	0.012937	0.010416	0.080441	0.062494	0.776894
28	0.0000000E+00	0.000000	0.000000	0.000000	0.000000	INDETERMINATE
29	0.0000000E+00	0.000000	0.000000	0.000000	0.000000	INDETERMINATE
30	0.0000000E+00	0.000000	0.000000	0.000000	0.000000	INDETERMINATE

APPENDIX I

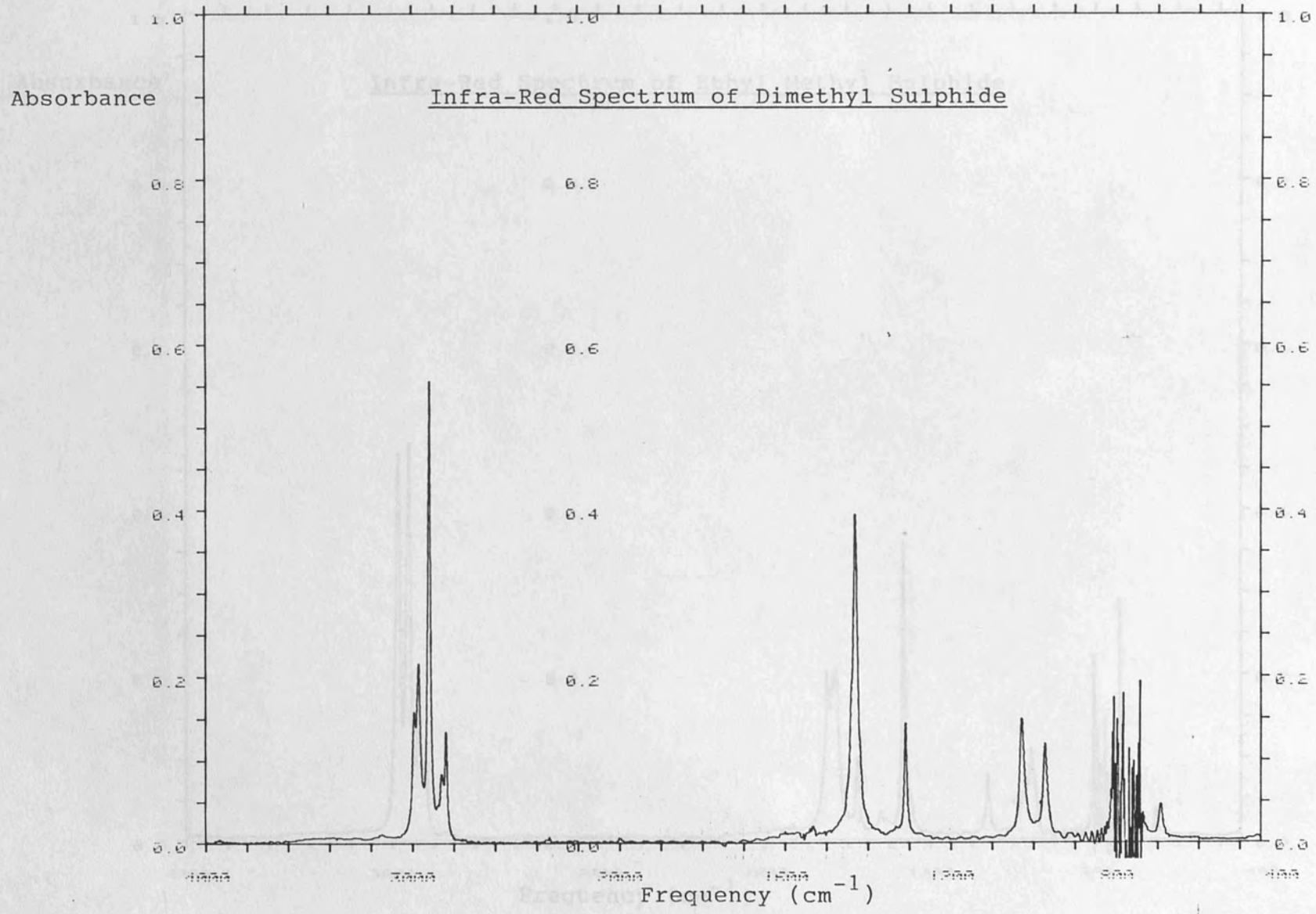
Absorbance
Infra-Red Spectrum of Dimethyl Sulphide
1.0
0.8
0.6
0.4
0.2
0.0
Frequency (cm^{-1})

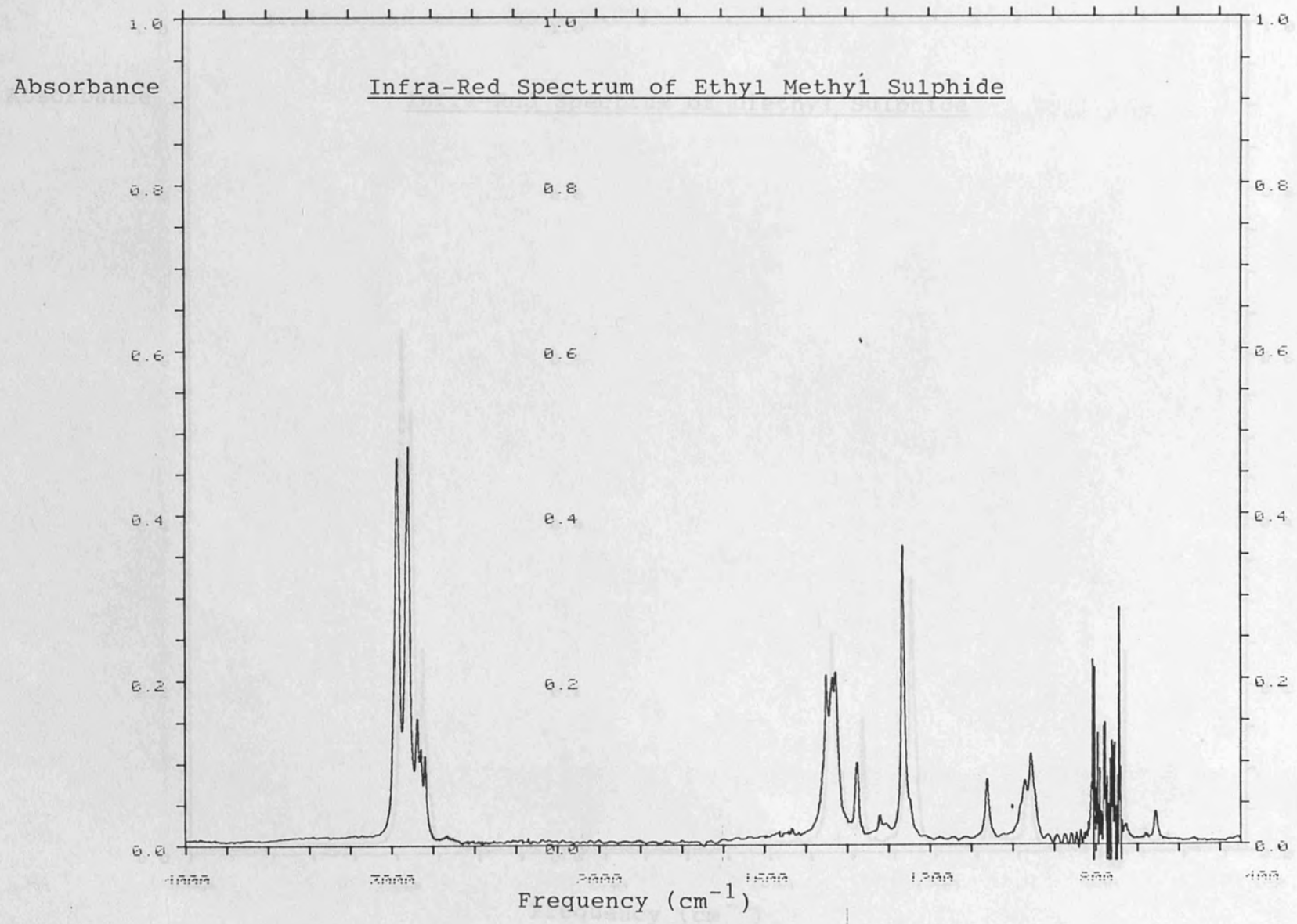
Infra-Red Spectrum of Ethyl Methyl Sulphide
Absorbance
1.0
0.8
0.6
0.4
0.2
0.0
Frequency (cm^{-1})

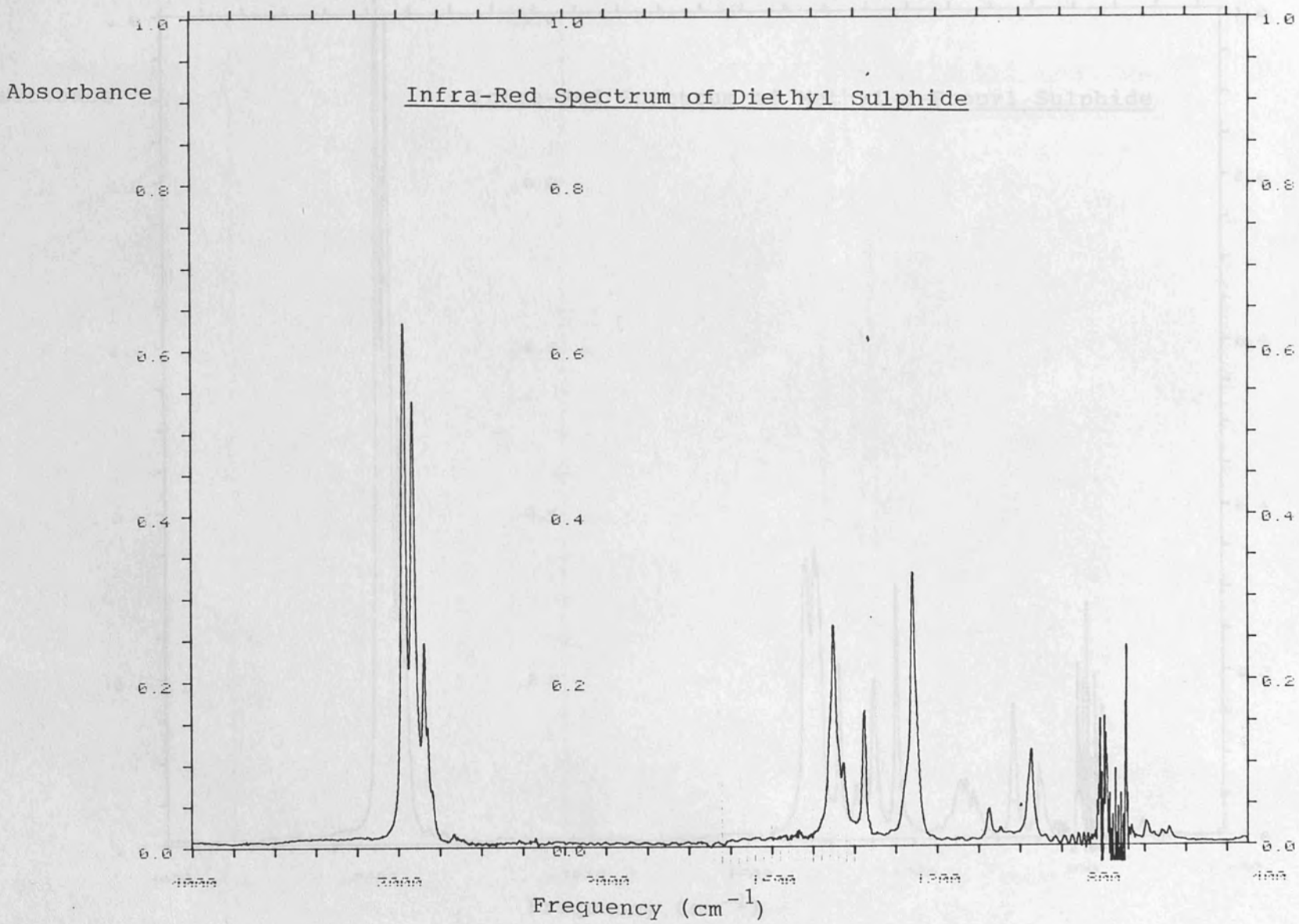
Absorbance
Infra-Red Spectrum of Diethyl Sulphide
1.0
0.8
0.6
0.4
0.2
0.0
Frequency (cm^{-1})

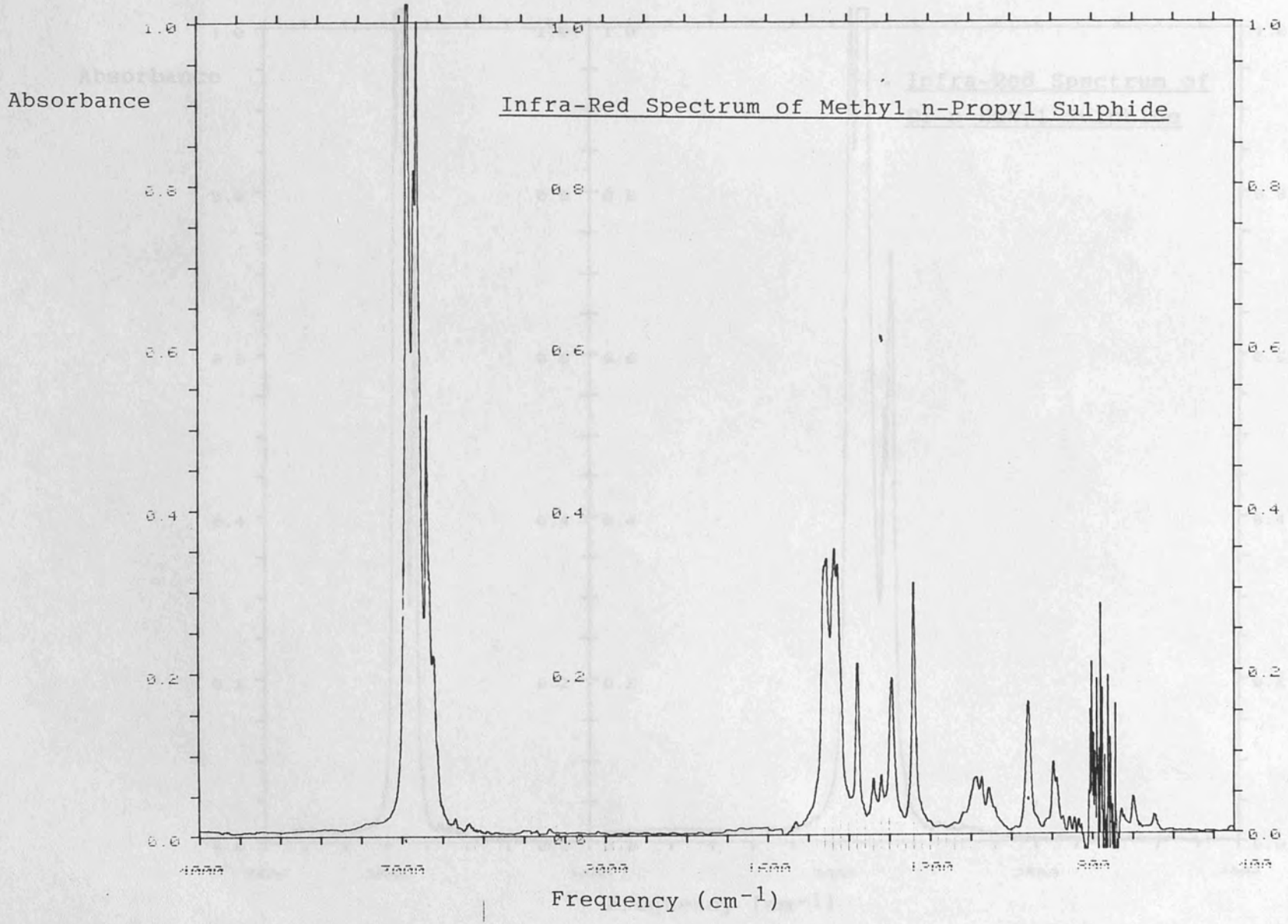
Infra-Red Spectrum of Methyl n-Propyl Sulphide
Absorbance
1.0
0.8
0.6
0.4
0.2
0.0
Frequency (cm^{-1})

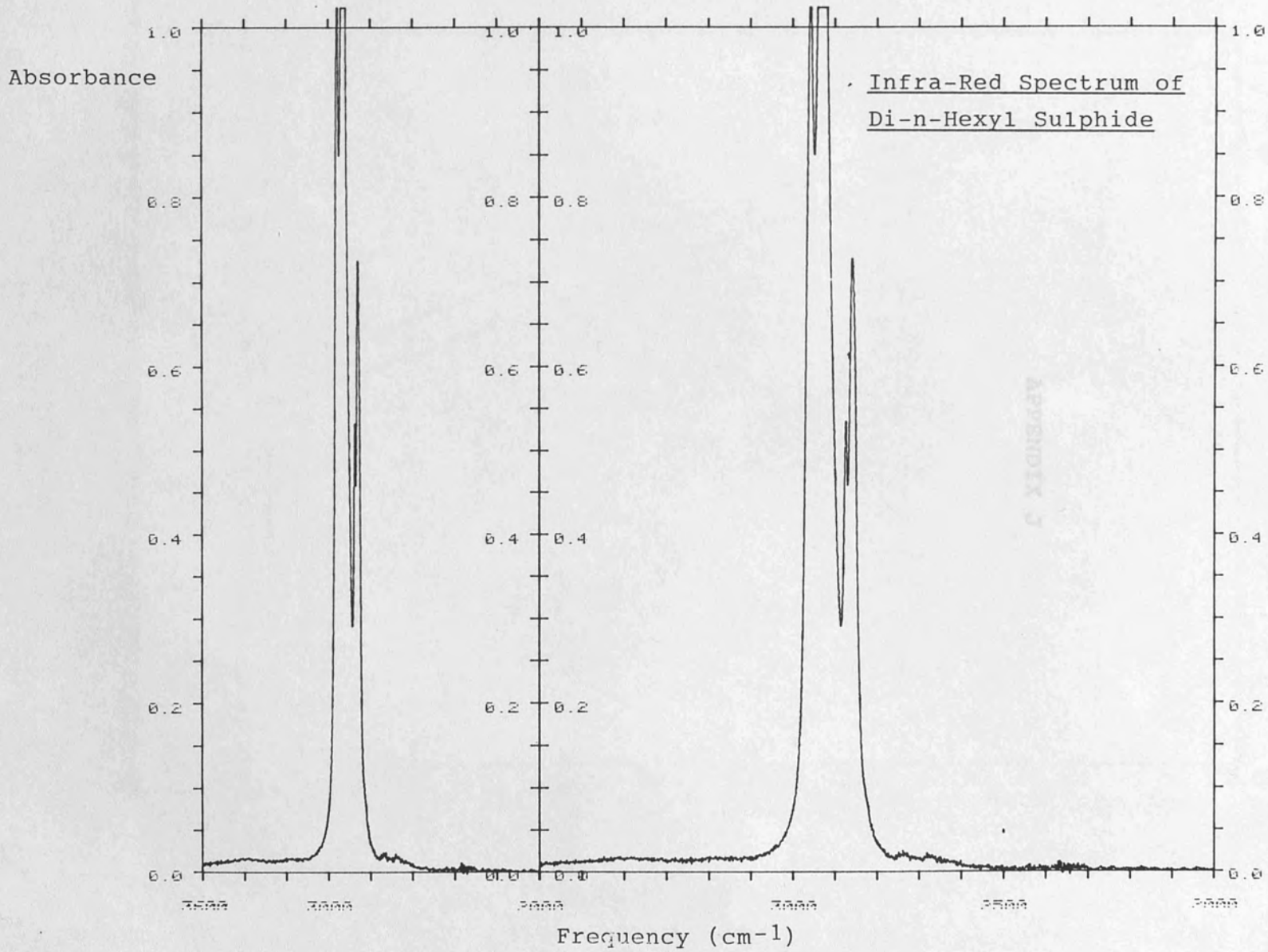

Infra-Red Spectrum of Di-n-Hexyl Sulphide

APPENDIX J

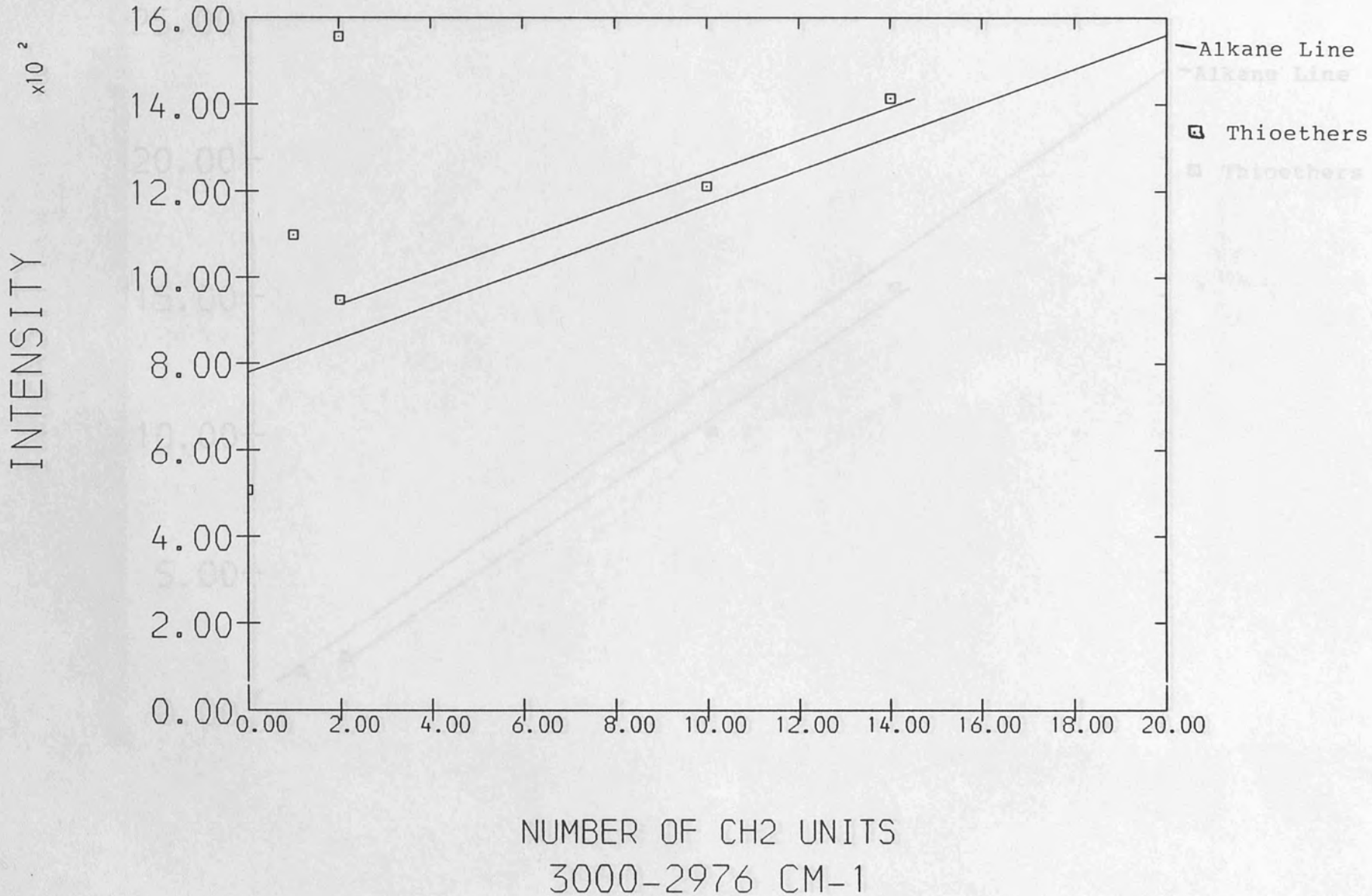
INTENSITY
x10 ²
16.00
14.00
12.00
10.00
8.00
6.00
4.00
2.00
0.00
0.00
2.00
4.00
6.00
8.00
10.00
12.00
14.00
16.00
18.00
20.00
Alkane Line
Thioethers
NUMBER OF CH2 UNITS
3000-2976 CM-1

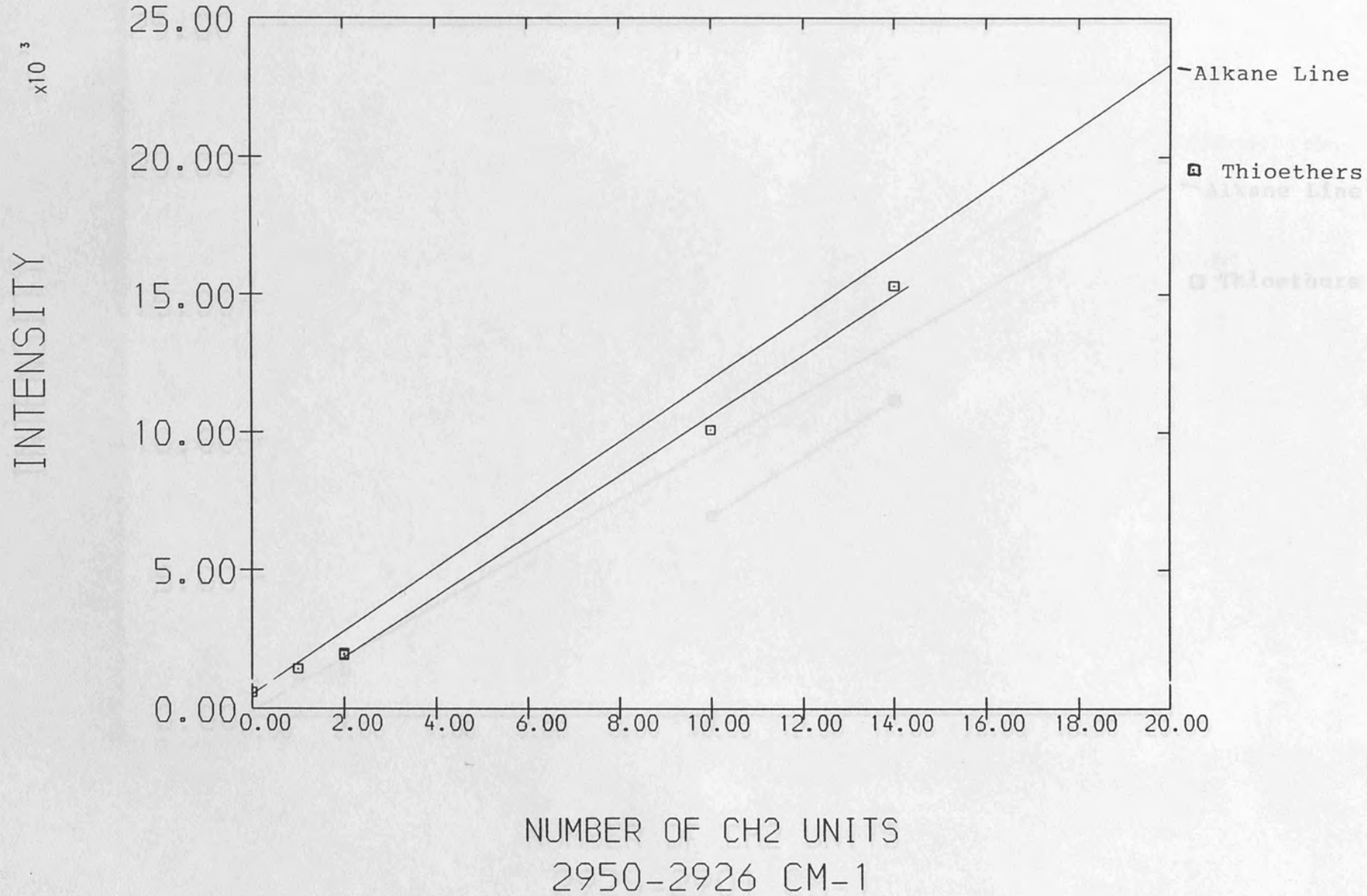
25.00
20.00
15.00
10.00
5.00
0.00
INTENSITY
x10 3
0.00
2.00
4.00
6.00
8.00
10.00
12.00
14.00
16.00
18.00
20.00
Alkane Line
Thioethers
NUMBER OF CH2 UNITS
2950-2926 CM-1

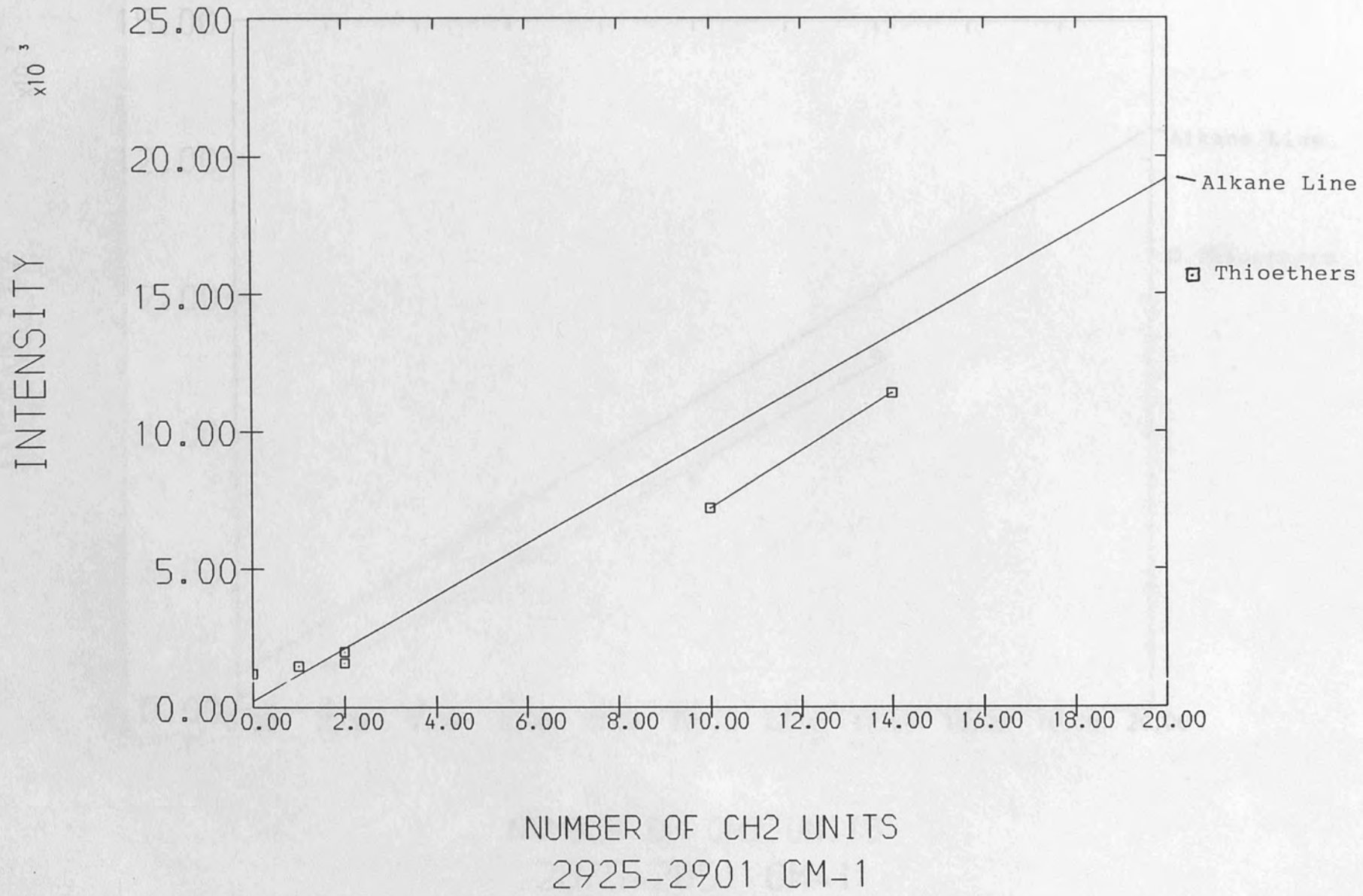
INTENSITY
x10 3
25.00
20.00
15.00
10.00
5.00
0.00
0.00
2.00
4.00
6.00
8.00
10.00
12.00
14.00
16.00
18.00
20.00
Alkane Line
Thioethers
NUMBER OF CH2 UNITS
2925-2901 CM-1

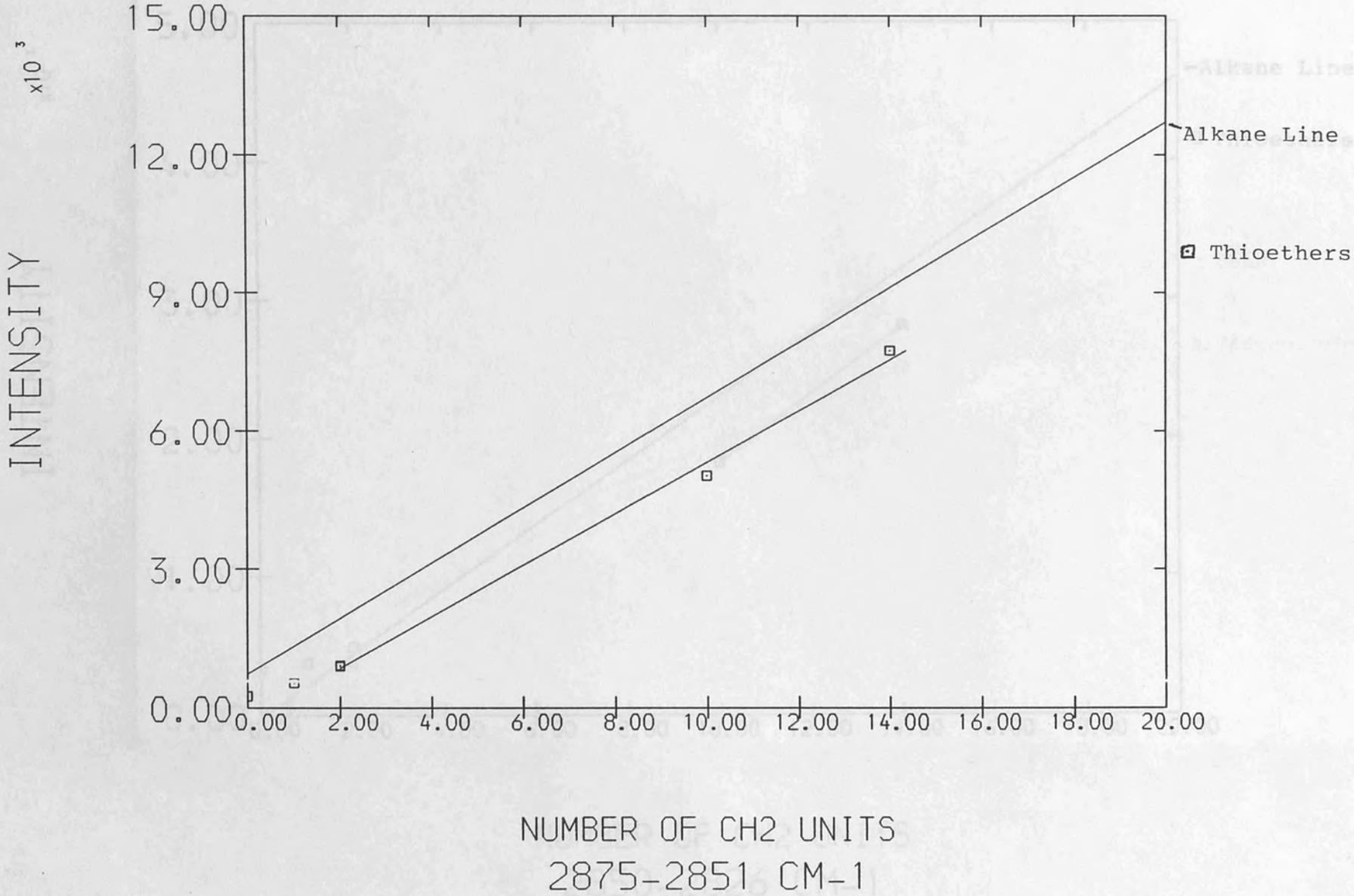
15.00
12.00
9.00
6.00
3.00
0.00
x10 3
INTENSITY
0.00
2.00
4.00
6.00
8.00
10.00
12.00
14.00
16.00
18.00
20.00
Alkane Line
Thioethers
NUMBER OF CH2 UNITS
2875-2851 CM-1

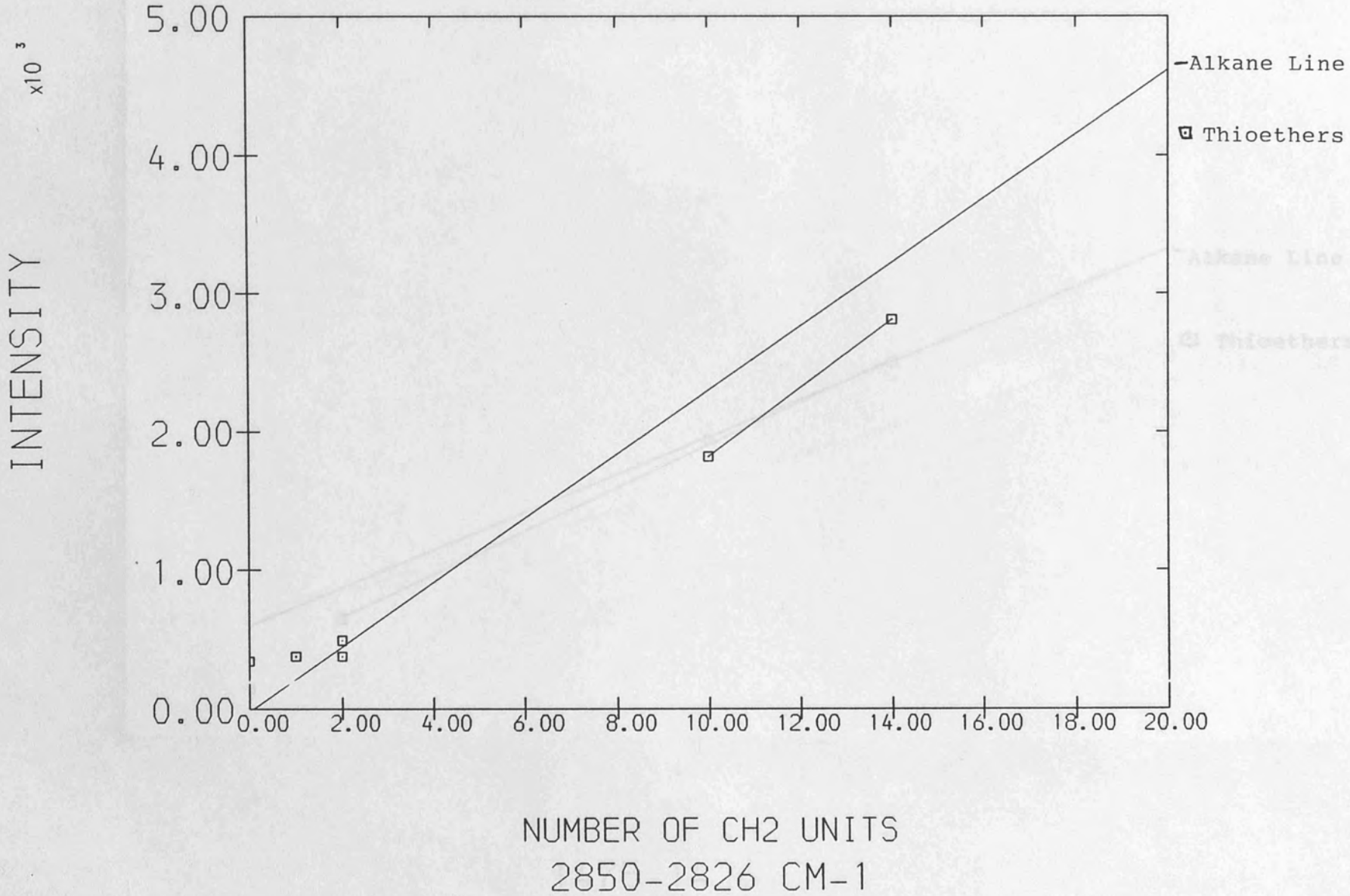
INTENSITY x10 3
5.00
4.00
3.00
2.00
1.00
0.00
0.00
2.00
4.00
6.00
8.00
10.00
12.00
14.00
16.00
18.00
20.00
Alkane Line
Thioethers
NUMBER OF CH2 UNITS
2850-2826 CM-1

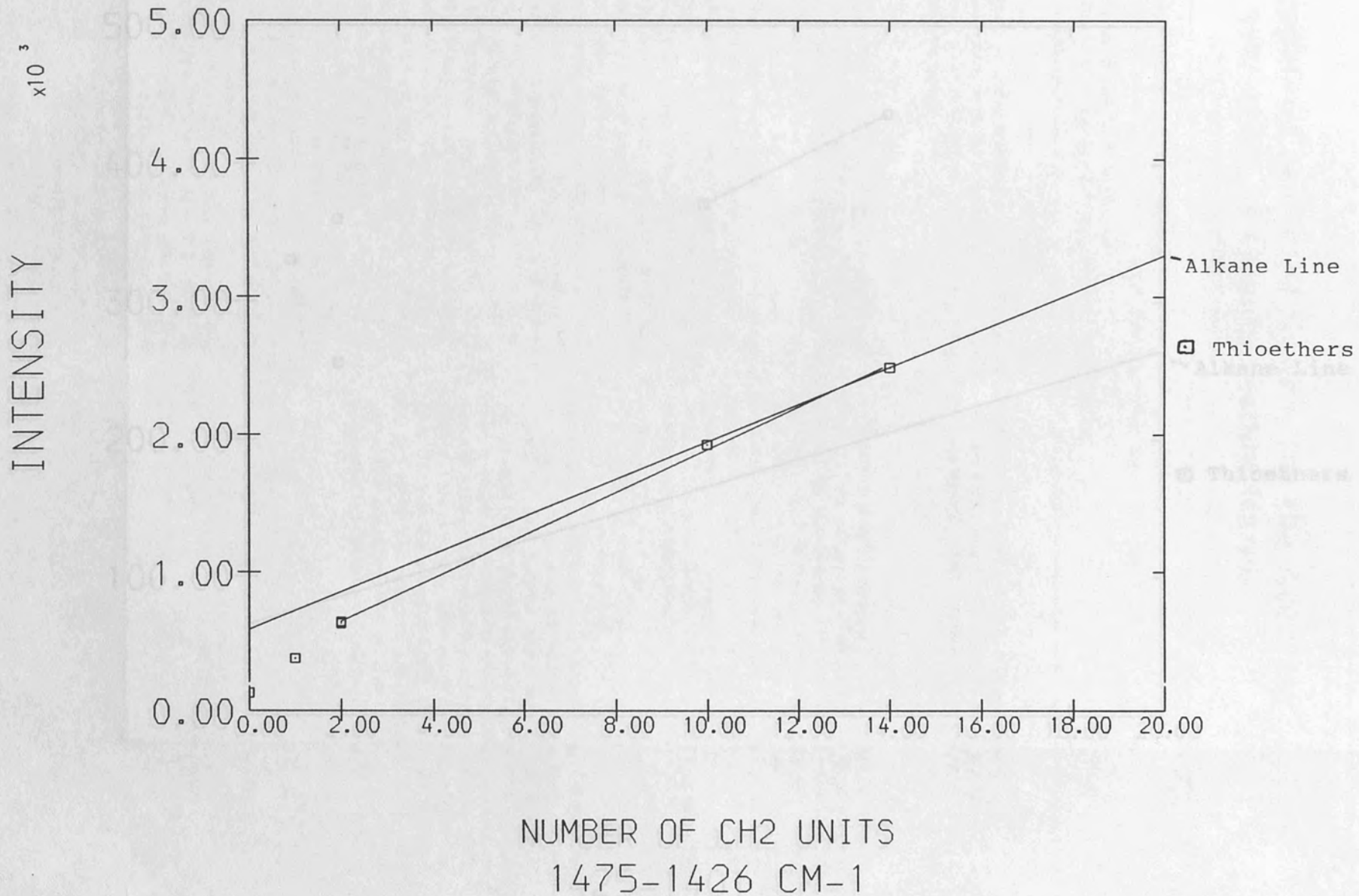
INTENSITY
x10 3
5.00
4.00
3.00
2.00
1.00
0.00
0.00
2.00
4.00
6.00
8.00
10.00
12.00
14.00
16.00
18.00
20.00
Alkane Line
Thioethers
NUMBER OF CH2 UNITS
1475-1426 CM-1

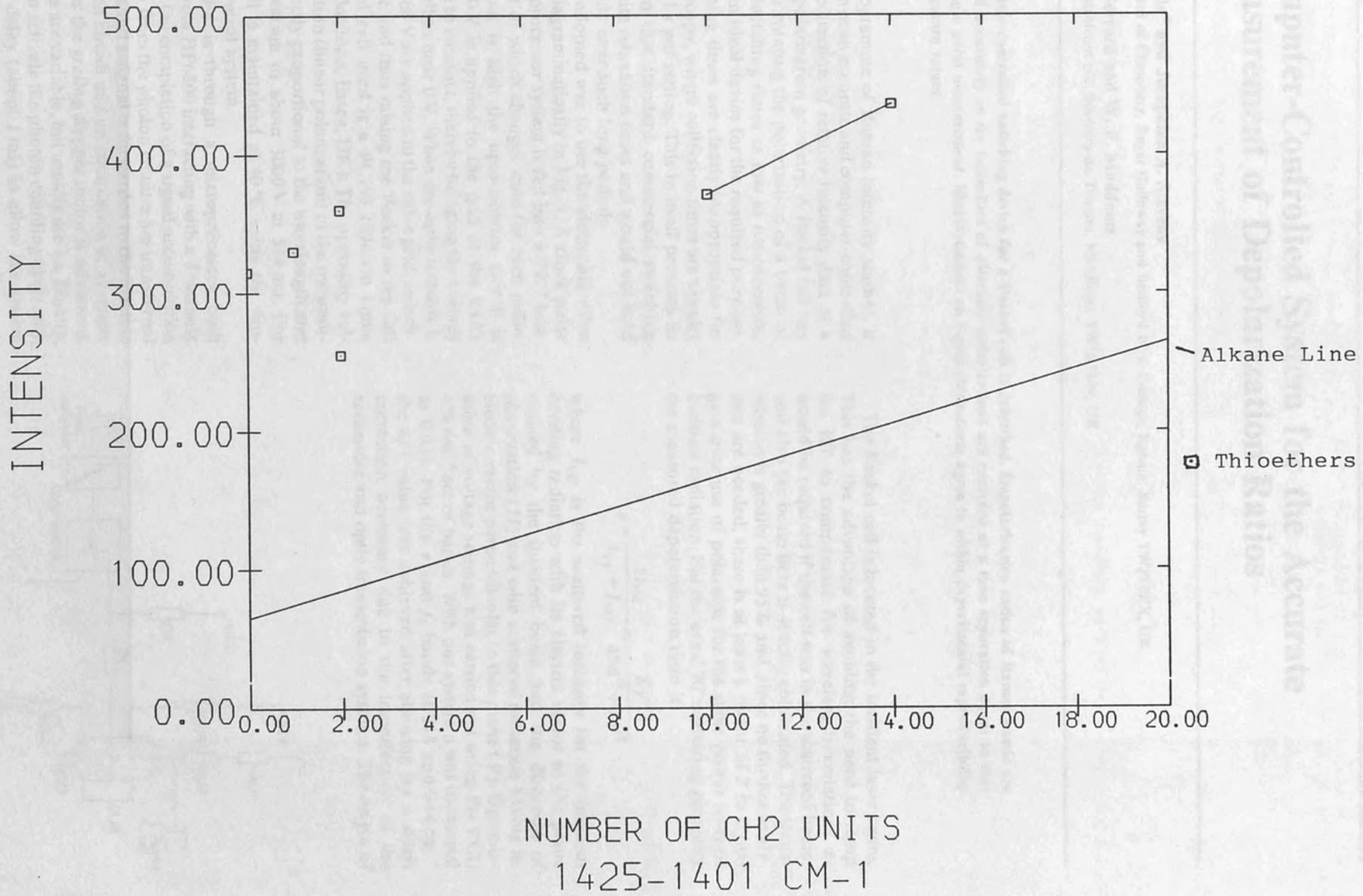
INTENSITY
500.00
400.00
300.00
200.00
100.00
0.00
0.00
2.00
4.00
6.00
8.00
10.00
12.00
14.00
16.00
18.00
20.00
Alkane Line
Thioethers
NUMBER OF CH2 UNITS
1425-1401 CM-1

JOURNAL OF RAMAN SPECTROSCOPY, VOL. 18, 373-374 (1987)

SHORT COMMUNICATION

Computer-Controlled System for the Accurate Measurement of Depolarization Ratios

D. Steele* and Josephine A. Stevens
Department of Chemistry, Royal Holloway and Bedford New College, Egham, Surrey TW20 0EX, UK

D. L. Gerrard and W. F. Maddams
British Petroleum plc, Sunbury-on-Thames, Middlesex TW16 7LN, UK

A computer-controlled switching device for a Pockel cell is described. Depolarization ratios of Raman bands are measured accurately as the intensities of alternate polarizations are recorded at a time separation equal to that for a single point measurement. Measurements on liquid chloroform agree to within experimental reproducibility with literature values.

As part of a programme of Raman intensity studies, it was desired to have an accurate and computer-controlled system for the collection of relative intensity data as a function of the polarization geometry. A Pockel cell has the capability of rotating the polarization of a beam of radiation with switching times as low as nanoseconds, thus making it an ideal device for the required purpose. Very fast switching times are clearly inappropriate for Raman spectroscopy, where collection times are usually of the order of 1 s per setting. This in itself presents its own problem in that standard commercial switching devices have finite relaxation times and would not hold the voltage steady over such long periods.

The solution adopted was to use the electronic valve switch shown diagrammatically in Fig. 1. A clock pulse from the microprocessor system is fed into a 7472 bistable, the output of which changes state for each pulse. When the output is high the opto-isolator switch is energized and 0 V is applied to the grid of the EL81 valve, causing it to conduct, thereby bringing the voltage at the Pockel cell to near 0 V. When the opto-isolator is not energized −60 V are applied to the valve grid, switching off the valve and thus raising the Pockel to the full HT. The Pockel cell used is a PC105 (Electro Optic Development, Basildon, Essex, UK). The operating voltage for 90° rotation (linear polarization) of the transmitted beam is directly proportional to the wavelength and is 6100 V at 1060 nm or about 3000 V at 514 nm. For stability the cell is maintained at 40 °C using the supplier's TC15 control system.

System control is through a microprocessor built around a Motorola HP6800 interacting with a Tektronix 4052 computer. On completion of a signal accumulation period, the data from the photon counter are transferred to the computer and a signal is forwarded to the bistable of the Pockel cell circuit and on completion of alternate collection cycles the grating stepper motor is advanced. Collection times are variable, but usually are 1 s. Finally, a pulse is sent to activate the photon counting cycle with a suitable time delay (about 1 ms) to allow the system to stabilize.

The Pockel cell is located in the incident laser beam. This has the advantage of avoiding the need to ramp the HT to compensate for wavelength variations as would be required if the cell was in the scattered beam, and also the beam here is strictly collimated. The transmission is greater than 95% and, since no further analysers are needed, there is at least a factor of 2 in signal gain over use of polaroids for the same power level of incident radiation. For the usual 90° scattering geometry the measured depolarization ratio is

$$\rho = \frac{2I_{VH}}{I_{VV}+I_{VH}} = \frac{6\gamma'^2}{45\bar{\alpha}'^2+7\gamma'^2}$$

where I_{VH} is the scattered intensity for the incident exciting radiation with its electric vector in the plane defined by the incident beam and the direction of observation (H) and with scattered radiation having its electric vector perpendicular to this plane (V). Optimization of voltage settings was carried out using the CCl_4 458 cm^{-1} set of bands. With our system ρ was measured as 0.035. For the e and f_2 bands at 218 and 314 cm^{-1} the 6/7 value was achieved after allowing for a small correction necessary due to the imperfection of the scrambler and optic transmission systems. The origin of

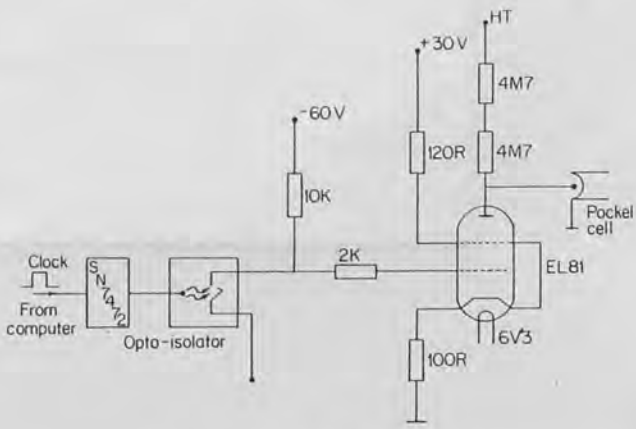

Figure 1. The Pockel cell control circuit.

* Author to whom correspondence should be addressed.

0377-0486/87/050373-02 $05.00
© 1987 by John Wiley & Sons, Ltd

Received 5 September 1986
Accepted 1 December 1986

residual intensity for the I_H arrangements was not apparent. Realigning of optics and axes of Pockel cell failed to reduce this further. Taking the 0.035 value for ν_1 as 'leakage' of $I_{VV}+I_{VH}$ through finite collection angles and incomplete beam rotation, spectra are readily corrected in the computer system by subtraction of 0.035 I_V from the I_H signals and scaling according to

$$\rho=\frac{[\rho(\text{obs})-0.035]\rho_{315}(\text{true})}{\rho_{315}(\text{obs})-0.035}$$

The spectrometer is a Coderg PHO double monochromator extensively modified with NPL holographic gratings, a cooled EMI 9863B photomultiplier and a Brookdeal 5Cl photon-counting system. A 2 W ionized argon laser (CRL) is used for excitation after passage through an Anaspec International Laserspec III premonochromator. The spectra reported here were recorded with about 300 mW of 514.5 nm radiation at the sample, 1 s recording times and frequency stepping intervals of 1 cm^{-1}. The linearity of the system was verified by measurements on $CHCl_3$ (Table 1). The results agree well with literature values[1] for the liquid phase. Agreement is also good with vapour phase results[2] for the ν_1, ν_3 A_1 bands. The ratio for the CH stretch is increased as a result of hydrogen bonding in liquid state.

In addition to convenience, speed and increased collection efficiency, there is an additional advantage in that errors due to drift in laser power are eliminated. The reproducibility is excellent and within statistical noise levels of the signals.

Table 1. Comparison of depolarization ratios of $CHCl_3$ as measured with the Pockel cell with literature values

	Depolarization ratio		
ν/cm^{-1}	This work[a]	Ref. 1 (liquid)	Ref. 2 (vapour)
263	0.868 (15)	0.857	
368	0.160 (13)	0.130	0.130
670	0.022 (8)	0.026	0.014
761	0.841 (9)	0.857	
1219	0.862 (22)	0.857	
3020	0.284 (5)	0.280	0.182

[a] Standard deviations of three measurements are shown in parentheses.

Acknowledgements

We thank L. Ellison and P. Willmore for assistance in the design and construction of the electronic control circuit, S. Eaton for assistance with programming of the microprocessor and British Petroleum Co. plc for financial support for J.S. and for the research programme.

REFERENCES

1. D. A. Long and R. B. Gravenor, *Trans. Faraday Soc.* **59**, 46 (1963).
2. S. Montero, D. Bermejo and W. Klockner, *Mol. Phys.* **33**, 1029 (1977).

R.H.B.N.C.
LIBRARY

CROATICA CHEMICA ACTA CCACAA **61** (3) 551—567 (1988)

CCA-1811

YU ISSN 0011-1643
UDC 543.42
Original Scientific Paper

The Use of Absolute Vibrational Band Intensities in Structural Analysis. I. *n*-Alkanes and Derived Ketones

Derek Steele, Kevin Hamilton, and (in part) Josephine Stevens

Department of Chemistry, Royal Holloway and Bedford New College, Egham Hill, Egham, Surrey, TW20 OEX, U.K.

Received March 18, 1988

A systematic investigation of group absorption band intensities in tetrachloromethane of *n*-alkanes and methyl *n*-alkyl ketones is described. Contributions to the total intensity in given regions from each structural group are established and the results used to predict the spectral intensities of methyl cyclohexane, di-*n*-hexyl ketone and cycloheptanone. The variations in CH_2 and CH_3 group contributions arising from proximity to the carbonyl are discussed in relation to the constancy of King's effective atomic charge.

Raman group frequencies and intensities of the CH_3S and CH_3CH_2S are established. It appears likely that Raman band intensities, though less easily measured, could also be useful in structural analysis.

INTRODUCTION

The prime role of vibrational spectroscopy in chemistry is in structural analysis. Since the vibrational spectrum is so complex (constituted out of $3N - 6$ fundamentals, where N is the number of atoms) the methods employed are almost invariably based on empirical correlations. In such procedures the chemist is using the long established observation that a particular group of atoms in a given local environment in different molecules has unchanged physical and chemical properties. Provided that the energies of certain fundamental modes arise primarily from distortions within that group of atoms then it follows that absorption or scattering resulting from excitation of those vibrations will result in bands at closely similar positions in the spectra of all the molecules containing that grouping. A vast compilation of such structure-band correlations exist in texts such as those of Bellamy[1,2], though the spectral data is restricted to frequency information and usually very qualitative intensity data. The latter is generally of the form "weak" or "strong", but these very imprecise terms are never defined, and what appears to be a strong band in perhaps a hydrocarbon spectrum may appear very weak compared with bands of a silicone.

Commencing in the 1930's detailed intensity studies were made of a number of molecules of high symmetry and attempts made to interpret the band intensities in terms of bond oriented parameters. The popularity of

such studies rapidly waned when it became clear that, even when experimental problems had been overcome, simple bond dipole models did not work. Different symmetry species led to different estimates for the bond dipole moment[3]. There are three theories explaining this. The first used the concept that as angles changed, then rehybridisation at the central nucleus caused electron flow in the opposite direction to the bond which was particularly marked when the bond moved in a plane perpendicular to that of π bonds[4,5]. Thus as the CH bond of ethene moves out of the equilibrium nuclear plane the hybridisation at carbon moves towards sp^3 and a lone electron pair builds up on the opposite side of the plane to CH. While some indirect experimental evidence for this exists, ab initio calculations suggested that incomplete bond following was responsible for the variable effective bond moment[6]. Not incompatible with this explanation are recent results[7] which show that in a variety of molecules, including CH_2F_2 and ethene the *ab initio* experiment of deforming one C—X bond produces a dipole change off the bond line for stretching and off the perpendicular for bending. Deforming two bonds (or angles) leads to a dipole change which is the vectorial sum of the individual components.

Even without these model problems serious difficulties have occurred because of force field uncertainties. Fortunately scaled *ab initio* computed fields are rapidly becoming far more reliable than experimentally derived fields and great progress is being made by combining the two.

Where does all of this leave the use of intensities in analysis? There are various hopeful signs in the morasse of data. King[8] defined an effective atomic charge ε_α related to infrared absorption intensities by

$$\sum_\alpha \frac{\varepsilon_\alpha^2}{M_\alpha} = \sum_i A_i + \Omega$$

where M_α is the mass of the α atom, A_i is the integrated absorbance and Ω is a rotational angular momentum correction necessary for polar molecules. ε_α is also related to the atomic polar tensor P_x^α by

$$\varepsilon_\alpha^2 = Tr\,[P_x^\alpha \tilde{P}_x^\alpha] = \left|\frac{\partial p}{\partial x_\alpha}\right|^2 + \left|\frac{\partial p}{\partial y_\alpha}\right|^2 + \left|\frac{\partial p}{\partial z_\alpha}\right|^2 + \qquad (1)$$

where P_x^α is the cartesian polar tensor for the atom, α and P is the dipole moment. Remarkably the effective atomic charge for the hydrogen atom is found to remain roughly constant in a diverse range of compounds and in all hydrocarbons except ethyne. Thus for saturated hydrocarbons, olefins and benzene $\varepsilon_H = 0.100 \pm 0.005$ e. These clearly indicate that wild variations in intensity parameters do not occur between similar bonds. Person and his coworkers have exploited the transferability of atomic polar tensors in metal fluorides and fluorocarbons by using transfered parameters to predict the spectra of unknown or related species[9,10].

In Raman scattering intensities were interpreted on the basis of the Wolkenstein assumptions, and polarisability bond derivatives for CC bonds were found to be approximately proportional to bond order[11]. CH derivatives were also found to be reasonably constant in aliphatic systems. It has often been

remarked that polarisabilities are less susceptible to intermolecular interactions and that higher derivatives than the first of the polarisability are generally very small as witnessed by general absence of combination bands. These points would indicate that characteristic vibration bands should show more intensity consistency in the Raman than in the infrared. It is remarkable then that little systematic work has been reported on Raman band intensities for characteristic bands in related series of molecules.

For infrared spectroscopy there is a considerable literature on band intensities, mostly dating from the 1960's. The data prior to 1967 is well reviewed by Wexler[12]. Many cases are well established where group intensities exist though in other situations complicated electron lone pair and inductive effects occur. Nevertheless with the vastly improved data handling facilities of modern spectrometers it is very surprising that group intensity studies have gone out of fashion and that few analysts ever seriously think of using infrared intensities in structural analysis. We shall present some initial results of a systematic study of some homologous series and demonstrate that the power of infrared and Raman analysis is greatly enhanced by the use of intensities.

EXPERIMENTAL

In measuring absorption intensities care needs to be taken to avoid the following sources of error.

1. Inadequate resolution. Instrumental slit widths need to be significantly less than half of the experimental half height width (HHW). For the compounds studied the narrowest bands had HHW of about 10 cm^{-1}.
2. Incorrect zero transmission measurements.
3. Non linearity of the detection system.
4. Interference effects due to internal reflection in the cell.
5. Incorrect allowance for background absorption.

Spectra were measured on a PE983 with spectral resolutions varying from 3.6 cm^{-1} at 3000 cm^{-1} to 2.1 at 1200 cm^{-1} (mode 5 filter 4). Data was collected and processed using a PE3600 data station. Before correction using the instrument's microprocessor routine (shift zero, page 4) the zero error was 0.1—0.2%. After correction the error was within the noise level. To ensure that all spectra were measured under the same conditions solutions in carbon tetrachloride were used at suitable concentrations between 3% and 20% and in a cell of path length of 0.103 mm. To correct for the cell background and for the CCl_4 absorption the following procedure was adopted.

i) Spectra of CCl_4 were measured at path lengths of 0.103 and 0.025 mm. By ratioing, the spectrum of CCl_4 was established in absorbance units.

ii) The spectrum of say a 10% (volume) solution (known weight ratios) was now recorded and ratioed against the spectrum of CCl_4 in the same cell. This overcompensates for the CCl_4 absorptions — in this case by 10% or 0.0103 mm. Addition to the spectrum of the absorbance spectrum of CCl_4 (as measured in (i)) of the appropriate path length serves to remove all traces of CCl_4 bands, except in the intensely absorbing 800 cm^{-1} region, while at the same time avoiding general cell background distortions.

During the procedure checks are made to ensure the correct positioning of the background (error source 5). In acquiring the initial difference spectrum (using SDIFF function) the VDU image is magnified by at least 30 using the EXPAND facility. At this level the noise is readily apparent and the backround is adjusted up or down so that at the point of minimum absorption, (usually 2200—2000 cm^{-1} in the scan range 3600—2000 cm^{-1}, and 2000—1800 cm^{-1} in the range 2000—400 cm^{-1}) the noise is fluctuating about the origin (located by bars on screen). Of course

regions of CCl_4 absorption, especially near 1550 cm^{-1} and 800 cm^{-1} are excluded in this procedure. Examination of the absorbance data in the memory using the TYPE facility can be used as a final verification that the origin is correctly located. The general noise level is found to be about 0.0010 absorbance units except where water vapour absorbs strongly when it may be 2—3 times as large. Occasionally there are some evidence of channel spectra but with the solutions or with pure CCl_4 in the cell these were weak. In such cases the background was adjusted to pass through the zero phase points (error source 2).

Linearity of the detection system was verified using calibrated sectors and by Beer's law plot tests. Linearity was better than 1%, thus error source 3 is negligible.

To maintain consistency with the majority of the literature on solution intensities the integrated intensities are defined by

$$\frac{1}{cl} \int_{\nu_e}^{\nu_H} \log_{10} (I_1/I)\, d\nu$$

By contrast most vapour studies use the more fundamental $\int \log_e (I_o/I)\, d\nu$ and preferably $\int \log_e (I_o/I)\, d \log_e \nu$.

Raman spectra were recorded using a modified Coderg PHO spectrometer with NPL holographic gratings, a low noise EMI 9863B photomultiplier and interfaced through a Brookdeal photoncounting system to a Tektronix 4052 computer with a 4907 disc system. Polarisations were recorded using a Pockel cell to rotate the plane of polarisation of the incident laser beam between acts of stepping the grating motor[13]. This has the merit of reducing the time separation between readings of intensities for parallel and perpendicular polarisations (actually $I_{VV} + I_{VH}$ and $2I_{HH}$) to time for a single reading, thereby significantly increasing measurement accuracy.

RESULTS

Separation into component bands is a process which is subject to considerable error due to uncertainties in the number of components and in the band contours. For this reason and because the intention is to develop a simple to apply analytical procedure no such band deconvolutions have been attempted. For the initial survey work reported here the CH stretching and deformation regions have been sub-divided at frequencies at which absorption minima occur in the higher *n*-alkanes. These are shown on a typical spectrum in Figure 1. For the stretching region the four regions so produced are, as is well established[1] and clear from the plots to follow, due primarily to CH_3 anti-symmetric, CH_2 anti-symmetric, CH_3 symmetric and CH_2 symmetric modes respectively from high to low frequencies. For the deformation region some extra subdivision was made to allow for the CH_2 bands which are significantly perturbed in frequency by the carbonyl. Plots of the integrated intensities of these regions against the number of CH_2 units in the alkane chain are shown in Figures 2. and 3. Good linear plots are obtained except for points for propanone (acetone) and butanone (methyl ethyl ketone). It is also to be noted that the gradients for the alkanes and the alk-2-ones are equal within experimental error (see Figures 2 and 3). The data was fitted by least squares analysis to

$$\text{Intensity} = YINT + GRAND \cdot N \qquad (2)$$

where N is the number of CH_2 units and $YINT$ and $GRAD$ are constants.

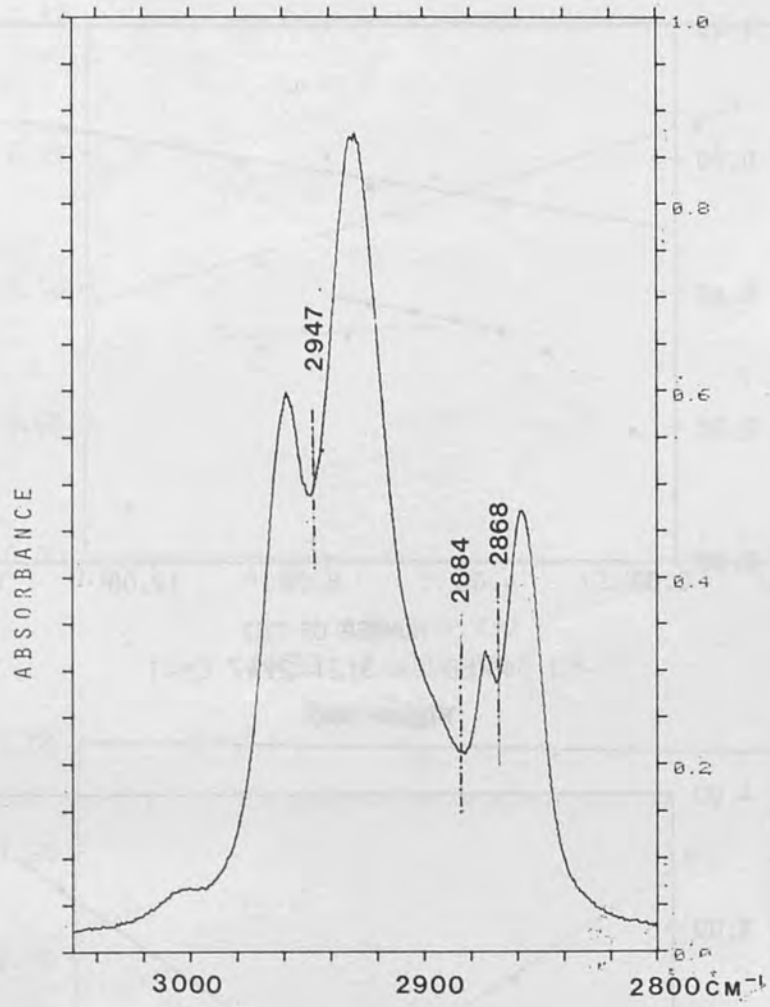

Figure 1. Spectrum of 2 nonanone in range 3050—2800 cm^{-1}; showing the break points used in integrating the intensities (concentration 0.2892 mol dm^{-3} in 0.0103 cm cell).

For the alkanes the intensity axis intercepts are all positive, though varying in *YINT* from magnitudes ranging from zero within two standard deviation to 7427 ± 275 dm^3 mol cm^{-2}. By contrast the methyl *n*-alkyl ketones generally show negative *YINT*. For the alkanes the gradient clearly represents the contribution to the integrated intensity in the spectral region per alkane CH_2 unit. *YINT* is the contribution to the intensity due to the two methyl units. Application of these results to alkyl cyclohexanes serves to check the wider applicability of the results. The measured and predicted intensities of methylcyclohexane, with the tertiary hydrogen atom ignored in the predictions, are shown in Table I. Some movement of intensity to lower frequencies in the CH stretching region is apparent though overall the result is very pleasing. Scaling of the intensity by 14/13 to allow for the tertiary H improves the total intensity. Clearly further studies of branched chain systems will allow more satisfactory allowance for this CH bond which does not give rise to any clearly identified band.

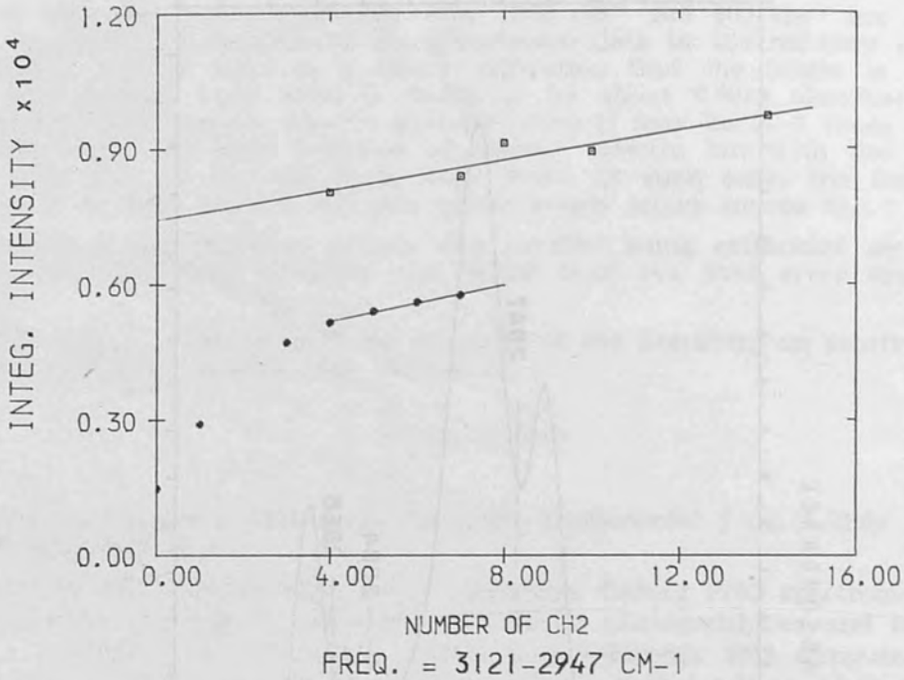

Figure 2(a)

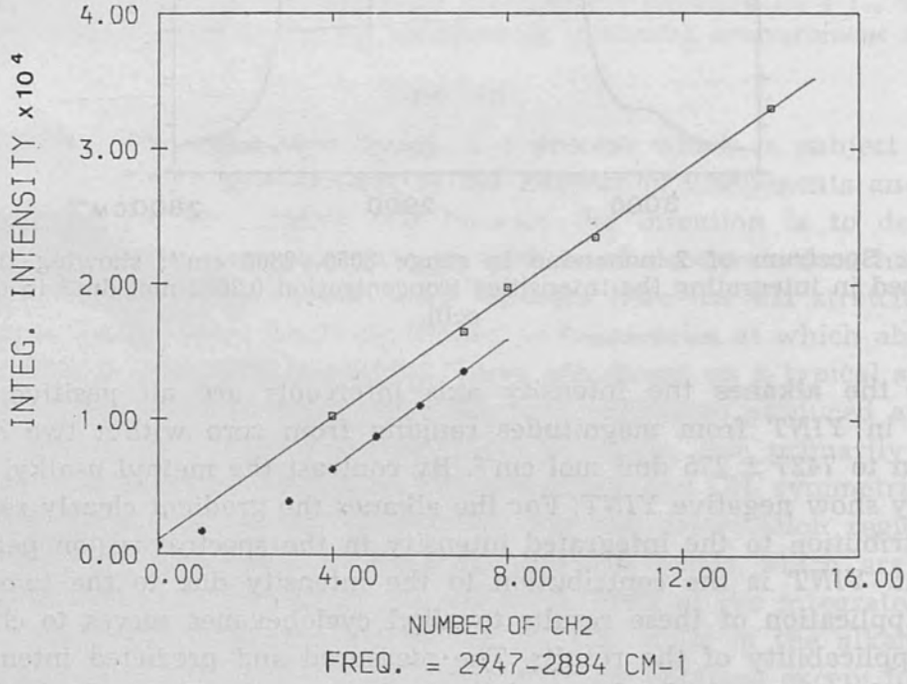

Figure 2(b)

In the alk-2-ones the parallel displacement of the lines for CH stretching to higher n is understandable as due to the general weakening of the CH bands in the CH_3COCH_2 unit. This weakening has long been recognised. What has not been ascertained is whether the effect is restricted to the CH bonds alpha to the carbonyl and whether the intensity effects are transferable bet-

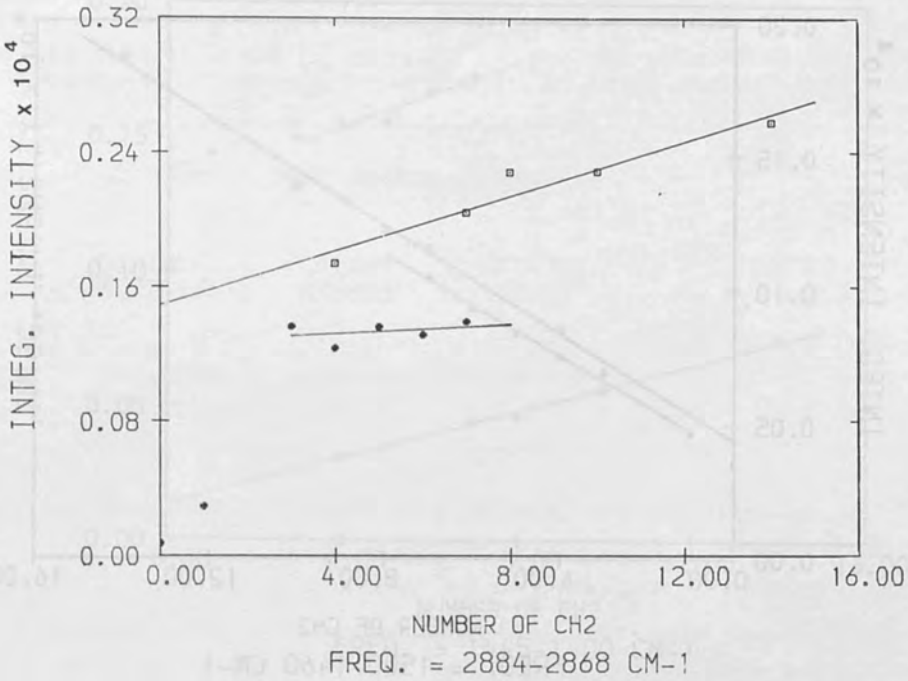

Figure 2(c)

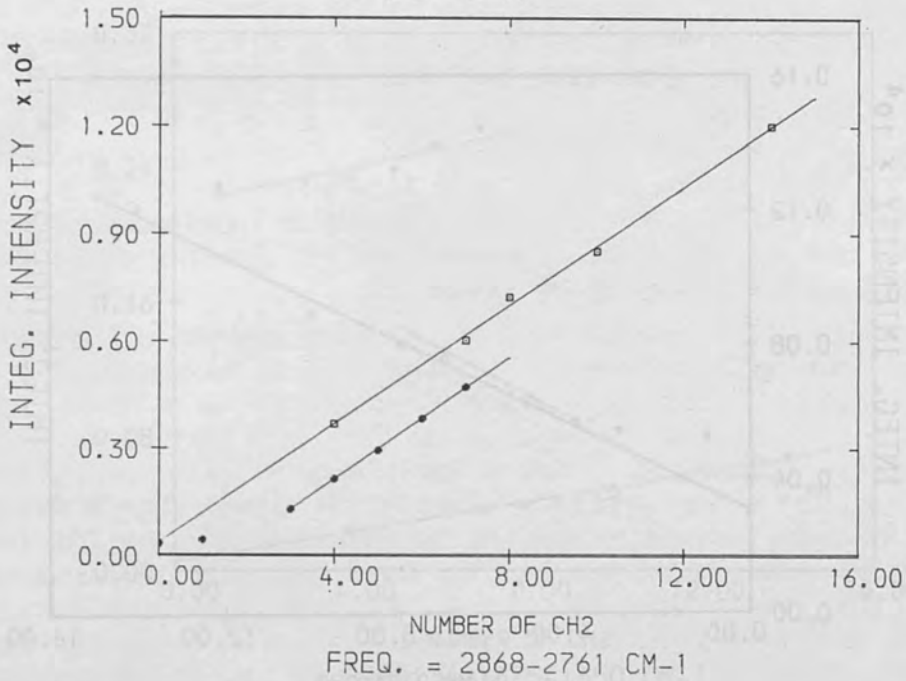

Figure 2(d)

Figure 2. Integrated absorption intensities (mol^{-1} dm^3 cm^{-2}) in defined spectral ranges (stretching region) for alkanes □ and methyl *n* alkyl ketones ✠ *versus* the number of CH_2 units in the alkyl chain.

ween similar molecules. Examination of the data shows that the answer to the former question is that the effect carries at least to the beta CH bonds.

Examination of Figures 2(a) and 2(b) in particular demonstrate that even for $n = 3$ there appears to be a slight deviation from the linear section of the

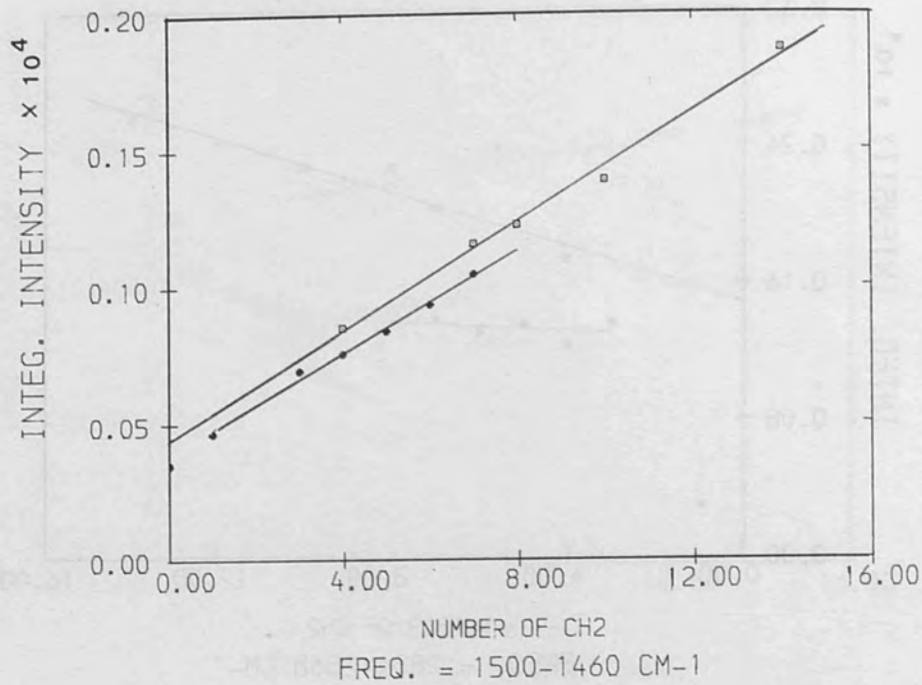

Figure 3(a)

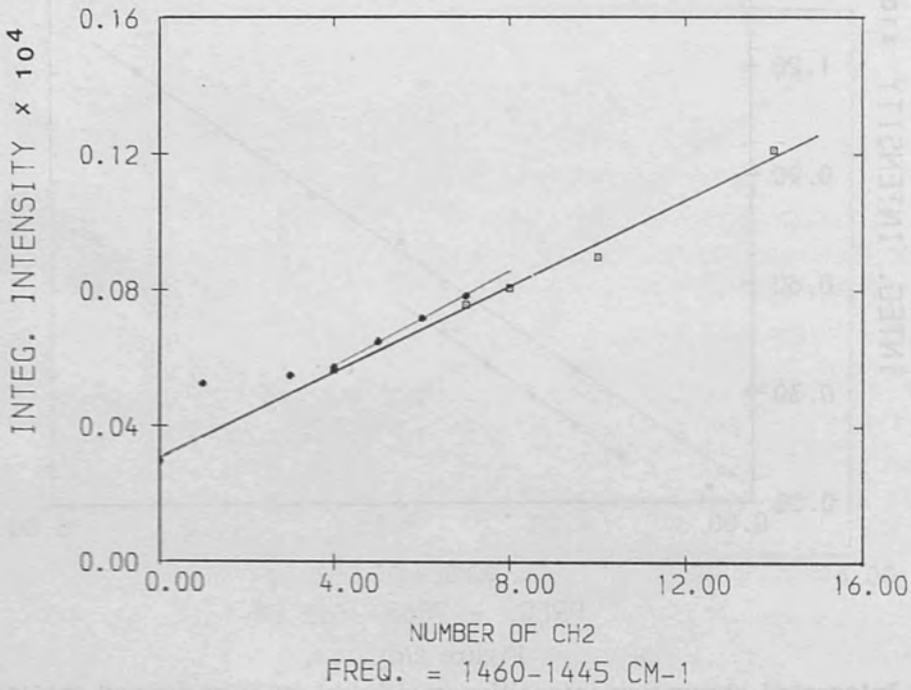

Figure 3(b)

graph. Possibly a very small intensity movement from the 3121—2947 cm^{-1} region to lower frequencies could explain the $n = 3$ points, but it seems highly probable by extrapolation that for $n = 2$ (no data currently available) the points lie off the lines. As we will see, data on such as cycloheptanone and methyl ethyl ketone reinforce the occurrence of an effect out to the β carbon.

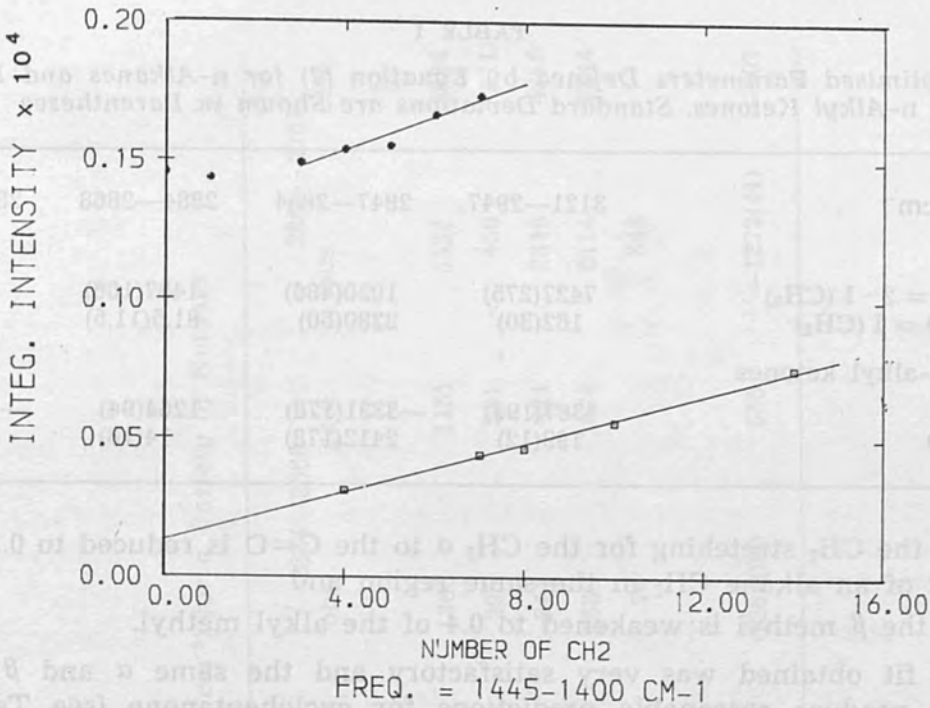

Figure 3(c)

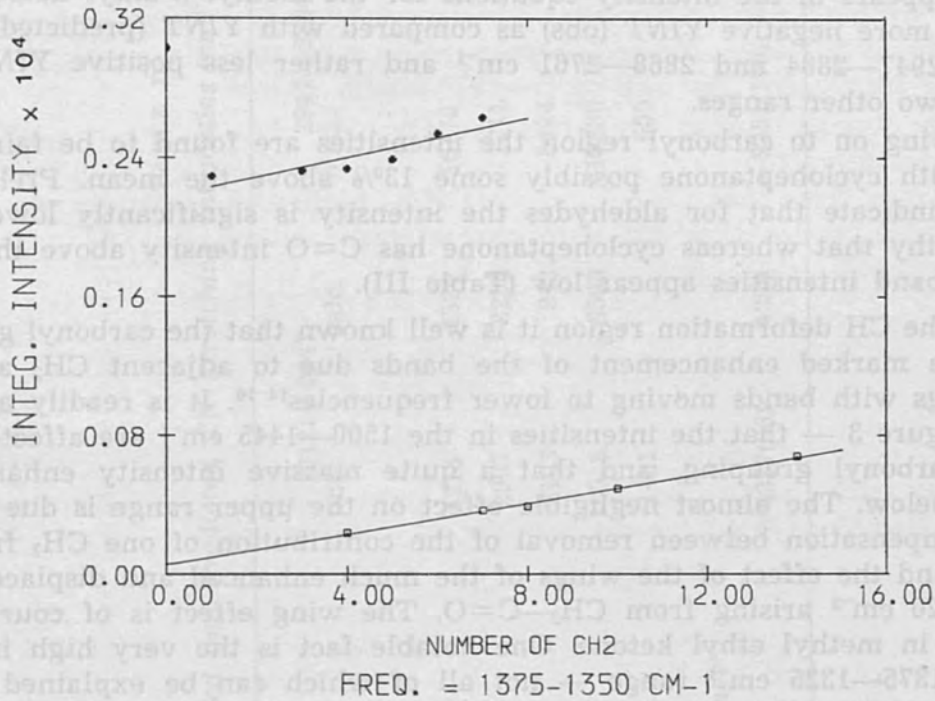

Figure 3(d)

Figure 3. Integrated absorption intensities (mol^{-1} dm^3 cm^{-2}) in defined spectral ranges (scissoring region) for alkanes □ and methyl *n*-alkyl ketones ✠ *versus* the number of CH_2 units in the alkyl chain.

For methyl ethyl ketone the following assumptions were tried:

(i) that the contribution of $CH_3(CO)$ to each region is equal to 1/2 of the intensity of acetone (propanone) in the same range;

TABLE I

The Optimised Parameters Defined by Equation (2) for n-*Alkanes and Methyl* n-*Alkyl Ketones. Standard Deviations are Shown in Parentheses*

ν Range/cm^{-1}	3121—2947	2947—2884	2884—2868	2868—2761
alkanes				
YINT = 2 · I (CH_3)	7427(275)	1030(486)	1487(106)	368(195)
GRAD = I (CH_2)	162(30)	2280(50)	81.5(11.5)	830(21)
methyl *n*-alkyl ketones				
YINT	4387(199)	—3331(178)	1264(94)	—1273(41)
GRAD	199(12)	2412(178)	14(18)	854(8)

(ii) the CH_2 stretching for the CH_2 α to the C=O is reduced to 0.2 of the intensity of an alkane CH_2 in the same region and

(iii) the β methyl is weakened to 0.4 of the alkyl methyl.

The fit obtained was very satisfactory and the same α and β factors serve to produce reasonable predictions for cycloheptanone (see Table II). There is some slight shift of intensity indicated towards lower frequencies, which appears in the intensity equations for the methyl *n*-alkyl ketones as a slightly more negative *YINT* (obs) as compared with *YINT* (predicted) in the ranges 2947—2884 and 2868—2761 cm^{-1} and rather less positive *YINT* (obs) in the two other ranges.

Moving on to carbonyl region the intensities are found to be fairly constant with cycloheptanone possibly some 13% above the mean. Preliminary studies indicate that for aldehydes the intensity is significantly lower. It is noteworthy that whereas cycloheptanone has C=O intensity above the mean its CH band intensities appear low (Table III).

In the CH deformation region it is well known that the carbonyl grouping causes a marked enhancement of the bands due to adjacent CH_2 and CH_3 groupings with bands moving to lower frequencies[14-16]. It is readily apparent from Figure 3 — that the intensities in the 1500—1445 cm^{-1} are affected little by a carbonyl grouping, and that a quite massive intensity enhancement occurs below. The almost negligible effect on the upper range is due in part to a compensation between removal of the contribution of one CH_2 from the region and the effect of the wings of the much enhanced and displaced band near 1420 cm^{-1} arising from CH_2—C=O. The wing effect is of course most marked in methyl ethyl ketone. One notable fact is the very high intensity in the 1375—1325 cm^{-1} range — not all of which can be explained by the CH_3 C=O umbrella vibration. Di-*n*-hexyl ketone shows about an extra 1000 cm^{-2} mol^{-1} dm^3 compared with expectations for an alkyl. There is clearly an enhancement of the CH_2 wagging vibration (alkanes near 1305 cm^{-1}) just as there is for the CH_3 umbrella vibration.

The results of fitting the observed intensities of the methyl deformation region to equation (2) for both *n*-alkanes and *n*-alk-2-ones are given in Table IV. The methyl umbrella region is enhanced by a factor of 10 and the CH_2 wagging region by a factor of 40. Taking half of the intensity of acetone

TABLE II

Observed and Predicted CH Stretching Intensities ($mol^{-1}\ dm^3\ cm^{-2}$) for a Variety of Ketones

$\bar{\nu}$ Range/cm^{-1}	3121—2947		2947—2884		2884—2868		2868—2761	
	obs.	calc.	obs.	calc.	obs.	calc.	obs.	calc.
compound								
methyl cyclohexane	4213	4524	16170	11915	1366	1151	5532	4334
methyl ethyl ketone	2907	2258	1711	985	295	351	456	411
cycloheptanone	2403	842	8494	11856	644	424	2345	4316
di *n*-hexyl ketone	10518	8593	17230	17446	2586	2074	6114	6344
acetone	1481		650		74		342	
methyl n-*alkyl ketones*								
YINT	4387(66)	4259	—3331(178)	—2353	1264(94)	555	—1273(41)	—807

TABLE III

Intensities of C = O Stretch (mol^{-1} dm^3 cm^{-2}) in Range 1750—1675 cm^{-1}

acetone	6640	non-2-one	6680
but-2-one	6490	dec-2-one	7170
hept-2-one	6700	cycloheptanone	7610
oct-2-one	6580	di-*n*-hexyl ketone	6570

as representative of the contribution of CH_3CO and half of *YINT* for alkanes as the intensity due to the alkane CH_3 then an estimate of the CH_2CO may be made from the intensities of methyl ethyl ketone (but-2-one). These figures are also given in Table IV. Using these the *YINT* for methyl *n*-alkyl ketones can be estimated by

$$YINT\,(\text{pred}) = I\,(CH_3CO) + I\,(CH_3\text{alk}) + I\,(CH_2CO) - GRAD(\text{alk}) \qquad (3)$$

The results agree very favourably with the observed, though a slight shift to higher frequencies is discernible. The group contributions can now be used to predict the intensities of cycloheptanone and of di-*n*-hexyl ketone, for both of which we have data. Agreement is very good for di *n*-hexyl ketone, though the experimental values for cycloheptanone do seem low. As mentioned earlier it may be significant that the carbonyl intensity is high.

In the Raman studies, for which we are only able to report preliminary results, measurements have been made on a series of dialkyl sulphides. From Table V. it is clear that CH_3S- and CH_3CH_2S- both lead to bands, not only at characteristic frequencies, but with characteristic intensities.

The intensities are defined by

$$I = \frac{I_{obs}\,(1 - \exp(-hc\bar{\nu}/kT))}{(\bar{\nu} - \bar{\nu}_e)^4\,\bar{\nu}} \qquad (4)$$

where I_{obs} is the measured intensity corrected for instrumental effects, $\bar{\nu}$ is the Raman shift and $\bar{\nu}_e$ is the exciting wave number. The intensities are scaled so that the 459 cm^{-1} band complex of CCl_4 has an intensity of 100 units.

DISCUSSION

The earliest integrated intensity studies of the characteristic bands of alkanes were carried out by Francis[17]. The integrated intensities of stretching and bending bands were shown to be approximately proportional to the number of hydrogen atoms, though strong substituent effects were later identified in a number of investigations exemplified by that of Higuchi, Kuno, Tanaka and Kamada[18]. For alkanes themselves the current results show values for CH_3 stretching (= (sum of *YINT*)/2) and for CH_2 stretching (= sum of *GRAD*) of 5150 (± 530) and 3353 (± 112) mol^{-1} dm^3 cm^{-2} respectively.* These are in the ratio 3 : 2 well within experimental error. Wexler[19] and Francis[17] quote

* 1 mol^{-1} dm^3 cm^{-2} ≡ 1 dark ≡ 0.01 km mol^{-1}, respectively.

TABLE IV

Observed and Predicted Intensities (mol^{-1} dm^3 cm^{-2}) for Methyl Deformation Regions of Alkanes and Alkones

$\bar{\nu}$ Range/cm^{-1}	1500—1460		1460—1445		1445—1400		1400—1375		1375—1325	
	AINT	GRAD	AINT	GRAD	AINT	GRAD	AINT	GRAD	AINT	GRAD
Alkanes	439(40)	100(4)	303(28)	63(3)	129(13)	44(1.4)	264(7)	12(1)	55(14)	44(1.5)
Alk-2-ones	385(16)	93(4)	294(8)	70.5(1.5)	1294(40)	61(18)	620(18)	6(4)	2176(57)	56(12)
Int/CH_3(alk)	220		152		65		132		28	
Int/$CH_3C:O$	175		149		728		258		1512	
Int*/$CH_2C:O$	70		224		640		90		720	
AINT predicted from above	365		461		1389		4689		2216	
di *n*-hexyl ketone										
pred.	1379		1255		1761		540		1847	
obs.	1434		969		1694		790		1904	
cycloheptanone										
pred.	940		700		1456		228		1616	
obs.	325		947		1251		164		1210	

* As derived by fitting methyl ethyl ketone taking contribution from CH_3 (CH_2) as in alkanes.

TABLE V

A Listing of Frequencies and Raman Scattering Cross Sections, as Defined by Equation (4), of Bands Which are Characteristic of CH_3S—, CH_3CH_2S— and of —CH_2S—. The Intesity Scale is such that the 459 cm^{-1} Band of CCl_4 has an Intensity of 100

CH_3SCH_3		$CH_3SC_2H_5$		$C_2H_5SC_2H_5$		$CH_3S(nC_3H_7)$		CD_3SCD_3		Mode
ν	I''	ν	I''	ν	I''	ν	I''	ν	I''	
		658	26.9	641	15.4	647	9.6			
				658	19.4	669	4.3			
		682	10.8	694	14.7	699	10.1			CS
693	48.0					724	10.8	642	37.1	
744	14.8	729	16.9	766	0.8	749	5.3	707	11.5	
						785	3.1			
600—800	62.8		53.6		50.3		43.2		48.6	Total ν_{c-s}
		1050	2.4	1048	4.6					ν (S—C_2H_5)
		2728	0.8	2733	2.5	2735	1.2			ν_{CH} (S — CH_2)
2834	4.6	2836	3.2			2829	2.1	2037	1.8	ν_{CH} (S — CH_3)
		2931	17.9	2932	18.6	2936	13.3			ν_{CH} (S — CH_2)
2987	13.3	2967*	21.3			2986	10.5	2240	15.3	ν_{CH} (S — CH_3)

4500 and 3700 and 3900 and 3300 mol^{-1} dm^3 cm^{-2} Francis's CH_3 values appear rather low and Wexler's CH_3 and CH_2 values seem to have some of CH_3 intensity transferred to the CH_2. In the deformation region it is necessary to define frequency limits and to be consistent in background definition. In the present work we consistently include all absorption in the spectral region of interest without seeking to decompose absorptions into contributions from different bands. Such latter procedures offer great scope for error and ambiguity. The presence of unidentified bands, of Fermi resonance components, of intrinsic band asymmetries (due for example to Coriolis coupling), and of uncertainties in wing shapes — all of these, and no doubt many others, render band deconvolution procedures undesirable. Jones[20] measured the molecular extinction coefficients of the component bands of *n*-alkanes — in the process identifying a third component at 1460 cm^{-1}. As quoted by Wexler[12] the data of references 19 and 17 both support values for the CH_3 antisymmetrical scissoring intensity (1460 cm^{-1}) of 480 mol^{-1} dm^3 cm^{-2} and for the umbrella mode of 200 mol^{-1} dm^3 cm^{-2}. Taking 1400 cm^{-1} as the separation point and extending the range of integration from 1500 to 1325 cm^{-1} leads to values of 435 and 160 mol^{-1} dm^3 cm^{-2} with uncertainties of about 10%.

Francis quoted an intensity reduction of CH stretching bands of 7 to 10 if a carbonyl groups is present (adjacent). In our interpretation of the intensity data the intensity ratio is given as

YINT (alkanes)/Intensity (acetone).

As the CH_3 symmetric stretch is moved to lower frequencies by the carbonyl it is necessary to combine the range 2884—2868 and 2868—2761 cm^{-1}. The ratios in the two upper ranges are little affected by the C=O but for consistency these too are combined. With these combinations the intensity reductions are 4.0 and 4.5 respectively, significantly less than proposed earlier.

Having established on a more quantitative basis than has previously been done the group intensities in CH stretching and deformation regions the question of the constancy of the effective atomic charge of the hydrogen atom can be re-examined. There does indeed appear to be a complimentarity in the effects of perturbing groups in that the carbonyl group greatly reduces the stretching intensity but enhances the bending intensities. We shall simply note at this stage that $\sum_i A_i/\nu_i^2$, where the sum is over the group vibrations, is much more constant that $\sum_i A_i$. Indeed for cycloheptanone where we note a general reduction in the CH_2 group intensities compared with that expected for an open chain ketone there is a compensatory increase in the C=O intensity, which may be a geometrical effect. This problem needs much more experimental and theoretical investigation.

So far we have not mentioned a recent important paper by Castiglioni, Gussoni and Zerbi[21]. The total integrated intensities in the CH stretching region and in the HCH scissoring region are reported for gaseous alkanes as well as a variety of ethenes, aldehydes, methanol, acetone and dimethylether. In Table VI. we compare the intensity predicted by the parameters in Table I. with the intensities as measured by Gussoni and colleagues. To conform with normal practice for gaseous intensity measurements our predictions are scaled by $\log_e(10)$. The intensity ratio of the solution and gaseous intensities is seen

TABLE VI

A Comparison of Solution Intensities of n-*Alkanes Based on This Work With Gaseous Phase Results from Reference 12. All Intensities are in mol⁻¹ dm³ cm². »A'« Refer to Intensities Defined Using* $\log_e(I_0/I)$ *and »A« to the Base 10 Counterparts*

Molecule	A^{CH}_{calc} (soln)	$A'^{CH}_{calc} \cdot 2.303 \equiv A^{CH}$ (soln)	A'^{CH} (gas) Ref. 21	A' (gas)/A' (soln)
C_2H_6	10302	23725	17088	1.388
C_3H_8	13656	31444	22496	1.398
C_4H_{10}	17020	39190	28720	1.365
C_5H_{12}	20374	46913	34752	1.350
C_6H_{14}	23718	54613	40376	1.353

to range only from 1.350 to 1.398. This is close to the predictions of the Polo Wilson equation

$$\frac{A_L}{A_S} = \frac{(n^2+2)^2}{9n}$$

where n is the refractive index. Using n_D for CCl_4 the ratio predicted is 1.299. An analysis of the intensities was made in terms of the electrooptical parameters, the charge fluxes, $\partial q/\partial r_{CH}$, and the atomic equilibrium charges, q_H°. It was shown that for all alkanes, alkenes and alkynes the ratio of the total intensity in the deformation region (1500—400 cm^{-1}) to the total CH stretching intensity (3000—2500 cm^{-1}) varies in a smooth fashion with the derived atomic charge q_H° as one might expect. However for the alkynes both the stretching and deformation intensities are considerably higher than for alkanes in accord with their higher King's effective charges.

REFERENCES

1. L. J. Bellamy, *The Infrared Spectra of Complex Molecules*, Volume **1**, 3rd edition, London, Chapman and Hall 1975.
2. L. J. Bellamy, *The Infrared Spectra of Complex Molecules*, Volume **2**, 2nd edition, London, Chapman and Hall 1980.
3. See for example reviews i) D. Steele, *Quart. Rev. (Chem. Soc., London)*, **18** (1964) 21, ii) J. Overed, *Infrared Spectroscopy and Molecular Structure*, M. Davies, (Ed.), Amsterdam, Elsevier 1963, p. 345.
4. D. C. McKean, *J. Chem. Physics* **24** (1956) 1002.
5. D. Steele and W. Wheatley, *J. Mol. Spectrosc.* **32** (1969) 265.
6. K. B. Wiberg and J. L. Wendoloski, *J. Computational Chem.* **2** (1981) 53; *J. Phys. Chem.* **88** (1984) 586.
7. Y. Dimitrova and D. Steele, *Spectrochim. Acta*, in press.
8. W. T. King, G. B. Mast, and P. P. Blanchette, *J. Chem. Physics*, **56** (1972) 4440.
9. J. H. Newton and W. B. Person, *Applied Spectrosc.* **32** (1978) 290.
10. J. H. Newton and W. B. Person, *J. Chem. Physics*, **68** (1978) 2799.
11. G. W. Chantry, Chapter 1 in *Raman Spectroscopy* edited by A. Anderson, New York, Dekker 1971.
12. A. S. Wexler, *Applied Spectroscopy Reviews* **1** (1967) 29.
13. J. A. Stevens, D. Steele, D. L. Gerrard, and W. F. Maddams, *J. Raman Spectrosc.* **18** (1987) 373.

14. S. A. Francis, *J. Chem. Physics* **19** (1951) 842.
15. R. N. Jones, A. R. H. Cole, and B. Nolin, *J. Amer. Chem. Soc.* **74** (1952) 5662.
16. B. Nolin and R. N. Jones, *J. Amer. Chem. Soc.* **75** (1953) 5626.
17. S. A. Francis, *J. Chem. Physics* **18** (1950) 861.
18. S. Higuchi, E. Kuno, S. Tanaka, and H. Kamada, *Spectrochim. Acta* **28A** (1972) 1335.
19. A. S. Wexler, *Spectrochim. Acta* **21** (1965) 1725.
20. R. N. Jones, *Spectrochim. Acta* **9** (1957) 235.
21. C. Castiglioni, M. Gussoni, and G. Zerbi, *J. Molecular Structure* **141** (1986) 341.

SAŽETAK

Uporaba apsolutnih intenziteta vibracijskih vrpci u strukturnoj analizi. I. *n*-Alkani i derivirani ketoni

Derek Steele, Kevin Hamilton i (dijelom) Josephine Stevens

Opisano je sustavno istraživanje intenziteta skupinskih apsorpcijskih vrpci *n*-alkana i metil-*n*-alkilketona u tetrakloruglji ku. Utvrđeni su doprinosi svake strukturne skupine ukupnom intenzitetu u određenom području, a rezultati su upotrijebljeni za procjenu spektralnih intenziteta metilcikloheksana, di-*n*-heksilketona i cikloheptanona. Varijacije u doprinosima skupina CH_2 i CH_3 uzrokovane blizinom karbonila, razmatraju se s obzirom na konstantnost Kingova efektivnog atomskog naboja.

Utvrđene su Ramanove skupinske frekvencije i intenziteti za CH_3S i CH_3CH_2S. Čini se da su intenziteti Ramanovih vrpci, iako teže mjerljivi, također uporabivi u strukturnoj analizi.